



City Research Online

City, University of London Institutional Repository

Citation: Bonomi, D. (2024). Analytic bootstrap for conformal defects. (Unpublished Doctoral thesis, City, University of London)

This is the accepted version of the paper.

This version of the publication may differ from the final published version.

Permanent repository link: <https://openaccess.city.ac.uk/id/eprint/33847/>

Link to published version:

Copyright: City Research Online aims to make research outputs of City, University of London available to a wider audience. Copyright and Moral Rights remain with the author(s) and/or copyright holders. URLs from City Research Online may be freely distributed and linked to.

Reuse: Copies of full items can be used for personal research or study, educational, or not-for-profit purposes without prior permission or charge. Provided that the authors, title and full bibliographic details are credited, a hyperlink and/or URL is given for the original metadata page and the content is not changed in any way.

Analytic bootstrap for conformal defects

Davide Bonomi

Thesis submitted in partial fulfillment of
the requirements for a doctorate of philosophy.



Department of Mathematics, City University of London

London, July 2024

Declaration

I, Davide Bonomi, confirm that the work presented in this thesis is my own. Where information has been derived from other sources, I confirm that this has been indicated in the thesis.

Abstract

Conformal Field Theories (CFTs) play a pivotal role in various areas of theoretical physics, including string theory, holography, and condensed matter physics. Many of these theories feature non-local excitations, known as defects. Conformal defects break some of the conformal symmetry of the bulk theory while preserving it on the defect. Therefore, it is natural to study them using similar methods to those employed for CFTs without defects, such as the analytic conformal bootstrap. In this thesis, we develop some analytic bootstrap techniques specifically for defect CFTs. We also apply these techniques to several defects that are relevant in the context of condensed matter physics or holography. We begin by reviewing the fundamental principles of conformal field theory and the analytic bootstrap. Following this, we derive dispersion relations that enable the reconstruction of defect and bulk correlators from their singularities. In favorable cases, these singularities are determined by a small set of data of defect and bulk operators. Specifically, we derive a new dispersion relation which computes the four-point function of defect operators in 1d CFTs (i.e. line defects) as an integral over its double discontinuity. Additionally, we construct two distinct dispersion relations for two-point functions of bulk operators in presence of a defect. The first one expresses the correlator as an integral over a single discontinuity governed by the bulk channel Operator Product Expansion (OPE). The second relation reconstructs the correlator from a double discontinuity controlled by the defect channel OPE. We also derive a different dispersion relation for the special case of codimension-one defects. In the last part of the thesis, we analyze the $O(N)$ model in presence of line defects, which correspond to magnetic impurities in condensed matter systems. In particular, using a dispersion relation, we compute the two-point function of the fundamental field at the first non-trivial order in the ε -expansion. From this result, we are able to extract an infinite set of new defect CFT data. Finally, we compute holographic correlators in presence of the supersymmetric Wilson line in $\mathcal{N} = 4$ Super Yang-Mills. Using the dispersion relation, we compute the four-point function of defect operators up to fourth order in the large t'Hooft coupling expansion. Our derivation validates the results previously obtained using an Ansatz. Similarly, we streamline the computation of two-point functions of half-BPS single trace bulk operators, thanks to the efficiency of the dispersion relation.

Contents

1	Introduction	9
1.1	Main results and structure of the thesis	11
2	A review of conformal field theory	15
2.1	The conformal algebra and its representations	15
2.2	Correlation functions and the OPE	17
2.3	The conformal bootstrap	20
2.3.1	Conformal block expansions and the crossing equation	20
2.3.2	The analytic bootstrap and the Lorentzian inversion formula	21
2.4	A special case: one-dimensional CFT	24
2.4.1	The Lorentzian inversion formulas in 1d CFTs	26
2.4.2	Regge-limit behaviour and the improved inversion formula	28
2.5	Conformal defects	30
2.5.1	The defect conformal bootstrap	32
2.5.2	Boundaries and interfaces	36
3	Dispersion relations for defect CFTs	38
3.1	Dispersion relation for the four-point function in a 1d CFT	39
3.1.1	Derivation of the dispersion relation	41
3.2	Dispersion relation for bulk two-point functions	44
3.2.1	Dispersion relation from defect inversion formula	46
3.2.2	Alternative derivation using Cauchy's theorem	48
3.2.3	A dispersion relation with the double discontinuity	50
3.2.4	The special case of boundary CFTs	52
4	Applications	55
4.1	The localized magnetic field in the $O(N)$ model	57
4.1.1	The observable: the bulk two-point function	58
4.1.2	Leading order	60
4.1.3	Next-to-leading order	63
4.1.4	Defect channel data	67

4.1.5	Bulk channel data	70
4.1.6	Diagrammatic check	74
4.2	The spin impurity in the $O(3)$ model	76
4.2.1	Defect β -function	77
4.2.2	Discrete symmetries	86
4.2.3	The defect spectrum	87
4.2.4	Analytic bootstrap of the bulk two-point function	102
4.2.5	Diagrammatic computation	109
4.3	The boundary in the $O(N)$ model	114
4.3.1	Next-to-leading order correlator	116
4.3.2	NNLO correlator	117
4.4	The supersymmetric Wilson line in $\mathcal{N} = 4$ SYM	120
4.4.1	Toy model: scalar theory in AdS_2	121
4.4.2	Defect four-point function on the Wilson line in $\mathcal{N} = 4$ SYM	125
4.4.3	Bulk correlator in presence of the Wilson line in $\mathcal{N} = 4$ SYM	132
5	Conclusions	138
	Appendices	141
A	Polyakov blocks from the dispersion relation	141
B	Details on the supersymmetric Wilson line in $\mathcal{N} = 4$ SYM	143
B.1	Superconformal block expansion for the defect four-point function	143
B.2	Defect correlators at two and three loop	146
B.3	Superconformal block expansion for the bulk two-point function	148
B.4	Bulk correlators for $P = 5$	149

List of Figures

3.1	Contour deformation leading to the dispersion relation.	49
3.2	Contour deformation for the boundary case.	53
4.1	One-, two-, and three-loop propagator diagrams.	78
4.2	Vertex diagrams up to three loops.	80

List of Tables

- 4.1 Defect twist-zero and twist-one primary operators with their quantum numbers and scaling dimensions. 101
- 4.2 Schematic perturbative definition of defect twist-zero and twist-one operators. 102

Acknowledgements

First and foremost, I want to thank my supervisor Valentina Forini for her guidance throughout my PhD journey. I am particularly grateful for her enthusiasm and unwavering encouragement.

I also extend my sincere thanks to Olalla Castro-Alvaredo for overseeing the final stages of my PhD.

The majority of the work presented in this thesis was done in collaboration with Lorenzo Bianchi. I am profoundly grateful to him for sharing his extensive knowledge, and for the opportunity to explore fascinating research topics together.

I would also like to express my sincerest gratitude to Aleix Gimenez-Grau and Elia de Sabbata for their invaluable collaboration.

I am thankful to Silvia Penati, who continued to support me after my master's degree, helping me to obtain first a PhD and then a postdoc position. I would also like to express my deep gratitude to Miguel Paulos for his support during the last round of applications and for giving me the opportunity to present my work to his group.

I am also thankful to Gabriel Bliard and Giulia Peveri for enriching discussions about physics and life.

I am grateful to City, University of London for funding my PhD through a SMCSE School Studentship. Over the last four years a significant part of my research has been conducted at Humboldt-Universität zu Berlin (Berlin, Germany), Institut des Hautes Études Scientifiques (Paris, France) and University of Turin (Turin, Italy), which I would like to warmly thank for the kind hospitality. I would like to specifically thank Humboldt-Universität for funding my research during the final eight months of my PhD. Additionally, I am grateful to the University of Turin for supporting my work with a Grant for Internationalization.

Finally, I want to thank my family and my friends for always being at my side. Their support is worth more than I can express. A special thanks goes to my friend Andrea, whose encouragement inspired me to chase my dreams and pursue a PhD.

To Chiara, the light of my life.

Chapter 1

Introduction

This thesis studies Conformal Field Theories (CFTs) that admit extended excitations, known as defects. CFTs are Quantum Field Theories (QFTs) that are invariant under the conformal group, which includes translations, rotations, dilatations, and special conformal transformations (transformations that map straight lines into circles). Conformal field theories are interesting due to their various applications, ranging from critical phenomena in condensed matter physics to string theory and the *AdS/CFT* correspondence.

In condensed matter physics, it is well-known that scale invariance arises when a system undergoes a second-order phase transition. This statement goes back to the experimental observation of critical opalescence near the critical point of CO_2 [1] which was interpreted as an indication of the diverging correlation length of the fluid density [2]. It was later proven that scale¹ invariance emerges at the critical point of the ferromagnetic phase transition in two-dimensional metals [5]. Therefore, second-order phase transitions are described by CFTs. A characteristic feature of critical phenomena is universality: the relevant parameters of completely different systems behave in the same way near the critical point. This means that, in order to describe a second-order phase transition, the microscopic details of a model are irrelevant and the behaviour of the system is determined only by general properties such as symmetries [6]. In other words, the same CFT can describe the behavior of different systems undergoing a second-order phase transition [7]. For example, the 3d Ising CFT describes both the liquid–vapor transition of water at the critical point and the ferromagnetic phase transition of uniaxial magnets. This connection to universality is one of the reasons why conformal field theory is such a fascinating and powerful tool.

Conformal field theories appear also in the context of high-energy physics. When quantum field theories are probed at different energy scales, their coupling constants change. For instance, the coupling of the strong interaction is small at high energies

¹Assuming unitarity, Poincaré invariance, a discrete spectrum and the existence of a scale current, scale invariance implies conformal invariance in dimension $d > 2$ [3, 4].

[8] but increases at low energies, leading to phenomena such as confinement. This evolution of the coupling constants as a function of energy or length scale is interpreted as a Renormalization Group (RG) flow [9–11] from a microscopic theory at very short distances or high energies (UV) to a theory defined at long distances (IR), which arises as one integrates out the degrees of freedom of the UV theory. The renormalization group explains the phenomenon of universality: different high-energy QFTs can give rise to the same low-energy physics. Scale invariant theories are fixed points of the RG flow. Therefore, studying CFTs allows us to identify the endpoints of RG flows and shed light on the space of QFTs.

Finally, conformal field theory has applications to string theory and holography. Indeed, the sigma model that describes the worldsheet of a string must be a two-dimensional CFT to ensure consistency of the string theory. Moreover, the *AdS/CFT* correspondence [12–14] states that string theory in Anti-de Sitter (*AdS*) spacetime is dual to a CFT defined on the boundary of *AdS*. In other words, this correspondence provides a non-perturbative definition of quantum gravity in *AdS* in terms of a CFT.

Many of the CFTs that are relevant for physical applications are strongly coupled. To study theories like the Ising model in three dimensions, various alternative expansion methods can be used. One approach is the ε -expansion [15], where we study the CFT in $d = 4 - \varepsilon$ dimension, with ε being small. Specifically, we set up a perturbative expansion around $\varepsilon = 0$ and extrapolate the results to $\varepsilon = 1$ [16, 17]. In the case of CFTs with internal symmetries, such as the $O(N)$ model, we can also perform a large N expansion [18]. In order to go beyond perturbation theory, we can perform numerical Monte Carlo simulations [19]. All these methods depend on having an explicit microscopic model to compute the observables of the CFT. An alternative approach is to focus on the general properties of CFTs and derive results based on consistency conditions. This is the crucial idea of the conformal bootstrap [20–23], which combines conformal invariance with the existence of a convergent and associative Operator Product Expansion (OPE) [24] to obtain constraints on CFT observables. This approach allows the precise determination of CFT data and, in certain cases, the exact solution of the theory. The conformal bootstrap program was initially implemented for two-dimensional CFTs [22] but has since been extended to higher dimensions [23]. A crucial breakthrough in this area was the development of a numerical method, based on linear programming, to compute scaling dimensions and OPE coefficients from the conformal bootstrap equations. This method has led to remarkable non-perturbative results for the CFT data of many strongly-coupled theories, such as² the 3d Ising model [27–29]. Alongside these numerical developments, a range of important analytic tools have been introduced [30–33]. These tools have proven extremely useful, particularly when the theory allows for a perturbative expansion in some small parameter.

²See [25, 26] and references therein for more numerical bootstrap results.

The spectrum of a CFT includes both local and non-local operators. The latter are often called *defects*. The expectation values of certain defects, such as Wilson and 't Hooft lines, are useful for diagnosing phases of theories [34, 35]. In condensed matter physics, defects like boundaries and interfaces naturally appear as consequence of the finite size of physical systems, while line defects extended in the time direction represent point-like impurities [36]. Additionally, topological defects correspond to symmetry generators [37]. In the context of CFTs, we usually consider conformal defects, which preserve part of the conformal symmetry of the bulk CFT [38]. Motivated by the success of the conformal bootstrap for homogeneous CFTs, it is natural to explore a similar approach for theories with conformal defects. In recent years, numerous new results for defect CFTs have emerged from both numerical [39–43] and analytic bootstrap [44–55] studies.

1.1 Main results and structure of the thesis

The aim of this thesis is to develop new tools for the analytic bootstrap of defect CFTs and to apply them to defects that are relevant in the context of condensed matter physics or holography. This work is structured as follows.

In Chapter 2, we review fundamental aspects of conformal field theory essential for understanding the main results of this thesis. The results discussed in this chapter are well-known in the literature. We begin by examining generic CFTs without defects. We present the conformal algebra and its implications for correlation functions. Next, we introduce the Operator Product Expansion, which allows to expand the product of two operators in correlation functions as a sum over primary operators. Then, we discuss the crossing equation and the conformal bootstrap program, with a particular focus on the analytic methods, specifically the Lorentzian inversion formula. This is an integral formula that can be used to extract conformal data from singularities of the four-point function in Lorentzian signature. In view of applications to line defects, we dedicate a section to one-dimensional CFTs, highlighting the main differences from the higher-dimensional case. In particular, we focus on the special features of the one-dimensional Lorentzian inversion formula. Towards the end of the chapter, we introduce conformal defects and we explain how correlation functions of local operators are modified in presence of a defect. We consider correlators of both defect and bulk operators. For the latter case, we introduce the bulk-defect (or simply defect) and bulk-bulk (bulk) OPE expansions and outline the concept of the defect analytic bootstrap. We discuss two distinct Lorentzian inversion formulas: the defect inversion formula, which extracts the CFT data of operators exchanged in the defect OPE channel from a single discontinuity controlled by the bulk OPE channel, and the bulk inversion formula, which extracts data in the bulk channel from a double discontinuity controlled by the defect spectrum.

Finally, we discuss the special case of boundaries and interfaces.

After this review, we present the main results of the thesis. In Chapter 3, we present new dispersion relations for correlators in defect CFTs. A dispersion relation is an integral formula that allows the reconstruction of a function from one or more of its discontinuities. We obtain novel dispersion relations for four-point functions in one-dimensional CFTs (i.e. line defects) and for two-point functions of bulk operators in the presence of a generic defect. Specifically, we derive the one-dimensional dispersion relation directly from the corresponding Lorentzian inversion formula. The input of the formula is the double discontinuity of the four-point function. We explicitly work out the integration kernel for correlators of identical operators with integer or half-integer dimensions. We also introduce two distinct dispersion relations to reconstruct two-point functions of bulk operators in the presence of a defect, up to low-spin ambiguities. The first formula involves a single discontinuity and we derive it using either a contour deformation argument, combined with the symmetries and the analytic structure of the correlator, or by re-summing the result of the defect Lorentzian inversion formula. The discontinuity is controlled by the bulk OPE, making this formula particularly suitable for theories where the bulk is well-understood. The second dispersion relation depends on a double discontinuity controlled by the defect channel. The derivation in this case is more complex, but for certain defect dimensions, we can relate the problem to the case without a defect. Finally, we present a dispersion relation for the special case of boundaries and interfaces. Here, it is not possible to find a relation controlled solely by either the bulk or the defect OPE. Instead, the dispersion relation involves two distinct discontinuities, each controlled by one of the OPE channels. The presentation of Chapter 3 is based on [56] and [57].

In Chapter 4, we present several applications of the defect analytic bootstrap. We begin by considering defects in the critical $O(N)$ model in $d = 4 - \varepsilon < 4$ dimensions, where the fundamental excitation is the vector of scalar fields ϕ_a with $a = 1, \dots, N$. Using a dispersion relation, we compute the two-point function of ϕ_a (i.e. the magnetic susceptibility) in the presence of a defect obtained by coupling the field ϕ_1 to a magnetic field localized on a line. In Lorentzian signature, this defect corresponds to a magnetic field localized at a point in space. Following [58], we determine the two-point function, at first order in ε -expansion and at the Wilson-Fisher critical point. The discontinuity of the correlator is governed by a single bulk conformal block, associated with the lightest operator exchanged in the bulk OPE channel, and is proportional to the anomalous dimension of this operator. Given that the anomalous dimensions of bulk operators are known from the analysis of the bulk theory without defects, we can reconstruct the non-trivial part of the order- ε correlator using only a single piece of known bulk CFT data. This is a universal feature of defects in the $O(N)$ critical model in ε -expansion. However, differences among defects may arise from low-spin ambiguities.

For the case of the localized magnetic field, we argue that the ambiguity corresponds to the contribution of the squared one-point function of the fundamental field ϕ_a . From the result for the two-point function, we can extract an infinite amount of new CFT data, including defect anomalous dimensions, bulk-to-defect couplings and bulk one-point functions.

Next, we consider a line defect corresponding to a spin impurity, following the analysis of [59]. In Lorentzian signature, this setup models a doped two-dimensional anti-ferromagnet at the quantum critical point. Among the various realizations of the spin impurity, we choose to work with a path-ordered exponential, which preserves the full global symmetry algebra only for $N = 3$. Thus, we focus on this case. We start by examining a free bulk theory and compute the beta function for the defect coupling up to three loops. We then analyze several important operators in the defect spectrum, particularly their explicit realization in the path-ordered exponential framework. Finally, we calculate the bulk two-point functions of ϕ_a using analytic bootstrap methods, in the case of a free or interacting bulk. For the free bulk case, the form of the correlator is completely fixed at all orders in ε , up to a single unknown (ε -dependent) constant which is essentially the one-point function of ϕ^2 . Evaluating this correlator at $\varepsilon = 1$ and assuming that the one-point function is non-zero, we obtain a correlator that cannot satisfy the defect bootstrap equations, leading to the inevitable conclusion that the defect CFT is trivial in this scenario. For the interacting bulk case, we compute the correlator up to order ε^2 . This computation is very similar to that for the localized magnetic field, the main difference being an extra contribution due to low-spin ambiguities. From the explicit form of the correlator, we extract an infinite amount of new CFT data. We also confirm and extend our results by diagrammatic computations.

As a last example of a defect in the $O(N)$ model, we consider a conformal boundary. In this case, we demonstrate that previously obtained results for the order ε^2 two-point correlator can be efficiently reproduced by the boundary dispersion relation. This section is based on [56].

In the final section of this chapter, we examine the supersymmetric Wilson line in $\mathcal{N} = 4$ SYM, which is holographically dual to a string worldsheet in $AdS_5 \times S^5$ ending on the line at the boundary. We compute the four-point function of fundamental fields inserted on the line, corresponding to fluctuations of the worldsheet of the dual fundamental string. Using the dispersion relation, we reproduce results in the planar limit up to the fourth order in a strong 't Hooft coupling expansion, which were previously obtained using an Ansatz in terms of polylogarithms and rational functions. Our first-principles computation retrospectively justifies the Ansatz. Additionally, by taking advantage of the simplicity of the dispersion relation, we efficiently reproduce known results for the bulk two-point function of 1/2 BPS operators at strong coupling. Previously, these correlators were derived using the Lorentzian inversion formula to extract

defect CFT data and then resumming the OPE expansion. We obtain the correlators directly, bypassing the technically challenging intermediate steps. This section is based on [56] and [57].

In Chapter 5, we summarize our results and discuss potential future research directions.

Chapter 2

A review of conformal field theory

In this chapter, we review the fundamental principles of conformal field theory. We begin by considering CFTs without defects. We introduce conformal transformations and their algebra, examining their implications for correlation functions. We also discuss the Operator Product Expansion and the crossing equation, which lay at the heart of the conformal bootstrap program. Furthermore, we provide a brief overview of the analytic methods used in the conformal bootstrap. Towards the end of the chapter, we introduce conformal defects, which will be the central focus of the subsequent chapters. This chapter is a short review of known results, we refer to the excellent reviews [25, 60–63] for a more comprehensive treatment.

2.1 The conformal algebra and its representations

A conformal transformation is a change of coordinates that preserves the metric up to a spacetime dependent scale factor

$$dx'^2 = \Omega^2(x)dx^2, \quad dx^2 = \eta_{\mu\nu}dx^\mu dx^\nu, \quad (2.1.1)$$

where $\eta_{\mu\nu}$ is the flat metric in Euclidean or Minkowski space. In what follows we will mostly focus on the Euclidean case. In order to see explicitly the form of such transformations, one considers an infinitesimal transformation $x'_\mu = x_\mu + \epsilon_\mu(x)$ with $\Omega(x) = 1 + \sigma(x)$ and expands the definition (2.1.1) at first order in ϵ and σ . One obtains the constraint

$$\partial_\mu \epsilon_\nu + \partial_\nu \epsilon_\mu = 2\sigma \delta_{\mu\nu}. \quad (2.1.2)$$

This is the so called *conformal Killing equation*. Its general solution reads ¹

$$\epsilon_\mu(x) = \underbrace{a_\mu}_{\text{translation}} + \underbrace{\omega_{\mu\nu}x^\nu}_{\text{rotation}} + \underbrace{\lambda x_\mu}_{\text{dilatation}} + \underbrace{b_\mu x^2 - 2x_\mu b_\nu x^\nu}_{\text{special conformal}}, \quad (2.1.3)$$

¹See for example [63] for more details about the solution of the conformal Killing equation.

where $\omega_{\mu\nu} = -\omega_{\nu\mu}$. In other words, the generic conformal transformation is a combination of translations, rotations, dilatations and special conformal transformations.

Given a conformal Killing vector $\epsilon = \epsilon^\mu \partial_\mu$, one can define the associated generator Q_ϵ . The commutation relations of the conformal generators can then be obtained from those of the Killing vectors as

$$[Q_{\epsilon_1}, Q_{\epsilon_2}] = Q_{-[\epsilon_1, \epsilon_2]}. \quad (2.1.4)$$

If we associate the generators $\{P_\mu, M_{\mu\nu}, D, K_\mu\}$ to the conformal Killing vectors with parameters $\{a_\mu, \omega_{\mu\nu}, \lambda, b_\mu\}$, we obtain

$$\begin{aligned} [M_{\mu\nu}, P_\rho] &= \delta_{\nu\rho} P_\mu - \delta_{\mu\rho} P_\nu, \\ [M_{\mu\nu}, K_\rho] &= \delta_{\nu\rho} K_\mu - \delta_{\mu\rho} K_\nu, \\ [M_{\mu\nu}, M_{\rho\sigma}] &= \delta_{\nu\rho} M_{\mu\sigma} - \delta_{\mu\rho} M_{\nu\sigma} + \delta_{\nu\sigma} M_{\rho\mu} - \delta_{\mu\sigma} M_{\rho\nu}, \\ [D, P_\mu] &= P_\mu, \\ [D, K_\mu] &= -K_\mu, \\ [K_\mu, P_\nu] &= 2\delta_{\mu\nu} D - 2M_{\mu\nu}, \end{aligned} \quad (2.1.5)$$

and all other commutators vanish. This is the conformal algebra. If we rearrange the generators as

$$\begin{aligned} L_{\mu\nu} &= M_{\mu\nu}, \\ L_{-1,0} &= D, \\ L_{0,\mu} &= \frac{1}{2}(P_\mu + K_\mu), \\ L_{-1,\mu} &= \frac{1}{2}(P_\mu - K_\mu), \end{aligned} \quad (2.1.6)$$

where $L_{ab} = -L_{ba}$ and $a, b \in \{-1, 0, 1, \dots, d\}$, then

$$[L_{ab}, L_{cd}] = \eta_{bc} L_{ad} - \eta_{ac} L_{bd} + \eta_{bd} L_{ca} - \eta_{ad} L_{cb}, \quad (2.1.7)$$

where $\eta_{ab} = \text{diag}(1, 1, \dots, -1)$. The equation above implies that the d -dimensional Euclidean conformal algebra is isomorphic to the algebra of $SO(d+1, 1)$, which is the Lorentz group in $d+1$ dimensions ².

Operators in a CFT transform in the representations of the conformal algebra. Exploiting the equivalence with the Lorentz algebra, one can easily construct such representations, following the same strategy that one uses for the Poincare group. For a given operator \mathcal{O} , we assume

$$[M_{\mu\nu}, \mathcal{O}^a(0)] = (S_{\mu\nu})_b^a \mathcal{O}^b(0) \quad [D, \mathcal{O}^a(0)] = \Delta \mathcal{O}^a(0), \quad (2.1.8)$$

²The Lorentzian conformal algebra is instead isomorphic to the algebra of $SO(d, 2)$.

where $S_{\mu\nu}$ are matrices satisfying the same algebra as $M_{\mu\nu}$ and a and b are spin indices for the $SO(d)$ representation of \mathcal{O} . The eigenvalue under the action of the dilatation generator, Δ , is called the *scaling dimension* of the operator. Operators in a CFT are uniquely characterized by their dimension Δ and representation under $SO(d)$. From now on, we will often suppress the spin indices to avoid cluttering.

From the conformal algebra (2.1.5), one can see that P_μ and K_μ are respectively rising and lowering operators for scaling dimensions. In physically sensible theories, the scaling dimension is bounded from below³. Therefore, there must exist operators such that

$$[K_\mu, \mathcal{O}(0)] = 0. \quad (2.1.9)$$

These are called *primary* operators. Given a primary, we can construct operators of higher dimension, called *descendants*, by acting with P_μ . The resulting conformal multiplet forms an irreducible representation of the conformal group.

The construction above can be generalised to operators inserted at an arbitrary point in spacetime, using

$$\mathcal{O}(x) = e^{x^\mu P_\mu} \mathcal{O}(0) e^{-x^\nu P_\nu}. \quad (2.1.10)$$

The action of the conformal generators on an operator in this case reads

$$\begin{aligned} [P_\mu, \mathcal{O}(x)] &= \partial_\mu \mathcal{O}(x), \\ [M_{\mu\nu}, \mathcal{O}(x)] &= (x_\nu \partial_\mu - x_\mu \partial_\nu + S_{\mu\nu}) \mathcal{O}(x), \\ [D, \mathcal{O}(x)] &= (x^\mu \partial_\mu + \Delta) \mathcal{O}(x), \\ [K_\mu, \mathcal{O}(x)] &= (2x_\mu x^\nu \partial_\nu - x^2 \partial_\mu + 2\Delta x_\mu - 2x^\nu S_{\mu\nu}) \mathcal{O}(x). \end{aligned} \quad (2.1.11)$$

2.2 Correlation functions and the OPE

Now we can introduce the main observables in conformal field theories, namely correlation functions of local primary operators,

$$\langle \mathcal{O}_1(x_1) \dots \mathcal{O}_n(x_n) \rangle \equiv \langle 0 | \mathcal{O}_1(x_1) \dots \mathcal{O}_n(x_n) | 0 \rangle. \quad (2.2.1)$$

Here the vacuum state $|0\rangle$ is defined as the state that is annihilated by all the conformal generators. For a general n -point function, conformal invariance implies

$$\langle 0 | [L_{ab}, \mathcal{O}_1(x_1) \dots \mathcal{O}_n(x_n)] | 0 \rangle = \sum_{i=1}^n \mathcal{L}^{(i)} \langle \mathcal{O}_1(x_1) \dots \mathcal{O}_n(x_n) \rangle = 0, \quad (2.2.2)$$

where L_{ab} are the generators (2.1.6) and $\mathcal{L}^{(i)}$ are the corresponding differential operators acting on $\mathcal{O}(x)$, see (2.1.11).

³As we shall see in the next section, if we had an operator with $\Delta < 0$, then its two-point function would grow with distance, violating cluster decomposition [61]. Moreover, unitarity/reflection positivity implies $\Delta \geq 0$.

The first non-trivial⁴ correlator is the two-point function. For scalar operators, the Ward identity (2.2.2) implies

$$\langle \mathcal{O}_1(x_1) \mathcal{O}_2(x_2) \rangle = \frac{C \delta_{\Delta_1 \Delta_2}}{x_{12}^{2\Delta_1}}, \quad (2.2.3)$$

where $x_{12} = x_1^\mu - x_2^\mu$. In other words, the two-point function is completely fixed in terms of the scaling dimension of the operators (and possibly an overall normalization constant C). One can generalize (2.2.3) to the case of spinning operators. In the case of a spin ℓ symmetric traceless tensor one obtains

$$\langle J^{\mu_1 \dots \mu_\ell}(x) J_{\nu_1 \dots \nu_\ell}(0) \rangle = C_J \left(\frac{I^{(\mu_1 \nu_1}(x) \dots I^{\mu_\ell) \nu_\ell}(x)}{x^{2\Delta_J}} - \text{traces} \right), \quad (2.2.4)$$

where

$$I^\mu{}_\nu(x) \equiv \delta^\mu{}_\nu - 2 \frac{x^\mu x_\nu}{x^2}. \quad (2.2.5)$$

Moving on, three-point functions of scalar operators read

$$\langle \mathcal{O}_1(x_1) \mathcal{O}_2(x_2) \mathcal{O}_3(x_3) \rangle = \frac{\lambda_{123}}{x_{12}^{\Delta_1 + \Delta_2 - \Delta_3} x_{23}^{\Delta_2 + \Delta_3 - \Delta_1} x_{31}^{\Delta_3 + \Delta_1 - \Delta_2}}, \quad (2.2.6)$$

whereas the three-point correlator of two scalars and a symmetric traceless tensors is given by

$$\begin{aligned} \langle \mathcal{O}_1(x_1) \mathcal{O}_2(x_2) J^{\mu_1 \dots \mu_\ell}(x_3) \rangle &= \frac{\lambda_{\mathcal{O}_1 \mathcal{O}_2 J} (Z^{\mu_1} \dots Z^{\mu_\ell} - \text{traces})}{x_{12}^{\Delta_1 + \Delta_2 - \Delta_J + \ell} x_{23}^{\Delta_2 + \Delta_J - \Delta_1 - \ell} x_{31}^{\Delta_J + \Delta_1 - \Delta_2 - \ell}}, \\ Z^\mu &\equiv \frac{x_{13}^\mu}{x_{13}^2} - \frac{x_{23}^\mu}{x_{23}^2}. \end{aligned} \quad (2.2.7)$$

The coefficients λ_{ijk} are called three-point couplings or *OPE coefficients*. The reason for this name will soon become clear.

The next correlator is the four-point function. In this case, conformal invariance (2.2.2) cannot fix the kinematic dependence completely and one obtains, for identical scalars⁵ ϕ ,

$$\langle \phi(x_1) \phi(x_2) \phi(x_3) \phi(x_4) \rangle = \frac{\mathcal{G}(z, \bar{z})}{x_{12}^{2\Delta_\phi} x_{34}^{2\Delta_\phi}}. \quad (2.2.8)$$

Here $\mathcal{G}(z, \bar{z})$ is an arbitrary function of z and \bar{z} , which are two (complex conjugate) conformal cross-ratios, satisfying

$$z\bar{z} = \frac{x_{12}^2 x_{34}^2}{x_{13}^2 x_{24}^2}, \quad (1-z)(1-\bar{z}) = \frac{x_{23}^2 x_{14}^2}{x_{13}^2 x_{24}^2}. \quad (2.2.9)$$

We can understand the meaning of the two cross-ratios by performing the following transformations [61]:

⁴One-point functions vanish because of translation and dilatation invariance, except in the case of the identity operator $\langle \mathbb{1} \rangle = 1$.

⁵Similar expressions exist for non-identical operators. We will not need them in what follows.

1. Using special conformal transformations we move x_4 to infinity.
2. We move x_1 to the origin using translations.
3. Using rotations and dilatations we set x_3 to $(1, 0, 0, \dots, 0)$.
4. Using rotations that fix x_3 , we move x_2 to a plane, i.e. $(x, y, 0, 0, \dots, 0)$.

This procedure leaves exactly two undetermined coordinates (x, y) , which parametrize a plane. We can then introduce lightcone coordinates for the plane, namely $z = x + iy$ and $\bar{z} = x - iy$. These are precisely the cross-ratios (2.2.9) in this frame. Notice that, if we Wick rotate to Lorentzian signature, the cross-ratios become two independent real numbers $z = x + y$, $\bar{z} = x - y$.

One could of course go on and study higher point functions, using (2.2.2) to constrain the form of the correlators up to an arbitrary function of an increasing number of cross-ratios. However, it turns out that all higher-points correlators can be constructed from two- and three-point functions using the Operator Product Expansion (OPE).

In a CFT one can expand the product of two operators inside any correlation function as an infinite sum over primary operators, namely

$$\phi(x_1)\phi(x_2) = \sum_{\mathcal{O}} \lambda_{\phi\phi\mathcal{O}} C_a(x_{12}, \partial_2) \mathcal{O}^a(x_2). \quad (2.2.10)$$

Above, C_a is a differential operator that encodes the contribution of descendants ⁶, a is a $SO(d)$ index ⁷ as before and finally $\lambda_{\phi\phi\mathcal{O}}$ is the three-point coupling introduced in (2.2.6). We now see why it is also called OPE coefficient. Contrary to what happens in the case of a generic quantum field theory, the OPE in a CFT is convergent [64], provided that one can surround the two operators with a sphere without crossing any other operator.

Using the OPE, any n -point function can be expressed as a sum of lower point functions,

$$\langle \phi(x_1)\phi(x_2) \cdots \phi_n(x_n) \rangle = \sum_{\mathcal{O}} \lambda_{\phi\phi\mathcal{O}} C(x_{12}, \partial_2) \langle \mathcal{O}(x_2) \cdots \phi_n(x_n) \rangle. \quad (2.2.11)$$

Applying the above equation recursively, one can in principle obtain any correlator just from two- and three-point functions. For this reason, one often says that the spectrum of scaling dimensions and OPE coefficients, collectively referred to as *CFT data*, completely determines a CFT.

⁶The explicit form of this operator can be computed by applying the OPE inside a three-point function and comparing with (2.2.6).

⁷Indeed, the OPE of scalars may contain spinning operators. In particular, in the case of two identical scalar operators, the OPE contains symmetric traceless tensors with even spin ℓ .

2.3 The conformal bootstrap

We can finally introduce the conformal bootstrap method for the study of CFTs [23, 65, 25]. Roughly speaking, the crucial idea is to consider four-point functions and perform the OPE between pairs of operators in different orders. This results in different expansions of the same correlator in terms of the CFT data. By imposing consistency between them, one obtains a *crossing equation* that constrains the allowed CFT data. One can rephrase the previous statement in more sophisticated terms by saying that associativity of the OPE imposes constraints on the CFT data.

The crossing equation can be (approximately) solved numerically [23, 65], leading to astonishing non-perturbative results for the CFT data of many strongly-coupled theories, such as the 3d Ising model [27–29]. Alternatively, one can tackle the bootstrap problem analytically, either by taking special kinematic limits of the crossing equation [32, 33] or by using alternative techniques such as analytic functionals [66, 67], the Mellin transform [68–71] and the Lorentzian inversion formula [31]. The analytic approach is viable when the CFT admits a small parameter expansion. In the next sections we will introduce the crossing equation and review one of the most powerful tools for the analytic bootstrap: the Lorentzian inversion formula.

2.3.1 Conformal block expansions and the crossing equation

We start by considering a four-point function (2.2.8) and taking the OPE between the first and the last couples of operators, schematically (12)(34),

$$\begin{aligned}
 \langle \phi(x_1) \phi(x_2) \phi(x_3) \phi(x_4) \rangle &= \sum_{\mathcal{O}, \mathcal{O}'} \lambda_{\phi\phi\mathcal{O}} \lambda_{\phi\phi\mathcal{O}'} C_a(x_{12}, \partial_2) C_b(x_{34}, \partial_4) \langle \mathcal{O}^a(x_2) \mathcal{O}'^b(x_4) \rangle \\
 &= \sum_{\mathcal{O}} \lambda_{\phi\phi\mathcal{O}}^2 C_a(x_{12}, \partial_2) C_b(x_{34}, \partial_4) \frac{I^{ab}(x_{24})}{x_{24}^{2\Delta_{\mathcal{O}}}} \\
 &= \frac{1}{x_{12}^{2\Delta_{\phi}} x_{34}^{2\Delta_{\phi}}} \sum_{\mathcal{O}} \lambda_{\phi\phi\mathcal{O}}^2 G_{\Delta, \ell}(z, \bar{z}) .
 \end{aligned} \tag{2.3.1}$$

In the last line we introduced the *conformal block* $G_{\Delta, \ell}(z, \bar{z})$, defined as

$$G_{\Delta, \ell}(z, \bar{z}) \equiv x_{12}^{2\Delta_{\phi}} x_{34}^{2\Delta_{\phi}} C_a(x_{12}, \partial_2) C_b(x_{34}, \partial_4) \frac{I^{ab}(x_{24})}{x_{24}^{2\Delta}} . \tag{2.3.2}$$

It turns out that conformal blocks are also eigenfunctions of the quadratic Casimir operator of the conformal algebra (2.1.5) and can be computed explicitly [72–74] in

$d = 1$ ⁸ or in even dimensions,

$$G_{\Delta,\ell}^{d=1}(z, \bar{z}) \equiv G_{\Delta}(z) = z^{\Delta} {}_2F_1(\Delta, \Delta, 2\Delta, z) \quad (2.3.3)$$

$$G_{\Delta,\ell}^{d=2}(z, \bar{z}) = G_{\frac{\Delta+\ell}{2}}(z)G_{\frac{\Delta-\ell}{2}}(\bar{z}) + G_{\frac{\Delta-\ell}{2}}(z)G_{\frac{\Delta+\ell}{2}}(\bar{z}), \quad (2.3.4)$$

$$G_{\Delta,\ell}^{d=4}(z, \bar{z}) = \frac{z\bar{z}}{z - \bar{z}} \left(G_{\frac{\Delta+\ell}{2}}(z)G_{\frac{\Delta-\ell-2}{2}}(\bar{z}) - G_{\frac{\Delta-\ell-2}{2}}(z)G_{\frac{\Delta+\ell}{2}}(\bar{z}) \right). \quad (2.3.5)$$

Above, ${}_2F_1(\Delta, \Delta, 2\Delta, z)$ is a Gaussian hypergeometric function. In general dimension, conformal blocks admit representations in terms of infinite sums, but no closed form is known. A useful representation is

$$G_{\Delta,\ell}(z, \bar{z}) = \sum_{n=0}^{\infty} \sum_{q=-n}^n A_{n,q}(\Delta, \ell) z^{\frac{\Delta-\ell}{2}+n} G_{\frac{\Delta+\ell+2q}{2}}(\bar{z}). \quad (2.3.6)$$

where the coefficients $A_{n,m}$ can be fixed recursively using the Casimir equation [33].

In analogy with scattering amplitudes, the expansion (2.3.1) is called "s-channel" conformal block expansion. As we already mentioned, there is another possible way of performing the OPE, namely (14)(23). This is the so-called t-channel expansion⁹. Following the same steps as in equation (2.3.1), one obtains

$$\langle \phi(x_1) \phi(x_2) \phi(x_3) \phi(x_4) \rangle = \frac{1}{x_{12}^{2\Delta_{\phi}} x_{34}^{2\Delta_{\phi}}} \sum_{\mathcal{O}} \lambda_{\phi\phi\mathcal{O}}^2 \left(\frac{z\bar{z}}{(1-z)(1-\bar{z})} \right)^{\Delta_{\phi}} G_{\Delta,\ell}(1-z, 1-\bar{z}). \quad (2.3.7)$$

Imposing consistency between the two expansions (2.3.1) and (2.3.7) one obtains the crossing equation

$$\sum_{\mathcal{O}} \lambda_{\phi\phi\mathcal{O}}^2 G_{\Delta,\ell}(z, \bar{z}) = \left(\frac{z\bar{z}}{(1-z)(1-\bar{z})} \right)^{\Delta_{\phi}} \left[\sum_{\mathcal{O}} \lambda_{\phi\phi\mathcal{O}}^2 G_{\Delta,\ell}(1-z, 1-\bar{z}) \right], \quad (2.3.8)$$

This is an infinite-dimensional system of equations for the CFT data $\{\Delta, \ell, \lambda_{\phi\phi\mathcal{O}}\}$.

In the case of identical operators, the crossing equation can also be written as

$$\mathcal{G}(z, \bar{z}) = \left(\frac{z\bar{z}}{(1-z)(1-\bar{z})} \right)^{\Delta_{\phi}} \mathcal{G}(1-z, 1-\bar{z}). \quad (2.3.9)$$

2.3.2 The analytic bootstrap and the Lorentzian inversion formula

The interplay between the CFT data in the two channels of the crossing equation (2.3.8) can also be captured using the Lorentzian inversion formula of [31].

In order to derive this powerful tool, one has to introduce yet another expansion of the four-point function (2.2.8). One introduces conformal partial waves $\Psi_{\Delta,\ell}(z, \bar{z})$,

⁸Notice that in $d = 1$ the conformal blocks, and the four-point function, depend only on one cross-ratio. We refer to section 2.4 for more details on one-dimensional CFTs.

⁹In the case of a four-point function of non-identical operators, there is also a u-channel and a corresponding additional crossing equation.

which are single-valued eigenfunctions of the Casimir operator that can be written as a linear combination of conformal blocks

$$\Psi_{\Delta,\ell}(z, \bar{z}) = \kappa_{d-\Delta,\ell} G_{\Delta,\ell}(z, \bar{z}) + \kappa_{\Delta,\ell} G_{d-\Delta,\ell}(z, \bar{z}), \quad (2.3.10)$$

$$\kappa_{\Delta,\ell} = \left(-\frac{1}{2}\right)^\ell \frac{\pi^{\frac{d}{2}} \Gamma(\Delta - \frac{d}{2}) \Gamma(\Delta + \ell - 1) \Gamma(\frac{d-\Delta+\ell}{2})^2}{\Gamma(\Delta-1) \Gamma(d-\Delta+\ell) \Gamma(\frac{\Delta+\ell}{2})^2}. \quad (2.3.11)$$

Harmonic analysis on the conformal group [75] shows that a complete and orthogonal basis is formed by partial waves with (unphysical) complex dimensions $\Delta = \frac{d}{2} + i\alpha$ with $\alpha > 0$, referred to as the principal series representation. The orthogonality condition reads

$$\left(\Psi_{\frac{d}{2}+i\alpha,\ell}, \Psi_{\frac{d}{2}-i\beta,\ell'}\right) \equiv \int dz d\bar{z} \mu(z, \bar{z}) \Psi_{\frac{d}{2}+i\alpha,\ell}(z, \bar{z}) \Psi_{\frac{d}{2}-i\beta,\ell'}(z, \bar{z}) = 2\pi n_{\frac{d}{2}+i\alpha,\ell} \delta(\alpha - \beta) \delta_{\ell,\ell'} \quad (2.3.12)$$

where $\mu(z, \bar{z})$ is the $SO(d+1, 1)$ invariant measure

$$\mu(z, \bar{z}) = \frac{|z - \bar{z}|^{d-2}}{|z\bar{z}|^d}, \quad (2.3.13)$$

and

$$n_{\Delta,\ell} = \frac{\kappa_{d-\Delta,\ell} \kappa_{\Delta,\ell} \text{vol}(S^{d-2}) (2\ell + d - 2) \pi \Gamma(\ell + 1) \Gamma(\ell + d - 2)}{2^{d-2} \Gamma(\ell + \frac{d}{2})^2}. \quad (2.3.14)$$

The four-point function can then be decomposed as [76]

$$\mathcal{G}(z, \bar{z}) = \sum_{\ell=0}^{\infty} \int_{\frac{d}{2}-i\infty}^{\frac{d}{2}+i\infty} \frac{d\Delta}{2\pi} c(\Delta, \ell) \Psi_{\Delta,\ell}(z, \bar{z}). \quad (2.3.15)$$

The s-channel OPE decomposition (2.3.1) is recovered by closing the integration contour to the right, so that terms of the OPE come from the poles of the coefficient $c(\Delta, \ell)$, namely

$$c(\Delta, \ell) = - \sum_{\mathcal{O}} \frac{\lambda_{\phi\phi\mathcal{O}}^2}{\Delta - \Delta_{\mathcal{O}}}, \quad \mathcal{O} \in \text{s-channel OPE}. \quad (2.3.16)$$

In other words, the coefficient $c(\Delta, \ell)$ encodes the s-channel OPE data. This coefficient can be obtained using orthogonality to invert equation (2.3.15),

$$c(\Delta, \ell) = 2n_{\Delta,\ell} \int_{\mathbb{C}} dz d\bar{z} \mu(z, \bar{z}) \Psi_{\Delta,\ell}(z, \bar{z}) \mathcal{G}(z, \bar{z}). \quad (2.3.17)$$

This is the so called *Euclidean* inversion formula. Exploiting the analytic structure of the correlator, which is determined by the conformal block expansions, Caron-Huot [31] performed a contour deformation of the Euclidean inversion formula and obtained a *Lorentzian*¹⁰ inversion formula. In the case of identical scalars, it reads

$$c(\Delta, \ell) = \frac{(1 + (-1)^\ell) \Gamma(\frac{\Delta+\ell}{2})^4}{8\pi^2 \Gamma(\Delta + \ell - 1) \Gamma(\Delta + \ell)} \int_0^1 dz \int_0^1 d\bar{z} \mu(z, \bar{z}) G_{\ell+d-1, \Delta-d+1}(z, \bar{z}) \text{dDisc}[\mathcal{G}(z, \bar{z})]. \quad (2.3.18)$$

¹⁰Notice that now the integration runs over a Lorentzian region, with (z, \bar{z}) independent and real, see the discussion below (2.2.9).

The contour deformation requires dropping contributions from arcs at infinity, which are controlled by the so-called Regge limit of the correlator ¹¹. It turns out that one can prove a bound on the growth of the correlator in the Regge limit [31] from the convergence of the OPE expansion and positivity of $\lambda_{\phi\phi\mathcal{O}}^2$. The latter is a consequence of unitarity, which implies $\lambda_{\phi\phi\mathcal{O}} \in \mathbb{R}$. At the end of the day, one finds that the contributions at infinity can be safely ignored only for $\ell > 1$, therefore the formula may miss contributions to the CFT data of spin $\ell = 0, 1$ operators.

The input of the formula is the *double discontinuity* of the correlator, defined as

$$\text{dDisc}[\mathcal{G}(z, \bar{z})] = \mathcal{G}(z, \bar{z}) - \frac{1}{2}\mathcal{G}^\circlearrowleft(z, \bar{z}) - \frac{1}{2}\mathcal{G}^\circlearrowright(z, \bar{z}), \quad (2.3.19)$$

where $\mathcal{G}^\circlearrowleft(z, \bar{z})$ and $\mathcal{G}^\circlearrowright(z, \bar{z})$ are two analytic continuations of $\mathcal{G}(z, \bar{z})$ around the branch point at $\bar{z} = 1$ in the directions specified by the arrows.

The double discontinuity of a four-point function can be computed by expanding $\mathcal{G}(z, \bar{z})$ in the t-channel and applying the definition (2.3.19) to the conformal blocks. One obtains

$$\begin{aligned} \text{dDisc}[\mathcal{G}(z, \bar{z})] &= \text{dDisc} \left[\left(\frac{z\bar{z}}{(1-z)(1-\bar{z})} \right)^{\Delta_\phi} \left[\sum_{\mathcal{O}} \lambda_{\phi\phi\mathcal{O}}^2 G_{\Delta, \ell}(1-z, 1-\bar{z}) \right] \right] \\ &= \sum_{\mathcal{O}} \lambda_{\phi\phi\mathcal{O}}^2 \text{dDisc} \left[\left(\frac{z\bar{z}}{(1-z)(1-\bar{z})} \right)^{\Delta_\phi} G_{\Delta, \ell}(1-z, 1-\bar{z}) \right] \\ &= \sum_{\mathcal{O}} 2 \sin^2 \frac{\pi}{2} (\Delta - 2\Delta_\phi - \ell) \lambda_{\phi\phi\mathcal{O}}^2 \left(\frac{z\bar{z}}{(1-z)(1-\bar{z})} \right)^{\Delta_\phi} G_{\Delta, \ell}(1-z, 1-\bar{z}). \end{aligned} \quad (2.3.20)$$

In the last line, we used an explicit series representation of the conformal blocks (2.3.6) and

$$\text{dDisc}[(1-\bar{z})^\alpha] = 2 \sin^2(\pi\alpha)(1-\bar{z})^\alpha. \quad (2.3.21)$$

We stress that the inversion formula (2.3.18) extracts the CFT data in the s-channel OPE from the double discontinuity (2.3.20), which is controlled by the t-channel expansion ¹². This is a manifestation of crossing symmetry (2.3.8).

A natural domain of application of the inversion formula is perturbation theory around a (generalized) free theory. The spectrum of these theories consists of the identity and *double-twist operators* ¹³ with dimensions

$$\Delta = 2\Delta_\phi + 2n + \ell. \quad (2.3.22)$$

¹¹We refer to the original work [31] for a thorough discussion of the contour deformation and of the Regge limit.

¹²In the case of non-identical operators, the inversion formula contains an extra term which receives contributions from the u-channel OPE data, see [31].

¹³In the literature, they are also referred to as double-trace operators.

When a small perturbation ¹⁴ is turned on, the scaling dimensions of these operators receive perturbative corrections. Crucially, the contribution of (approximately) double-twist operators to the double discontinuity at any given order in perturbation theory depends entirely on lower order data. In other words, in this case, the double discontinuity is considerably simpler than the full correlator. Therefore, the inversion formula can be used to bootstrap the CFT data order by order in perturbation theory. This is a consequence of the fact that the double discontinuity (2.3.20) has double zeros at $\Delta = 2\Delta_\phi + 2n + \ell$. The inversion formula has been heavily exploited to analytically bootstrap various theories that admit a small parameter expansion, see for example [77–80].

Let us conclude this section by mentioning an important feature of the Lorentzian inversion formula (2.3.18), namely that it is analytic in spin. This property justifies a posteriori the convergence of large-spin expansions of the CFT data all the way down to spin $\ell = 2$ [32, 33, 81–83].

2.4 A special case: one-dimensional CFT

In this section we specialize to the case of one-dimensional CFTs, in view of applications to line defects. It is often said that 1d CFTs are trivial, since the conformal Killing equation (2.1.2) is identically satisfied for any smooth coordinate transformation [63]. Moreover, the traceless condition on the stress-energy tensor ¹⁵ implies that it vanishes, i.e. the Hamiltonian is trivial. However, one can relax the assumption of the existence of a conserved stress-tensor and study theories invariant under the one-dimensional conformal group $SO(2, 1) \cong SL(2, \mathbb{R})$. This is natural in the context of line defects, where one considers correlators of operators inserted on a line immersed in a higher-dimensional bulk CFT.

The one-dimensional conformal group has just three generators $\{P, D, K\}$ (2.1.5), and operators are labeled by their scaling dimension Δ . There is no spin in $d = 1$ and fermions are just anti-commuting scalars. Correlators of one-dimensional CFTs share many of the properties of their higher-dimensional cousins, in particular two- and three-point functions have the same form as in (2.2.3) and (2.2.6).

Four-point function of identical scalar operators ϕ with dimension Δ_ϕ have the structure

$$\langle \phi(\tau_1)\phi(\tau_2)\phi(\tau_3)\phi(\tau_4) \rangle = \frac{1}{(\tau_{12} \tau_{34})^{2\Delta_\phi}} \mathcal{G}(z), \quad (2.4.1)$$

¹⁴The small parameter can be the coupling of an interaction, but also $1/N$ in large N theories or ε in the ε -expansion.

¹⁵In generic CFT, the stress tensor is conserved, $\partial_\mu T^{\mu\nu} = 0$, and traceless, $T^\mu_\mu = 0$. One can prove that these conditions imply the conformal Killing equation (2.1.2), see [61] for a proof.

where τ is the coordinate on the line and z is the single invariant cross-ratio

$$z = \frac{\tau_{12} \tau_{34}}{\tau_{13} \tau_{24}}, \quad \tau_{ij} = \tau_i - \tau_j . \quad (2.4.2)$$

Comparing with the higher-dimensional case (2.2.8), one can see that restricting to a line corresponds to setting $z = \bar{z}$. This is the so-called diagonal limit. Given the ordering $\tau_1 < \tau_2 < \tau_3 < \tau_4$ on the line, conformal symmetry can be exploited to set $\tau_1 = 0$, $\tau_3 = 1$, $\tau_4 = \infty$, see the discussion below (2.2.9). This results in $\tau_2 = z$ falling in the interval $(0, 1)$. Changing the ordering of the points alters the range of z . Unlike the higher-dimensional case, correlators derived from (2.4.1) through the exchange $1 \leftrightarrow 2$ (placing z in the region $z < 0$) and $2 \leftrightarrow 3$ (corresponding to $z > 1$) are not related by analytic continuation. The correlator $\mathcal{G}(z)$ is given by three separate functions in the intervals $(-\infty, 0)$, $(0, 1)$ and $(1, \infty)$ [84, 85],

$$\mathcal{G}(z) = \begin{cases} \mathcal{G}^{(-)}(z) & \text{for } z \in (-\infty, 0) \\ \mathcal{G}^{(0)}(z) & \text{for } z \in (0, 1) \\ \mathcal{G}^{(+)}(z) & \text{for } z \in (1, \infty). \end{cases} \quad (2.4.3)$$

As discussed in details in [85], in the case of identical operators Bose (or Fermi) symmetry implies relations between the three functions above. In particular, $\mathcal{G}^{(0)}(z)$ is sufficient to determine the correlator on the whole real axis as

$$\begin{aligned} \mathcal{G}^{(-)}(z) &= \mathcal{G}^{(0)}\left(\frac{z}{z-1}\right), \\ \mathcal{G}^{(+)}(z) &= \pm z^{2\Delta_\phi} \mathcal{G}^{(0)}\left(\frac{1}{z}\right), \end{aligned} \quad (2.4.4)$$

where the plus sign is for bosons and the minus sign for fermions. The exchange $\tau_1 \leftrightarrow \tau_3$ (or equivalently, $\tau_2 \leftrightarrow \tau_4$) is the sole true symmetry of the correlator, as it consistently maps the interval $(0, 1)$ onto itself. This symmetry is none other than the crossing relation (2.3.9), which in this case reads

$$\mathcal{G}^{(0)}(z) = \frac{z^{2\Delta_\phi}}{(1-z)^{2\Delta_\phi}} \mathcal{G}^{(0)}(1-z) . \quad (2.4.5)$$

Just like in the higher-dimensional case (2.3.8), the four-point function (2.4.1) can be expanded using the OPE in two different channels

$$\mathcal{G}^{(0)}(z) = \sum_{\Delta} a_{\Delta} G_{\Delta}(z) = \frac{z^{2\Delta_\phi}}{(1-z)^{2\Delta_\phi}} \sum_{\Delta} a_{\Delta} G_{\Delta}(1-z), \quad (2.4.6)$$

where the sum runs over primary operators with scaling dimension Δ and we defined $a_{\Delta} = \lambda_{\phi\phi\mathcal{O}}^2$ for convenience. Above, $G_{\Delta}(z)$ are the one-dimensional conformal blocks defined in (2.3.3).

2.4.1 The Lorentzian inversion formulas in 1d CFTs

As in higher-dimension, one can introduce a conformal partial wave expansion (2.3.10). However, in this case the representation theory of $SL(2, \mathbb{R})$ [86] shows that, in order to have a complete and orthogonal basis, one needs *two* sets of partial waves: the principal series with complex dimensions $\Delta = \frac{1}{2} + i\alpha$ with $\alpha > 0$, and the discrete series with $\Delta = 2m$, $m \in \mathbb{N}$. The orthogonality relations for partial waves in the $d = 1$ case are ¹⁶

$$\begin{aligned} (\Psi_{\frac{1}{2}+i\alpha}(z), \Psi_{\frac{1}{2}+i\beta}(z)) &= 2\pi n_{\frac{1}{2}+i\alpha} \delta(\alpha - \beta), \quad \alpha, \beta \in \mathbb{R}^+ \\ (\Psi_{2m}(z), \Psi_{2n}(z)) &= \frac{4\pi^2}{4m-1} \delta_{mn}, \quad m, n \in \mathbb{N} \end{aligned} \quad (2.4.7)$$

with $(\Psi_{1/2+i\alpha}(z), \Psi_m(z)) = 0$ and $n_{\Delta, \ell}$ is defined in (2.3.14). The four-point function can be decomposed in partial waves as

$$\mathcal{G}(z) = \int_{\frac{1}{2}-i\infty}^{\frac{1}{2}+i\infty} \frac{d\Delta}{2\pi i} \frac{I_\Delta}{2\kappa_\Delta} G_\Delta(z) + \sum_{m=0}^{\infty} \frac{\Gamma^2(2m+2)}{2\pi^2 \Gamma(4m+3)} \tilde{I}_{2m+2} G_{2m+2}(z), \quad (2.4.8)$$

The s-channel OPE decomposition (2.4.6) is recovered by closing the principal series integration contour to the right. The contributions to the OPE expansion come from the poles of $c(\Delta) = I_\Delta/2\kappa_\Delta$ and from the discrete series. Notice that, in general, the coefficient of the discrete series \tilde{I}_m is different from $I_\Delta|_{\Delta=m}$. The coefficients I_Δ and \tilde{I}_m can be obtained using orthogonality to invert the conformal partial wave expansion (2.4.8), namely

$$I_\Delta = \int_{-\infty}^{\infty} dw w^{-2} \mathcal{G}(w) \Psi_\Delta(w), \quad \tilde{I}_m = \int_{-\infty}^{\infty} dw w^{-2} \mathcal{G}(w) \Psi_m(w). \quad (2.4.9)$$

However, in the case of identical operators, there are also two Lorentzian ¹⁷ inversion formulas that allow to reconstruct \tilde{I}_m [84] and I_Δ [85] from the double discontinuity of the four-point function,

$$I_\Delta = 2 \int_0^1 dw w^{-2} H_\Delta^{B/F}(w) \text{dDisc}[\mathcal{G}(w)], \quad (2.4.10)$$

$$\tilde{I}_m = \frac{4\Gamma^2(m)}{\Gamma(2m)} \int_0^1 dw w^{-2} G_m(w) \text{dDisc}[\mathcal{G}(w)]. \quad (2.4.11)$$

Notice that none of the two formulas can be obtained from a diagonal limit ($z = \bar{z}$) of the higher-dimensional expression (2.3.18).

¹⁶In what follows $\Psi_\Delta(z) \equiv \Psi_{\Delta,0}(z, \bar{z})|_{G_{\Delta,\ell}(z,\bar{z}) \rightarrow G_\Delta(z)}$ and $n_\Delta \equiv n_{\Delta,0}$, see (2.3.10) and (2.3.14).

¹⁷In $d = 1$ there is no distinction between Euclidean and Lorentzian signature, the name Lorentzian means only that the input of the formula is a double discontinuity, as in the original Lorentzian inversion formula (2.3.18).

The double discontinuity in the equations above is defined as

$$\text{dDisc}[\mathcal{G}(z)] = \mathcal{G}(z) - \frac{\mathcal{G}^\frown(z) + \mathcal{G}^\smile(z)}{2}, \quad (2.4.12)$$

where $\mathcal{G}^\frown(z)$ is the value of $\mathcal{G}(z)$ moving counterclockwise around the branch cut at $z = 1$ and viceversa for $\mathcal{G}^\smile(z)$. For identical operators, (2.4.3) implies

$$\mathcal{G}^\frown(z) = \mathcal{G}^{(+)}(z + i\epsilon), \quad \mathcal{G}^\smile(z) = \mathcal{G}^{(+)}(z - i\epsilon). \quad (2.4.13)$$

For a bosonic correlator, using the explicit form of the conformal blocks (2.3.3) and following the same steps as in (2.3.20), one obtains

$$\text{dDisc}[\mathcal{G}(z)] = \sum_{\Delta} 2 \sin^2 \frac{\pi}{2} (\Delta - 2\Delta_\phi) a_{\Delta} \frac{z^{2\Delta_\phi}}{(1-z)^{2\Delta_\phi}} G_{\Delta}(1-z), \quad (2.4.14)$$

whereas, in the case of fermions, one finds

$$\text{dDisc}[\mathcal{G}(z)] = \sum_{\Delta} 2 \cos^2 \frac{\pi}{2} (\Delta - 2\Delta_\phi) a_{\Delta} \frac{z^{2\Delta_\phi}}{(1-z)^{2\Delta_\phi}} G_{\Delta}(1-z). \quad (2.4.15)$$

The difference between the two cases is due to a different sign in $\mathcal{G}^{(+)}(z)$, see (2.4.4).

Notice that, as in the higher-dimensional case, the double discontinuity has double zeros at the dimensions of double-trace operators, namely $\Delta = 2\Delta_\phi + 2n$ in the bosonic case and $\Delta = 2\Delta_\phi + 2n + 1$ in the fermionic one.

In the case of identical bosons (B) or fermions (F), the inversion kernels $H_{\Delta}^{B/F}(w)$ in (2.4.10) can be determined requiring consistency between the Lorentzian inversion (2.4.10) and the Euclidean one (2.4.9), as discussed in [85]. It turns out that $H_{\Delta}^{B/F}(w)$ must be holomorphic functions in $w \notin (1, \infty)$ and satisfy the constraints $H_{\Delta}^{B/F}(w) = H_{\Delta}^{B/F}(w/(w-1))$ and

$$\begin{aligned} & z^{2\Delta_\phi-2} H_{\Delta}^{B/F}(z) + (1-z)^{2\Delta_\phi-2} H_{\Delta}^{B/F}(1-z) \pm \frac{H_{\Delta}^{B/F}\left(\frac{1}{z} + i\epsilon\right) + H_{\Delta}^{B/F}\left(\frac{1}{z} - i\epsilon\right)}{2} = \\ & = z^{2\Delta_\phi-2} \Psi_{\Delta}(z) + (1-z)^{2\Delta_\phi-2} \Psi_{\Delta}(1-z) \pm \frac{\Psi_{\Delta}\left(\frac{1}{z} + i\epsilon\right) + \Psi_{\Delta}\left(\frac{1}{z} - i\epsilon\right)}{2}. \end{aligned} \quad (2.4.16)$$

The explicit solution of such constraints is only known in the case of identical bosons (fermions) with integer (half-integer) conformal dimension [85], and reads

$$H_{\Delta}^{B/F}(w) = \pm \frac{2\pi}{\sin(\pi\Delta)} \left[w^{2-2\Delta_\phi} p_{\Delta}(w) + \left(\frac{w}{w-1}\right)^{2-2\Delta_\phi} p_{\Delta}\left(\frac{w}{w-1}\right) + q_{\Delta}^{\Delta_\phi}(w) \right] \quad (2.4.17)$$

$$p_{\Delta}(w) = {}_2F_1(\Delta, 1-\Delta, 1, w), \quad (2.4.18)$$

$$q_{\Delta}^{\Delta_\phi}(w) = a_{\Delta}^{\Delta_\phi}(w) + b_{\Delta}^{\Delta_\phi}(w) \log(1-w). \quad (2.4.19)$$

In (2.4.19), $a_{\Delta}^{\Delta\phi}(w)$ and $b_{\Delta}^{\Delta\phi}(w)$ are polynomials in Δ ¹⁸ and w ,

$$\begin{aligned} a_{\Delta}^{\Delta\phi}(w) &= \sum_{m=0}^{2\Delta_{\phi}-2} \sum_{n=0}^{2\Delta_{\phi}-4} \alpha_{m,n} w^{m+2-2\Delta_{\phi}} \Delta^n (\Delta-1)^n, \\ b_{\Delta}^{\Delta\phi}(w) &= \sum_{m=0}^{2\Delta_{\phi}-2} \sum_{n=0}^{2\Delta_{\phi}-4} \beta_{m,n} w^{m+2-2\Delta_{\phi}} \Delta^n (\Delta-1)^n. \end{aligned} \quad (2.4.20)$$

The coefficients $\alpha_{m,n}$ and $\beta_{m,n}$ above have to be fixed case-by-case in Δ_{ϕ} , by demanding that $H_{\Delta}^{B/F}(w)$ satisfies the constraint (2.4.16) and is holomorphic in $w = 0$. The first few examples read

$$\begin{aligned} a_{\Delta}^1(w) &= 0, & b_{\Delta}^1(w) &= 0, \\ a_{\Delta}^2(w) &= w^2 + 2w - 2, & b_{\Delta}^2(w) &= 0, \\ a_{\Delta}^{1/2}(w) &= 0, & b_{\Delta}^{1/2}(w) &= 0, \\ a_{\Delta}^{3/2}(w) &= (2\Delta^2 - 2\Delta - 1)w, & b_{\Delta}^{3/2}(w) &= 0. \end{aligned} \quad (2.4.21)$$

We stress that there is a crucial difference between the Lorentzian inversion formula in $d = 1$ and the original one (2.3.18). In higher dimensions the inversion kernel does not depend on the external dimensions Δ_{ϕ} and it is simply a conformal block, see (2.3.18). Here the kernel depends on the external dimensions. However, it turns out that the coefficient function I_{Δ} corresponding to a single t-channel conformal block of dimension Δ encapsulates the CFT data of the *crossing-symmetric* sum of exchange Witten diagrams in AdS_2 with the same dimension, the so-called Polyakov block $\mathcal{P}_{\Delta}^{\Delta\phi}(z)$ [85]. In this sense, the one-dimensional inversion formula is manifestly crossing symmetric.

2.4.2 Regge-limit behaviour and the improved inversion formula

In unitary CFTs, four-point functions are bounded in the Regge limit [87, 31]. In $d = 1$, the Regge bound reads

$$\left(\frac{1}{2} + it\right)^{-2\Delta_{\phi}} \mathcal{G}\left(\frac{1}{2} + it\right) < \infty \quad \text{for } t \rightarrow \infty. \quad (2.4.22)$$

The inversion formulas (2.4.10) and (2.4.11), with kernels (2.4.17), hold for any Regge-bounded fermionic four-point functions. In the bosonic case, the inversion formula (2.4.10) holds only for Regge super-bounded four-point functions, namely correlators that satisfy

$$\left(\frac{1}{2} + it\right)^{-2\Delta_{\phi}} \mathcal{G}\left(\frac{1}{2} + it\right) \sim t^{-1-\epsilon} \quad \text{for } t \rightarrow \infty, \quad (2.4.23)$$

¹⁸Notice that the definition of the conformal partial waves (2.3.10) and of the inversion formula (2.4.9) and (2.4.10) imply $H_{\Delta}^{B/F}(w) = H_{1-\Delta}^{B/F}(w)$. Therefore $a_{\Delta}^{\Delta\phi}(w)$ and $b_{\Delta}^{\Delta\phi}(w)$ are polynomials in $\Delta(\Delta-1)$.

with $\epsilon > 0$.

In general, one can relate the behaviour of the correlator in the Regge limit with the behaviour at $w = 0$ of the inversion kernel [85],

$$\left(\frac{1}{2} + it\right)^{-2\Delta_\phi} \mathcal{G}\left(\frac{1}{2} + it\right) \sim t^n \text{ for } t \rightarrow \infty \implies H_\Delta(w) \sim w^{2+2n} \text{ for } w \rightarrow 0. \quad (2.4.24)$$

From the explicit expressions (2.4.17), one can see that $H_\Delta^B(w) \sim w^0$ and $H_\Delta^F(w) \sim w^2$. To derive an inversion formula applicable to Regge-bounded bosonic correlators, it is necessary to enhance the behavior of the inversion kernel $H_\Delta^B(w)$ at $w = 0$. This can be achieved by subtracting any function that shares all the properties of $H_\Delta^B(w)$ except that it satisfies (2.4.16) with vanishing RHS. There are two natural choices for the subtraction, $\widehat{H}_{n,2}^B(w)$ and $\widehat{H}_{n,1}^B(w)$, which are defined by expanding $H_\Delta^B(w)$ at $\Delta = 2\Delta_\phi + 2n$,

$$\frac{H_\Delta^B(w)}{\kappa_\Delta} = \frac{\widehat{H}_{n,2}^B(w)}{(\Delta - 2\Delta_\phi - 2n)^2} + \frac{\widehat{H}_{n,1}^B(w)}{\Delta - 2\Delta_\phi - 2n} + O(1), \quad \Delta \rightarrow 2\Delta_\phi + 2n. \quad (2.4.25)$$

Using for instance $\widehat{H}_{0,2}^B(w)$, one obtains for bounded bosons [85]

$$H_\Delta^{\text{bd}}(w) \equiv H_\Delta^B(w) - \frac{\pi^2 2^{2(\Delta_\phi-1)} \Gamma(\Delta_\phi + \frac{1}{2}) \Gamma(\Delta_\phi - \frac{\Delta}{2})^2 \Gamma(\Delta_\phi - \frac{1-\Delta}{2})^2}{\Gamma(\Delta_\phi)^3 \Gamma(2\Delta_\phi - \frac{1}{2}) \Gamma(1 - \frac{\Delta}{2})^2 \Gamma(1 - \frac{1-\Delta}{2})^2} \frac{2\pi}{\sin(\pi\Delta)} \widehat{H}_{0,2}^B(w), \quad (2.4.26)$$

The coefficient in front of $\widehat{H}_{0,2}^B(w)$ is determined by requiring that $H_\Delta^{\text{bd}}(w) \sim w^2$ for $w \rightarrow 0$.

The function $\widehat{H}_{0,2}^B(w)$ has a pole in $w = 1$ for all Δ_ϕ , potentially spoiling the convergence of the inversion formula (2.4.10). Therefore, beyond the kernel redefinition in (2.4.26), it may be necessary to define a regularized correlator $\mathcal{G}^{\text{reg}}(z)$ by subtracting a crossing symmetric and Regge-bounded function from $\mathcal{G}(z)$, to eliminate the singularity in the integral. Generally, the regularized correlator is defined as

$$\mathcal{G}^{\text{reg}}(z) = \mathcal{G}(z) - \sum_{\Delta < 2\Delta_\phi} a_\Delta \mathcal{P}_\Delta^{\Delta_\phi}(z), \quad (2.4.27)$$

where $\mathcal{P}_\Delta^{\Delta_\phi}(z)$ are the Polyakov blocks¹⁹ we mentioned earlier, which are crossing symmetric and Regge-bounded functions with the same double discontinuity as the conformal blocks [85]. For example, in the bosonic case

$$\text{dDisc}[\mathcal{P}_\Delta^{\Delta_\phi}(z)] = 2 \sin^2 \frac{\pi}{2} (\Delta - 2\Delta_\phi) \frac{z^{2\Delta_\phi}}{(1-z)^{2\Delta_\phi}} G_\Delta(1-z). \quad (2.4.28)$$

¹⁹In Appendix A we briefly discuss the properties of Polyakov blocks and show some explicit examples. Specifically, we compute Polyakov blocks for integer and half-integer Δ_ϕ using a dispersion relation introduced in Section 3.1.1.

Therefore

$$\begin{aligned} \text{dDisc}[\mathcal{G}^{\text{reg}}(z)] &= \sum_{\Delta > 2\Delta_\phi} 2a_\Delta \sin^2 \frac{\pi}{2} (\Delta - 2\Delta_\phi) \frac{z^{2\Delta_\phi}}{(1-z)^{2\Delta_\phi}} G_\Delta(1-z) \\ &\sim (1-z)^\epsilon \quad \text{with } \epsilon > 0, \end{aligned} \quad (2.4.29)$$

ensuring that the integral in (2.4.10) converges. While the definition (2.4.27) of $\mathcal{G}^{\text{reg}}(z)$ is general, it is difficult to use because Polyakov blocks are complicated functions. In practical applications, it is often more convenient to use different, ad hoc subtractions. We shall see examples in Section 4.4.

In summary, the inversion formula for Regge-bounded bosonic correlators reads [85]

$$I_\Delta = \int_0^1 \frac{2dw}{w^2} H_\Delta^{\text{bd}}(w) \text{dDisc}[\mathcal{G}^{\text{reg}}(w)] + \lim_{\rho \rightarrow 0} \left[\int_{C_\rho^+} \frac{dw}{w^2} H_\Delta^{\text{bd}}(w) \mathcal{G}^{\text{reg}}(w) + \int_{C_\rho^-} \frac{dw}{w^2} H_\Delta^{\text{bd}}(w) \mathcal{G}^{\text{reg}}(w) \right] \quad (2.4.30)$$

where C_ρ^\pm are semicircular contours of radius ρ centered in $w = 1$, going above and below the real axis, introduced to avoid the pole of $\widehat{H}_{0,2}^B(w)$.

One can extend all the above results to the case of correlators *unbounded*²⁰ in the Regge limit. Given a specific asymptotic behaviour in the Regge limit, the corresponding inversion kernel is

$$H_\Delta^{\text{unbd}}(w) \equiv H_\Delta^B(w) - \sum_{m,n} A_{m,n} \widehat{H}_{m,2}^B(w) \frac{2\pi \Delta^n (\Delta-1)^n}{\sin(\pi\Delta)} - \sum_{m,n} B_{m,n} \widehat{H}_{m,1}^B(w) \frac{2\pi \Delta^n (\Delta-1)^n}{\sin(\pi\Delta)} \quad (2.4.31)$$

where the coefficients $A_{m,n}$ and $B_{m,n}$ are fixed by the imposing that $H_\Delta^{\text{unbd}}(w)$ vanishes at small w according to (2.4.24). The more severe the divergence in the Regge limit, the more terms will be needed in equation (2.4.31), resulting in increasingly strong singularities at $w = 1$ ²¹.

2.5 Conformal defects

In this last section we extend the previous discussion on the analytic bootstrap to the case of defect conformal field theory.

We consider flat defects of dimension p and codimension $q = d - p$ in d spacetime dimensions. We find convenient to separate the coordinates $x^\mu = (x^a, x^i)$ into coordinates parallel to the defect, with $a = 1, \dots, p$, and orthogonal, with $i = p + 1, \dots, d$.

Conformal defects are extended operators that preserve a subgroup of the full conformal symmetry of the bulk theory

$$SO(d+1, 1) \rightarrow SO(p+1, 1) \times SO(q). \quad (2.5.1)$$

²⁰The bound in the Regge limit is a non-perturbative feature of CFTs. However, this constraint can be violated at each order in perturbation theory, if the theory involves derivative interactions.

²¹The functions $\widehat{H}_{n,2}^B(w)$ have poles at $w = 1$, with order that increases as n increases, while $\widehat{H}_{n,1}^B(w)$ also exhibit logarithmic singularities.

In presence of a defect, there are two kinds of operators:

- Defect operators ²² $\hat{\mathcal{O}}$, which are inserted in the worldvolume of the defect and transform in the representations of the broken symmetry group. They are labeled by scaling dimensions $\hat{\Delta}$, parallel spin $\hat{\ell}$ and transverse ²³ spin s .
- Bulk operators \mathcal{O} , which are the operators inserted in the bulk (i.e. away from the defect). They are the same operators that exist in the CFT in absence of the defect and transform in the representations of $SO(d+1, 1)$. They are labeled by scaling dimensions Δ and spin ℓ .

In a defect CFT, correlation functions are defined as

$$\langle \mathcal{O}_1(x_1) \dots \hat{\mathcal{O}}_n(x_n) \rangle_{\mathcal{D}} \equiv \frac{\langle \mathcal{O}_1(x_1) \dots \hat{\mathcal{O}}_n(x_n) \mathcal{D} \rangle}{\langle \mathcal{D} \rangle}, \quad (2.5.2)$$

where \mathcal{D} is the non-local operator that represents the defect. Just like in the case without defects (2.2.2), the action of the generators of the unbroken conformal subgroup $SO(p+1, 1) \times SO(q)$ constrains correlation functions

$$\sum_{i=1}^n \hat{\mathcal{L}}^{(i)} \langle \mathcal{O}_1(x_1) \dots \mathcal{O}_n(x_n) \rangle_{\mathcal{D}} = 0 \quad (2.5.3)$$

Here $\hat{\mathcal{L}}^i$ are the differential operators associated to the unbroken generators, see (2.1.11). Correlators involving only defect operators have the same structure as in the case of a p -dimensional CFT without defects, for example

$$\begin{aligned} \langle \hat{\mathcal{O}}_1(x_1) \hat{\mathcal{O}}_2(x_2) \rangle_{\mathcal{D}} &= \frac{C \delta^{\hat{\Delta}_1 \hat{\Delta}_2}}{x_{12}^{2\hat{\Delta}_1}}, \\ \langle \hat{\mathcal{O}}_1(x_1) \hat{\mathcal{O}}_2(x_2) \hat{\mathcal{O}}_3(x_3) \rangle_{\mathcal{D}} &= \frac{\hat{\lambda}_{123}}{x_{12}^{\hat{\Delta}_1 + \hat{\Delta}_2 - \hat{\Delta}_3} x_{23}^{\hat{\Delta}_2 + \hat{\Delta}_3 - \hat{\Delta}_1} x_{31}^{\hat{\Delta}_3 + \hat{\Delta}_1 - \hat{\Delta}_2}}. \end{aligned} \quad (2.5.4)$$

On the other hand, correlators of bulk operators change dramatically. Since the defect breaks translation invariance in the directions orthogonal to the defect, bulk operators can acquire non-trivial one-point functions ²⁴ [38]

$$\langle \phi(x) \rangle_{\mathcal{D}} = \frac{a_\phi}{|x^i|^{\Delta_\phi}}. \quad (2.5.6)$$

²²In what follows, we will often indicate defect quantities with a hat.

²³Transverse spin is the quantum number associated to the group $SO(q)$ of rotations in directions orthogonal to the defect.

²⁴Here we consider the case of a scalar, but analogous expressions exist for spinning operators, see [38]. Schematically, they read

$$\langle J_{\mu_1 \dots \mu_\ell}(x) \rangle_{\mathcal{D}} = \frac{a_{\mathcal{O}}}{|x_i|^{\Delta_J}} I_{\mu_1 \dots \mu_\ell}(x_i), \quad (2.5.5)$$

For generic codimension q ²⁵, the two-point functions of bulk operators is no longer fixed as in (2.2.3), but instead depends on an arbitrary function of two cross-ratios [38]

$$\langle \phi(x_1)\phi(x_2) \rangle_{\mathcal{D}} = \frac{F(z, \bar{z})}{|x_1^i|^{\Delta_\phi} |x_2^i|^{\Delta_\phi}}, \quad (2.5.7)$$

with

$$\frac{1 + z\bar{z}}{\sqrt{z\bar{z}}} = \frac{|x_{12}^a|^2 + |x_1^i|^2 + |x_2^i|^2}{|x_1^i||x_2^i|}, \quad \frac{z + \bar{z}}{2\sqrt{z\bar{z}}} = \frac{x_1^i x_2^i}{|x_1^i||x_2^i|}. \quad (2.5.8)$$

The interpretation of the cross-ratios is similar to the one in the case of four-point functions in absence of a defect: they are complex conjugate coordinates that parametrize the plane orthogonal to the defect. In Lorentzian signature they are real and independent. It is clear from the definition of the cross-ratios that $F(z, \bar{z}) = F(\bar{z}, z)$. Sometimes we will find useful to switch to radial coordinates r and w , defined by

$$z = rw, \quad \bar{z} = \frac{r}{w}. \quad (2.5.9)$$

In Euclidean signature, w is the phase and r the modulus of the complex number z , whereas in the Lorentzian regime they are independent real numbers. In radial coordinates, one has that $F(r, w) = F(r, \frac{1}{w})$.

One can of course consider mixed correlators, involving both defect and bulk operators, such as [38]

$$\langle \phi(x_1)\hat{\mathcal{O}}(x_2) \rangle_{\mathcal{D}} = \frac{b_{\phi\hat{\mathcal{O}}}}{|x_1^i|^{\Delta_\phi - \hat{\Delta}} (|x_1^i|^2 + x_2^2)^{\hat{\Delta}}}. \quad (2.5.10)$$

The constants $b_{\phi\hat{\mathcal{O}}}$ are the so-called bulk-to-defect couplings. Using (2.5.3), one can constrain higher points functions, but we will not pursue this direction further.

2.5.1 The defect conformal bootstrap

Just like in the case without defects, associativity of the OPE inside correlators (2.5.2) can be used to impose constraints on the CFT data of bulk and defect operators. In a defect CFTs, one can consider three kinds of OPEs: the bulk-bulk, defect-defect and bulk-defect expansions. The bulk-bulk OPE is the one described in the previous sections in absence of defects, see (2.2.10). The defect-defect OPE is the analogue result for defect operators, namely it is the expansion of a product of two defect operators as a sum of defect primaries

$$\hat{\phi}(x_1)\hat{\phi}(x_2) = \sum_{\hat{\mathcal{O}}} \hat{\lambda}_{\hat{\phi}\hat{\phi}\hat{\mathcal{O}}} C(x_{12}, \partial_2) \hat{\mathcal{O}}(x_2). \quad (2.5.11)$$

Finally, the bulk-defect OPE is an expansion of a bulk operator as an infinite sum of defect operators

$$\phi(x) = \sum_{\hat{\mathcal{O}}} b_{\phi\hat{\mathcal{O}}} \hat{C}(x, \partial) \hat{\mathcal{O}}(x), \quad \text{for } x^i \rightarrow 0. \quad (2.5.12)$$

²⁵For $q = 1$ the structure of the two-point function is simpler, see Section 2.5.2.

Just like in the absence of defects, one can use different OPEs inside a correlator to obtain different expansions. By demanding consistency between them, one obtains a crossing equation that can be used to bootstrap the CFT data of the theory. In defect CFT, one can obtain a crossing equation from the four-point functions of defect operators, similar to what happens in (2.3.8), but also from the two-point functions of bulk operators. If one considers the four-point correlator of defect scalars $\langle \hat{\phi}\hat{\phi}\hat{\phi}\hat{\phi} \rangle$, the first crossing equation reads

$$\sum_{\hat{\mathcal{O}}} \hat{\lambda}_{\hat{\phi}\hat{\phi}\hat{\mathcal{O}}}^2 G_{\hat{\Delta},\hat{\ell}}(\hat{z},\hat{\bar{z}}) = \left(\frac{\hat{z}\hat{\bar{z}}}{(1-\hat{z})(1-\hat{\bar{z}})} \right)^{\Delta_{\phi}} \left[\sum_{\hat{\mathcal{O}}} \hat{\lambda}_{\hat{\phi}\hat{\phi}\hat{\mathcal{O}}}^2 G_{\hat{\Delta},\hat{\ell}}(1-\hat{z},1-\hat{\bar{z}}) \right], \quad (2.5.13)$$

where $G_{\hat{\Delta},\hat{\ell}}$ and $\hat{z},\hat{\bar{z}}$ are respectively p -dimensional conformal blocks (2.3.3) and cross-ratios(2.2.9). For the special case of a line defect, the crossing equation was given in (2.4.5).

One can also consider the two point function of bulk operators (2.5.7) and expand it in two ways:

1. Using the bulk-bulk OPE $\phi(x_1)\phi(x_2) = \sum_{\mathcal{O}} \lambda_{\phi\phi\mathcal{O}} C(x_{12},\partial_2)\mathcal{O}$ and then using the bulk-defect OPE (2.5.12) to expand \mathcal{O} .
2. Using the bulk-defect OPE (2.5.12) on the two ϕ first and then summing over the resulting defect two-point functions.

The consistency between these two OPE expansions imposes constraints on both the bulk and the defect CFT data. Following the same steps as in (2.3.1), one can translate the above OPEs into conformal block expansions and find a crossing equation ²⁶

$$F(z,\bar{z}) = \sum_{\mathcal{O}} \lambda_{\phi\phi\mathcal{O}} a_{\mathcal{O}} \left(\frac{\sqrt{z\bar{z}}}{(1-z)(1-\bar{z})} \right)^{\Delta_{\phi}} f_{\Delta,\ell}(z,\bar{z}) = \sum_{\hat{\mathcal{O}}} b_{\phi\hat{\mathcal{O}}}^2 \hat{f}_{\hat{\Delta},s}(z,\bar{z}), \quad (2.5.14)$$

where $a_{\mathcal{O}}$ are the one-point couplings (2.5.6) and $b_{\phi\hat{\mathcal{O}}}$ are the bulk-to-defect couplings (2.5.10). Notice that, compared to the four-point crossing (2.3.8), the equation above lacks positivity in the bulk channel, since $\lambda_{\phi\phi\mathcal{O}} a_{\mathcal{O}}$ can have arbitrary sign. In (2.5.14), $\hat{f}_{\hat{\Delta},s}(z,\bar{z})$ and $f_{\Delta,\ell}(z,\bar{z})$ are conformal blocks. With an abuse of notation, we will often refer to the former as *defect conformal blocks* and the latter as *bulk conformal blocks*. The explicit expression of the defect blocks can be obtained by solving a Casimir differential equation [38] and reads ²⁷

$$\hat{f}_{\hat{\Delta},s}(z,\bar{z}) = z^{\frac{\hat{\Delta}-s}{2}} \bar{z}^{\frac{\hat{\Delta}+s}{2}} {}_2F_1\left(-s, \frac{q}{2}-1, 2-\frac{q}{2}-s, \frac{z}{\bar{z}}\right) {}_2F_1\left(\hat{\Delta}, \frac{p}{2}, \hat{\Delta}+1-\frac{p}{2}, z\bar{z}\right). \quad (2.5.15)$$

²⁶For the special case of $q=1$ we refer to Section 2.5.2.

²⁷Since we consider the two-point function of bulk scalars, the operators exchanged in the defect OPE do not carry longitudinal spin $\hat{\ell}$. Correspondingly, the defect blocks depend only on the transverse spin s .

It terms of the radial coordinates introduced in (2.5.9), the blocks factorize

$$\hat{f}_{\hat{\Delta},s}(r, w) = \hat{f}_{\hat{\Delta}}(r) \hat{g}_s(w) \quad (2.5.16)$$

with

$$\hat{f}_{\hat{\Delta}}(r) = r^{\hat{\Delta}} {}_2F_1\left(\hat{\Delta}, \frac{p}{2}, \hat{\Delta} + 1 - \frac{p}{2}, r^2\right), \quad \hat{g}_s(w) = w^{-s} {}_2F_1\left(-s, \frac{q}{2} - 1, 2 - \frac{q}{2} - s, w^2\right)$$

The angular part, for integer s , is actually a Gegenbauer polynomial in the variable $\eta = \frac{1}{2}\left(w + \frac{1}{w}\right)$

$$\hat{g}_s(w) = \left(s + \frac{q}{2} - 2\right)^{-1} C_s^{q/2-1}(\eta) \quad (2.5.17)$$

The bulk conformal blocks are not known in closed form, similarly to what happens for conformal blocks in generic dimension d in a setup without defect, but can be expressed as a sum of Harish-Chandra functions [88]

$$f_{\Delta,\ell}(z, \bar{z}) = 2^{-\ell} f_{\Delta,\ell}^{HS}(z, \bar{z}) + \frac{\Gamma(\ell + d - 2)\Gamma(-\ell - \frac{d-2}{2})}{2^\ell \Gamma(\ell + \frac{d-2}{2})\Gamma(-\ell)} \frac{\Gamma(\frac{\ell+d-p-1}{2})\Gamma(\frac{1-\ell}{2})}{\Gamma(\frac{\ell+d-1}{2})\Gamma(\frac{1-\ell-p}{2})} f_{\Delta,2-d-\ell}^{HS}(z, \bar{z}), \quad (2.5.18)$$

where $f_{\Delta,\ell}^{HS}(z, \bar{z})$ can be expressed as a double infinite sum

$$\begin{aligned} f_{\Delta,\ell}^{HS}(z, \bar{z}) &= \sum_{m,n=0}^{\infty} [(1-z)(1-\bar{z})]^{\frac{\Delta-\ell}{2}+m+n} h_n(\Delta, \ell) h_m(1-\ell, 1-\Delta) \frac{4^{m-n}}{n!m!} \frac{(\frac{\Delta+\ell}{2})_{n-m}}{(\frac{\Delta+\ell}{2} - \frac{1}{2})_{n-m}} \\ &\times {}_4F_3\left(-n, -m, \frac{1}{2}, \frac{\Delta-\ell}{2} - \frac{d}{2} + 1; -\frac{\Delta+\ell}{2} + 1 - n, \frac{\Delta+\ell}{2} - m, \frac{\Delta-\ell}{2} - \frac{d}{2} + \frac{3}{2}; 1\right) \\ &(1-z\bar{z})^{\ell-2m} {}_2F_1\left(\frac{\Delta+\ell}{2} - m + n, \frac{\Delta+\ell}{2} - m + n, \Delta + \ell - 2(m-n), 1 - z\bar{z}\right), \end{aligned} \quad (2.5.19)$$

and

$$h_n(\Delta, \ell) = \frac{(\frac{\Delta}{2} - \frac{1}{2})_n (\frac{\Delta}{2} - \frac{p}{2})_n (\frac{\Delta+\ell}{2})_n}{(\Delta - \frac{d}{2} + 1)_n (\frac{\Delta+\ell}{2} + \frac{1}{2})_n}. \quad (2.5.20)$$

The crossing equations (2.5.13) and (2.5.14) are the foundation of the defect conformal bootstrap. As we saw before in the case of CFTs without defects, the crossing equation can be translated into a Lorentzian inversion formula. For the defect case, there are two analogous formulas that invert the two-point function of bulk operators.

The first formula is the so called defect inversion formula, and was derived in [44] from a contour deformation argument. It reads ²⁸

$$\begin{aligned} b(\hat{\Delta}, s) &= \int_0^1 \frac{dz}{2z} z^{-\frac{\hat{\Delta}}{2}} \int_1^{\frac{1}{z}} \frac{d\bar{z}}{2\pi i} (1-z\bar{z})(\bar{z}-z)\bar{z}^{-\frac{\hat{\Delta}+s}{2}-2} {}_2F_1\left(s+1, 2 - \frac{q}{2}, \frac{q}{2} + s, \frac{z}{\bar{z}}\right) \times \\ &\times {}_2F_1\left(1 - \hat{\Delta}, 1 - \frac{p}{2}, 1 + \frac{p}{2} - \hat{\Delta}, z\bar{z}\right) \text{Disc}[F(z, \bar{z})]. \end{aligned} \quad (2.5.21)$$

²⁸The formula is slightly different in the case of $q=2$ monodromy defects, see [54]. We will ignore this subtlety in what follows.

The coefficient function $b(\hat{\Delta}, s)$ has simple poles for $\hat{\Delta}$ equal to the dimensions of operators exchanged in the defect OPE and residues given by the couplings $b_{\Delta, s}^2$. The input of this inversion formula is the *single* discontinuity

$$\text{Disc}[F(z, \bar{z})] = F(z, \bar{z} + i\epsilon) - F(z, \bar{z} - i\epsilon), \quad (2.5.22)$$

where $F(z, \bar{z} + i\epsilon)$ and $F(z, \bar{z} - i\epsilon)$ indicate that \bar{z} should be taken above or below the branch cut at $\bar{z} = 1$, leaving z fixed. One can obviously express the inversion formula in radial coordinates (2.5.9). In that case, the discontinuity is computed with respect to a branch cut running from $w = 0$ to $w = r$,

$$\text{Disc}[F(r, w)] = F(r, w + i\epsilon) - F(r, w - i\epsilon). \quad (2.5.23)$$

The discontinuity can be computed by expanding the two-point function in bulk blocks (2.5.18), following a similar strategy as in (2.3.20). The end result is

$$\text{Disc}[F(z, \bar{z})] = \sum_{\mathcal{O}} -2i \sin\left[\frac{\pi}{2}(\Delta - 2\Delta_{\phi} - \ell)\right] a_{\mathcal{O}} \lambda_{\phi\phi\mathcal{O}} (z\bar{z})^{\frac{\Delta_{\phi}}{2}} [(1-z)(\bar{z}-1)]^{\Delta_{\phi} - \frac{\Delta - \ell}{2}} \tilde{f}_{\Delta, \ell}(z, \bar{z}), \quad (2.5.24)$$

where $\tilde{f}_{\Delta, \ell}(z, \bar{z}) = [(1-z)(1-\bar{z})]^{-\frac{\Delta - \ell}{2}} f_{\Delta, \ell}(z, \bar{z})$. Just like in the case without defects, the Lorentzian inversion formula allows to extract the CFT data in one channel (the defect one in this case) from a discontinuity controlled by the other channel (the bulk channel). Notice that the discontinuity has single zeros at the dimensions of double trace operators. This implies that it will be useful to study perturbative theories that contain operators with scaling dimensions close to the double-trace spectrum. In those cases, the discontinuity at any given order depends on lower order OPE data and on the anomalous dimensions of bulk operators at the order one is working at²⁹. We shall see explicit examples in Chapter 4.

The defect inversion formula is derived from a contour deformation argument in the w complex plane, assuming that $F(r, w)$ decays fast enough at large w ³⁰,

$$F(r, w) \sim w^{s^*}, \quad w \rightarrow \infty, \quad s^* < 0. \quad (2.5.25)$$

If instead $s^* \geq 0$, the inversion formula misses contributions to the CFT data of defect operators with low transverse spin $s \leq s^*$. This looks similar to what happens in the original inversion formula (2.3.18), however there is a big difference: in that case positivity of the OPE expansion can be used to prove the existence of a bound on the growth of the correlator and find $\ell^* = 1$. Since in the defect case we lack positivity, see below (2.5.14), we cannot derive a bound on s^* following the same strategy that worked in the case without defects [44]. However, in all known examples $s^* = 1$, suggesting the

²⁹Notice that the single discontinuity is less powerful than the double discontinuity, since the latter depends only on lower order data in perturbation theory.

³⁰One can rephrase (2.5.25) into a condition for the behaviour at small w , using $F(r, w) = F(r, \frac{1}{w})$.

existence of a bound also in this setup. It would be interesting to prove this conjecture, but we will not pursue this direction here.

Instead, we introduce the bulk inversion formula, which is very similar to the original Lorentzian inversion formula (2.3.18) and allows to extract the bulk OPE data from a double discontinuity in the defect channel. The formula reads [45]

$$c(\Delta, \ell) = \frac{(1+(-1)^\ell)\Gamma(\frac{\Delta+\ell}{2})^4}{4\pi^2\Gamma(\Delta+\ell)\Gamma(\Delta+\ell-1)} \int_0^1 d^2z \mu(z, \bar{z}) f_{\ell+d-1, \Delta-d+1}(z, \bar{z}) \text{dDisc} \left[\left(\frac{(1-z)(1-\bar{z})}{\sqrt{z\bar{z}}} \right)^{\Delta_\phi} F(z, \bar{z}) \right] \quad (2.5.26)$$

with

$$\mu(z, \bar{z}) = \frac{|z - \bar{z}|^{d-p-2} |1 - z\bar{z}|^p}{(1-z)^d (1-\bar{z})^d}, \quad (2.5.27)$$

and where $f_{\Delta, \ell}(z, \bar{z})$ are the bulk blocks. In this case, the coefficient function $c(\Delta, \ell)$ has poles corresponding to the dimensions of the operators that are exchanged in the bulk OPE and corresponding residues given by the product of bulk three-point functions and one-point functions, $\lambda_{\phi\phi\mathcal{O}} a_{\mathcal{O}}$. The input of the formula is the double discontinuity defined by

$$\text{dDisc}[F(z, \bar{z})] = F(z, \bar{z}) - \frac{1}{2} F^\circ(z, \bar{z}) - \frac{1}{2} F^\circ(z, \bar{z}), \quad (2.5.28)$$

where the functions $F^\circ(z, \bar{z})$ and $F^\circ(z, \bar{z})$ are obtained by taking the analytic continuation around the point $\bar{z} = 0$, leaving z fixed. Similar to the case of the original formula (2.3.18), the bulk inversion formula might fail for low spins ℓ . More precisely, the formula is valid for spins $\ell > \ell_*$ where ³¹

$$\left(\frac{(w-r)(1-wr)}{rw} \right)^{\Delta_\phi} F(r, w) \lesssim w^{1-\ell_*}, \quad w \rightarrow 0. \quad (2.5.29)$$

As we already mentioned below (2.5.25), there is no universal bound on the behaviour of $F(r, w)$ for large w , or equivalently for $w \rightarrow 0$. Therefore, ℓ_* has to be determined case-by-case.

2.5.2 Boundaries and interfaces

In the discussion above, we considered a defect with generic codimension q . In the special case of boundaries and interfaces, namely $q = 1$, the kinematics of bulk correlators simplifies [46, 89]. In particular, the two-point function of bulk operators reads ³²

$$\langle \phi(x_1) \phi(x_2) \rangle_{\mathcal{D}} = \frac{F(z)}{(4|x_1^i||x_2^i|)^{\Delta_\phi}}, \quad (2.5.30)$$

³¹Here we give a condition for the behaviour of $F(r, w)$ at small w . This is equivalent to a condition at large w , since $F(r, w) = F(r, \frac{1}{w})$.

³²Notice that the conventions used in the $q = 1$ case are slightly different compared to the case of general codimension.

where z is a single cross-ratio, defined as

$$\frac{1-z}{z} = \frac{|x_{12}^a|^2}{4x_1^i x_2^i}. \quad (2.5.31)$$

One can expand the two-point function (2.5.30) in the defect (or boundary) channel

$$F(z) = \sum_{\hat{\mathcal{O}}} b_{\phi\hat{\mathcal{O}}}^2 \hat{f}_{\hat{\Delta}}(z), \quad (2.5.32)$$

or in the bulk channel,

$$F(z) = \left(\frac{z}{1-z}\right)^{\Delta_\phi} \sum_{\mathcal{O}} a_{\mathcal{O}} \lambda_{\phi\phi\mathcal{O}} f_{\Delta}(z), \quad (2.5.33)$$

where the conformal blocks are given by ³³

$$\hat{f}_{\hat{\Delta}}(z) = z^{\hat{\Delta}} {}_2F_1\left(\hat{\Delta}, \hat{\Delta} + 1 - \frac{d}{2}, 2\hat{\Delta} + 2 - d, z\right), \quad (2.5.34)$$

and

$$f_{\Delta}(z) = (1-z)^{\frac{\Delta}{2}} {}_2F_1\left(\frac{\Delta}{2}, \frac{\Delta}{2} + 1 - \frac{d}{2}, \Delta + 1 - \frac{d}{2}, 1-z\right). \quad (2.5.35)$$

Notice that, contrary to what happens for generic codimension (2.5.18), the bulk blocks here have a simple expression.

Imposing consistency between the two OPE expansions, one finds a crossing equation

$$F(z) = \sum_{\hat{\mathcal{O}}} b_{\phi\hat{\mathcal{O}}}^2 \hat{f}_{\hat{\Delta}}(z) = \left(\frac{z}{1-z}\right)^{\Delta_\phi} \sum_{\mathcal{O}} a_{\mathcal{O}} \lambda_{\phi\phi\mathcal{O}} f_{\Delta}(z), \quad (2.5.36)$$

One can derive two Lorentzian inversion formulas for boundaries and interfaces. However, the structure of the Lorentzian inversion formulas is very different compared to the generic case, see (2.5.21) and (2.5.26). In the $q = 1$ case, the two formulas receive a contribution from both the single discontinuity, which is controlled by the bulk OPE, and the double discontinuity, controlled by the boundary OPE. For identical operators, the two formulas read [48]

$$\begin{aligned} \hat{I}_{\hat{\Delta}} &= 2 \int_0^1 dz (1-z)^{\frac{2\Delta_{\hat{\phi}}-3}{2}} \hat{H}_{\hat{\Delta}}(z) \text{dDisc}[F(z)] - i \int_1^\infty dz (z-1)^{-\frac{1}{2}} \hat{H}_{\hat{\Delta}}\left(\frac{z}{z-1}\right) \text{Disc}[F(z)] \\ I_{\Delta} &= 2 \int_0^1 dz (1-z)^{\frac{2\Delta_{\phi}-3}{2}} H_{\Delta}(z) \text{dDisc}[F(z)] - i \int_1^\infty dz (z-1)^{-\frac{1}{2}} H_{\Delta}\left(\frac{z}{z-1}\right) \text{Disc}[F(z)] \end{aligned}$$

The single and double discontinuity are taken with respect to $z = 1$ and $z = 0$, respectively. The inversion kernels $\hat{H}_{\hat{\Delta}}(z)$ and $H_{\Delta}(z)$ are not known in closed form, except in the case of a two-point function of operators with dimensions that differ by an odd integer, see [48].

³³Notice that there is no transverse spin s when $q = 1$.

Chapter 3

Dispersion relations for defect CFTs

In this chapter, we introduce new tools for the analytic bootstrap of defect CFTs, namely conformal dispersion relations. By dispersion relation we mean an integral formula that reconstructs a function from its discontinuity. Such a formula is typically derived, using a contour deformation argument, from the knowledge of the analytic structure and the behaviour at infinity of the function. Dispersion relations have a long history in theoretical physics, going back to the the work of Kramers and Kronig [90,91] in optics. These authors exploited the analyticity properties of the refractive index to find a relation between its real and imaginary parts, the latter being related to the absorption coefficient of the optical medium. In other words, the Kramers–Kronig relations allow one to calculate the refractive index of an optical material solely from its absorption coefficient. Before the advent of QCD, dispersion relations were also used to constrain the S-matrix [92], in an attempt of bootstrapping strong interactions. Dispersion relations are most useful in perturbative setups, where one can often compute the imaginary part without knowing the full function. For example, in the context of perturbative scattering amplitudes, the imaginary part of an amplitude at any given order can be efficiently computed in terms of lower-order amplitudes [93,94].

In the context of CFTs in dimension $d > 1$, a dispersion relation was first developed in [95], starting from the Lorentzian inversion formula (2.3.18), and reads

$$\mathcal{G}(z, \bar{z}) = \int_0^1 dw d\bar{w} K(z, \bar{z}, w, \bar{w}) \text{dDisc}[\mathcal{G}(w, \bar{w})], \quad (3.0.1)$$

where $\mathcal{G}(z, \bar{z})$ is the four-point function (2.2.8) and $K(z, \bar{z}, w, \bar{w})$ is a known kernel ¹. The input of the formula is the double discontinuity $\text{dDisc}[\mathcal{G}(z, \bar{z})]$, which we defined in (2.3.19). The double discontinuity is the analogue, in the CFT case, of the imaginary part of an amplitude. Just like the latter, it is positive definite and can be computed at any given order in perturbation theory from lower-order data, as we mentioned below (2.3.20).

¹See (3.2.32) below for the (cumbersome) explicit expression.

In Section 3.1, we derive the analogue of the dispersion relation (3.0.1) for four-point functions of one-dimensional CFTs (i.e. correlators on a line defect). The derivation is based on [57].

Next, in Section 3.2, we present two distinct dispersion relations for two-point functions of bulk operators in presence of a defect. The first relation expresses the correlator through an integral over a *single* discontinuity governed by the bulk channel OPE. We also introduce a second relation that reconstructs the correlator using a double discontinuity controlled by the defect channel OPE. Finally, we derive a dispersion relation for codimension-one defects (boundaries and interfaces), which incorporates contributions from both OPE channels. The exposition is based on [56].

3.1 Dispersion relation for the four-point function in a 1d CFT

In the case of one-dimensional correlators, a dispersion relation was constructed in [96] building on previous work on analytic functionals [66, 97, 98]. In [96], the application of a class of functionals to the crossing equation was shown to generate a family of dispersive sum rules², which can be rephrased as dispersion relations for the four-point function. The functional kernels can be computed numerically, for identical operators with generic scaling dimension. In the case of a four-point function of operators with integer or half-integer dimension, they can be determined analytically, on a case-by-case basis, using an Ansatz and a series of consistency conditions.

Here we complement this derivation, computing the kernel of the dispersion relation directly from the Lorentzian inversion formulas (2.4.10) and (2.4.11). The dispersion relation reads

$$\mathcal{G}(z) = \int_0^1 dw w^{-2} \text{dDisc}[\mathcal{G}(w)] K_{\Delta_\phi}(z, w). \quad (3.1.1)$$

The input of the formula is the double discontinuity defined in (2.4.12). As mentioned below (2.4.15), the double discontinuity has double zeros at the dimensions of double trace operators. This property allows to derive dispersive sum rules for the OPE data from the dispersion relation, as explained in [85, 96]. We are able to find an explicit expression for the kernel $K_{\Delta_\phi}(z, w)$ for correlators of identical operators with integer or half-integer dimension. For Regge-(super)bounded³ (bosonic) fermionic correlators, it

²A sum rule is dispersive if it has double zeros for the dimensions of double-trace operators.

³See (2.4.23) and (2.4.22) for the meaning of Regge-(super)bounded.

reads

$$\begin{aligned}
K_{\Delta_\phi}(z, w) &= \frac{w z^2 (w-2) \log(1-w)}{\pi^2 (w-z)(w+z-wz)} - \frac{z w^2 (z-2) \log(1-z)}{\pi^2 (w-z)(w+z-wz)} \\
&\pm \frac{z^2}{\pi^2} \left[\log(1-w) \frac{(1-2w)w^{2-2\Delta_\phi}}{(w-1)wz^2+z-1} + \frac{\log(1-z)}{z} \frac{w^{2-2\Delta_\phi}}{wz-1} + \log(z) \frac{(1-2w)w^{2-2\Delta_\phi}}{(w-1)wz^2+z-1} + (w \rightarrow \frac{w}{w-1}) \right] \\
&+ \sum_{m=0}^{2\Delta_\phi-2} \sum_{n=0}^{2\Delta_\phi-4} (\alpha_{m,n} + \beta_{m,n} \log(1-w)) w^{m+2-2\Delta_\phi} \mathcal{C}^n \left[\frac{2}{\pi^2} \left(\frac{z^2 \log(z)}{1-z} + z \log(1-z) \right) \right].
\end{aligned} \tag{3.1.2}$$

where the plus sign is for bosons, the minus for fermions. Here $\mathcal{C} = z^2(1-z)\partial^2 - z^2\partial$ is the Casimir operator of the 1d conformal group. The coefficients $\alpha_{m,n}$ and $\beta_{m,n}$ are fixed by a system of equations,

$$\begin{aligned}
&\sum_{m=0}^{2\Delta_\phi-2} \sum_{n=0}^{2\Delta_\phi-4} (\alpha_{m,n} + \beta_{m,n} \log(1-w)) w^{m+2-2\Delta_\phi} \left(\mathcal{C}^n \left[\frac{2}{\pi^2} \left(\frac{z^2 \log(z)}{1-z} + z \log(1-z) \right) \right] - \text{crossing} \right) \\
&= \frac{z^{2\Delta_\phi}}{(1-z)^{2\Delta_\phi}} \left(K^{\text{discrete}}(1-z, w) + K_{\Delta_\phi}^p(1-z, w) \right) - K^{\text{discrete}}(z, w) - K_{\Delta_\phi}^p(z, w)
\end{aligned} \tag{3.1.3}$$

where $K^{\text{discrete}}(z, w)$ and $K_{\Delta_\phi}^p(z, w)$ are given explicitly below, in (3.1.8) and (3.1.14).

As for the Lorentzian inversion formula, the dispersion relation receives extra contributions in the case of Regge-bounded bosonic correlators. In particular, it requires a regularisation of the correlator, see the discussion around (2.4.30). It has the form

$$\begin{aligned}
\mathcal{G}^{\text{reg}}(z) &= \int_0^1 \frac{dw}{w^2} K_{\Delta_\phi}^{\text{bd}}(z, w) \text{dDisc} \mathcal{G}^{\text{reg}}(w) + \\
&+ \lim_{\rho \rightarrow 0} \int_{C_\rho^+} \frac{dw}{2w^2} K_{\Delta_\phi}^{\text{bd}}(z, w) \mathcal{G}^{\text{reg}}(w) + \lim_{\rho \rightarrow 0} \int_{C_\rho^-} \frac{dw}{2w^2} K_{\Delta_\phi}^{\text{bd}}(z, w) \mathcal{G}^{\text{reg}}(w),
\end{aligned} \tag{3.1.4}$$

where the kernel $K_{\Delta_\phi}^{\text{bd}}(z, w)$ is given below in (3.1.23). A dispersion relation can also be constructed for correlators that are not bounded in the Regge limit.

Notice that it is not possible to derive the 1d dispersion relation from the higher-dimensional expression (3.0.1), as the one-dimensional case is intrinsically different⁴. At variance with the higher-dimensional case (3.0.1), the kernel (3.1.2) depends explicitly on the dimensions Δ_ϕ of the external operators and it is manifestly crossing symmetric. As pointed out in [96], this fact implies the equivalence between the dispersion relation and the so-called Polyakov bootstrap. This is the idea of replacing the conformal block expansion with a similar expansion in terms of crossing symmetric Polyakov blocks $\mathcal{P}_{\Delta}^{\Delta_\phi}(z)$ such that [21, 70, 99–102]

$$\mathcal{G}(z) = \sum_{\Delta} a_{\Delta} G_{\Delta}(z) = \sum_{\Delta} a_{\Delta} \mathcal{P}_{\Delta}^{\Delta_\phi}(z). \tag{3.1.5}$$

The dispersion relation can be used to obtain explicit expressions for Polyakov blocks in position space. We show some examples in Appendix A.

⁴See Section 2.4 for more details.

3.1.1 Derivation of the dispersion relation

We begin by examining the case of Regge-(super)bounded (bosonic) fermionic correlators, see (2.4.22). Starting with the conformal partial wave expansion given in equation (2.4.8), we substitute the inversion formulas (2.4.10)-(2.4.11) and then exchange the order of integration.

$$\begin{aligned}
\mathcal{G}(z) &= \int_0^1 dw w^{-2} d\text{Disc}[\mathcal{G}(w)] \int_{\frac{1}{2}-i\infty}^{\frac{1}{2}+i\infty} \frac{d\Delta}{2\pi i} \frac{H_{\Delta}^{B/F}(w)}{\kappa_{\Delta}} G_{\Delta}(z) \\
&+ \int_0^1 dw w^{-2} d\text{Disc}[\mathcal{G}(w)] \sum_{m=0}^{\infty} \frac{2\Gamma(2m+2)^4}{\pi^2\Gamma(4m+4)\Gamma(4m+3)} G_{2m+2}(w) G_{2m+2}(z) \\
&\equiv \int_0^1 dw w^{-2} d\text{Disc}[\mathcal{G}(w)] K_{\Delta_{\phi}}(z, w),
\end{aligned} \tag{3.1.6}$$

Using (2.4.17), $K_{\Delta_{\phi}}(z, w)$ is explicitly defined as

$$\begin{aligned}
K_{\Delta_{\phi}}(z, w) &= \sum_{m=0}^{\infty} \frac{2\Gamma(2m+2)^4}{\pi^2\Gamma(4m+4)\Gamma(4m+3)} G_{2m+2}(w) G_{2m+2}(z) + \\
&\pm \int_{\frac{1}{2}-i\infty}^{\frac{1}{2}+i\infty} \frac{d\Delta}{2\pi i} \frac{G_{\Delta}(z)}{\kappa_{\Delta}} \frac{2\pi}{\sin(\pi\Delta)} \left[w^{2-2\Delta_{\phi}} p_{\Delta}(w) + \left(\frac{w}{w-1}\right)^{2-2\Delta_{\phi}} p_{\Delta}\left(\frac{w}{w-1}\right) + q_{\Delta}^{\Delta_{\phi}}(w) \right] \\
&\equiv K^{\text{discrete}}(z, w) + K_{\Delta_{\phi}}^p(z, w) + K_{\Delta_{\phi}}^q(z, w).
\end{aligned} \tag{3.1.7}$$

The three terms in the last line represent respectively the contributions from the discrete series and from the integrals of p_{Δ} and $q_{\Delta}^{\Delta_{\phi}}$.

The discrete contribution does not depend on the external dimension Δ_{ϕ} and is identical for both fermions and bosons. It reads

$$\begin{aligned}
K^{\text{discrete}}(z, w) &\equiv \sum_{m=0}^{\infty} \frac{2\Gamma(2m+2)^4}{\pi^2\Gamma(4m+4)\Gamma(4m+3)} G_{2m+2}(w) G_{2m+2}(z) \\
&= \sum_{m=0}^{\infty} \frac{8(4m+3)}{\pi^2} Q_{2m+1}\left(\frac{2}{w}-1\right) Q_{2m+1}\left(\frac{2}{z}-1\right).
\end{aligned} \tag{3.1.8}$$

In the last line we introduced the Legendre functions of the second kind $Q_n(z)$ and we used that

$$G_{2m+2} = \frac{2^{4m+4}\Gamma(2m+\frac{1}{2}+2)}{\sqrt{\pi}\Gamma(2m+2)} Q_{2m+1}\left(\frac{2}{z}-1\right). \tag{3.1.9}$$

The discrete sum can be computed using a representation of $Q_n(z)$ as an integral of a Legendre function of first kind $P_n(z)$,

$$Q_{2m+1}\left(\frac{2}{z}-1\right) = \int_{-1}^1 dv \frac{P_{2m+1}(v)}{2(-v+\frac{2}{z}-1)}, \tag{3.1.10}$$

and using

$$\sum_{m=0}^{\infty} (4m+3) P_{2m+1}(x) P_{2m+1}(y) = \delta(x-y) - \delta(x+y), \quad (3.1.11)$$

At the end of the day, we find

$$\begin{aligned} K^{\text{discrete}}(z, w) &= \sum_{m=0}^{\infty} \frac{8(4m+3)}{\pi^2} Q_{2m+1}\left(\frac{z}{w} - 1\right) Q_{2m+1}\left(\frac{z}{z} - 1\right) \\ &= \int_{-1}^1 dv \int_{-1}^1 du \frac{1}{2\left(\frac{z}{w}-1-v\right)} \frac{1}{2\left(\frac{z}{z}-1-u\right)} \sum_{m=0}^{\infty} (4m+3) P_{2m+1}(v) P_{2m+1}(u) \\ &= \frac{w z^2 (w-2) \log(1-w)}{\pi^2 (w-z)(w+z-wz)} - \frac{z w^2 (z-2) \log(1-z)}{\pi^2 (w-z)(w+z-wz)}. \end{aligned} \quad (3.1.12)$$

The second term in (3.1.7) is defined by

$$K_{\Delta_\phi}^p(z, w) \equiv \pm \int_{\frac{1}{2}-i\infty}^{\frac{1}{2}+i\infty} \frac{d\Delta}{2\pi i} \frac{G_\Delta(z)}{\kappa_\Delta} \frac{2\pi}{\sin(\pi\Delta)} \left[w^{2-2\Delta_\phi} p_\Delta(w) + \left(\frac{w}{w-1}\right)^{2-2\Delta_\phi} p_\Delta\left(\frac{w}{w-1}\right) \right], \quad (3.1.13)$$

with $p_\Delta(z)$ in (2.4.18). Closing the contour on the right and using the residue theorem, one obtains

$$\begin{aligned} K_{\Delta_\phi}^p(z, w) &= \mp \sum_{m=0}^{\infty} \partial_m \left[\frac{2(4m+3)}{\pi^2} Q_{2m+1}\left(\frac{z}{z} - 1\right) \left(w^{2-2\Delta_\phi} P_{2m+1}(1-2w) + \left(w \rightarrow \frac{w}{w-1}\right) \right) \right] \\ &= \pm \frac{z^2}{\pi^2} \left[\log(1-w) \frac{(1-2w)w^{2-2\Delta_\phi}}{(w-1)wz^2+z-1} + \frac{\log(1-z)}{z} \frac{w^{2-2\Delta_\phi}}{wz-1} + \log(z) \frac{(1-2w)w^{2-2\Delta_\phi}}{(w-1)wz^2+z-1} + \left(w \rightarrow \frac{w}{w-1}\right) \right]. \end{aligned} \quad (3.1.14)$$

In order to perform the sum in the first line, we used integral representations of Legendre functions,

$$P_n(z) = \frac{2^n}{\pi} \int_{-\infty}^{\infty} du \frac{(z+iu)^n}{(u^2+1)^{n+1}} \quad (3.1.15)$$

$$Q_\nu^\mu(z) = \frac{1}{\Gamma(\nu+1)} e^{\pi i \mu} 2^{-\nu-1} (z^2-1)^{\mu/2} \Gamma(\mu+\nu+1) \int_{-1}^1 dt (1-t^2)^\nu (z-t)^{-\mu-\nu-1}$$

and then we exchanged the order of sum and integral.

The last contribution to $K_{\Delta_\phi}(z, w)$ in (3.1.7) is defined as

$$K_{\Delta_\phi}^q(z, w) \equiv \int_{\frac{1}{2}-i\infty}^{\frac{1}{2}+i\infty} \frac{d\Delta}{2\pi i} \frac{G_\Delta(z)}{\kappa_\Delta} \frac{2\pi}{\sin(\pi\Delta)} q_{\Delta_\phi}^{\Delta}(w), \quad (3.1.16)$$

where $q_{\Delta_\phi}^{\Delta}(w)$ is defined in (2.4.19).

Since $q_{\Delta_\phi}^{\Delta}(w)$ is a polynomial in w and $\Delta(\Delta-1)$, see (2.4.19) and (2.4.20), we obtain

$$K_{\Delta_\phi}^q(z, w) = \sum_{m=0}^{2\Delta_\phi-2} \sum_{n=0}^{2\Delta_\phi-4} (\alpha_{m,n} + \beta_{m,n} \log(1-w)) w^{m+2-2\Delta_\phi} \int_{\frac{1}{2}-i\infty}^{\frac{1}{2}+i\infty} \frac{d\Delta}{2\pi i} \frac{G_\Delta(z)}{\kappa_\Delta} \frac{2\pi}{\sin(\pi\Delta)} \Delta^n (\Delta-1)^n \quad (3.1.17)$$

The coefficients $\alpha_{m,n}$ and $\beta_{m,n}$ have to be determined on a case-by-case basis, requiring that $H_{\Delta}^{B/F}(w)$ has no poles in $w = 0$.

The integral in (3.1.17) can be evaluated using that

$$\int_{\frac{1}{2}-i\infty}^{\frac{1}{2}+i\infty} \frac{d\Delta}{2\pi i} \frac{G_{\Delta}(z)}{\kappa_{\Delta}} \frac{2\pi}{\sin(\pi\Delta)} \Delta^n (\Delta-1)^n = \mathcal{C}^n \left[K_{\Delta_{\phi}=1}^p(z, 0) \right] = \mathcal{C}^n \left[-\frac{2}{\pi^2} \left(\frac{z^2 \log(z)}{1-z} + z \log(1-z) \right) \right] \quad (3.1.18)$$

where $\mathcal{C} = z^2(1-z)\partial^2 - z^2\partial$ is the Casimir operator of the one-dimensional conformal group, which acts as $\mathcal{C}G_{\Delta}(z) = \Delta(\Delta-1)G_{\Delta}(z)$ on the conformal blocks, and we used the definition (3.1.13) of $K_{\Delta_{\phi}=1}^p(z, w=0)$. All in all, the kernel reads

$$\begin{aligned} K_{\Delta_{\phi}}(z, w) &= \frac{w z^2 (w-2) \log(1-w)}{\pi^2 (w-z)(w+z-wz)} - \frac{z w^2 (z-2) \log(1-z)}{\pi^2 (w-z)(w+z-wz)} \quad (3.1.19) \\ &\pm \frac{z^2}{\pi^2} \left[\log(1-w) \frac{(1-2w)w^{2-2\Delta_{\phi}}}{(w-1)wz^2+z-1} + \frac{\log(1-z)}{z} \frac{w^{2-2\Delta_{\phi}}}{wz-1} + \log(z) \frac{(1-2w)w^{2-2\Delta_{\phi}}}{(w-1)wz^2+z-1} + (w \rightarrow \frac{w}{w-1}) \right] \\ &+ \sum_{m=0}^{2\Delta_{\phi}-2} \sum_{n=0}^{2\Delta_{\phi}-4} (\alpha_{m,n} + \beta_{m,n} \log(1-w)) w^{m+2-2\Delta_{\phi}} \mathcal{C}^n \left[\frac{2}{\pi^2} \left(\frac{z^2 \log(z)}{1-z} + z \log(1-z) \right) \right]. \end{aligned}$$

Once all the coefficients are fixed as explained below (2.4.20), the kernel is explicitly crossing symmetric. If the coefficients are not determined first, the requirement of crossing symmetry of the kernel can be used to fix them. To be more explicit, we write the crossing equation for the kernel

$$K_{\Delta_{\phi}}(z, w) = \frac{z^{2\Delta_{\phi}}}{(1-z)^{2\Delta_{\phi}}} K_{\Delta_{\phi}}(1-z, w). \quad (3.1.20)$$

and expand it using (3.1.19). The end result is

$$\begin{aligned} &\sum_{m=0}^{2\Delta_{\phi}-2} \sum_{n=0}^{2\Delta_{\phi}-4} (\alpha_{m,n} + \beta_{m,n} \log(1-w)) w^{m+2-2\Delta_{\phi}} \left(\mathcal{C}^n \left[\frac{2}{\pi^2} \left(\frac{z^2 \log(z)}{1-z} + z \log(1-z) \right) \right] - \text{crossing} \right) \\ &= \frac{z^{2\Delta_{\phi}}}{(1-z)^{2\Delta_{\phi}}} \left(K^{\text{discrete}}(1-z, w) + K_{\Delta_{\phi}}^p(1-z, w) \right) - K^{\text{discrete}}(z, w) - K_{\Delta_{\phi}}^p(z, w), \quad (3.1.21) \end{aligned}$$

which is a system of equations that can be used to determine $\alpha_{m,n}$ and $\beta_{m,n}$, without referring to the inversion kernel $H_{\Delta}^{B/F}(w)$. Plotting (3.1.19) for several values of the external dimension Δ_{ϕ} and $(z, w) \in (0, 1)$ we found that the kernel is always positive.

The dispersion kernel (3.1.19) is applicable only to super-bounded bosonic correlators (2.4.23). To extend this result to bounded bosonic correlators, one must use the improved inversion kernel (2.4.26) in (3.1.6). The dispersion relation is then given by

$$\begin{aligned} \mathcal{G}^{\text{reg}}(z) &= \int_0^1 \frac{dw}{w^2} K_{\Delta_{\phi}}^{\text{bd}}(z, w) d\text{Disc} \mathcal{G}^{\text{reg}}(w) + \\ &+ \lim_{\rho \rightarrow 0} \int_{C_{\rho}^+} \frac{dw}{2w^2} K_{\Delta_{\phi}}^{\text{bd}}(z, w) \mathcal{G}^{\text{reg}}(w) + \lim_{\rho \rightarrow 0} \int_{C_{\rho}^-} \frac{dw}{2w^2} K_{\Delta_{\phi}}^{\text{bd}}(z, w) \mathcal{G}^{\text{reg}}(w). \quad (3.1.22) \end{aligned}$$

with

$$K_{\Delta_\phi}^{\text{bd}}(z, w) = K_{\Delta_\phi}(z, w) - \widehat{H}_{0,2}^B(w) \sum_{n=0}^{2\Delta_\phi-2} A_n \mathcal{C}^n \left[\frac{2}{\pi^2} \left(\frac{z^2 \log(z)}{1-z} + z \log(1-z) \right) \right]. \quad (3.1.23)$$

In order to compute the extra term, we have followed the same procedure as for $K_{\Delta_\phi}^q$. Indeed, we noticed that for every integer Δ_ϕ the ratio of gamma functions appearing in (2.4.26) reduces to a polynomial in $\Delta(\Delta-1)$, exactly like $K_{\Delta_\phi}^q$. Explicitly, we find

$$\frac{\pi^2 2^{2(\Delta_\phi-1)} \Gamma(\Delta_\phi + \frac{1}{2}) \Gamma(\Delta_\phi - \frac{\Delta}{2})^2 \Gamma(\Delta_\phi - \frac{1-\Delta}{2})^2}{\Gamma(\Delta_\phi)^3 \Gamma(2\Delta_\phi - \frac{1}{2}) \Gamma(1-\frac{\Delta}{2})^2 \Gamma(1-\frac{1-\Delta}{2})^2} = \sum_{n=0}^{2\Delta_\phi-2} A_n \Delta^n (\Delta-1)^n, \quad (3.1.24)$$

where the coefficients A_n can be easily determined case-by-case in Δ_ϕ . The function $\widehat{H}_{0,2}^B(w)$ is defined in (2.4.25). As with the inversion formula, the kernel redefinition (3.1.23) introduces an additional pole at $w=1$, potentially affecting the convergence of the integral. To ensure convergence, a crossing-symmetric, Regge-bounded subtraction is necessary, as discussed below (2.4.26).

Following the same strategy that works for the bounded case, using (2.4.31) and (3.1.18), we can also derive a dispersion formula for unbounded correlators. In general, it reads

$$\begin{aligned} K_{\Delta_\phi}^{\text{unbd}}(z, w) &= K_{\Delta_\phi}(z, w) - \sum_{m,n} A_{m,n} \widehat{H}_{m,2}^B(w) \mathcal{C}^n \left[\frac{2}{\pi^2} \left(\frac{z^2 \log(z)}{1-z} + z \log(1-z) \right) \right] \\ &- \sum_{m,n} B_{m,n} \widehat{H}_{m,1}^B(w) \mathcal{C}^n \left[\frac{2}{\pi^2} \left(\frac{z^2 \log(z)}{1-z} + z \log(1-z) \right) \right] \\ &- \sum_{m,n} \tilde{A}_{m,n} \widehat{H}_{m,2}^B(w) G_{2+2n}(z) - \sum_{m,n} \tilde{B}_{m,n} \widehat{H}_{m,1}^B(w) G_{2+2n}(z), \end{aligned} \quad (3.1.25)$$

where the coefficients $A_{m,n}, B_{m,n}, \tilde{A}_{m,n}, \tilde{B}_{m,n}$ are fixed as in (2.4.31). The final two coefficients are necessary to enhance the behavior of the contribution coming from the discrete inversion kernel (2.4.11).

3.2 Dispersion relation for bulk two-point functions

In the case of bulk two-point functions in a defect CFT, the existence of two Lorentzian inversion formulas, (2.5.21) and (2.5.26), implies that we can formulate two distinct dispersion relations.

The first dispersion relation can be derived from the defect inversion formula (2.5.21) and depends on a single discontinuity of the two-point function, which is controlled by the the bulk OPE. It can also be obtained directly from Cauchy's theorem⁵. For general

⁵A similar approach can also be used to derive a dispersion relation for four-point functions in CFTs without defects [103].

codimension $q > 1$, the dispersion relation reads ⁶

$$F(r, w) = \int_0^r \frac{dw'}{2\pi i} \left(\frac{1}{w' - w} + \frac{1}{w' - \frac{1}{w}} - \frac{1}{w'} \right) \text{Disc}[F(r, w')]. \quad (3.2.1)$$

Since the bulk OPE controls the discontinuity, see (3.2.16), this formula allows to reconstruct the full correlator using only a subset of bulk data (with defect information encoded in the one-point functions of bulk operators). This approach is especially powerful for theories where the bulk is well understood and we can leverage that knowledge to gain insights about the defect.

As in the case of the defect inversion formula (2.5.21), the dispersion relation may miss contributions from defect operators with low transverse spin, as discussed in (2.5.25). This issue arises because both the inversion formula and dispersion relations are derived from a contour deformation argument, which involves neglecting contributions from arcs at infinity. If the defect OPE includes operators with low transverse spin, these contributions are not suppressed. To address this in the context of the dispersion relation, we can introduce a suitable prefactor to enhance the behavior of the correlator without altering its analytic structure, see (3.2.24) below. Alternatively, we have to subtract the divergent contributions and add them back after using the dispersion relation, as in (3.2.17).

The second dispersion relation involves the double discontinuity and is controlled by the defect channel. Deriving this relation is more complex, but for certain specific values of the defect dimension, the problem can be related to the case of four-point functions without the defect (3.0.1). Since the dispersion relation is a mathematical statement that is valid for any function of two complex variables with a specific analytical structure, we conjecture a general formula. This formula is essentially similar to (3.0.1) and, like it, is technically challenging to use.

A slightly different discussion is needed for codimension-one defects. In this case, the bulk two-point function depends on a single cross-ratio, leading to a different form of the dispersion relation. In particular, it is impossible to derive a relation controlled only by either the bulk or the defect OPE. A similar drawback is present in the Lorentzian inversion formula, as seen in (2.5.37). Therefore, we propose a dispersion relation that includes contributions from two distinct cuts, dominated by the two OPE channels,

$$F(z) = \frac{z^{\Delta_\phi+1}}{2\pi i} \int_{-\infty}^0 dz' \frac{\text{Disc}_{z'<0} \left[\frac{F(z')}{(z')^{\Delta_\phi+1}} \right]}{z' - z} + \frac{z^{\Delta_\phi+1}}{2\pi i} \int_1^\infty dz' \frac{\text{Disc}_{z'>1} \left[\frac{F(z')}{(z')^{\Delta_\phi+1}} \right]}{z' - z}. \quad (3.2.2)$$

Our boundary formula involves two single discontinuities, while the Lorentzian inversion formula depends on a single discontinuity controlled by the bulk channel and a double discontinuity controlled by the defect OPE. It would be interesting to explore whether

⁶For the special case of $q = 2$ monodromy defects, see [104].

a dispersion relation could be formulated which exhibits these same features. Such a formula would be more powerful because the double discontinuity is typically simpler than the single one. However, this problem appears technically challenging, as no closed form is known for the kernel of the Lorentzian inversion formula [48].

3.2.1 Dispersion relation from defect inversion formula

We can obtain a defect dispersion relation following the same strategy that worked for four-point functions in absence of defects, see for example Section 3.1.1.

We introduce the defect conformal partial wave decomposition [44],

$$F(r, w) = \sum_{s=0}^{\infty} \int_{p/2-i\infty}^{p/2+i\infty} \frac{d\hat{\Delta}}{2\pi i} b(\hat{\Delta}, s) \hat{g}_s(w) \hat{\Psi}_{\hat{\Delta}}(r), \quad (3.2.3)$$

with

$$\hat{\Psi}_{\hat{\Delta}}(r) = \frac{1}{2} \left(\hat{f}_{\hat{\Delta}}(r) + \frac{\hat{K}_{p-\hat{\Delta}}}{\hat{K}_{\hat{\Delta}}} \hat{f}_{p-\hat{\Delta}}(r) \right), \quad \hat{K}_{\hat{\Delta}} \equiv \frac{\Gamma(\hat{\Delta})}{\Gamma(\hat{\Delta}-\frac{p}{2})}. \quad (3.2.4)$$

The functions $\hat{f}_{\hat{\Delta}}(r)$ and $\hat{g}_s(w)$ are defined in (2.5.16). The coefficient $b(\hat{\Delta}, s)$ encodes the CFT data in the defect channel and can be computed using the Lorentzian inversion formula (2.5.21). In radial coordinates, the formula reads

$$b(\hat{\Delta}, s) = -\frac{\hat{K}_{\hat{\Delta}}}{i\pi \hat{K}_{p-\hat{\Delta}}} \int_0^1 dr \int_0^r dw \hat{\mu}(r, w) \hat{g}_{2-q-s}(w) \hat{\Psi}_{\hat{\Delta}}(r), \text{Disc}[F(r, w)] \quad (3.2.5)$$

where the integration measure is

$$\hat{\mu}(r, w) = w^{1-q}(1-w^2)^{q-2} r^{-p-1} (1-r^2)^p. \quad (3.2.6)$$

Using (3.2.5) inside the partial wave expansion (3.2.3) and exchanging the order of integration, we find an expression of the form

$$F(r, w) = \int_0^1 dr' \int_0^{r'} dw' S(w, w') I(r, r') \text{Disc}[F(r', w')], \quad (3.2.7)$$

where the discontinuity is defined in (2.5.23) and

$$\begin{aligned} S(w, w') &= \sum_{s=0}^{\infty} w^{1-q}(1-w^2)^{q-2} \hat{g}_{2-q-s}(w') \hat{g}_s(w) \\ I(r, r') &= \int_{\frac{p}{2}-i\infty}^{\frac{p}{2}+i\infty} \frac{d\hat{\Delta}}{2\pi i} (r')^{-p-1} (1-(r')^2)^p \frac{\hat{K}_{\hat{\Delta}}}{i\pi \hat{K}_{p-\hat{\Delta}}} \hat{\Psi}_{\hat{\Delta}}(r') \Psi_{\hat{\Delta}}(r) \end{aligned} \quad (3.2.8)$$

Note that the contributions from the angular and radial parts factorize. The angular contribution $S(w, w')$ can be computed using the integral representations of the Gegenbauer polynomials and of the hypergeometric function. Exchanging the sum over spin with the integrals from these representations, we obtain

$$S(w, w') = \frac{1}{2\pi i} \left(\frac{1}{w' - w} + \frac{1}{w' - \frac{1}{w}} - \frac{1}{w'} \right). \quad (3.2.9)$$

The remaining contribution $I(r, r')$ can be evaluated exploiting the orthogonality of conformal partial waves, namely

$$\int_0^1 dr r^{-p-1} (1-r^2)^p \Psi_{\hat{\Delta}_1}(r) \Psi_{\hat{\Delta}_2}(r) = \frac{\pi}{2} \frac{K_{p-\hat{\Delta}_2}}{K_{\hat{\Delta}_1}} (\delta(\nu_1 - \nu_2) + \delta(\nu_1 + \nu_2)). \quad (3.2.10)$$

where $\hat{\Delta} = \frac{1}{2} + i\nu$, and the identity

$$\Psi_{p-\hat{\Delta}}(r) = \frac{K_{\hat{\Delta}}}{K_{p-\hat{\Delta}}} \Psi_{\hat{\Delta}}(r). \quad (3.2.11)$$

It turns out that $I(r, r') = \delta(r' - r)$. We can prove it by introducing a generic function $f(r)$ and expanding it on the $\Psi_{\hat{\Delta}}(r)$ basis as

$$f(r) = \int_{\frac{p}{2}-i\infty}^{\frac{p}{2}+i\infty} \frac{d\Delta'}{2\pi i} \hat{f}(\Delta') \Psi_{\Delta'}(r). \quad (3.2.12)$$

Using the properties of the conformal partial waves, we find

$$\begin{aligned} \int_0^1 dr I(r, r') f(r') &= \int_0^1 dr I(r, r') \int_{\frac{1}{2}-i\infty}^{\frac{1}{2}+i\infty} \frac{d\Delta'}{2\pi i} \hat{f}(\Delta') \Psi_{\Delta'}(r') \\ &= \int_{\frac{p}{2}-i\infty}^{\frac{p}{2}+i\infty} \frac{d\hat{\Delta}}{2\pi i} \int_{\frac{p}{2}-i\infty}^{\frac{p}{2}+i\infty} \frac{d\Delta'}{2\pi i} \frac{K_{\hat{\Delta}}}{K_{p-\hat{\Delta}}} \Psi_{\hat{\Delta}}(r) \hat{f}(\Delta') \int_0^1 dr' (r')^{-p-1} (1-(r')^2)^p \Psi_{\hat{\Delta}}(r') \Psi_{\Delta'}(r') \\ &= \int_{\frac{p}{2}-i\infty}^{\frac{p}{2}+i\infty} \frac{d\hat{\Delta}}{2\pi i} \int_{\frac{p}{2}-i\infty}^{\frac{p}{2}+i\infty} \frac{d\Delta'}{2\pi i} \frac{K_{\hat{\Delta}}}{K_{p-\hat{\Delta}}} \Psi_{\hat{\Delta}}(r) \hat{f}(\Delta') \frac{\pi}{2} \frac{K_{p-\Delta'}}{K_{\hat{\Delta}}} (\delta(\hat{\nu} - \nu') + \delta(\hat{\nu} + \nu')) \\ &= \int_{\frac{p}{2}-i\infty}^{\frac{p}{2}+i\infty} \frac{d\hat{\Delta}}{2\pi i} \Psi_{\hat{\Delta}}(r) \hat{f}(\hat{\Delta}) \\ &= f(r), \end{aligned} \quad (3.2.13)$$

which implies

$$I(r, r') = \delta(r - r'). \quad (3.2.14)$$

We can finally collect the pieces, (3.2.9)- (3.2.14), and obtain

$$\begin{aligned} F(r, w) &= \int_0^1 dr' \int_0^{r'} \frac{dw'}{2\pi i} \delta(r - r') \left(\frac{1}{w' - w} + \frac{1}{w' - \frac{1}{w}} - \frac{1}{w'} \right) \text{Disc}[F(r', w')] \\ &= \int_0^r \frac{dw'}{2\pi i} \left(\frac{1}{w' - w} + \frac{1}{w' - \frac{1}{w}} - \frac{1}{w'} \right) \text{Disc}[F(r, w')], \end{aligned} \quad (3.2.15)$$

which is the defect dispersion relation (3.2.1). The input of the formula is the discontinuity (2.5.23), which can be computed from the bulk expansion as in (2.5.24). In radial coordinates it reads

$$\text{Disc}[F(r, w)] = - \sum_{\mathcal{O}} 2i \sin\left[\frac{\pi}{2}(\Delta - 2\Delta_{\phi} - \ell)\right] a_{\mathcal{O}} \lambda_{\phi\phi\mathcal{O}} r^{\Delta_{\phi}} [(1-rw)\left(\frac{r}{w} - 1\right)]^{\Delta_{\phi} - \frac{\Delta - \ell}{2}} \tilde{f}_{\Delta, \ell}(r, w). \quad (3.2.16)$$

We conclude this section by noting that in the above derivation, we ignored the fact that the inversion formula (2.5.21) reconstructs $b(\hat{\Delta}, s)$ up to low-spin ambiguities, as discussed around (2.5.25). Since the dispersion relation is derived from the inversion formula, it has the same ambiguities. Specifically, it will miss a contribution given by the sum of defect conformal blocks (2.5.16) with transverse spin lower than a certain s^* . If $s^* \geq 0$, one has to subtract these contribution when applying the dispersion relation and then add them back at the end. All in all, in the most general case, the correlator reads

$$F(r, w) = \text{dispersion relation} + \sum_{s=0}^{s^*} \sum_{\hat{\Delta}} b_{\phi_{\hat{\Delta}, s}}^2 \hat{f}_{\hat{\Delta}, s}(r, w). \quad (3.2.17)$$

In the next section we will see a different approach to fix this ambiguity.

3.2.2 Alternative derivation using Cauchy's theorem

There is an alternative, and perhaps more transparent, way to derive the defect dispersion relation. If we set $r \in (0, 1)$, we observe from the bulk and defect block expansions that the two-point function is regular everywhere in the complex w plane except for two branch cuts at $(0, r)$ and $(\frac{1}{r}, \infty)$ ⁷. Thus, we can directly apply Cauchy's theorem to the variable w and write

$$F(r, w) = \oint \frac{dw'}{2\pi i} \frac{F(r, w')}{w' - w}. \quad (3.2.18)$$

We can now deform the contour and wrap it around the branch cuts as shown in Figure 3.1. For now, we assume that we can neglect the contributions from all the circles, including the circle at infinity and the small circles around $w = 0, r, 1/r$ ⁸. Under this assumption, we can write:

$$F(r, w) = \int_0^r \frac{dw'}{2\pi i} \frac{1}{w' - w} \text{Disc}_{0 < w' < r}[F(r, w')] + \int_{\frac{1}{r}}^{\infty} \frac{dw'}{2\pi i} \frac{1}{w' - w} \text{Disc}_{w' > \frac{1}{r}}[F(r, w')], \quad (3.2.19)$$

Finally, we can change variable $w' \rightarrow \frac{1}{w'}$ in the second integral and use the symmetry $F(r, w) = F(r, \frac{1}{w})$ to obtain

$$F(r, w) = \int_0^r \frac{dw'}{2\pi i} \left(\frac{1}{w' - w} + \frac{1}{w' - \frac{1}{w}} - \frac{1}{w'} \right) \text{Disc}[F(r, w')], \quad (3.2.20)$$

where the discontinuity is taken around the branch point at $w = r$ as in (2.5.23).

We now discuss the behavior at $w' = 0$ and $w' = r$. The behavior near $w' = r$ is controlled by the bulk OPE, specifically the block expansion (2.5.18). The bulk

⁷See [44] for a detailed analysis of the analytic structure of $F(r, w)$.

⁸Notice that, thanks to the symmetry $F(r, w) = F(r, \frac{1}{w})$, it is sufficient to require good behavior at $w = 0$ and $w = r$.

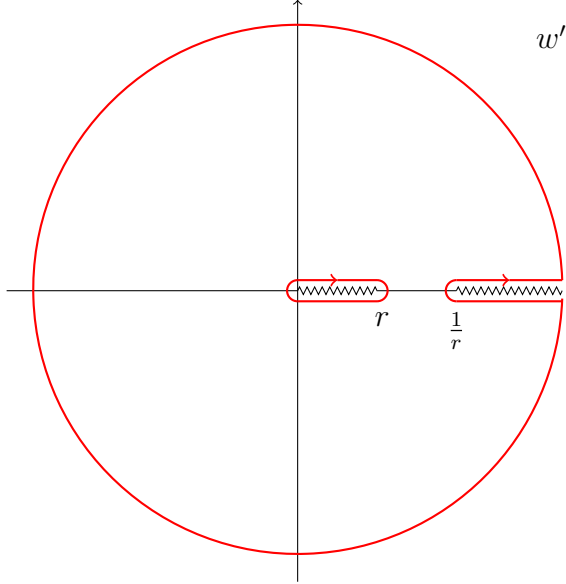


Figure 3.1: Contour deformation leading to the dispersion relation.

blocks $f_{\Delta,\ell}(r, w)$ behave like $(w - r)^{\Delta - \ell}$ for $w \rightarrow r$ so the correlator is dominated by the operator with the lowest twist ⁹, which is the identity. Therefore, as $w \rightarrow r$, the correlator behaves as

$$F(r, w) \sim (w - r)^{-\Delta_\phi}. \quad (3.2.21)$$

For $\Delta_\phi > 1$, we need to interpret the formula (3.2.20) carefully. Since the original integral (3.2.18) was finite, and assuming no other singularities are present, the combined contribution from the small circle around $w' = r$ and the integral in (3.2.20) must also be finite. This implies that the discontinuity in equation (3.2.20) should be understood in a distributional sense with values of $\Delta_\phi > 1$ giving additional finite contributions localized at $w' = r$.

For the behaviour near $w = 0$, or equivalently at infinity, the situation is similar to that in the Lorentzian inversion formula (2.5.21). While the inversion formula allows us to extract defect CFT data for sufficiently high spin ($s > s_*$), the dispersion relation (3.2.20) reconstructs only part of the full correlator. The missing terms are given by low-spin conformal blocks, see (3.2.17), which are polynomials in w but can be arbitrarily complicated functions of r . The derivation from Cauchy's theorem makes it clear how to improve the dispersion formula to include the missing contributions. This can be done once the behavior of the correlator for $w \rightarrow 0$ (or equivalently for $|w| \rightarrow \infty$) is

⁹By definition, the twist τ of an operator is $\tau = \Delta - \ell$.

known. In particular, if we know ¹⁰ that

$$F(r, w) \sim w^{-s^*} \quad \text{for } w \rightarrow 0, \quad (3.2.22)$$

then we can define

$$\tilde{F}(r, w) = \left(\frac{wr}{(w-r)(1-wr)} \right)^{s^*+1} F(r, w), \quad (3.2.23)$$

which, by construction, goes like w^{-1} at large w . Therefore, formula (3.2.20) applies to the function \tilde{F} . We can then write an improved version of the dispersion relation for $F(r, w)$,

$$\frac{F(r, w)}{(w-r)^{s^*+1} \left(\frac{1}{w} - r \right)^{s^*+1}} = \int_0^r \frac{dw'}{2\pi i} \left(\frac{1}{w'-w} + \frac{1}{w'-\frac{1}{w}} - \frac{1}{w'} \right) \text{Disc} \left[\frac{F(r, w')}{(w'-r)^{s^*+1} \left(\frac{1}{w'} - r \right)^{s^*+1}} \right]. \quad (3.2.24)$$

This improved formula offers an alternative to (3.2.17). Depending on the context, one approach may be better than the other. The main drawback of using the prefactor is that it worsens the behavior near $w \rightarrow r$, and introduces additional contributions to the discontinuity¹¹.

3.2.3 A dispersion relation with the double discontinuity

A second dispersion relation can be obtained starting from the bulk conformal partial wave expansion [45]

$$F(z, \bar{z}) = \sum_{\ell} \int_{d/2-i\infty}^{d/2+i\infty} \frac{d\Delta}{2\pi i} c(\Delta, \ell) \Psi_{\Delta, \ell}(z, \bar{z}), \quad (3.2.25)$$

with

$$\Psi_{\Delta, \ell}(z, \bar{z}) = \frac{1}{2} \left(f_{\Delta, \ell}(z, \bar{z}) + \frac{K_{d-\Delta, \ell}}{K_{\Delta, \ell}} f_{d-\Delta, \ell}(z, \bar{z}) \right), \quad (3.2.26)$$

and ¹²

$$K_{\Delta, \ell} = \frac{\Gamma(\Delta - p - 1) \Gamma(\frac{\Delta-1}{2})}{\Gamma(\Delta - \frac{d}{2}) \Gamma(\frac{\Delta-p-1}{2})} \kappa_{\Delta+\ell}, \quad \kappa_{\Delta+\ell} = \frac{\Gamma(\frac{\Delta+\ell}{2})^2}{2\pi^2 \Gamma(\Delta + \ell) \Gamma(\Delta + \ell - 1)}. \quad (3.2.27)$$

By substituting the result of the Lorentzian inversion formula (2.5.26) into the partial wave decomposition (3.2.25) and summing over spin and dimension, one should obtain a dispersion relation involving the double discontinuity at $\bar{z} = 0$. This computation is

¹⁰As we mentioned multiple times, the value of the low-spin threshold s^* is not known for general defect theories.

¹¹More precisely, the prefactor may introduce extra poles in the correlator, which correspond to delta-function contributions to the discontinuity.

¹²The factors $K_{\Delta, \ell}$ and $\kappa_{\Delta+\ell}$ should not be confused with (3.1.19) and (2.3.10).

challenging because no closed form exists for the bulk blocks. However, this is the case also in the defect-free case. The strategy employed in the case without defects [95] was to derive a formula for $d = 4$ and $d = 2$ and then argue for its validity in general. We believe that a similar approach can be applied to our case. For $p = 2$ and generic d , we can exploit the following fact [45]

$$f_{\Delta,l}(z, \bar{z}) = \frac{(1-z)(1-\bar{z})}{1-z\bar{z}} G_{\Delta-1,l+1}^{d-2}(1-z, 1-\bar{z}), \quad (3.2.28)$$

where $f_{\Delta,l}(z, \bar{z})$ is the bulk block and $G_{\Delta,l}^d(z, \bar{z})$ is the conformal block for a four-point function without the defect in dimension d , see (2.3.3). Then, if we rewrite the defect two-point function as

$$F(z, \bar{z}) = \left(\frac{\sqrt{z\bar{z}}}{(1-z)(1-\bar{z})} \right)^{\Delta_\phi} \frac{(1-z)(1-\bar{z})}{1-z\bar{z}} \mathcal{G}(1-z, 1-\bar{z}), \quad (3.2.29)$$

the function $\mathcal{G}(z, \bar{z})$ can be expanded using ordinary conformal blocks for four-point functions. This implies that it can be computed using the dispersion relation for Regge-bounded four-point functions. The formula is given by [95]

$$\begin{aligned} \mathcal{G}(u, v) &= \mathcal{G}^t(u, v) + \mathcal{G}^u(u, v), \\ \frac{u}{v} \mathcal{G}^t(u, v) &= \int_0^1 du' dv' K(u, v, u', v') d\text{Disc} \left(\frac{u'}{v'} \mathcal{G}(u', v') \right), \end{aligned} \quad (3.2.30)$$

where the u-channel expression is obtained by sending $z \rightarrow \frac{z}{z-1}$ and we have introduced the variables

$$u = z\bar{z}, \quad v = (1-z)(1-\bar{z}). \quad (3.2.31)$$

In these coordinates the kernel $K(u, v, u', v')$ is

$$K(u, v, u', v') = \frac{u-v+u'-v'}{64\pi(uvu'v')^{\frac{3}{4}}} x^{\frac{3}{2}} {}_2F_1 \left(\frac{1}{2}, \frac{3}{2}, 2, 1-x \right) (\theta(x-1) - 4\delta(x-1)), \quad (3.2.32)$$

where

$$x = \frac{16\sqrt{uvu'v'}}{[(\sqrt{u} + \sqrt{v})^2 - (\sqrt{u'} + \sqrt{v'})^2][(\sqrt{u} - \sqrt{v})^2 - (\sqrt{u'} - \sqrt{v'})^2]}. \quad (3.2.33)$$

Therefore for our correlator we obtain

$$\begin{aligned} F^t(z, \bar{z}) &= \left(\frac{\sqrt{z\bar{z}}}{(1-z)(1-\bar{z})} \right)^{\Delta_\phi} \frac{z\bar{z}}{1-z\bar{z}} \int_0^1 dw d\bar{w} K(1-z, 1-\bar{z}, 1-w, 1-\bar{w}) \\ &\quad \times d\text{Disc} \left[F(w, \bar{w}) \left(\frac{(1-w)(1-\bar{w})}{\sqrt{w\bar{w}}} \right)^{\Delta_\phi} \frac{1-w\bar{w}}{w\bar{w}} \right]. \end{aligned} \quad (3.2.34)$$

This formula is derived for $p = 2$ and arbitrary d . However, we observe that the function $F(z, \bar{z})$ has the same analytic structure for all p and the prefactors in the formula do not introduce new singularities. Given that the original derivation relied on a contour deformation argument based on the analytic properties of the functions involved, we conjecture that this formula extends to defects of arbitrary dimensions. Due to the complicated nature of the dispersion kernel in (3.2.34), we could only check the formula explicitly for the bulk identity correlator, which corresponds to

$$\mathcal{G}(1 - z, 1 - \bar{z}) = \frac{1 - z\bar{z}}{(1 - z)(1 - \bar{z})} \quad (3.2.35)$$

In this case, the check reduces to the one performed in [95] for generalized free fields.

3.2.4 The special case of boundary CFTs

In this section, we turn our attention to codimension-one defects, such as boundaries and interfaces. The main difference with general defects lies in the absence of transverse spin and the presence of a single cross-ratio z . As noted in [48], this feature implies a different structure for the Lorentzian inversion formula, see (2.5.37). Specifically, the formula includes two distinct contributions: one involving a single discontinuity controlled by the bulk OPE (2.5.33), and another involving a double discontinuity controlled by the boundary (defect) OPE (2.5.32).

Another drawback of this case is that the integration kernels are not generally known in closed form, except when the difference of external dimensions is an odd integer.

Fortunately, we can employ a straightforward contour deformation argument, as in Section 3.2.2, to derive a dispersion relation involving two discontinuities. However, in contrast with the general case, there is no symmetry that relates these two contributions.

Explicitly, we start from

$$F(z) = \frac{1}{2\pi i} \oint dz' \frac{F(z')}{z' - z}, \quad (3.2.36)$$

where the integration contour encircle any regular point z . Based on the explicit expressions of the conformal blocks, (2.5.34) and (2.5.35), and the convergence properties of the two OPE expansions [48], it is clear that the correlator exhibits branch cuts originating at $z = 0$ and $z = 1$.

We can deform the contour as depicted in Figure 3.2. Assuming once more that we can disregard the contribution from the circle at infinity and the two small circles at $z' = 0$ and $z' = 1$, we obtain

$$F(z) = \frac{1}{2\pi i} \int_{-\infty}^0 dz' \frac{\text{Disc}_{z' < 0}[F(z')]}{z' - z} + \frac{1}{2\pi i} \int_1^{\infty} dz' \frac{\text{Disc}_{z' > 1}[F(z')]}{z' - z}. \quad (3.2.37)$$

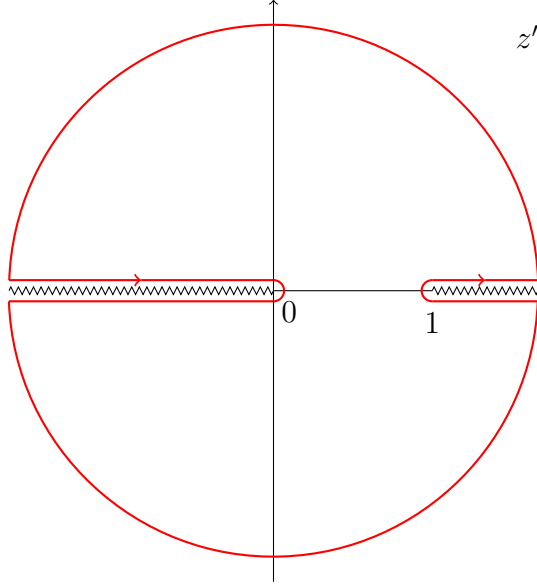


Figure 3.2: Contour deformation for the boundary case.

The discontinuities can be computed from the two OPE expansions, in a similar way as in (2.5.24). Explicitly,

$$\begin{aligned} \text{Disc}_{z<0}[F(z)] &= \sum_{\hat{\mathcal{O}}} 2i \sin(\pi \hat{\Delta}) b_{\phi \hat{\mathcal{O}}}^2 (-z)^{\hat{\Delta}} {}_2F_1 \left(\hat{\Delta}, \hat{\Delta} + 1 - \frac{d}{2}, 2\hat{\Delta} + 2 - d, z \right), \\ \text{Disc}_{z>1}[F(z)] &= \sum_{\mathcal{O}} 2i \sin \left[\frac{\pi}{2} (\Delta - 2\Delta_{\phi}) \right] a_{\mathcal{O}} \lambda_{\phi \phi \mathcal{O}} z^{\Delta_{\phi}} (z-1)^{\frac{\Delta-2\Delta_{\phi}}{2}} \tilde{f}_{\Delta}(z), \end{aligned} \quad (3.2.38)$$

where we used the explicit forms of the blocks, (2.5.34) and (2.5.35), and we defined $\tilde{f}_{\Delta}(z) = (1-z)^{-\frac{\Delta}{2}} f_{\Delta}(z)$.

Let us now discuss the convergence at $z' = 0, 1, \infty$. In the boundary channel, the lightest exchanged operator is the boundary identity, corresponding to $\hat{\Delta} = 0$ in (2.5.34). All other boundary operators contribute terms that vanish for $z = 0$, so this limit does not pose any problem. At $z = 1$, the dominant contribution comes from the bulk identity, which, according to (2.5.33), implies $F(z) \sim (1-z)^{-\Delta_{\phi}}$. This is similar to the behavior observed in the case of a generic defect for $w \rightarrow r$ (see (3.2.21)). Therefore, the same argument that was applied in that context is applicable here: if $\Delta_{\phi} > 1$, one interprets the singular terms as giving rise to a discontinuity with distributional values (i.e. a delta-function and its derivatives).

The circle at $|z| \rightarrow \infty$ presents a subtler situation since it is not directly governed by an OPE expansion. However, compared to higher codimension cases, the situation is under much greater control. In [48], the authors managed to derive an upper bound on the behavior of a boundary correlator as $|z| \rightarrow \infty$

$$F(z) \sim z^{\Delta_{\phi}}, \quad \text{for } |z| \rightarrow \infty. \quad (3.2.39)$$

We can then improve the dispersion relation (3.2.37) by introducing a suitable prefactor as we did in (3.2.24). A possible choice is

$$F(z) = \frac{z^{\Delta_\phi+1}}{2\pi i} \int_{-\infty}^0 dz' \frac{\text{Disc}_{z'<0} \left[\frac{F(z')}{(z')^{\Delta_\phi+1}} \right]}{z' - z} + \frac{z^{\Delta_\phi+1}}{2\pi i} \int_1^\infty dz' \frac{\text{Disc}_{z'>1} \left[\frac{F(z')}{(z')^{\Delta_\phi+1}} \right]}{z' - z}. \quad (3.2.40)$$

Clearly this choice affects the behavior of the integrand at $z' = 0$ and one should reconsider the contribution from the small circle around $z' = 0$, in case the integral diverges. It's important to note that the choice of prefactor $z^{-\Delta_\phi-1}$ in (3.2.40) is not unique. For example, one could use a different prefactor $(1-z)^{-\Delta_\phi-1}$, or a combination of the two. In a perturbative context, different choices may reduce the number of exchanged operators required to compute the discontinuities. We shall see an example in Section 4.3.

Chapter 4

Applications

In this chapter, we apply the tools of the analytic bootstrap, introduced in Chapters 2 and 3, to several defect CFTs that are relevant in the context of condensed matter physics or holography.

We begin by examining three distinct types of defects in the critical $O(N)$ model. The $O(N)$ model is a well-known field theory which can be realized by deforming the four-dimensional free theory of N scalar fields by a quartic $O(N)$ invariant interaction. It is characterized by the following action

$$S = \int d^d x \left[\frac{1}{2} (\partial_\mu \phi_a)^2 + \frac{\lambda_0}{4!} (\phi_a \phi_a)^2 \right], \quad a = 1, \dots, N, \quad (4.0.1)$$

where λ_0 is the bare coupling and the fundamental fields ϕ_a transform in the vector representation of $O(N)$. For $d = 4 - \varepsilon < 4$, the coupling λ is relevant and it triggers a renormalization group flow, which can be studied perturbatively in ε . The β -function for the quartic coupling reads

$$\beta_\lambda = \frac{\partial \lambda}{\partial \log \mu} = -\varepsilon \lambda + \frac{N+8}{48\pi^2} \lambda^2 + O(\lambda^3), \quad (4.0.2)$$

and a non-trivial fixed point is reached for

$$\lambda_* = \frac{48\pi^2}{N+8} \varepsilon + \frac{144\pi^2(3N+14)}{(N+8)^3} \varepsilon^2 + \mathcal{O}(\varepsilon^3). \quad (4.0.3)$$

This is the so-called Wilson-Fisher fixed point. This solution is perturbative in ε and this is the regime we are going to be interested in. The critical $O(N)$ model has numerous applications in condensed matter physics. Notable examples of critical models within the same universality class include the Ising model for $N = 1$, the XY model and the Helium superfluid transition for $N = 2$, and isotropic magnets for $N = 3$.

In Section 4.1, we consider the *localized magnetic field* defect. It is obtained by turning on a magnetic field along a line, breaking the $O(N)$ symmetry down to $O(N-1)$ along the defect. In Lorentzian signature, it can be viewed as a point-like impurity

generated by an external magnetic field, extended over the time direction. This line defect can be effectively realized on the lattice and has been studied through Monte Carlo simulations in [105, 106]. Experimental applications are also conceivable, either in quantum simulators [107] or in a mixture of two liquids with a colloidal impurity [108, 109, 106]. Therefore, it is crucial to produce predictions for the defect CFT data of this critical system. The localized magnetic field was studied using traditional field-theoretic methods, either in the large N limit or using the ε -expansion, in [110–112]. More recently, [42] analyzed this defect for $N = 2$ using numerical bootstrap techniques for the four-point function of defect operators. Here we calculate, for the first time, the two-point function of the bulk operator ϕ_a up to order ε using both the analytic bootstrap and diagrammatic methods, extracting an infinite set of defect CFT data. This analysis is based on [58].

Next, in Section 4.2, we conduct a similar analysis for a different line defect known as the *spin impurity*. This defect was originally introduced in [113, 114] to model a doped two-dimensional antiferromagnet at the quantum critical point. Recently, there has been renewed interest in this setup. In [115], it was analyzed at large N with the goal of understanding the interplay between symmetry-protected topological phases and quantum criticality. Additionally, [116] provided a semiclassical description of this defect in the limit of large spin. It was also noted in [117] that these defects emerge in a specific scaling limit of superconformal Wilson lines in $\mathcal{N} = 4$ SYM theory. We examine this defect in both the free ($\lambda = 0$) and interacting bulk cases. Specifically, for the free case, we compute the defect β -function up to three loops. We also analyze the spectrum of defect operators and bootstrap the two-point functions of bulk operators up to order ε^2 , comparing the results with explicit diagrammatic computations. This section is based on [59].

Finally, in Section 4.3, we use the boundary dispersion relation (3.2.2) to bootstrap the two-point function of ϕ_a in the presence of a boundary. We successfully reproduce the results of [47] up to order ε^2 . This section is based on [56].

In the final section of this chapter, Section 4.4, we consider a different bulk theory, specifically $\mathcal{N} = 4$ Super Yang-Mills (SYM), which is defined by the following action

$$S = \int dx^4 \text{Tr} \left\{ -\frac{1}{2g_{YM}^2} F_{\mu\nu} F^{\mu\nu} + \frac{\Theta}{8\pi^2} F_{\mu\nu} \tilde{F}^{\mu\nu} - i\bar{\chi}^a \bar{\sigma}^\mu D_\mu \chi_a - D_\mu \Phi^I D^\mu \Phi^I \right. \\ \left. + g_{YM} C_I^{ab} \chi_a [\Phi^I, \chi_b] + g_{YM} \bar{C}_{Iab} \bar{\chi}^a [\Phi^I, \bar{\chi}^b] + \frac{g_{YM}^2}{2} [\Phi^I, \Phi^J]^2 \right\}, \quad (4.0.4)$$

where g_{YM} is the gauge coupling, Θ is the instanton angle, $F_{\mu\nu}$ is the field strength associated to the $SU(N)$ gauge field A_μ , χ^a are Weyl fermions, σ^μ are the Pauli matrices, D_μ are covariant derivatives, Φ^I are six real scalars that transform in the vector of $SO(6)$, and C_I^{ab} represents the structure constants of the R-symmetry group $SU(4) \cong$

$SO(6)$. This theory is (super)conformal and holographically¹ dual to type IIB string theory in $AdS_5 \times S^5$ [12]. We analyze this theory at large N in the presence of a supersymmetric Wilson line (or Maldacena-Wilson line [121]) and consider correlators of both defect and bulk operators. Specifically, we compute the four-point function of the fundamental scalars Φ^I inserted on the defect and the two-point function of single trace 1/2 BPS bulk operators² $\mathcal{O}_P \propto \text{Tr}(Y \cdot \Phi)^P$, using the dispersion relations (3.1.1) and (3.2.1). In the former case, we reproduce state-of-the-art results up to fourth order in a perturbative expansion at strong 't Hooft coupling $\lambda = g_{YM}^2 N$ [51]. In the latter case, we reproduce the results of [104] at large N and strong coupling. The content of Section 4.4 is based on [56] and [57].

4.1 The localized magnetic field in the $O(N)$ model

In this section, we apply analytic bootstrap techniques to study the two-point correlator of local operators in the $O(N)$ critical model in the presence of a defect, which is created by coupling the field ϕ_1 to a magnetic field localized on a line [112]

$$\mathcal{D} = e^{h_0 \int d\tau |\dot{x}(\tau)| \phi_1(x(\tau))}. \quad (4.1.1)$$

Here, $x(\tau)$ represents a straight line (or equivalently, a circle) as the real parameter τ varies, and h_0 is a new coupling constant. The defect explicitly breaks the $O(N)$ global symmetry of the model down to $O(N-1)$. In the free theory in four dimensions, this perturbation provides a straightforward example of a conformal defect, as the operator ϕ has dimension one, and h_0 is a defect marginal parameter [122]. As we move away from four dimensions, the bulk theory flows to the Wilson-Fisher fixed point, and the operator ϕ becomes a weakly relevant defect deformation (the bulk dimension is $4 - \varepsilon$, but the defect dimension remains fixed at one). Consequently, this perturbation, along with the quartic interaction, triggers a renormalization group flow in the two coupling constants. One can investigate this joint flow using standard diagrammatic techniques without needing to work perturbatively in h_0 . Indeed, any diagram contributing to a correlator at a fixed order in λ will only include insertions of h_0 up to a finite power. In other words, h_0 is not treated as a small coupling constant. The RG flow reaches an infrared fixed point at the following values of the renormalized coupling constants [111, 112]

$$\lambda_* = \frac{48\pi^2}{N+8}\varepsilon + \mathcal{O}(\varepsilon^2), \quad h_* = \sqrt{N+8} + \frac{4N^2 + 45N + 170}{4(N+8)^{\frac{3}{2}}}\varepsilon + \mathcal{O}(\varepsilon^2). \quad (4.1.2)$$

This implies that the fixed point can be described by a defect conformal field theory.

¹We refer to [118–120] for an introduction to the AdS/CFT correspondence and holography.

²See equation (4.4.63) and the discussion above it for a proper definition of single trace 1/2 BPS operators \mathcal{O}_P .

4.1.1 The observable: the bulk two-point function

The main observable we consider is the two-point function of the vector of scalar fields ϕ_a with $a = 1, \dots, N$. Conformal and global symmetries constrain this correlator to take the following form

$$\langle \phi_a(x_1) \phi_b(x_2) \rangle_{\mathcal{D}} = \frac{F_1(z, \bar{z}) \delta_{ab} + F_2(z, \bar{z}) \delta_{a1} \delta_{b1}}{|x_1^i|^{\Delta_\phi} |x_2^i|^{\Delta_\phi}}, \quad (4.1.3)$$

where $F_1(z, \bar{z})$ and $F_2(z, \bar{z})$ are arbitrary functions of the two conformally invariant cross-ratios z and \bar{z} , defined in (2.5.7). We recall that correlation functions in presence of a defect are defined as in (2.5.2).

As discussed in Section 2.5.1, in a defect conformal field theory there are bulk-bulk and bulk-defect OPE channels, see (2.2.10) and (2.5.12). These expansions can be further refined to explicitly account for the internal symmetry structure of the theory.

In the bulk channel, the OPE of two operators transforming under the representations R_1 and R_2 of the internal symmetry group must involve exchanged operators in irreducible representations contained in the Clebsch-Gordan decomposition of $R_1 \otimes R_2$. For our model, the OPE for two fundamental scalar fields can be written as:

$$\phi_a(x_1) \phi_b(x_2) = \sum_{\Delta, \ell, R} \lambda_{\phi\phi\mathcal{O}}^{abI} \mathcal{C}(x_{12}, \partial_2) \mathcal{O}_{\Delta, \ell}^R(x_2), \quad (4.1.4)$$

where R denotes the $O(N)$ irreducible representations in the tensor product $V \otimes V$ of two vector representations V , which include the singlet (S), symmetric traceless (T) and antisymmetric (A) representations. We have suppressed spacetime indices. Since this OPE is between scalar operators, only operators in even spin- ℓ traceless symmetric representations of $SO(d)$ can appear in the decomposition. The tensor structure of the three-point function coefficients $\lambda_{\phi\phi\mathcal{O}_S}^{ab}$ can be explicitly written down for $R = S, T, A$ as

$$\lambda_{\phi\phi\mathcal{O}_S}^{ab} = \lambda_{\phi\phi\mathcal{O}_S} \delta_{ab}, \quad \lambda_{\phi\phi\mathcal{O}_T}^{ab(cd)} = \lambda_{\phi\phi\mathcal{O}_T} \left(\delta_{a(c} \delta_{bd)} - \frac{1}{N} \delta_{ab} \delta_{cd} \right), \quad \lambda_{\phi\phi\mathcal{O}_A}^{ab[cd]} = \lambda_{\phi\phi\mathcal{O}_A} \delta_{a[c} \delta_{bd]}, \quad (4.1.5)$$

where the (anti-)symmetrization has been taken with weight $1/2$.

In the defect OPE, the operators are categorized into $O(N-1)$ representations since the presence of the defect breaks the $O(N)$ symmetry. Generally, when a symmetry group G is broken down to a subgroup H by a defect, bulk operators originally in a representation R of G will transform according to irreducible representations found in the decomposition of R under H . Hence we can write

$$\phi_a(x) = \sum_{\hat{\Delta}, s, R} b_{\phi\hat{\mathcal{O}}}^{aR} \hat{\mathcal{C}}(x, \partial) \hat{\mathcal{O}}_{\hat{\Delta}, s}^R(x), \quad (4.1.6)$$

where $\hat{\Delta}$ and s represent the conformal dimension and transverse spin of the defect operator $\hat{\mathcal{O}}_{\hat{\Delta},s}^R$, respectively. Since $\phi_a(x)$ is a scalar field, the exchanged operators in this OPE do not possess longitudinal spin. From the branching rule $V^{O(N)} \rightarrow S^{O(N-1)} \oplus V^{O(N-1)}$, it is clear that the only permissible representations R are the singlet S and the vector V of $O(N-1)$. The tensor structures for the bulk-defect two-point function coefficients $b_{\phi\hat{\mathcal{O}}}^{aR}$ are

$$b_{\phi\hat{\mathcal{O}}_S}^a = b_{S,\hat{\Delta},s}\delta_{a1}, \quad b_{\phi\hat{\mathcal{O}}_V}^{a\hat{b}} = b_{V,\hat{\Delta},s}\delta_{a\hat{b}}, \quad (4.1.7)$$

where $\hat{b} = 2, \dots, N$, and δ_{a1} and $\delta_{a\hat{b}}$ are projectors from the representation space of $V^{O(N)}$ to those of $S^{O(N-1)}$ and $V^{O(N-1)}$, respectively.

These different OPE decompositions result in two distinct conformal block expansions. To analyze the bulk block expansion, it is helpful to express the bulk two-point function as

$$\langle \phi_a(x_1)\phi_b(x_2) \rangle_{\mathcal{D}} = \frac{F_S(z, \bar{z})\delta_{ab} + F_T(z, \bar{z})\left(\delta_{a1}\delta_{b1} - \frac{1}{N}\delta_{ab}\right)}{|x_1^i|^{\Delta_\phi}|x_2^i|^{\Delta_\phi}}, \quad (4.1.8)$$

where $F_S(z, \bar{z})$ and $F_T(z, \bar{z})$ are linear combinations of the functions $F_1(z, \bar{z})$ and $F_2(z, \bar{z})$ introduced in (4.1.3). Explicitly,

$$\begin{aligned} F_1(z, \bar{z}) &= F_S(z, \bar{z}) - \frac{1}{N}F_T(z, \bar{z}), \\ F_2(z, \bar{z}) &= F_T(z, \bar{z}). \end{aligned} \quad (4.1.9)$$

In terms of lightcone coordinates, this bulk channel decomposition reads

$$F_S(z, \bar{z})\delta_{ab} + F_T(z, \bar{z})\left(\delta_{a1}\delta_{b1} - \frac{1}{N}\delta_{ab}\right) = \left(\frac{\sqrt{z\bar{z}}}{(1-z)(1-\bar{z})}\right)^{\Delta_\phi} \sum_{\substack{\Delta,\ell \\ R=S,T}} \lambda_{\phi\hat{\mathcal{O}}}^{abR} a_{\hat{\mathcal{O}}}^R f_{\Delta,\ell}(z, \bar{z}), \quad (4.1.10)$$

where the explicit form of the bulk conformal blocks $f_{\Delta,\ell}(z, \bar{z})$ is given in (2.5.18). Note that the only bulk operators that have a non vanishing one-point function are those who exchange the identity operator in their defect OPE. Therefore, the tensor structures for the coefficients $a_{\hat{\mathcal{O}}}^R$ are obtained by projecting $O(N)$ representations into the singlet $S^{O(N-1)}$. It immediately follows that operators in antisymmetric representations have zero one-point functions. Hence, the sum in (4.1.10) only includes the singlet S and the symmetric traceless T representations of $O(N)$. The tensor structures of the one-point functions for $R = T, S$ are

$$a_{\mathcal{O}_S}, \quad a_{\mathcal{O}_T}^{(ab)} = a_{\mathcal{O}_T} \left(\delta_{a1}\delta_{b1} - \frac{1}{N}\delta_{ab} \right). \quad (4.1.11)$$

Inserting (4.1.5) and (4.1.11) into (4.1.10) we get the following block decompositions

$$F_S(z, \bar{z}) = \left(\frac{\sqrt{z\bar{z}}}{(1-z)(1-\bar{z})} \right)^{\Delta_\phi} \sum_{\Delta, \ell} \lambda_{\phi\phi\mathcal{O}_S} a_{\mathcal{O}_S} f_{\Delta, \ell}(z, \bar{z}), \quad (4.1.12)$$

$$F_T(z, \bar{z}) = \left(\frac{\sqrt{z\bar{z}}}{(1-z)(1-\bar{z})} \right)^{\Delta_\phi} \sum_{\Delta, \ell} \lambda_{\phi\phi\mathcal{O}_T} a_{\mathcal{O}_T} f_{\Delta, \ell}(z, \bar{z}). \quad (4.1.13)$$

Similarly, for the defect channel, it is useful to rewrite the bulk two-point function as

$$\langle \phi_a(x_1) \phi_b(x_2) \rangle_{\mathcal{D}} = \frac{\hat{F}_S(z, \bar{z}) \delta_{a1} \delta_{b1} + \hat{F}_V(z, \bar{z}) (\delta_{ab} - \delta_{a1} \delta_{b1})}{|x_1^i|^{\Delta_\phi} |x_2^i|^{\Delta_\phi}}, \quad (4.1.14)$$

where again $\hat{F}_S(z, \bar{z})$ and $\hat{F}_V(z, \bar{z})$ are linear combinations of $F_1(z, \bar{z})$ and $F_2(z, \bar{z})$,

$$\begin{aligned} F_1(z, \bar{z}) &= \hat{F}_V(z, \bar{z}), \\ F_2(z, \bar{z}) &= \hat{F}_S(z, \bar{z}) - \hat{F}_V(z, \bar{z}). \end{aligned} \quad (4.1.15)$$

The defect channel decomposition is

$$\hat{F}_S(z, \bar{z}) \delta_{a1} \delta_{b1} + \hat{F}_V(z, \bar{z}) (\delta_{ab} - \delta_{a1} \delta_{b1}) = \sum_{\substack{\hat{\Delta}, s \\ R=S, V}} b_{\phi\hat{\mathcal{O}}}^{aR} b_{\phi\hat{\mathcal{O}}}^{bR} \hat{f}_{\hat{\Delta}, s}(z, \bar{z}), \quad (4.1.16)$$

where the explicit form of the defect conformal blocks $\hat{f}_{\hat{\Delta}, s}(z, \bar{z})$ is given in (2.5.15).

Using (4.1.7) one gets

$$\hat{F}_S(z, \bar{z}) = \sum_{\hat{\Delta}, s} b_{S, \hat{\Delta}, s}^2 \hat{f}_{\hat{\Delta}, s}(z, \bar{z}), \quad \hat{F}_V(z, \bar{z}) = \sum_{\hat{\Delta}, s} b_{V, \hat{\Delta}, s}^2 \hat{f}_{\hat{\Delta}, s}(z, \bar{z}). \quad (4.1.17)$$

4.1.2 Leading order

We are now ready to compute the two-point function (4.1.3) in $d = 4 - \varepsilon$

$$F(r, w) = F^{(0)}(r, w) + \varepsilon F^{(1)}(r, w) + \mathcal{O}(\varepsilon^2), \quad \varepsilon \ll 1. \quad (4.1.18)$$

At leading order, the correlator has two components: the free correlator without the defect, which contributes to F_1 in (4.1.3), and the square of the one-point function

$$\langle \phi_a(x) \rangle_{\mathcal{D}} = \delta_{a1} \frac{a_\phi}{|x^i|^{\Delta_\phi}}. \quad (4.1.19)$$

which provides the leading contribution ³ to F_2 . The dimension of ϕ_a is

$$\begin{aligned} \Delta_\phi &= \frac{d-2}{2} + \varepsilon \gamma_\phi^{(1)} + \varepsilon^2 \gamma_\phi^{(2)} + \mathcal{O}(\varepsilon^3) \\ &= 1 - \frac{\varepsilon}{2} + \varepsilon^2 \frac{N+2}{4(N+8)^2} + \mathcal{O}(\varepsilon^3), \end{aligned} \quad (4.1.20)$$

³The defect coupling at the fixed point is not infinitesimally small, so the one-point function (4.1.19) is not suppressed in the ε -expansion.

and a_ϕ in (4.1.19) reads [111, 112]

$$a_\phi^2 = \frac{N+8}{4} + \varepsilon \frac{(N^2 - 3N + (N+8)^2 \log(4) - 22)}{8(N+8)} + \mathcal{O}(\varepsilon^2). \quad (4.1.21)$$

The leading-order contributions to the two-point function are

$$F_1^{(0)}(r, w) = \frac{rw}{(w-r)(1-rw)}, \quad F_2^{(0)}(r, w) = a_\phi^2. \quad (4.1.22)$$

Notice that we switched to the radial coordinates introduced in (2.5.9). Each term has a straightforward interpretation in one of the two channels. The correlator $F_1^{(0)}$ corresponds to the exchange of the identity operator in the bulk channel, while the squared one-point function corresponds to the exchange of the identity in the defect channel. As usual, to represent the identity in one channel, an infinite tower of operators is necessary in the crossed channel. Let us review the CFT data of these exchanged operators.

Rewriting (4.1.22) in terms of F_S and F_T introduced in (4.1.8), we find

$$\begin{aligned} F_S^{(0)}(r, w) &= \frac{a_\phi^2}{N} + \frac{rw}{(w-r)(1-rw)}, \\ F_T^{(0)}(r, w) &= a_\phi^2. \end{aligned} \quad (4.1.23)$$

This expression shows that the bulk identity contributes solely to the singlet exchange. On the other hand, the constant term a_ϕ^2 is reproduced by the exchange of two infinite towers of twist-two spin- ℓ operators of the schematic form

$$\mathcal{J}_{S,0,\ell} = \phi^a \partial_{\mu_1} \dots \partial_{\mu_\ell} \phi_a, \quad \mathcal{J}_{T,0,\ell}^{ab} = \phi^a \partial_{\mu_1} \dots \partial_{\mu_\ell} \phi^b - \text{trace}. \quad (4.1.24)$$

Their CFT data can be extracted by comparing (4.1.23) with the block expansion (4.1.12) or using the Lorentzian inversion formula (2.5.26) with ⁴

$$\begin{aligned} \text{dDisc} \left[\left(\frac{(1-z)(1-\bar{z})}{\sqrt{z\bar{z}}} \right)^{\Delta_\phi} F_S^{(0)}(z, \bar{z}) \right] &= 2 \frac{a_\phi^2}{N} \frac{(1-z)(1-\bar{z})}{\sqrt{z\bar{z}}}, \\ \text{dDisc} \left[\left(\frac{(1-z)(1-\bar{z})}{\sqrt{z\bar{z}}} \right)^{\Delta_\phi} F_T^{(0)}(z, \bar{z}) \right] &= 2a_\phi^2 \frac{(1-z)(1-\bar{z})}{\sqrt{z\bar{z}}}. \end{aligned} \quad (4.1.25)$$

The result is ⁵ [45]

$$\begin{aligned} \Delta_{S,0,\ell}^{(0)} &= \Delta_{T,0,\ell}^{(0)} = 2\Delta_\phi + \ell, \\ a\lambda_{T,0,\ell}^{(0)} &= a\lambda_{S,0,\ell}^{(0)} N = a_\phi^2 \frac{2^{-\ell} \Gamma\left(\frac{\ell+1}{2}\right)^3}{\pi \Gamma\left(\frac{\ell}{2} + 1\right) \Gamma\left(\ell + \frac{1}{2}\right)}. \end{aligned} \quad (4.1.26)$$

⁴As we mentioned above (2.5.29), the Lorentzian inversion formula does not work for low spins. In this case, it misses the contribution of the bulk identity. Nevertheless, it still reproduces correctly all the defect CFT data of the twist-two operators.

⁵The twist-two operators have the same dimensions in both channel at tree level, however they are distinct operators and have different anomalous dimensions and OPE coefficients.

where the spin ℓ is even. Let us clarify our notations for the CFT data and the labeling of the operators, which will remain consistent at order ε . We define $a\lambda_{R,k,\ell}^{(0)} \equiv a_{\mathcal{J}_{R,k,\ell}}^{(0)} \lambda_{\phi\phi\mathcal{J}_{R,k,\ell}}^{(0)}$ and we use the index k to label the classical twist $\tau^{(0)} = \Delta^{(0)} - \ell$, specifically $k = \frac{\tau^{(0)}}{2} - \Delta_\phi$. At this order, only two families of operators appear in the bulk OPE: the identity and the twist-two operators ($k = 0$), see (4.1.24). Furthermore, for the specific case $k = 0$ we know that there is a single primary operator for any given spin ℓ . However, for higher values of k , corresponding to operators of the schematic form $\mathcal{J}_{S/T,k,\ell} \sim \phi \square^k \partial_{\mu_1} \dots \partial_{\mu_\ell} \phi$, degeneracies may occur. Thus, our notation will not differentiate between degenerate operators, but since our observable does not make this distinction either, we find this notation convenient.

Turning to the defect channel, we have

$$\begin{aligned}\hat{F}_S^{(0)}(r, w) &= a_\phi^2{}^{(0)} + \frac{rw}{(w-r)(1-rw)}, \\ \hat{F}_V^{(0)}(r, w) &= \frac{rw}{(w-r)(1-rw)}.\end{aligned}\tag{4.1.27}$$

The defect identity contributes only to the singlet channel, while the bulk identity is represented by two infinite towers of defect operators of the schematic form ⁶

$$\hat{\mathcal{O}}_{S,0,s} = \partial_\perp^s \phi^1, \quad \hat{\mathcal{O}}_{V,0,s}^{\hat{a}} = \partial_\perp^s \phi^{\hat{a}}.\tag{4.1.28}$$

These operators have transverse spin s and transverse twist $\hat{\tau} = \hat{\Delta} - s = 1$. By comparing (4.1.27) with the block expansion (4.1.17) or using the inversion formula (2.5.21) with ⁷

$$\begin{aligned}\text{Disc}[\hat{F}_S^{(0)}(r, w)] &= 2\pi i \left(\frac{rw}{1-rw} \right) \delta(r-w), \\ \text{Disc}[\hat{F}_V^{(0)}(r, w)] &= 2\pi i \left(\frac{rw}{1-rw} \right) \delta(r-w).\end{aligned}\tag{4.1.29}$$

we find [44, 38]

$$\begin{aligned}\hat{\Delta}_{S,0,s}^{(0)} &= \hat{\Delta}_{V,0,s}^{(0)} = 1 + s, \\ b_{S,m,s}^{2(0)} &= b_{V,m,s}^{2(0)} = \delta_{m,0},\end{aligned}\tag{4.1.30}$$

where $b_{R,m,s}^{2(0)} = b_{\phi\hat{\mathcal{O}}_{R,m,s}}^{2(0)}$. As in the bulk case, we use an additional label m for the classical transverse twist, $m = \frac{\hat{\tau}^{(0)} - 1}{2}$. At this order, only twist-one operators ($m = 0$) appear in the OPE, as expected from the equation of motion of the bulk field [44].

⁶Here ∂_\perp stands for the derivative in the direction orthogonal to the defect, therefore $\partial_\perp^s \phi$ are not defect descendants.

⁷In this case the Lorentzian inversion formula fails to reproduce the contribution of the defect identity.

4.1.3 Next-to-leading order

Now we turn our attention to the order ε correlator, which we compute using the methods outlined in Section 3.2. The idea of the defect analytic bootstrap is to use information from the bulk theory to compute correlators in the presence of the defect. Specifically, the discontinuity relevant to the dispersion relation (3.1.1) is governed by the bulk block expansion, as detailed in (2.5.24). We consider the following perturbative expansion of the bulk channel CFT data

$$\begin{aligned}\Delta &= \Delta^{(0)} + \varepsilon \gamma^{(1)} + \mathcal{O}(\varepsilon^2), \\ a\lambda &= a\lambda^{(0)} + \varepsilon a\lambda^{(1)} + \mathcal{O}(\varepsilon^2).\end{aligned}\tag{4.1.31}$$

Operators that appeared at tree level, specifically twist-two operators, enter the one-loop OPE with their anomalous dimensions given by

$$\Delta_{S/T,0,\ell} = 2\Delta_\phi + \ell + \varepsilon \gamma_{S/T,0,\ell}^{(1)} + \mathcal{O}(\varepsilon^2).\tag{4.1.32}$$

These anomalous dimensions are known from previous studies of the $O(N)$ model without defects (see for example [123] and references therein)

$$\gamma_{S,0,\ell}^{(1)} = \frac{N+2}{N+8} \delta_{0,\ell}, \quad \gamma_{T,0,\ell}^{(1)} = \frac{2}{N+8} \delta_{0,\ell}.\tag{4.1.33}$$

Importantly, only the spin-zero operators of each representation, $\mathcal{J}_{S,0,0} = \phi^2$ and $\mathcal{J}_{T,0,0}^{ab} \equiv T_{ab} = \phi_a \phi_b - \frac{\delta_{ab}}{N} \phi^2$, have a non-zero anomalous dimension at order ε . This fact will greatly simplify the computation of the discontinuity.

At this order higher-twist operators can appear, with their classical dimensions given by

$$\Delta_{S/T,k,\ell} = 2\Delta_\phi + 2k + \ell + \mathcal{O}(\varepsilon), \quad k > 0.\tag{4.1.34}$$

We anticipate the appearance of operators up to twist four ⁸ because the bulk OPE coefficients $\lambda_{\phi\phi\mathcal{J}}$ of higher-twist operators are of order ε^2 [79, 80].

All in all, at order ε , the bulk block expansion for the singlet reads

$$\begin{aligned}F_S^{(1)}(r, w) &= -\frac{rw}{2(1-rw)(w-r)} \log\left(\frac{rw}{(1-rw)(w-r)}\right) + \\ &+ \frac{rw}{2(1-rw)} a\lambda_{\phi^2}^{(0)} \gamma_{\phi^2}^{(1)} \left(\tilde{f}_{2,0}(r, w) \log(w-r) + \partial_\Delta \tilde{f}_{2,0}(r, w) \right) + \\ &+ \sum_{k=0}^1 \sum_{\ell} \frac{rw}{1-rw} a\lambda_{S,k,\ell}^{(1)} (w-r)^k \tilde{f}_{2+2k+\ell,\ell}(r, w),\end{aligned}\tag{4.1.35}$$

⁸While twist-two operators consist of a single family, meaning a single primary operator for each spin, from twist four onwards, degeneracies may arise that cannot be resolved by analyzing a single correlator. However, these operators do not contribute to the discontinuity in (3.2.1), hence this does not affect the computation of the correlator.

where we defined $\tilde{f}_{\Delta,\ell}(r, w) = (w - r)^{-\frac{\Delta+\ell}{2}} f_{\Delta,\ell}$, with $f_{\Delta,\ell}$ given in (2.5.19).

Notice that the first line in (4.1.35) originates from the contribution of the bulk identity operator

$$\left(\frac{rw}{(w-r)(1-rw)}\right)^{\Delta_\phi} = \frac{rw}{(r-w)(rw-1)} + \varepsilon \left(\gamma_\phi^{(1)} - \frac{1}{2}\right) \frac{rw}{(1-rw)(w-r)} \log\left(\frac{rw}{(1-rw)(w-r)}\right) + \mathcal{O}(\varepsilon^2). \quad (4.1.36)$$

Specifically, the anomalous dimension $\gamma_\phi^{(1)}$ is well-known to be vanishing at this order, see (4.1.20).

For the symmetric traceless part, the bulk OPE reads

$$F_T^{(1)}(r, w) = \frac{rw}{2(1-rw)} a\lambda_T^{(0)} \gamma_T^{(1)} \left(\tilde{f}_{2,0}(r, w) \log(w-r) + \partial_\Delta \tilde{f}_{2,0}(r, w)\right) + \sum_{k=0}^1 \sum_{\ell} \frac{rw}{1-rw} a\lambda_{T,k,\ell}^{(1)} (w-r)^k \tilde{f}_{2+2k+\ell}(r, w). \quad (4.1.37)$$

With the bulk OPE expansions (4.1.35) and (4.1.37), we can compute the discontinuity and then use the dispersion relation (3.2.1) to determine the full correlator. We assume that after subtracting the defect identity a_ϕ^2 , the rest of the correlator vanishes for $w \rightarrow \infty$. In other words, we assume that the dispersion relation is able to reconstruct the correlator up to a single low-spin ambiguity

$$F_{\text{amb}}(r, w) = a_\phi^2. \quad (4.1.38)$$

While we cannot prove this fact rigorously, we can derive it from the assumption that, at order ε , only the twist-one family appears in the defect OPE. This assumption is motivated by the fact ⁹ that higher-twist defect operators have bulk-to-defect couplings $b_{\phi\hat{\mathcal{O}}}$ of order ε and therefore their squared coefficients are at least of order ε^2 . Provided the assumption is true, the most general ansatz for the ambiguity is

$$F_{\text{amb}}(r, w) = (q_0 + r_0 \partial_{\hat{\Delta}}) \hat{f}_{0,0} + (q_1 + r_1 \partial_{\hat{\Delta}}) \hat{f}_{1,0} + \sum_{s=1}^{s_*} (q_{s+1} + r_{s+1} \partial_{\hat{\Delta}}) \hat{f}_{s+1,s}, \quad (4.1.39)$$

where q and r are arbitrary constants. For any finite $s_* \in \mathbb{N}$, the conformal blocks in this sum can be written as polylogarithms using HypExp [124, 125]. For example, the lowest lying ones take a very simple form:

$$\hat{f}_{0,0}(r, w) = 1, \quad \partial_{\hat{\Delta}} \hat{f}_{0,0}(r, w) = \log \frac{r}{1-r^2}, \quad \hat{f}_{1,0}(r, w) = \tanh^{-1} r, \quad \dots \quad (4.1.40)$$

Expanding the ansatz (4.1.39) in the bulk channel is generally not feasible due to spurious terms incompatible with bulk-channel conformal blocks (2.5.19). Experimenting with low values of $s_* \leq 5$, we conclude that the most general truncated solution is

$$F_{\text{amb}}(r, w) = q_0 \hat{f}_{0,0}(r, w) + r_0 \left(\partial_{\hat{\Delta}} \hat{f}_{0,0}(r, w) - 2\hat{f}_{1,0}(r, w)\right) = q_0 + r_0 \log \frac{r}{(1+r)^2}. \quad (4.1.41)$$

⁹This fact follows from elementary diagrammatic considerations.

The constant term can be interpreted as the defect identity, while the logarithm signals the presence of a defect operator with $\hat{\Delta} \sim \varepsilon$. No such operator can be constructed from the fundamental field ϕ^a in presence of the defect (4.1.1). Therefore, we conclude that this contribution is absent¹⁰ and we obtain (4.1.38).

We will check at the end that our assumption is correct by comparing the full correlator obtained from the dispersion relation (4.1.44) with the result from Feynman diagrams, see Section 4.1.6.

Computation of the correlator

Starting with the singlet representation, we observe from (4.1.35) that the discontinuity in the first order of the ε -expansion arises solely from the logarithmic terms. This is because the rescaled blocks $\tilde{f}_{\Delta,\ell}(r, w)$ and their derivatives, evaluated at the tree-level dimensions (4.1.26), are regular as w approaches r . Importantly, the logarithmic terms depend linearly on leading order coefficients and next-to-leading order anomalous dimensions. Notice that (4.1.33), combined with (4.1.35), implies that the one-loop discontinuity of the singlet is just given by two terms: one represents the correction to the bulk identity coming from the engineering dimension of the external field, while the other is proportional to a single bulk block. Using

$$\text{Disc}[\log(w - r)] = 2\pi i, \quad (4.1.42)$$

and the explicit form of the bulk blocks as a series expansion (2.5.19) we find¹¹

$$\begin{aligned} \text{Disc}[F_S^{(1)}(r, w)] &= -i\pi \frac{rw}{(w-r)(1-rw)} + i\pi \frac{rw}{(w-r)(1-rw)} a\lambda_{\phi^2}^{(0)} \gamma_{\phi^2}^{(1)} f_{2,0}(r, w) = \\ &= -\pi i \frac{(rw)}{(r-w)(rw-1)} + \frac{N+2}{8N} \frac{4\pi\sqrt{rw} \left(F\left(\sin^{-1}\left(\sqrt{r}\sqrt{\frac{r-w}{1-rw}}\right) \middle| \frac{(rw-1)^2}{(r-w)^2}\right) - F\left(\sin^{-1}\left(\frac{\sqrt{\frac{r-w}{1-rw}}}{\sqrt{r}}\right) \middle| \frac{(rw-1)^2}{(r-w)^2}\right) \right)}{r-w}, \end{aligned} \quad (4.1.43)$$

where $F(x, k)$ is the incomplete elliptic integral of the first kind. It's important to emphasize that this contribution arises solely from a single operator in the bulk expansion, specifically the twist-two, spin-zero operator ϕ^2 , whose anomalous dimension (4.1.33) serves as our primary input. The intricate form of the function (4.1.43) is due to the presence of the bulk conformal block $f_{2,0}$, which is a particular case of the complicated expression in (2.5.19).

The first term in (4.1.43) trivially reproduces the correction to the bulk identity (4.1.36), as we expected. The second contribution, however, proves to be quite complicated and we could not solve the corresponding integral in the dispersion relation

¹⁰In the case of a spin impurity, a defect operator with vanishing classical dimension will indeed appear. We refer to Section 4.2.3 for a thorough discussion.

¹¹Alternatively, the discontinuity can be obtained using the general formula (3.2.16) by inserting the perturbative OPE data and expanding up to order ε .

in terms of simple functions. Nonetheless, we are able to provide a simple integral representation of the result or express it through a variety of special functions. We find

$$\begin{aligned}
F^{(1)}(r, w)_{S, \text{not id}} &= - \int_0^1 dx \frac{6r \tanh^{-1} \left[\frac{(1+(rw-1)x)(1+(\frac{r}{w}-1)x)}{1+x(r-1)} \right]}{\sqrt{(1+(rw-1)x)(1+(\frac{r}{w}-1)x)(1+x(r-1))}} = \\
&= \frac{N+2}{8N} \sum_{m=0}^{\infty} \frac{2^{1-m} rw(1-r^2)^m G_{4,4}^{4,2} \left(\frac{4w}{wr^2-(w^2+1)r+w} \middle| \begin{matrix} 0, 0, \frac{m}{2}, \frac{m+1}{2} \\ -\frac{1}{2}, 0, m, m \end{matrix} \right)}{(m!) (rw^2 - wr^2 + r - w)} = \tag{4.1.44}
\end{aligned}$$

$$= \frac{N+2}{8N} \frac{\partial}{\partial t} \left[\left(\frac{(r-w)(rw-1)}{(1+r)^2 w} \right)^t \frac{4r}{(1+r)^{2(2t+1)}} F_{101}^{112} \left(\begin{matrix} 1+t : \frac{1}{2}; \frac{1}{2} + t, 1; \\ \frac{3}{2} + t : -; 1 + t; \end{matrix} \left(\frac{1-r}{1+r} \right)^2, \frac{(r-w)(rw-1)}{(1+r)^2 w} \right) \right] \Bigg|_{t=0} \tag{4.1.45}$$

For later convenience, we define

$$F^{(1)}(r, w)_{S, \text{not id}} \equiv \frac{N+2}{8N} H(r, w) \tag{4.1.46}$$

The result (4.1.44) is expressed in terms of an infinite sum of Meijer G-functions or as a derivative of a Kampè de Fèriet function F_{101}^{112} , which can be represented as a triple hypergeometric sum [126]. A more compact representation of $H(r, w)$ is [127]

$$H(r, w) = \frac{rw}{(w-r)(1-rw)} (\partial_{\Delta} - 1 - \log 2) f_{\Delta,0}(r, w)|_{\Delta=2}, \tag{4.1.47}$$

where $f_{\Delta,0}(r, w)$ is a bulk block (2.5.18). Combining (4.1.44), (4.1.36) and the contribution of the defect identity, the singlet contribution reads

$$F_S^{(1)}(r, w) = \frac{a_{\phi}^2{}^{(1)}}{N} - \frac{rw}{2(1-rw)(w-r)} \log \left(\frac{rw}{(1-rw)(w-r)} \right) + \frac{N+2}{8N} H(r, w). \tag{4.1.48}$$

The analysis for the symmetric traceless is similar, the only difference being the absence of the bulk identity contribution and a change in the overall factor due to the OPE data (4.1.26) and (4.1.33). The discontinuity in this case is given by

$$\begin{aligned}
\text{Disc}[F_T^{(1)}(r, w)] &= \pi i \frac{rw}{(1-rw)(w-r)} a\lambda_T^{(0)} \gamma_T^{(1)} f_{2,0}(r, w) = \tag{4.1.49} \\
&= \frac{\pi \sqrt{rw} \left(F \left(\sin^{-1} \left(\sqrt{r} \sqrt{\frac{r-w}{1-rw}} \right) \middle| \frac{(rw-1)^2}{(r-w)^2} \right) - F \left(\sin^{-1} \left(\frac{\sqrt{\frac{r-w}{1-rw}}}{\sqrt{r}} \right) \middle| \frac{(rw-1)^2}{(r-w)^2} \right) \right)}{r-w},
\end{aligned}$$

and we find

$$F_T^{(1)}(r, w) = a_{\phi}^2{}^{(1)} + \frac{1}{4} H(r, w). \tag{4.1.50}$$

Using (4.1.9) and (4.1.15), we can rewrite the results (4.1.48) and (4.1.50) in terms of the functions \hat{F}_S and \hat{F}_T that are natural in the defect channel,

$$\begin{aligned}\hat{F}_S^{(1)}(r, w) &= a_\phi^{2(1)} - \frac{rw}{2(1-rw)(w-r)} \log \left(\frac{rw}{(1-rw)(w-r)} \right) + \frac{3}{8}H(r, w), \\ \hat{F}_V^{(1)}(r, w) &= -\frac{rw}{2(1-rw)(w-r)} \log \left(\frac{rw}{(1-rw)(w-r)} \right) + \frac{1}{8}H(r, w).\end{aligned}\tag{4.1.51}$$

In summary, using the dispersion relation (3.1.1), we are able to compute the full correlator at first order in ε -expansion just from the knowledge of zeroth order data and three (known) bulk data $\{\Delta_\phi, \gamma_{S,0,0}^{(1)}, \gamma_{T,0,0}^{(1)}\}$, given in (4.1.33) and (4.1.20). While the full result looks complicated, we shall see that we can easily extract from it new defect and bulk CFT data.

4.1.4 Defect channel data

We consider an expansion for the defect channel CFT data

$$\begin{aligned}\hat{\Delta} &= \hat{\Delta}^{(0)} + \varepsilon \hat{\gamma}^{(1)} + \mathcal{O}(\varepsilon^2), \\ b_{\phi\hat{\phi}} &= b^{(0)} + \varepsilon b^{(1)} + \mathcal{O}(\varepsilon^2).\end{aligned}\tag{4.1.52}$$

Similar to the bulk scenario, operators that appeared at leading order contribute to the block expansion with their anomalous dimensions

$$\hat{\Delta}_{S/V,0,s} = 1 + s + \varepsilon \hat{\gamma}_{S/T,0,s}^{(1)} + \mathcal{O}(\varepsilon^2).\tag{4.1.53}$$

In contrast, higher-twist operators, which are absent at leading order, contribute with their classical dimensions

$$\hat{\Delta}_{S/V,m,s} = 1 + 2m + s + \mathcal{O}(\varepsilon), \quad m > 0.\tag{4.1.54}$$

As we already mentioned, at order ε , only defect operators of transverse twist one ($m = 0$) are expected to appear. This expectation will be independently confirmed by the inversion formula.

The defect block expansions at one loop read

$$\begin{aligned}\hat{F}_S^{(1)}(r, w) &= a_\phi^{2(1)} + \sum_s b_{S,0,s}^{2(1)} \hat{f}_{1+s,s}(r, w) + b_{S,0,s}^{2(0)} \hat{\gamma}_{S,0,s}^{(1)} \partial_{\hat{\Delta}} \hat{f}_{1+s,s}(r, w), \\ \hat{F}_V^{(1)}(r, w) &= \sum_s b_{V,0,s}^{2(1)} \hat{f}_{1+s,s}(r, w) + b_{V,0,s}^{2(0)} \hat{\gamma}_{V,0,s}^{(1)} \partial_{\hat{\Delta}} \hat{f}_{1+s,s}(r, w).\end{aligned}\tag{4.1.55}$$

To extract CFT data from this expansion, we plug the discontinuity into the defect inversion formula (2.5.21). Following the strategy outlined in [31], and specialized to

the case of defects in [44], we perform a small z expansion in the inversion formula and then integrate each term in the expansion. Expanding the inversion formula, we find

$$b(\hat{\Delta}, s) = \int_0^1 \frac{dz}{2z} z^{-\frac{\hat{r}}{2}} \sum_{m=0} z^m \sum_{k=-m}^m c_{m,k}(\hat{\Delta}, s) B(z, \beta + 2k), \quad (4.1.56)$$

$$B(z, \beta) = \int_1^\infty \frac{d\bar{z}}{2\pi i} \bar{z}^{-\frac{\beta}{2}-1} \text{Disc}[\hat{F}_{S,V}(z, \bar{z})],$$

where $\beta = \hat{\Delta} + s = \hat{r} + 2s$ and where $c_{m,k}(\hat{\Delta}, s)$ are the coefficients obtained from the small z expansion of the integrand of (2.5.21). Observe that a term proportional to z^α in the small z expansion corresponds to a contribution of an operator of twist 2α in the coefficient $b(\hat{\Delta}, s)$, because the last integral is

$$\int_0^1 dz \frac{z^{-\frac{\hat{r}}{2}}}{2z} z^\alpha = -\frac{1}{\hat{r} - 2\alpha}. \quad (4.1.57)$$

We will explicitly demonstrate the computation of the coefficient only for the leading order in the small z expansion, which enables us to extract the CFT data for transverse twist equal to one. For higher orders, we will simply present the results, as the expressions become increasingly complex.

Starting from (4.1.43) and (4.1.49) and performing the linear combinations (4.1.9) and (4.1.15), we obtain

$$\text{Disc}[\hat{F}_S^{(1)}] = -\frac{\pi i(rw)}{(r-w)(rw-1)} + \frac{3\pi\sqrt{rw} \left[F\left(\sin^{-1}\left(\sqrt{r}\sqrt{\frac{r-w}{1-rw}}\right) \middle| \frac{(rw-1)^2}{(r-w)^2}\right) - F\left(\sin^{-1}\left(\frac{\sqrt{\frac{r-w}{1-rw}}}{\sqrt{r}}\right) \middle| \frac{(rw-1)^2}{(r-w)^2}\right) \right]}{2(r-w)},$$

$$\text{Disc}[\hat{F}_V^{(1)}] = -\frac{\pi i(rw)}{(r-w)(rw-1)} + \frac{\pi\sqrt{rw} \left[F\left(\sin^{-1}\left(\sqrt{r}\sqrt{\frac{r-w}{1-rw}}\right) \middle| \frac{(rw-1)^2}{(r-w)^2}\right) - F\left(\sin^{-1}\left(\frac{\sqrt{\frac{r-w}{1-rw}}}{\sqrt{r}}\right) \middle| \frac{(rw-1)^2}{(r-w)^2}\right) \right]}{2(r-w)}. \quad (4.1.58)$$

We see that both the singlet and vector defect representations contain two contributions in the discontinuity ¹². The first one originates from the the bulk identity operator. This contribution was already considered in [44] for a generic value of Δ_ϕ and it gives

$$B(z, \beta)_{\text{id}} = \frac{\sin(\pi\Delta_\phi)\Gamma(1 - \Delta_\phi) \left(\frac{\sqrt{z}}{1-z}\right)^{\Delta_\phi} \Gamma\left(\frac{\beta+\Delta_\phi}{2}\right)}{\pi\Gamma\left(\frac{1}{2}(\beta - \Delta_\phi + 2)\right)}. \quad (4.1.59)$$

Expanding in ε and selecting the first order gives

$$B(z, \beta)_{\text{id}}^{(1)} = \frac{\sqrt{z} \left(\psi^{(0)}\left(\frac{\beta+1}{2}\right) + \log\left(\frac{\sqrt{z}}{1-z}\right) + \gamma \right)}{2(z-1)} =$$

$$= \frac{1}{4}\sqrt{z} \left(-2\psi^{(0)}\left(\frac{1+\beta}{2}\right) - \log(z) - 2\gamma \right) + O(z^{\frac{3}{2}}), \quad (4.1.60)$$

¹²Note that in both representations, the discontinuity does not depend on N , then the only defect OPE data that will depend on N is the defect identity correction, which is not captured by the inversion formula.

where $\psi^{(0)}(z)$ is the digamma function and γ is the Euler-Mascheroni constant. This result has to be combined with the contribution coming from the second term in (4.1.58). The latter can be expanded as

$$\begin{aligned} \text{Disc}\hat{F}_S(z, \bar{z})_{\text{not id}} &= \frac{3}{4}i\pi\sqrt{z} \left(\log(z) + \log(\bar{z}) - 4 \log \left(\frac{2\sqrt{\bar{z}}}{\sqrt{\bar{z}} + 1} \right) \right) + O(z^{\frac{3}{2}}), \\ \text{Disc}\hat{F}_V(z, \bar{z})_{\text{not id}} &= \frac{1}{4}i\pi\sqrt{z} \left(\log(z) + \log(\bar{z}) - 4 \log \left(\frac{2\sqrt{\bar{z}}}{\sqrt{\bar{z}} + 1} \right) \right) + O(z^{\frac{3}{2}}). \end{aligned} \quad (4.1.61)$$

Inserting these discontinuities into (4.1.56) we find

$$\begin{aligned} B_S(z, \beta)_{\text{not id}} &= \frac{3\sqrt{z} \left[2(\beta+1) - 2(\beta-1)\beta \left(\psi^{(0)}\left(\frac{\beta}{2}\right) + \gamma \right) + (\beta-1)\beta \left(2H_{\frac{\beta-3}{2}} + \log(z) \right) \right]}{4(\beta-1)\beta^2}, \\ B_V(z, \beta)_{\text{not id}} &= \frac{\sqrt{z} \left[2(\beta+1) - 2(\beta-1)\beta \left(\psi^{(0)}\left(\frac{\beta}{2}\right) + \gamma \right) + (\beta-1)\beta \left(2H_{\frac{\beta-3}{2}} + \log(z) \right) \right]}{4(\beta-1)\beta^2}. \end{aligned} \quad (4.1.62)$$

where H_z are harmonic numbers. Combining both contributions (4.1.60) and (4.1.62) in (4.1.56), we obtain

$$\begin{aligned} b_S(\hat{\Delta}, s) &\sim \frac{s-1}{(2s+1)(\hat{\tau}-1)^2} + \frac{2(s-1)H_s + 3H_{s+\frac{1}{2}}}{2(2s+1)(\hat{\tau}-1)}, \\ b_V(\hat{\Delta}, s) &\sim \frac{s}{(2s+1)(\hat{\tau}-1)^2} + \frac{(2s+1) \left(2sH_s + H_{s-\frac{1}{2}} \right) + 2}{2(2s+1)^2(\hat{\tau}-1)}. \end{aligned} \quad (4.1.63)$$

The presence of double poles indicates the existence of anomalous dimensions, indeed

$$b(\hat{\Delta}, s) \sim \frac{b^{(0)} + \varepsilon b^{(1)}}{\hat{\tau}^{(0)} + \varepsilon \hat{\gamma}^{(1)} - 1} = \frac{b^{(1)}}{\hat{\tau}^{(0)} - 1} - \frac{b^{(0)}\hat{\gamma}^{(1)}}{(\hat{\tau}^{(0)} - 1)^2}. \quad (4.1.64)$$

Comparing with (4.1.63), we find the next-to-leading order defect data

$$\begin{aligned} \hat{\gamma}_{S,0,s}^{(1)} &= \frac{1-s}{(2s+1)}, & b_{S,0,s}^{2(1)} &= \frac{-2(s-1)H_s - 3H_{s+\frac{1}{2}}}{2(2s+1)}, \\ \hat{\gamma}_{V,0,s}^{(1)} &= -\frac{s}{(2s+1)}, & b_{V,0,s}^{2(1)} &= -\frac{(2s+1) \left(2sH_s + H_{s-\frac{1}{2}} \right) + 2}{2(2s+1)^2}. \end{aligned} \quad (4.1.65)$$

We can validate these results through several sanity checks. First, we see that $\hat{\gamma}_{S,0,1}^{(1)} = 0$, indicating the presence of the displacement operator in the defect OPE of the fundamental field. The displacement operator is a protected operator, which is related to the explicit breaking of translational symmetry¹³. For a line defect, it has dimension

¹³See equation (4.2.74) below for the explicit definition of the displacement operator.

two and transverse spin one, and it is a singlet under global symmetries. In the present case, it is the operator $\partial_{\perp}\hat{\phi}^1$, which is indeed associated to the vanishing anomalous dimension $\hat{\gamma}_{S,0,1}^{(1)}$.

Another universal protected operator is the tilt operator, which emerges when the defect breaks part of the internal symmetry of the bulk theory. In this setup, the defect breaks $O(N)$ to $O(N-1)$ and each of the $N-1$ broken generators is associated to a tilt operator forming a vectorial representation of the preserved subgroup. This vector, represented by the $N-1$ scalars $\hat{\phi}^{\hat{a}}$, has dimension one and orthogonal spin zero. Correspondingly, we find $\hat{\gamma}_{V,0,0}^{(1)} = 0$.

For other defect operators, some results are already available in the literature. The anomalous dimensions for the spin-zero singlet $\hat{\phi}^1$ and the spin-one vector operators $\partial_{\perp}\hat{\phi}^{\hat{a}}$ have been computed in equations (3.19) and (3.52) of [112] and our results agree with those findings. Our results for the bulk-to-defect couplings are entirely new.

As previously mentioned, the order ε result provides information about the anomalous dimensions of operators already present at leading order. By considering additional terms in the small- z expansion of (4.1.56) and (4.1.61), we can also determine the bulk-to-defect couplings for higher-twist operators. As anticipated from a diagrammatic perspective and noted in (4.1.55), all higher-twist coefficients are zero at this order in perturbation theory

$$b_{S,m,s}^{2(1)} = b_{V,m,s}^{2(1)} = 0, \quad m > 0. \quad (4.1.66)$$

Therefore the only non zero OPE data in the defect channel are (4.1.65) and the defect identity at one loop (4.1.21), which is missed by the inversion formula.

4.1.5 Bulk channel data

Finally, we can extract the bulk data at next-to-leading order using the bulk inversion formula (2.5.26). While the bulk anomalous dimensions are well-known and reproducing them serves only as a consistency check for our method, the product $a\lambda^{(1)}$ is influenced by the defect through the one-point function. Thus, we can provide new predictions for operators that are not affected by perturbative degeneracies, specifically all twist-two operators and the first two operators in the twist-four family.

To use formula (2.5.26), we need to analyze the behavior of $\left(\frac{(1-z)(1-\bar{z})}{\sqrt{z\bar{z}}}\right)^{\Delta_{\phi}} F(z, \bar{z})$ as $w \rightarrow 0$, according to (2.5.29)¹⁴. By expanding the results of the dispersion relation (4.1.48) and (4.1.50) around $w = 0$ and comparing with (2.5.29), we identify $\ell^* = 2$. Therefore the inversion formula will be applicable for $\ell > 2$.

¹⁴Note that for the bulk inversion, we must consider an additional factor in front of the correlator $F(r, w)$. For this reason the behaviour at small w is different from the one discussed in the defect inversion section.

Since the integral in (2.5.26) is too complex to solve directly, we use a similar approach to that employed for the defect inversion. We expand the integrand around $z = 1$ and compute the coefficient term by term in the expansion, as explained in [45]. We find

$$c(\Delta, \ell) = \int_0^1 \frac{dz}{(1-z)} (1-z)^{\frac{\ell-\Delta}{2}} \sum_{m=0} (1-z)^m \sum_{k=-m}^m B_{m,k}(\Delta, \ell) C(z, \Delta + \ell + 2k),$$

$$C(z, \beta) = \kappa_\beta \int_0^z \frac{d\bar{z}}{(1-\bar{z})^2} G_{\frac{\beta}{2}}(1-\bar{z}) \text{dDisc} \left[\left(\frac{(1-z)(1-\bar{z})}{\sqrt{z\bar{z}}} \right)^{\Delta_\phi} F(z, \bar{z}) \right], \quad (4.1.67)$$

where κ_β is defined in (3.2.27), $G_\Delta(z)$ is the $d = 1$ conformal block (2.3.3) and $B_{m,k}(\Delta, \ell)$ are coefficients that can be fixed by expanding the kernel in (2.5.26) and comparing with (4.1.67), namely

$$(1-z)(1-\bar{z})^2 (1-z)^{\frac{\Delta-l}{2}} \mu(z, \bar{z}) f_{d+l-1, -d+\Delta+1}^{HS} =$$

$$= \sum_m (1-z)^m \sum_{k=-m}^m \frac{\kappa_{\Delta+2k+l}}{\kappa_{\Delta+l}} B_{m,k}(\Delta, \ell) G_{\frac{\Delta+\ell+2k}{2}}(1-\bar{z}). \quad (4.1.68)$$

Just like in the defect case, each term in the series expansion around $z = 1$ (4.1.67) reproduces the contribution of a given twist to the coefficient.

To compute the double discontinuity at order ε , we first multiply the full correlator expressions (4.1.48) and (4.1.50) by $\frac{(1-z)(1-\bar{z})}{\sqrt{z\bar{z}}}$ and expand them in $z = 1$. We find that every term in the expansion of the non-trivial part $\frac{(1-z)(1-\bar{z})}{\sqrt{z\bar{z}}} H(z, \bar{z})$ contains only integer powers of \bar{z} . This indicates that this part of the correlator does not contribute to the double discontinuity. The same is true for the contribution from the correction to the bulk identity. Thus, the only contributions to the double discontinuity in both representations are the terms proportional to the defect identity, $a_\phi^{2(1)} \frac{(1-z)(1-\bar{z})}{\sqrt{z\bar{z}}}$. However, the coefficient (4.1.67) also receives contributions from the leading double discontinuity. This occurs because the factors dependent on Δ_ϕ and d introduce terms of order ε when combined with the order zero double discontinuity (4.1.25). In particular both $C(z, \beta)$ and $B_{m,k}(\Delta, \ell)$ depend on ε through Δ_ϕ and d . Therefore, we need to consider

$$\text{dDisc} \left[\left(\frac{(1-z)(1-\bar{z})}{\sqrt{z\bar{z}}} \right)^{\Delta_\phi} F_S \right] = \left(\frac{a_\phi^{2(0)}}{N} + \varepsilon \frac{a_\phi^{2(1)}}{N} \right) 2 \sin^2 \left(\frac{\pi \Delta_\phi}{2} \right) \left(\frac{(1-z)(1-\bar{z})}{\sqrt{z\bar{z}}} \right)^{\Delta_\phi}$$

$$\text{dDisc} \left[\left(\frac{(1-z)(1-\bar{z})}{\sqrt{z\bar{z}}} \right)^{\Delta_\phi} F_T \right] = (a_\phi^{2(0)} + \varepsilon a_\phi^{2(1)}) 2 \sin^2 \left(\frac{\pi \Delta_\phi}{2} \right) \left(\frac{(1-z)(1-\bar{z})}{\sqrt{z\bar{z}}} \right)^{\Delta_\phi}.$$

Using the double discontinuities above, the first few orders in the $z = 1$ expansion of

the one-loop generating function $C_T(z, \beta)$ (4.1.67) read

$$\begin{aligned}
C_T(z, \beta) = & a_\phi^2(0) \left\{ (1-z)^{\Delta_\phi} \left[\frac{\sqrt{\pi} \Gamma\left(\frac{\beta+1}{2}\right) \Gamma\left(1-\frac{\Delta_\phi}{2}\right)^2 \Gamma\left(\frac{\beta}{2}+\Delta_\phi-1\right)}{\Gamma\left(\frac{\beta+2}{4}\right)^2 \Gamma\left(\frac{1}{4}(\beta-2\Delta_\phi+4)\right) \Gamma\left(\frac{1}{4}(\beta+2\Delta_\phi)\right)} + \right. \\
& + \left(\frac{(z-1)^2 (-\beta^3 - 4\beta^2 \Delta_\phi - 6\beta^2 - 4\beta \Delta_\phi^2 - 20\beta \Delta_\phi - 8\beta - 4\Delta_\phi^2 - 16\Delta_\phi)}{192(\beta+1)} + \frac{2}{(z-1)(\beta+2\Delta_\phi-2)} - \frac{1}{2} + \right. \\
& \left. \left. + \frac{(z-1)(\beta^3 + 4\beta^2 \Delta_\phi + 4\beta^2 + 4\beta \Delta_\phi^2 + 12\beta \Delta_\phi + 4\beta + 4\Delta_\phi^2 + 8\Delta_\phi)}{16(\beta+1)(\beta+2\Delta_\phi+2)} \right) (1-z)^{\frac{\beta}{2}+\Delta_\phi} \right] \times \\
& \times \left[\frac{\Gamma\left(\frac{\beta}{2}\right)^4 \sin^2\left(\frac{\pi \Delta_\phi}{2}\right)}{\pi^2 \Gamma(\beta-1) \Gamma(\beta)} + \frac{(\Delta_\phi^2 + 2\Delta_\phi)(z-1)^2 \Gamma\left(\frac{\beta}{2}\right)^4 \sin^2\left(\frac{\pi \Delta_\phi}{2}\right)}{8\pi^2 \Gamma(\beta-1) \Gamma(\beta)} - \frac{\Delta_\phi(z-1) \Gamma\left(\frac{\beta}{2}\right)^4 \sin^2\left(\frac{\pi \Delta_\phi}{2}\right)}{2\pi^2 \Gamma(\beta-1) \Gamma(\beta)} \right. \\
& \left. - \frac{(\Delta_\phi^3 + 6\Delta_\phi^2 + 8\Delta_\phi)(z-1)^3 \Gamma\left(\frac{\beta}{2}\right)^4 \sin^2\left(\frac{\pi \Delta_\phi}{2}\right)}{48\pi^2 \Gamma(\beta-1) \Gamma(\beta)} \right] \left. \right\} - a_\phi^2(1) \frac{\Gamma\left(\frac{\beta}{4}\right)^2 (1-z)^{\Delta_\phi} \Gamma\left(\frac{\beta}{4} + \frac{\Delta_\phi}{2} - \frac{1}{2}\right)}{\Gamma\left(\frac{\beta}{2} - \frac{1}{2}\right) \left(2^{\frac{\beta}{2} - \Delta_\phi + 1} \Gamma\left(\frac{\Delta_\phi}{2}\right)^2\right) \Gamma\left(\frac{\beta}{4} - \frac{\Delta_\phi}{2} + 1\right)} \\
& + \mathcal{O}((z-1)^4), \tag{4.1.69}
\end{aligned}$$

where Δ_ϕ needs to be expanded at order ε . The singlet contribution is simply $C_S(z, \beta) = \frac{1}{N} C_T(z, \beta)$. By substituting these expressions into (4.1.67), using (4.1.21), and expanding to first order in ε , we can determine the coefficients $c_{S/T}(\Delta, \ell)$ and extract

$$\begin{aligned}
a\lambda_{T,0,\ell}^{(1)} &= -\frac{2^{-\ell-5} \Gamma\left(\frac{\ell}{2} + \frac{1}{2}\right)^3}{\pi \Gamma\left(\frac{\ell}{2} + 1\right) \Gamma\left(\ell + \frac{1}{2}\right)} \left(-32a_\phi^2(0) H_{\ell-\frac{1}{2}} + 35a_\phi^2(0) H_{\ell-\frac{1}{2}} + 19a_\phi^2(0) \psi^{(0)}(\ell) + \right. \\
& \quad \left. -38a_\phi^2(0) \psi^{(0)}(2\ell) - 19\gamma a_\phi^2(0) + 6a_\phi^2(0) \log(2) + 32a_\phi^2(1) \right), \\
\langle a\lambda_{T,1,\ell}^{(1)} \rangle &= -\frac{a_\phi^2(0) 2^{-\ell-3} \Gamma\left(\frac{\ell+1}{2}\right) \Gamma\left(\frac{\ell+3}{2}\right)^2}{\pi \Gamma\left(\frac{\ell}{2} + 2\right) \Gamma\left(\ell + \frac{3}{2}\right)}, \\
a\lambda_{S,0,\ell}^{(1)} &= \frac{1}{N} a\lambda_{T,0,\ell}^{(1)}, \\
\langle a\lambda_{S,1,\ell}^{(1)} \rangle &= \frac{1}{N} \langle a\lambda_{T,1,\ell}^{(1)} \rangle, \tag{4.1.70}
\end{aligned}$$

with a_ϕ^2 given in (4.1.21). We write $\langle \dots \rangle$ to stress that the data we derived for twist-four (4.1.70) should be interpreted as an average over degenerate operators of a given spin. Indeed, starting at spin $\ell = 2$, the twist-four operators are degenerate, meaning that multiple operators share the same classical scaling dimensions and are therefore indistinguishable from the perspective of bootstrap. Using known expressions for the

bulk three-point couplings [123],

$$\begin{aligned}
\lambda_{\phi\phi\mathcal{J}_{T,0,\ell}}^2 &= \frac{2^{\ell+1}(\Delta_\phi)_\ell^2}{\ell!(2\Delta_\phi + \ell - 1)_\ell} + O(\varepsilon^2), \\
\langle \lambda_{\phi\phi\mathcal{J}_{T,1,\ell}}^2 \rangle &= \frac{2^\ell \Gamma(\ell + 2)^2 (N + 2) (\ell^2 + 3\ell + 8) - 4N}{\Gamma(2\ell + 3) 4N(N + 8)^2 (\ell + 1)(\ell + 2)} \varepsilon^2 + O(\varepsilon^3), \\
\lambda_{\phi\phi\mathcal{J}_{S,0,\ell}}^2 &= \frac{2^{\ell+1}(\Delta_\phi)_\ell^2}{N\ell!(2\Delta_\phi + \ell - 1)_\ell} + O(\varepsilon^2), \\
\langle \lambda_{\phi\phi\mathcal{J}_{S,1,\ell}}^2 \rangle &= \frac{2^\ell \Gamma(\ell + 2)^2 (N + 2) (\ell^2 + 3\ell + 8)}{\Gamma(2\ell + 3) 4N(N + 8)^2 (\ell + 1)(\ell + 2)} \varepsilon^2 + O(\varepsilon^3) \dots \quad (4.1.71)
\end{aligned}$$

and the definition $a\lambda^{(1)} = a^{(0)}\lambda^{(1)} + a^{(1)}\lambda^{(0)}$, we can extract the one-point functions coefficients

$$\begin{aligned}
a_{\mathcal{J}_{T,0,\ell}}^{(1)} &= \frac{(N + 8)(\ell!)^3}{2^{\frac{3\ell+7}{2}} \left(\frac{\ell!}{2}\right)^4 \sqrt{(2\ell)!}} \left(\frac{N^2 - 3N - 22}{(N + 8)^2} - 2H_{\frac{\ell-1}{2}} + H_{\ell-\frac{1}{2}} + 2H_\ell - H_{2\ell} \right), \\
a_{\mathcal{J}_{S,0,\ell}}^{(1)} &= \frac{(N + 8)(\ell!)^3}{\sqrt{N} 2^{\frac{3\ell+7}{2}} \left(\frac{\ell!}{2}\right)^4 \sqrt{(2\ell)!}} \left(\frac{N^2 - 3N - 22}{(N + 8)^2} - 2H_{\frac{\ell-1}{2}} + H_{\ell-\frac{1}{2}} + 2H_\ell - H_{2\ell} \right), \\
\langle a_{\mathcal{J}_{T,1,\ell}}^{(0)} \rangle &= \frac{2^{-\frac{3\ell+6}{2}} ((\ell + 1)!)^3}{\left(\frac{\ell!}{2}\right)^4 \sqrt{(2\ell + 2)!}} \frac{(N + 8)^2}{\sqrt{(\ell + 1)(\ell + 2)[(\ell^2 + 3\ell + 8)(N + 2) - 4N]}}, \\
\langle a_{\mathcal{J}_{S,1,\ell}}^{(0)} \rangle &= \frac{2^{-\frac{3\ell+6}{2}} ((\ell + 1)!)^3}{\left(\frac{\ell!}{2}\right)^4 \sqrt{(2\ell + 2)!}} \frac{(N + 8)^2}{\sqrt{N(N + 2)} \sqrt{(\ell + 1)(\ell + 2)(\ell^2 + 3\ell + 8)}}, \quad (4.1.72)
\end{aligned}$$

The anomalous dimensions are all zero for $\ell > 0$, as expected. We also computed $C(z, \beta)$ and (4.1.67) to higher order in the $z = 1$ expansion to extract the coefficients and anomalous dimensions of higher-twist operators, confirming that they are zero.

For low-spin operators, the inversion formula does not converge, so a different approach is needed. We can compute the missing data by expanding the full results (4.1.48) and (4.1.50) in series and comparing them to the bulk OPE expansion. Although we anticipated the inversion formula to fail at spins $\ell = 0, 2$, we find that the only data missed by the inversion formula are the coefficients of the twist-two operators with $\ell = 0$, namely ϕ^2 and $T_{ab} = \phi_a \phi_b - \frac{\delta_{ab}}{N} \phi^2$. For these operators, we obtain

$$\begin{aligned}
a\lambda_T^{(1)} &= a_\phi^{2(1)} - \frac{1}{2} - \frac{\log(2)}{2}, \\
a\lambda_{\phi^2}^{(1)} &= -\frac{-4a_\phi^{2(1)} + N + N \log(2) + 2 + \log(4)}{4N}. \quad (4.1.73)
\end{aligned}$$

and

$$\begin{aligned}
a_T^{(1)} &= \frac{(N + 6)(N + 8) \log 4 + N^2 - 5N - 38}{8\sqrt{2}(N + 8)}, \\
a_{\phi^2}^{(1)} &= \frac{12(N + 8) \log 2 - 13N - 38}{8\sqrt{2}N(N + 8)}. \quad (4.1.74)
\end{aligned}$$

These last two one-point functions match the diagrammatic results of [112]. As another non-trivial check of our results for twist-4 operators at low spin, we can derive the coefficient of the operator ϕ^4 , namely $a\lambda_{S/T,1,0}^{(1)}$, using an alternative method and compare it with the result from the inversion formula. For simplicity, we set $N = 1$ and focus only on the singlet representation. We compute the two-point function of the operator ϕ^2 at leading order, and extract the bulk CFT data. Similar to the two-point function of ϕ , the leading order correlator receives contributions from the squared one-point function and from the bulk identity, with $\Delta_{\phi^2} = 2 + \mathcal{O}(\varepsilon)$. It reads

$$F^{(0)}(r, w) = a_{\phi^2}^{2(0)} + a_{\phi}^{2(0)} \frac{rw}{(w-r)(1-rw)} + \left(\frac{rw}{(w-r)(1-rw)} \right)^2. \quad (4.1.75)$$

A family of double-twist operators with twist 4 appears in the bulk spectrum at this order. Specifically, we can extract the coefficient of the spin-zero double-twist operator $a_{\phi^4}^{(0)} \lambda_{\phi^2\phi^2\phi^4}^{(0)}$ from the bulk expansion and we find that it perfectly matches with what we expect from (4.1.70). This approach can be generalized to any N . Examining other correlators not only would be useful to validate our findings but also it would help to resolve the degeneracy issue.

4.1.6 Diagrammatic check

In this section, we compute the two-point function (4.1.3) using Feynman diagrams, as an independent verification of our bootstrap result. To construct Feynman diagrams, we use the scalar propagator

$$\text{---} \equiv \langle \phi_a(x_1) \phi_b(x_2) \rangle_{\lambda_0=h_0=0} = \frac{\kappa \delta_{ab}}{(x_{12}^2)^{1-\frac{\varepsilon}{2}}}, \quad \kappa = \frac{\Gamma(\frac{d}{2})}{2\pi^{d/2}(d-2)}. \quad (4.1.76)$$

and the vertices

$$\text{X} \equiv -\lambda_0 \int d^d x \dots, \quad \text{---} \equiv -h_0 \int_{-\infty}^{\infty} d\tau \dots \quad (4.1.77)$$

The blue double line at the bottom represents the defect. The value of the couplings at the fixed point is given in (4.1.2). In particular, $\lambda_* \sim \mathcal{O}(\varepsilon)$ and $h_* \sim \mathcal{O}(1)$.

Up to the first order in ε (one loop), the diagrams that contribute to the two-point function of ϕ are

$$\langle \phi_a \phi_b \rangle_{\mathcal{D}} = \text{---} + \text{---} + \text{X} + \text{---} \quad (4.1.78)$$

The disconnected contributions in (4.1.78) naturally correspond to the defect and bulk identity in (4.1.48) and (4.1.50). The former is the squared one-point function (4.1.21), which was computed diagrammatically up to order ε^2 in [112].

The only non-trivial term is the cross diagram, given by

$$-\kappa (\delta_{ab} + 2\delta_{a1}\delta_{b1}) \frac{\lambda h^2}{2!} \int d\tau_1 \int d\tau_2 \int d^{4-\varepsilon}q G(x_1 - q)G(x_2 - q)G(q - x(\tau_1))G(q - x(\tau_2)), \quad (4.1.79)$$

where $x(\tau_i)$ are the coordinates of the points on the defect, with $|\dot{x}(\tau_{1,2})| = 1$, q is the coordinate of the bulk vertex and $G(x)$ is the free propagator. At the fixed point, performing the τ_1 and τ_2 integrals, we obtain

$$-(\delta_{ab} + 2\delta_{a1}\delta_{b1}) \frac{3}{8\pi^2} \int d^4q \frac{1}{|q^i|^2 |x_1 - q|^2 |x_2 - q|^2} = (\delta_{ab} + 2\delta_{a1}\delta_{b1}) \frac{H(x_1, x_2)}{8|x_1^i||y_2^i|}, \quad (4.1.80)$$

where $H(x_1, x_2)$ is a conformally invariant function, according to (4.1.3). Thanks to conformal invariance, it is enough to evaluate $H(x_1, x_2)$ at a specific coordinate along the defect, for instance $x_1^0 = x_2^0 = 0$. Even with this simplification, solving the integral in (4.1.80) analytically is challenging.

A simplified integral representation can be derived starting with

$$H(x_1, x_2) = -\frac{3}{\pi^2} \int d^3q^i \int dq \frac{|x_1^i||x_2^i|}{|q^i|^2 (q^2 + |x_1^i - q^i|^2) (q^2 + |x_2^i - q^i|^2)}, \quad (4.1.81)$$

where we defined $q \equiv q^0$. Introducing a Feynman parameter α for the last two factor in the denominator, we get

$$H(x_1, x_2) = -\frac{3}{\pi^2} \int_0^1 d\alpha \int d^3q^i \int dq \frac{|x_1^i||x_2^i|}{|q^i|^2 (q^2 + \alpha|x_1^i - q^i|^2 + (1 - \alpha)|x_2^i - q^i|^2)^2}. \quad (4.1.82)$$

Performing the q integral and rearranging the terms, we obtain

$$H(x_1, x_2) = -\frac{3}{2\pi} \int_0^1 d\alpha \int d^3q^i \frac{|x_1^i||x_2^i|}{|q^i|^2 (|q^i - \tilde{q}^i|^2 + L^2)^{\frac{3}{2}}}, \quad (4.1.83)$$

where

$$\tilde{q}^i = \alpha x_1^i + (1 - \alpha)x_2^i, \quad L^2 = \alpha(1 - \alpha)|x_1^i - x_2^i|^2. \quad (4.1.84)$$

Introducing another Feynman parameter ξ , the expression becomes

$$H(x_1, x_2) = -\frac{9}{4\pi} \int_0^1 d\alpha \int_0^1 d\xi \int d^3q^i \frac{\xi^{\frac{1}{2}} \cdot |x_1^i||x_2^i|}{(|q^i - \xi\tilde{q}^i|^2 + \xi(1 - \xi)|\tilde{q}^i|^2 + \xi L^2)^{\frac{5}{2}}}. \quad (4.1.85)$$

Shifting $q^i \rightarrow q^i + \xi\tilde{q}^i$ and integrating over q^i , we find

$$H(x_1, x_2) = -3|x_1^i||x_2^i| \int_0^1 d\alpha \int_0^1 d\xi \frac{1}{\xi^{\frac{1}{2}} (L^2 + (1 - \xi)|\tilde{q}^i|^2)}. \quad (4.1.86)$$

If we introduce lightcone coordinates and change variable as $\xi = \eta^2$, we get

$$H(z, \bar{z}) = -6\sqrt{z\bar{z}} \int_0^1 d\alpha \int_0^1 d\eta \frac{1}{(1 + \alpha(z\bar{z} - 1) - \eta^2(1 + (z - 1)\alpha)(1 + (\bar{z} - 1)\alpha))}. \quad (4.1.87)$$

This integral representation can be further evaluated by integrating either over α or η . Integrating over α leads to

$$H(z, \bar{z}) = -6\sqrt{z\bar{z}} \int_0^1 d\eta \frac{\log \left[P(z, \bar{z}, \eta) + \sqrt{Q(z, \bar{z}, \eta)} \right] - \log \left[P(z, \bar{z}, \eta) - \sqrt{Q(z, \bar{z}, \eta)} \right]}{\sqrt{Q(z, \bar{z}, \eta)}}, \quad (4.1.88)$$

where $P(z, \bar{z}, \eta)$ and $Q(z, \bar{z}, \eta)$ are the following polynomials

$$\begin{aligned} P(z, \bar{z}, \eta) &= 1 + z\bar{z} - \eta^2(z + \bar{z}), \\ Q(z, \bar{z}, \eta) &= (z\bar{z} - 1)^2 - 2\eta^2(z + \bar{z} + z\bar{z}(z + \bar{z} - 4)) + \eta^4(z - \bar{z})^2. \end{aligned} \quad (4.1.89)$$

Alternatively, integrating over η in (4.1.87), we find

$$H(z, \bar{z}) = -6\sqrt{z\bar{z}} \int_0^1 d\alpha \frac{\tanh^{-1} \left[\frac{(1+(z-1)\alpha)(1+(\bar{z}-1)\alpha)}{1+\alpha(z\bar{z}-1)} \right]}{\sqrt{(1+(z-1)\alpha)(1+(\bar{z}-1)\alpha)(1+\alpha(z\bar{z}-1))}}. \quad (4.1.90)$$

Both expressions (4.1.88) and (4.1.90) allow us to obtain series expansions of $H(z, \bar{z})$. In particular, we recognize that (4.1.90) is one of the representations of the bootstrap result (4.1.44). In other words, we see that the Feynman diagram computation reproduces the bootstrap prediction. This justifies our decision to overlook potential ambiguities at low transverse spins in the dispersion relation (3.2.1).

4.2 The spin impurity in the $O(3)$ model

In this section, we examine the spin impurity in the $O(3)$ model. Following the approach of [116], we represent the defect using the trace of the path-ordered exponential

$$\mathcal{D}_j(u, v) = \mathcal{P} \exp \left(\frac{\zeta_0}{\sqrt{\kappa}} \int_u^v d\tau \phi^a(\tau) T_a \right), \quad (4.2.1)$$

where $a = 1, 2, 3$ and the factor κ was introduced in (4.1.76). Explicitly, (4.2.1) amounts to the definition

$$\mathcal{D}_j(u, v) = \sum_{n=0}^{\infty} \frac{\zeta_0^n}{\kappa^{\frac{n}{2}}} \int_{u < \tau_1 < \dots < \tau_n < v} d\tau_1 \dots d\tau_n \phi_{a_1}(\tau_1) \dots \phi_{a_n}(\tau_n) T^{a_1} \dots T^{a_n}. \quad (4.2.2)$$

The defect extends over the imaginary time direction,¹⁵ and for brevity, we denote $\phi_a(\tau) \equiv \phi_a(\tau, 0, \dots, 0)$. We will be primarily interested in the infinite defect $\mathcal{D}_j \equiv \mathcal{D}_j(-\infty, \infty)$, but the finite version of (4.2.1) will also be considered at some point.

¹⁵Another interesting observable is the circular loop, which is monotonic under RG flow [128]. The two configurations are related by a conformal transformation, and despite potential conformal anomalies at the level of the defect expectation value [129], our conclusions about defect correlators are adaptable to the circular case. The straight line has a clearer interpretation as an impurity in a condensed-matter system.

The matrices T^a form a spin- j representation of $\mathfrak{su}(2)$, meaning they are $(2j+1) \times (2j+1)$ matrices. We normalize them such that the commutation relations and Casimir read

$$[T^a, T^b] = i\epsilon^{abc}T^c, \quad T_a T_a = j(j+1). \quad (4.2.3)$$

The defect $\text{Tr } \mathcal{D}_j$ preserves the connected component of the $O(3)$ global symmetry.¹⁶ Thus, it can be realized in a lattice by inserting a spin- j impurity that interacts with other lattice sites through $SU(2)$ -preserving interactions. The coupling ζ_0 is marginally irrelevant in four dimensions, but it becomes relevant for $d < 4$, driving the system to a non-trivial interacting defect CFT in the IR. Notably, this defect CFT remains non-trivial even when the bulk is at the free fixed point $\lambda_0 = 0$. To illustrate this, we outline the computation of the β -function, both in the free and interacting bulk cases. For the free case, we present a new result at order ζ^7 , which for the first time reveals the dependence of the beta function on the spin j . We then explore the spectrum of operators on the spin impurity defect, motivated by the need to identify which defect operators appear in the OPE, for an efficient application of the analytic bootstrap techniques. Finally, we analyze the bulk two-point function of ϕ_a using the analytic bootstrap method and we compare our results with diagrammatic computations.

4.2.1 Defect β -function

The computation of the β -function for line defects originates from the work of [130] on non-abelian gauge theories, see also [131] for a comprehensive review. For the magnetic impurities relevant to our discussion, the β -function has been calculated up to two loops in [132, 133]. The standard approach involves selecting a specific observable and renormalizing the coupling ζ_0 to ensure UV-finiteness. Since renormalization focuses on the UV behavior of the theory, we can consider a finite line $\tau \in [u, v]$ for our calculations. We choose to impose the UV-finiteness of the vertex operator

$$\mathcal{V}(x) = \frac{\text{Tr} \langle \phi_a(x) T^a \mathcal{D}_j(0, \tau) \rangle}{\text{Tr} \langle \mathcal{D}_j(0, \tau) \rangle}, \quad (4.2.4)$$

where $\phi_a(x)T^a$ is inserted in the trace, but it is placed in a point x in the bulk.

Free bulk

Let's start with the case of a free bulk, where the operator ϕ_a does not require renormalization. In this case, all the divergences in (4.2.4) are attributed to the renormalization

¹⁶Strictly speaking, we take the trace over $SU(2)$ representations instead of $O(3)$ to allow for half-integer j . From now on, we will overlook this subtlety, since it does not affect our results.

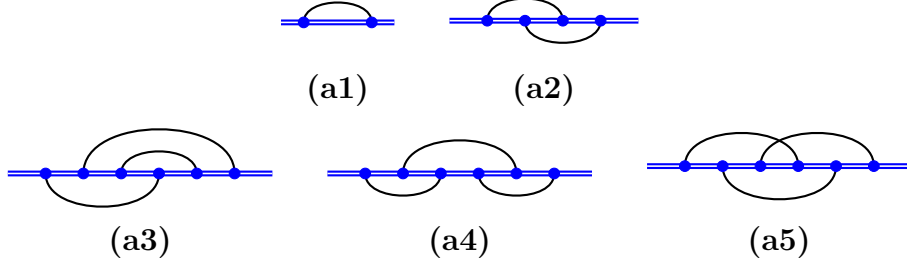


Figure 4.1: One-, two-, and three-loop propagator diagrams.

of the coupling ζ_0 . Our main goal is to find the divergent part of (4.2.4) and relate the bare coupling ζ_0 to the renormalized coupling ζ , given in the MS scheme by

$$\zeta_0 = \mu^{\varepsilon/2} \zeta \left(1 + \frac{a_{11}\zeta^2 + a_{12}\zeta^4 + a_{13}\zeta^6}{\varepsilon} + \frac{a_{22}\zeta^4 + a_{23}\zeta^6}{\varepsilon^2} + \frac{a_{33}\zeta^6}{\varepsilon^3} + O(\zeta^8) \right). \quad (4.2.5)$$

In essence, our task is to find the coefficients a_{ij} above. Once determined, we can impose the condition that the bare coupling remains independent of the renormalization scale μ , namely $d\zeta_0/d\mu = 0$, and extract the beta function

$$\beta(\zeta) = \mu \frac{d\zeta}{d\mu} = -\frac{\varepsilon}{2} \zeta + a_{11}\zeta^3 + 2a_{12}\zeta^5 + 3a_{13}\zeta^7 + O(\zeta^9). \quad (4.2.6)$$

To compute (4.2.4), we first need to discuss the expectation value of the defect. Given that $\langle \text{Tr } \mathcal{D}_j(\tau) \rangle$ exponentiates, it's convenient to study its logarithm. Here is the final result, which we will derive below

$$\frac{\log \langle \text{Tr } \mathcal{D}_j(\tau) \rangle}{j(j+1)(2j+1)} = \zeta_0^2 (\mathbf{a1}) - \zeta_0^4 (\mathbf{a2}) + \zeta_0^6 (2(\mathbf{a3}) + 2(\mathbf{a4}) + (\mathbf{a5})) + \dots \quad (4.2.7)$$

In this expression, (a1)–(a5) correspond to integrals represented diagrammatically in Figure 4.1. The integrals are evaluated over the interval $[0, \tau]$, with implicit time-ordering and unit-normalized propagators. For instance

$$(\mathbf{a1}) = \text{diagram (a1)} = \int_{0 < \tau_1 < \tau_2 < \tau} \frac{d\tau_1 d\tau_2}{\tau_{21}^{2-\varepsilon}}, \quad (4.2.8)$$

$$(\mathbf{a2}) = \text{diagram (a2)} = \int_{0 < \tau_1 < \tau_2 < \tau_3 < \tau_4 < \tau} \frac{d\tau_1 d\tau_2 d\tau_3 d\tau_4}{(\tau_{31} \tau_{42})^{2-\varepsilon}}. \quad (4.2.9)$$

While these integrals are straightforward to compute, their explicit value is unnecessary as they cancel out between the numerator and denominator in (4.2.4).

In order to find (4.2.7), we start by computing $\langle \mathcal{D}_j(\tau) \rangle$ up to order ζ_0^6 , performing all possible Wick contractions. Each diagram consists of an integral multiplied by a trace. The traces take the form $\text{Tr } T_{a_1} T_{a_2} \dots T_{a_l}$, where all indices a_1, \dots, a_l are contracted.

These traces can be computed iteratively using the commutation relations (4.2.3). Although the process is tedious, it can be automated with the help of `Mathematica`.

Regarding the integrals, we encounter a significant number of them, far exceeding those depicted in Figure 4.1. However, many of these integrals can be decomposed into products of lower-point integrals. To clarify, let's consider an example. Consider the following sum of diagrams

We can think of it as the lower diagram “passing through” the upper diagram. Since all possible orderings of points are accounted for, this sum is equal to the diagram **(a1)** squared. Each diagram appears twice, so we obtain

$$\left[\text{diagram} \right]^2 = 2 \text{diagram} + 2 \text{diagram} + 2 \text{diagram}. \quad (4.2.10)$$

A similar pattern emerges for other combinations of diagrams. The crucial idea is that a product of diagrams equals the sum of all time-ordered diagrams where the relative order of the legs within each subdiagram is maintained. This combinatorial problem can be automated. By decomposing sums of diagrams as illustrated in the example, we observe an exponentiation of the result, leading to equation (4.2.7).

We now consider the complete vertex $\mathcal{V}(x)$ (4.2.4). As before, we'll present the final result first and then derive it:

$$\begin{aligned} \frac{\mathcal{V}(x)}{\zeta_0 \sqrt{\kappa} j(j+1)} &= (\mathbf{b1}) - (\mathbf{b2})\zeta_0^2 + ((\mathbf{b3}) + 2(\mathbf{b4}) + 2(\mathbf{b5}))\zeta_0^4 + \\ &+ \left(-2(\mathbf{b6}) - 4(\mathbf{b7}) - (\mathbf{b8}) - (\mathbf{b9}) - 2(\mathbf{b10}) - 2(\mathbf{b11}) - 2(\mathbf{b12}) - 2(\mathbf{b13}) + \right. \\ &- 2(\mathbf{b14}) - 4(\mathbf{b15}) + 2(2j(j+1) - 5)(\mathbf{b16}) + 4(j(j+1) - 2)(\mathbf{b17}) - 2(\mathbf{b18}) + \\ &\left. - 4(\mathbf{b19}) + 2(2j(j+1) - 5)(\mathbf{b20}) + (2j(j+1) - 7)(\mathbf{b21}) \right) \zeta_0^6 + \dots \end{aligned} \quad (4.2.11)$$

The diagrams **(b1)**–**(b21)** are shown in Figure 4.2. In this figure, the cross (\times) indicates the point where the bulk field connects to the defect. For instance, if the bulk field is located at $x = (\tau', x^i)$, where x^i are directions orthogonal to the defect, then

$$(\mathbf{b5}) = \text{diagram} = \int_{0 < \tau_1 < \tau_2 < \tau_3 < \tau_4 < \tau_5 < \tau} \frac{d\tau_1 d\tau_2 d\tau_3 d\tau_4 d\tau_5}{\tau_{41}^{2-\epsilon} \tau_{53}^{2-\epsilon} (|x^i|^2 + (\tau' - \tau_2)^2)^{1-\frac{\epsilon}{2}}}. \quad (4.2.12)$$

The value of these integrals is necessary to determine the beta function, and we will soon explain how to calculate them. Regarding the derivation of equation (4.2.11), the procedure is similar to (4.2.7). We start by generating all Wick contractions that contribute to $\text{Tr}\langle \phi(x) \mathcal{D}_j(\tau) \rangle$. For each term, we compute the traces using the commutation relations, then factorize the integrals using relations analogous to (4.2.10). It

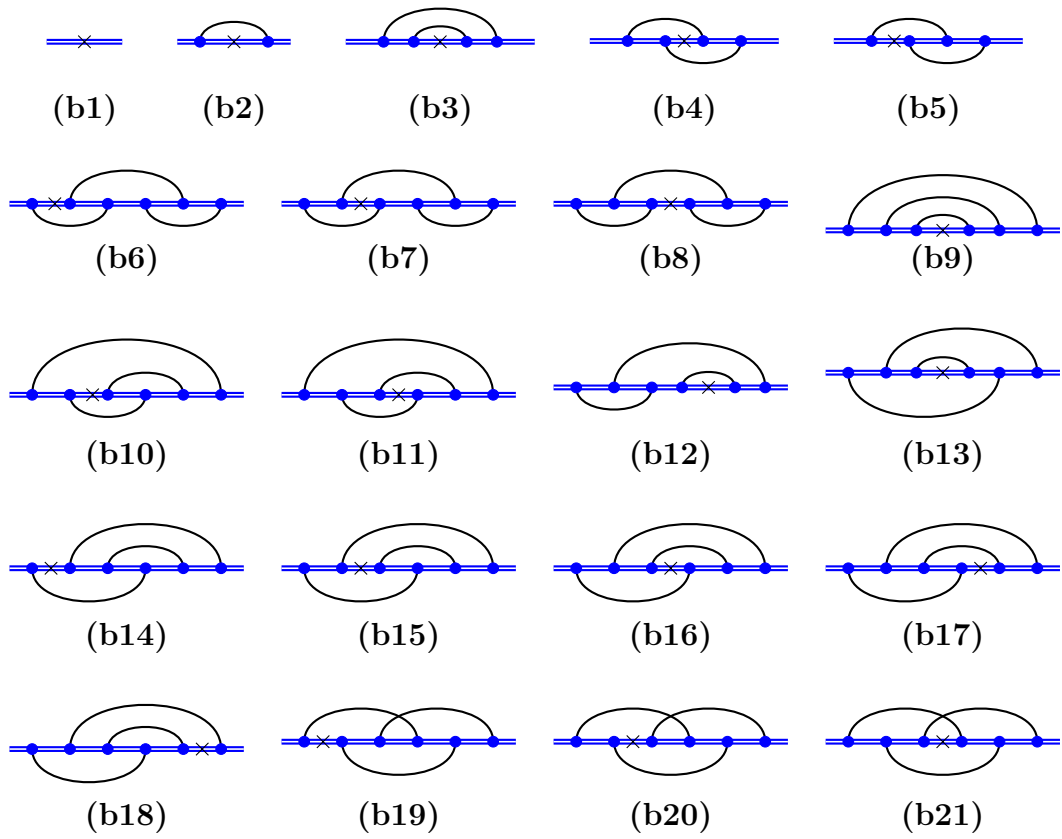


Figure 4.2: Vertex diagrams up to three loops.

turns out that the result is proportional to the right-hand side of (4.2.11) multiplied by $\text{Tr}(\mathcal{D}_j(\tau))$ in (4.2.7). These steps are tedious, but we have automated them with a computer. To obtain the beta function, we need to extract the divergent part of the integrals in equation (4.2.11). For illustration, we compute diagram **(b5)** in (4.2.12) in detail. We then explain how this approach can be generalized and automated for all other diagrams.

The first observation is that, since we are only interested in the divergent part of $\mathcal{V}(x)$, it is convenient to place the ϕ insertion far from the defect. Specifically, we take $|x^i| \gg \tau$, where τ is the length of the defect operator $\mathcal{D}_j(\tau)$. In this limit, the dependence on x^i , τ' and τ_2 drops out

$$\overline{\text{(b5)}} \equiv \lim_{|x^i| \rightarrow \infty} |x^i|^{2-\varepsilon} \text{(b5)} = \int_{0 < \tau_1 < \tau_2 < \tau_3 < \tau_4 < \tau_5 < \tau} \frac{d\tau_1 d\tau_2 d\tau_3 d\tau_4 d\tau_5}{\tau_{41}^{2-\varepsilon} \tau_{53}^{2-\varepsilon}}. \quad (4.2.13)$$

An important observation is that we can choose the order in which we integrate the variables. Since τ_2 does not appear in the integrand, it is convenient to perform its integral first

$$\overline{\text{(b5)}} = \int_{0 < \tau_1 < \tau_3 < \tau_4 < \tau_5 < \tau} d\tau_1 d\tau_3 d\tau_4 d\tau_5 \int_{\tau_1}^{\tau_3} \frac{d\tau_2}{\tau_{41}^{2-\varepsilon} \tau_{53}^{2-\varepsilon}} = \int_{1345} \frac{\tau_{31}}{\tau_{41}^{2-\varepsilon} \tau_{53}^{2-\varepsilon}}. \quad (4.2.14)$$

In the second equality, we introduce the shorthand notation $\int_{ij\dots k} = \int_{0 < \tau_i < \tau_j < \dots < \tau_k < \tau}$, omitting $d\tau_i$ for brevity. The strategy is to continue integrating the simplest variable next. For instance, since τ_4 appears only once, it has a simple integral

$$\overline{\text{(b5)}} = \int_{135} \int_{\tau_3}^{\tau_5} d\tau_4 \frac{\tau_{31}}{\tau_{41}^{2-\varepsilon} \tau_{53}^{2-\varepsilon}} = \frac{1}{\varepsilon - 1} \int_{135} \left[\tau_{51}^{\varepsilon} \tau_{53}^{\varepsilon-2} - \tau_{51}^{\varepsilon-1} \tau_{53}^{\varepsilon-1} - \tau_{31}^{\varepsilon} \tau_{53}^{\varepsilon-2} \right]. \quad (4.2.15)$$

In the right-hand side we used $\tau_{31} = \tau_{51} - \tau_{53}$ to simplify the result. An important observation is that, as we integrate, many terms are generated, each requiring a different order of integration to minimize complexity. For the first two terms in (4.2.15), we should integrate first τ_1 and τ_3 , and only then τ_5 . In this way, all integrals are elementary

$$\begin{aligned} \int_{135} \left[\tau_{51}^{\varepsilon} \tau_{53}^{\varepsilon-2} - \tau_{51}^{\varepsilon-1} \tau_{53}^{\varepsilon-1} \right] &= \int_0^{\tau} d\tau_5 \int_0^{\tau_5} d\tau_3 \int_0^{\tau_3} d\tau_1 \left[\tau_{51}^{\varepsilon} \tau_{53}^{\varepsilon-2} - \tau_{51}^{\varepsilon-1} \tau_{53}^{\varepsilon-1} \right] \\ &= \frac{\tau^{2\varepsilon+1}}{2(\varepsilon - 1)\varepsilon^2(2\varepsilon + 1)}. \end{aligned} \quad (4.2.16)$$

Instead, for the last term in (4.2.15) it is better to integrate first τ_1 and τ_5 , and only then τ_3 :

$$\begin{aligned} \int_{135} \tau_{31}^{\varepsilon} \tau_{53}^{\varepsilon-2} &= \int_0^{\tau} d\tau_3 \int_{\tau_3}^{\tau} d\tau_5 \int_0^{\tau_3} d\tau_1 \tau_{31}^{\varepsilon} \tau_{53}^{\varepsilon-2} = \int_0^{\tau} d\tau_3 \frac{\tau_3^{\varepsilon+1} (\tau - \tau_3)^{\varepsilon-1}}{(\varepsilon - 1)(\varepsilon + 1)} \\ &= \frac{2\Gamma(\varepsilon - 1)\Gamma(\varepsilon + 2)}{\Gamma(2\varepsilon + 3)} \tau^{2\varepsilon+1}. \end{aligned} \quad (4.2.17)$$

The last τ_3 integral is the so-called Euler integral. By carefully selecting the order of integrations, we encounter this more challenging integral only at the last step. If instead we had chosen the order of integration poorly, intermediate results would have included hypergeometric functions, and simplification would have occurred only at the end.

For completeness, the value of the diagram of interest is

$$\overline{\mathbf{(b5)}} = \left(\frac{1}{2\varepsilon^2(2\varepsilon+1)} - \frac{2\Gamma(\varepsilon)\Gamma(\varepsilon+2)}{\Gamma(2\varepsilon+3)} \right) \frac{\tau^{2\varepsilon+1}}{(\varepsilon-1)^2}. \quad (4.2.18)$$

We can now apply the insights gained from computing diagram **(b5)** to all other integrals. To summarize:

1. We first take the limit $|x^i| \gg \tau$.
2. We integrate the variables τ_i that appear at most once in the integrand.
3. This process generates many terms, and for each term, we may need to choose different integration orders to minimize complexity. Sometimes relations of the form $\tau_{ij} = \tau_{ik} + \tau_{kj}$ are convenient to simplify intermediate expressions.

At the end of the day, we encounter only two integrals that are not elementary:

$$H_1 = \int_0^\tau du u^a (\tau - u)^b, \quad H_2 = \int_0^\tau du \int_0^u dv u^a (u - v)^b (\tau - v)^c. \quad (4.2.19)$$

These integrals may arise in the final integration step or as subdiagrams within a larger diagram. Fortunately, they can be evaluated straightforwardly

$$H_1 = \frac{\Gamma(a+1)\Gamma(b+1)}{\Gamma(a+b+2)} \tau^{a+b+1}, \quad (4.2.20)$$

$$H_2 = \frac{\Gamma(a+b+2)\Gamma(b+c+2)}{(b+1)\Gamma(a+2b+c+4)} {}_3F_2 \left(\begin{matrix} b+1, a+b+2, b+c+2 \\ b+2, a+2b+c+4 \end{matrix}; 1 \right) \tau^{a+b+c+2}. \quad (4.2.21)$$

By implementing this algorithm in **Mathematica**, we successfully computed all the integrals in 4.2 in closed form. The expressions are not particularly illuminating, so we do not present them here.

The final step is to combine all the components. We substitute the values of the integrals into equation 4.2 for the vertex $\mathcal{V}(x)$. Demanding the result to be finite, we obtain

$$\zeta_0 = \mu^{\varepsilon/2} \zeta \left(1 + \frac{\zeta^2}{\varepsilon} - \frac{\zeta^4}{2\varepsilon} + \frac{3\zeta^4}{2\varepsilon^2} + \frac{\zeta^6}{3\varepsilon} \left(2 - \pi^2 \left(j(j+1) - \frac{1}{3} \right) \right) - \frac{11\zeta^6}{6\varepsilon^2} + \frac{5\zeta^6}{2\varepsilon^3} + O(\zeta^8) \right). \quad (4.2.22)$$

Consequently, the β -function reads

$$\beta_\zeta = -\frac{\varepsilon}{2} \zeta + \zeta^3 - \zeta^5 + \left(2 - \pi^2 \left(j(j+1) - \frac{1}{3} \right) \right) \zeta^7 + \dots \quad (4.2.23)$$

Notably, starting at $O(\zeta^7)$, the β -function depends on the spin j , which complicates the resummation of the perturbative series, even for a free bulk. However, for large spin j , one can consider a double-scaling limit where $\zeta \rightarrow 0$, $j \rightarrow \infty$ and $\zeta^2 j$ is kept fixed. The β -function was recently computed in this limit in [116] and our result is in perfect agreement for large j . Solving the fixed point equation $\beta(\zeta) = 0$ perturbatively in ε leads to a defect fixed point for

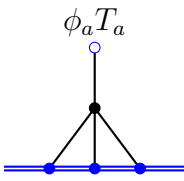
$$\zeta_*^2 = \frac{\varepsilon}{2} + \frac{\varepsilon^2}{4} + \left(j(j+1) - \frac{1}{3} \right) \frac{\pi^2 \varepsilon^3}{8} + O(\varepsilon^4). \quad (4.2.24)$$

In four dimensions, the defect coupling is irrelevant, leading to a trivial fixed point at $\varepsilon = 0$. For $\varepsilon > 0$ there is a non-trivial fixed point, even though the bulk is free. The existence of this fixed point in three dimensions, *i.e.* for $\varepsilon \rightarrow 1$, was questioned in [116], based on a large spin analysis. In Section 4.2.4 we will confirm that indeed this fixed point is trivial.

Interacting bulk

For an interacting bulk, extending the calculation to higher orders in perturbation theory is more challenging due to the presence of diagrams with quartic bulk interactions. We perform the calculation to order $\lambda\zeta^3$, where a single Feynman diagram contributes to the vertex renormalization. The result of this computation was presented without derivation in [133].

At the order we are focusing on, the majority of contributions to the β -function arise from diagrams either without bulk interactions or from corrections to the bulk propagator. The only exception is the diagram



$$(4.2.25)$$

where we set the length of the defect operator to be one, since the integral is homogeneous. We first compute the symmetry factor of this diagram. It's crucial to note that T_a also participates in the trace, according to the definition of the vertex (4.2.4). One of the three legs attached to the defect carries a generator T_a with the same index as the external field ϕ_a , while the other two legs carry generators T_b with contracted indices. Out of the three possible permutations, two configurations place the contracted generators T_b adjacent to each other and they simplify to $j(j+1)T_a$. The remaining configuration reads $T_b T_a T_b = (j(j+1) - 1)T_a$. Thus, the total contribution is $(j(j+1) - \frac{1}{3})T_a$. Additionally, note that the integral is path-ordered, but, thanks

to permutation symmetry, we can divide by $3!$ and instead compute the unordered integral. Therefore, the contribution of this diagram to the vertex is

$$\frac{\mathcal{V}(x)}{\zeta_0 \sqrt{\kappa} j(j+1)} \supset -\frac{\lambda_0 \zeta_0^2 \kappa^2}{6} \left(j(j+1) - \frac{1}{3} \right) I(x), \quad (4.2.26)$$

where the integral is

$$I(x) = \int \frac{d^{4-\varepsilon} y}{((\tau' - \tau'')^2 + |x^i - y^i|^2)^{\frac{2-\varepsilon}{2}}} \left(\int_0^1 \frac{dt}{(|y^i|^2 + (t - \tau'')^2)^{\frac{2-\varepsilon}{2}}} \right)^3. \quad (4.2.27)$$

where $\phi_a T^a$ is inserted at (τ', x^i) and the bulk interaction is localized at (τ'', y^i) . For our purposes, it is enough to extract the leading contribution in the limit $|x^i| \rightarrow \infty$ that is also divergent for $\varepsilon \rightarrow 0$. It's important to note that divergences in ε only arise for small $|y^i|$ and when τ'' lies near the interval $[0, 1]$.

Without loss of generality, we can set $x^i = (\frac{1}{2}, L, 0, \dots)$, and then pass to cylindrical coordinates $(\tau'', y^i) \rightarrow (\tau'', \rho, \theta, \dots)$:

$$I(L) = \int_0^\infty d\rho \int_{-\infty}^{+\infty} d\tau'' \int_0^\pi d\theta \int d\Omega_{1-\varepsilon} \frac{\rho^{2-\varepsilon} (\sin \theta)^{1-\varepsilon}}{\left(\left(\frac{1}{2} - \tau'' \right)^2 + \rho^2 + L^2 - 2\rho L \cos \theta \right)^{\frac{2-\varepsilon}{2}}} \times \left(\int_0^1 \frac{dt}{(\rho^2 + (t - \tau'')^2)^{\frac{2-\varepsilon}{2}}} \right)^3. \quad (4.2.28)$$

Here Ω_{d-1} is the volume of the $d - 1$ -dimensional sphere. We are interested in the leading term as $L \rightarrow \infty$. In order to extract the divergent part, we can assume that ρ and τ'' are bounded. Therefore, we obtain

$$I(L) \sim \frac{1}{L^{2-\varepsilon}} \int_0^\delta d\rho \int_{-\delta}^{1+\delta} d\tau'' \int_0^\pi d\theta \int d\Omega_{1-\varepsilon} \rho^{2-\varepsilon} (\sin \theta)^{1-\varepsilon} \times \left(\int_0^1 \frac{dt}{(\rho^2 + (t - \tau'')^2)^{\frac{2-\varepsilon}{2}}} \right)^3 + O(\varepsilon^0), \quad (4.2.29)$$

where $\delta > 0$ is some arbitrarily small parameter. The integrals over dt , $d\Omega_{1-\varepsilon}$ and $d\theta$ are easily performed and one finds

$$I(L) \sim \frac{1}{L^{2-\varepsilon}} \frac{2\pi^{\frac{3-\varepsilon}{2}}}{\Gamma\left(\frac{3-\varepsilon}{2}\right)} \int_0^\delta d\rho \int_{-\delta}^{1+\delta} d\tau'' \rho^{-4+2\varepsilon} \left((1 - \tau'') {}_2F_1\left(\frac{1}{2}, 1 - \frac{\varepsilon}{2}; \frac{3}{2}; -\frac{(1-\tau'')^2}{\rho^2}\right) + \tau'' {}_2F_1\left(\frac{1}{2}, 1 - \frac{\varepsilon}{2}; \frac{3}{2}; -\frac{\tau''^2}{\rho^2}\right) \right)^3. \quad (4.2.30)$$

Computing this integral in full generality is challenging, but given that $\rho < \delta$ is small, we can straightforwardly expand the integrand. The crucial observation is that only terms of the form $\rho^{-1+c\varepsilon}$ produce divergent contributions, since

$$\int_0^\delta d\rho \rho^{-1+c\varepsilon} = \frac{1}{c\varepsilon} + O(\varepsilon^0). \quad (4.2.31)$$

All in all, only one term contributes to the divergence, and the remaining $d\rho$ and $d\tau''$ integrations are elementary:

$$\begin{aligned} I(L) &\sim \frac{1}{L^{2-\varepsilon}} \frac{2\pi^{\frac{3-\varepsilon}{2}}}{\Gamma\left(\frac{3-\varepsilon}{2}\right)} \frac{\pi^{\frac{3}{2}} \Gamma\left(\frac{1-\varepsilon}{2}\right)^3}{8 \Gamma\left(1 - \frac{\varepsilon}{2}\right)^3} \int_0^\delta d\rho \int_{-\delta}^{1+\delta} d\tau'' \rho^{-1+2\varepsilon} (\text{sgn}(1 - \tau'') + \text{sgn}(\tau''))^3 \\ &= \frac{1}{L^{2-\varepsilon}} \frac{2\pi^4}{\varepsilon} + O(\varepsilon^0). \end{aligned} \quad (4.2.32)$$

Inserting this into (4.2.26) we finally get

$$\frac{\mathcal{V}(L)}{\zeta_0 \sqrt{\kappa} j(j+1)} \supset -\frac{1}{L^2} \frac{\lambda_0 \zeta_0^2}{48\varepsilon} \left(j(j+1) - \frac{1}{3} \right), \quad (4.2.33)$$

Combining this result with the free-theory contributions (4.2.11) and with the two-loop correction to the bulk propagator, which is known from previous work on the theory without defects, we obtain

$$\zeta_0 = \mu^{\varepsilon/2} \zeta \left(1 + \frac{\zeta^2}{\varepsilon} - \frac{\zeta^4}{2\varepsilon} + \frac{3\zeta^4}{2\varepsilon^2} + \frac{5\lambda^2}{72(4\pi)^4\varepsilon} + \frac{\left(j(j+1) - \frac{1}{3}\right)\zeta^2\lambda}{48\varepsilon} + \dots \right). \quad (4.2.34)$$

From this, we can extract the β -function [113, 114, 133]

$$\beta_\zeta = -\frac{\varepsilon}{2} \zeta + \zeta^3 - \zeta^5 + \frac{5}{36} \frac{\zeta\lambda^2}{(4\pi)^4} + \left(j(j+1) - \frac{1}{3} \right) \frac{\zeta^3\lambda}{24} + \dots \quad (4.2.35)$$

After setting the bulk coupling to the fixed-point value λ_* , the equation $\beta_\zeta(\zeta_*, \lambda_*) = 0$ can be solved perturbatively, yielding

$$\zeta_*^2 = \frac{\varepsilon}{2} + \varepsilon^2 \left(\frac{29}{121} - \frac{\pi^2}{11} \left(j(j+1) - \frac{1}{3} \right) \right) + O(\varepsilon^3). \quad (4.2.36)$$

Notice that in the interacting theory, the dependence on j appears already at order ε^2 .

When the bulk and defect couplings are tuned to their fixed-point values, we obtain an interacting defect conformal field theory. While the bulk spectrum remains unaffected by the presence of the defect, it is crucial to understand how to characterize the defect operators. This topic will be explored in detail in Section 4.2.3.

4.2.2 Discrete symmetries

It is important to examine the discrete symmetries preserved by the defect, as they imply selection rules in correlation functions and help in classifying defect operators. The bulk theory, both in the free and interacting cases, is invariant under time reversal symmetry¹⁷ and a global \mathbb{Z}_2 symmetry

$$T_t : \phi^a(\tau, x^i) \mapsto \phi^a(-\tau, x^i), \quad T_{\mathbb{Z}_2} : \phi^a(\tau, x^i) \mapsto -\phi^a(\tau, x^i). \quad (4.2.37)$$

A sufficient condition to extend these symmetries to the defect theory is that they leave the trace of the defect operator $\text{Tr } \mathcal{D}_j$ invariant. This is exactly what happens to the $SU(2)$ global symmetry. In contrast, the generators $T_{\mathbb{Z}_2}$ and T_t modify the defect. It is straightforward to see that the net effect of $T_{\mathbb{Z}_2}$ is to change the sign of the defect coupling constant [115]

$$T_{\mathbb{Z}_2} \mathcal{D}_j^\zeta = \mathcal{D}_j^{-\zeta}, \quad (4.2.38)$$

where \mathcal{D}_j^ζ is the defect extended operator with coupling constant ζ . On the other hand, T_t flips the signs of the arguments of all the fields in (4.2.2). However, by a convenient change of integration variables and name redefinitions, this is equivalent to reversing the order of the generators inside the trace. For generators of representations of $\mathfrak{su}(2)$, the following relation holds¹⁸

$$\text{Tr}(T^{a_n} \dots T^{a_1}) = (-1)^n \text{Tr}(T^{a_1} \dots T^{a_n}). \quad (4.2.39)$$

From this it follows that also T_t also effectively changes the sign of the defect coupling constant

$$T_t \text{Tr } \mathcal{D}_j^\zeta = \text{Tr } \mathcal{D}_j^{-\zeta}. \quad (4.2.40)$$

We can now define a modified time reversal symmetry for the defect theory by requiring that the fundamental fields are odd under this symmetry

$$\bar{T}_t = T_{\mathbb{Z}_2} \circ T_t : \phi^a(\tau, x^i) \mapsto -\phi^a(-\tau, x^i). \quad (4.2.41)$$

Now \bar{T}_t is both a symmetry of the homogeneous theory and leaves $\text{Tr } \mathcal{D}_j^\zeta$ invariant (it changes the sign of ζ two times). Therefore, it is a symmetry of the defect theory as well. To derive useful selection rules, we need to understand how this symmetry acts on defect operators. This will be briefly discussed in Section 4.2.3, after we have gained a general understanding of the defect operators in this model.

¹⁷In the context of defects, the inversion of the defect coordinate is also known as \mathcal{S} -parity [39, 134].

¹⁸This is due to the facts that the generators T^a are taken to be Hermitean and that the $\mathfrak{su}(2)$ representation given by the complex conjugated generators $(T^a)^*$ is equivalent to the original one, so that $(T^a)^T = P T^a P^{-1}$ for some matrix P .

4.2.3 The defect spectrum

In this section, we investigate the spectrum of operators localized on the spin impurity defect. We begin with the free-bulk theory, because the spectrum is simpler and Ward identities protect several defect operators. When bulk interactions are introduced, the dimensions of these operators are corrected by additional terms proportional to powers of λ_* , which remains perturbatively small in the ε -expansion. Our analysis enables us to understand the perturbative definition of defect operators, which is surprisingly complex in some instances. This will in turn clarify how to enumerate all possible defect operators within perturbation theory and help us in the analytic bootstrap analysis of Section 4.2.4.

The defect spin operator

As noted in [116], an interesting Ward identity is obtained by considering the shift of the fields $\phi_a(x) \rightarrow \phi_a(x) + c_a$ for some constants c_a . This is a symmetry of the free-bulk theory without the defect. The Noether currents for these symmetries are $J_a^\mu(x) = -\partial^\mu \phi_a(x)$, and their conservation is equivalent to the equations of motion since $0 = \partial_\mu J_a^\mu(x) = -\square \phi_a(x)$. The defect interaction explicitly breaks this shift symmetry and the conservation equation is modified by a term localized on the defect

$$\partial_\mu J^{\mu a}(0, x^i) = -\frac{\zeta_0}{\sqrt{\kappa}} \hat{S}_0^a(0) \delta^{d-1}(x^i), \quad (4.2.42)$$

where the minus sign is introduced for future convenience. We will often assume that the coordinate of bulk operators parallel to the defect is zero, thanks to translational invariance along the defect. Since the bulk is free, the bulk fundamental field ϕ_a do not renormalize. Introducing renormalization factors such that $\hat{S}_0^a = Z_{\hat{S}} \hat{S}^a$ and $\zeta_0 = \mu^{\frac{\varepsilon}{2}} Z_\zeta \zeta$, it follows that in the MS scheme

$$Z_{\hat{S}} = Z_\zeta^{-1}, \quad (4.2.43)$$

at all orders in perturbation theory, since the right hand side of (4.2.42) must be finite. This relation holds even when substituting renormalized quantities for the bare ones¹⁹. The operator \hat{S}_a responsible for symmetry breaking is a defect primary operator at the fixed point, known as the *defect spin* operator. As argued in [116], the Ward identity protects its dimension to $\hat{\Delta}_{\hat{S}} = \varepsilon/2$.²⁰ The explicit form of the defect spin operator

¹⁹More precisely, for renormalized quantities we would have $\partial_\mu J^{\mu a}(0, x^i) = -\frac{\mu^{\frac{\varepsilon}{2}} \zeta}{\sqrt{\kappa}} \hat{S}^a(0) \delta^{d-1}(x^i)$. We will often forget about the scale factor μ and set it to one, as is customary in the CFT literature, because we are ultimately interested in correlation functions at the fixed point and they depend on μ in a trivial way.

²⁰This result can also be derived using diagrammatic considerations, as originally done in [113].

\hat{S}_a in the perturbative setup can be derived via the Schwinger-Dyson equations. The defect contributes an extra term to the full action $S = S_{\text{bulk}} + S_{\text{defect}}$, where

$$S_{\text{defect}} = -\log \text{Tr } \mathcal{D}_j. \quad (4.2.44)$$

Inside correlation functions, it holds that

$$\square \phi_a(\tau, x^i) = \frac{\delta S_{\text{defect}}}{\delta \phi_a(\tau, x^i)} = -\frac{\zeta_0}{\sqrt{\kappa}} \delta^{d-1}(x^i) \frac{\text{Tr}(\mathcal{D}_j(-\infty, \tau) T_a \mathcal{D}_j(\tau, \infty))}{\text{Tr } \mathcal{D}_j}. \quad (4.2.45)$$

Thus, comparing with (4.2.42), correlators involving a defect spin operator $\hat{S}_0^a(\tau)$ inserted at a point τ on the defect satisfy ²¹

$$\langle \mathcal{O}_1(x_1) \dots \hat{S}_0^a(\tau) \dots \mathcal{O}_n(x_n) \rangle_{\mathcal{D}_j} = -\langle \mathcal{O}_1(x_1) \dots T^a(\tau) \dots \mathcal{O}_n(x_n) \rangle_{\mathcal{D}_j}, \quad (4.2.47)$$

Hence, we can write

$$\hat{S}_a(\tau) = -Z_{\hat{S}}^{-1} T_a(\tau). \quad (4.2.48)$$

In this sense, the \hat{S}_a operators in perturbation theory are just normal matrices that acquire an anomalous dimension when inserted into the defect ²².

Another interesting consequence of (4.2.42) is that we can rewrite it as

$$\square \phi_a(0, x^i) = \frac{\zeta}{\sqrt{\kappa}} \hat{S}_a(0) \delta^{d-1}(x^i), \quad (4.2.49)$$

which can be inverted as

$$\phi_a(0, x^i) = \sqrt{\kappa} \zeta \int d\tau \frac{\hat{S}_a(\tau)}{(|x^i|^2 + \tau^2)^{1-\frac{\epsilon}{2}}} + \phi_a^{\text{free}}(0, x^i), \quad (4.2.50)$$

where we set the defect coordinate of ϕ_a to zero and ϕ_a^{free} is a free field that does not interact with the defect. Using (4.2.50), correlators involving fundamental fields and their orthogonal derivatives can be reduced to integrals of defect correlators involving \hat{S}_a (not necessarily at the fixed point).

Understanding the conformal descendants of the operator \hat{S}_a at the fixed point is

²¹From the general definition (2.5.2), correlators of operators inserted on the spin impurity read

$$\langle \hat{\mathcal{O}}_1(\tau_1) \dots \hat{\mathcal{O}}_n(\tau_n) \rangle_{\mathcal{D}_j} = \frac{\langle \text{Tr} [\mathcal{D}_j(-\infty, \tau_1) \hat{\mathcal{O}}(\tau_1) \mathcal{D}_j(\tau_1, \tau_2) \hat{\mathcal{O}}(\tau_2) \dots \hat{\mathcal{O}}(\tau_n) \mathcal{D}_j(\tau_n, \infty)] \rangle}{\langle \text{Tr } \mathcal{D}_j \rangle}. \quad (4.2.46)$$

Note that matrix-valued operators interact non-trivially with the trace.

²²The appearance of this non-trivial constant operator could be avoided here by choosing a different representation of the defect in terms of one-dimensional fermions [117, 59]

crucial. These descendants are obtained by acting with the defect covariant derivative ²³

$$D_\tau \hat{\mathcal{O}}(\tau) = \partial_\tau \hat{\mathcal{O}}(\tau) + \frac{\zeta_0}{\sqrt{\kappa}} \phi^a(\tau) [T_a, \hat{\mathcal{O}}(\tau)]. \quad (4.2.52)$$

In the case of the \hat{S}_a operator, we get

$$D_\tau \hat{S}^a(\tau) = -i \frac{\zeta_0}{\sqrt{\kappa}} \epsilon^{abc} \phi_b T_c(\tau), \quad (4.2.53)$$

where the generator on the right hand side has to be inserted inside the path ordering, as in (4.2.47). This example shows that in this setup the question of whether an operator is a primary or not can be hard to address, because even though (4.2.53) contains no ∂_τ derivatives, it is still a descendant.

Once the bulk quartic interaction is introduced, the shift symmetry is explicitly broken in the bulk, so the above analysis does not directly apply. However, one can still consider the operators \hat{S}_a , defined by (4.2.47). Their dimensions, no longer protected, are given by

$$\hat{\Delta}_{\hat{S}} = \left(\beta_\zeta \frac{\partial \log Z_{\hat{S}}}{\partial \zeta} + \beta_\lambda \frac{\partial \log Z_{\hat{S}}}{\partial \lambda} \right) \Big|_{\zeta_*, \lambda_*}, \quad (4.2.54)$$

where now $Z_{\hat{S}}$ depends also on the bulk coupling constant λ . Interestingly, up to two loops in perturbation theory, $Z_{\hat{S}}$ does not receive any divergent corrections from the bulk interaction. Thus, we can still write

$$Z_{\hat{S}} = (Z_\zeta|_{\lambda=0})^{-1} + O(\zeta^2 \lambda^2, \zeta^4 \lambda), \quad (4.2.55)$$

allowing us to compute the first correction to $\Delta_{\hat{S}}$ using only the result for the β -function in the interacting case, without further diagrammatic computations [113]

$$\hat{\Delta}_{\hat{S}} = \beta_\zeta \frac{\partial \log Z_{\hat{S}}}{\partial \zeta} \Big|_{\zeta_*, \lambda_*} + O(\varepsilon^3) = \frac{\varepsilon}{2} - \varepsilon^2 \left[\frac{5}{484} + \frac{\pi^2}{11} \left(j(j+1) - \frac{1}{3} \right) \right] + O(\varepsilon^3). \quad (4.2.56)$$

Correlators of defect spin operators in perturbation theory

Once the explicit form of the defect spin operator in perturbation theory is determined, it is possible to evaluate correlators using standard diagrammatic techniques. This section focuses on computing the two-point function $\langle \hat{S}_a(\tau_1) \hat{S}_b(\tau_2) \rangle_{\mathcal{D}_j}$ at two loops, both for the free and interacting bulk cases. The overall normalization of the two-point

²³Correlators depend on the coordinate of an operator $\hat{\mathcal{O}}(\tau)$ also through the endpoints of the neighbouring defect operators $\mathcal{D}_j(\cdot, \tau)$ and $\mathcal{D}_j(\tau, \cdot)$. Therefore, it is convenient to introduce the defect covariant derivative

$$\mathcal{D}_j(u, \tau) D_\tau \hat{\mathcal{O}}(\tau) \mathcal{D}_j(\tau, v) \equiv \frac{d}{d\tau} (\mathcal{D}_j(u, \tau) \hat{\mathcal{O}}(\tau) \mathcal{D}_j(\tau, v)), \quad (4.2.51)$$

function in the free theory is physically significant, as the normalization of \hat{S} is fixed by the Ward identity (4.2.42).

Neglecting renormalization factors, for the moment, this two-point function represents the expectation value of the defect with generators T_a and T_b inserted at τ_1 and τ_2 , respectively. Since in (2.5.2) we divide by the defect expectation value, we can normalize traces by dividing by $2j + 1$, which is the classical expectation value. It is also convenient to define the "connected part" of a diagram as the part remaining after subtracting contributions that are products of lower-order diagrams or pieces containing "defect bubbles." Using this terminology, the defect correlator is the sum of all connected diagrams.

The leading order term is given by the following diagram

$$\begin{array}{c} \hat{S}_a \quad \hat{S}_b \\ \bullet \quad \bullet \\ \hline \tau_1 \quad \tau_2 \end{array} \quad (4.2.57)$$

Here, the blue line represents the defect, and the blue points indicate where a generator is inserted into the trace. Since there are no lower-order diagrams, this diagram is already connected and gives

$$I_c^{(0)}(\tau_1, \tau_2) = \frac{1}{2j+1} \text{Tr}(T_a T_b) = \frac{j(j+1)}{3} \delta_{ab}. \quad (4.2.58)$$

At one loop, only two diagrams contribute to the connected term. All other diagrams factor exactly into an order-zero diagram times a piece of a one-loop bubble, which must be subtracted

$$\begin{array}{cc} \begin{array}{c} \hat{S}_a \quad \hat{S}_b \\ \bullet \quad \bullet \\ \hline \tau_1 \quad \tau_2 \\ \text{---} \end{array} & \begin{array}{c} \hat{S}_a \quad \hat{S}_b \\ \bullet \quad \bullet \\ \hline \tau_1 \quad \tau_2 \\ \text{---} \end{array} \end{array} \quad (4.2.59)$$

Here, the additional blue points indicate interactions with a generator insertion, and the black line represents a free propagator (4.1.76). The interactions must be integrated along the defect, but without crossing any other generator insertions. These two diagrams have the same color factor

$$I^{(1)} \sim \frac{1}{2j+1} \text{Tr}(T_c T_a T_c T_b) = \frac{j(j+1)(j(j+1)-1)}{3} \delta_{ab}. \quad (4.2.60)$$

Subtracting the product of the order-zero diagram and one-loop defect bubbles, which have the same kinematic integral but a different color factor, gives

$$I_c^{(0)} \times \text{bubbles}^{(1)} \sim \frac{1}{(2j+1)^2} \text{Tr}(T_a T_b) \text{Tr}(T_c T_c) = \frac{j^2(j+1)^2}{3} \delta_{ab}. \quad (4.2.61)$$

Thus, we obtain

$$I_c^{(1)}(\tau_1, \tau_2) = -\zeta_0^2 \frac{j(j+1)}{3} \delta_{ab} \left(\int_{-\infty < \tau < \tau_1 < \tau' < \tau_2} \frac{d\tau d\tau'}{|\tau - \tau'|^{2-\varepsilon}} + \int_{\tau_1 < \tau < \tau_2 < \tau' < +\infty} \frac{d\tau d\tau'}{|\tau - \tau'|^{2-\varepsilon}} \right). \quad (4.2.62)$$

After performing the integrals, we find

$$I_c^{(1)}(\tau_1, \tau_2) = -\frac{2\zeta_0^2 j(j+1)}{3(1-\varepsilon)\varepsilon} |\tau_1 - \tau_2|^\varepsilon \delta_{ab}. \quad (4.2.63)$$

This contribution has a pole for $\varepsilon \rightarrow 0$, as expected, since we are computing the bare two-point function.

At the next order, many new diagrams contribute. Similarly to what has been done at one loop, we focus on computing connected diagrams. At two loops, this involves subtracting not only the zeroth-order connected contribution multiplied by two-loop bubbles, but also the first-order connected contributions multiplied by one-loop bubbles. For example

$$\begin{aligned} \text{Diagram 1} &= \text{Diagram 2} - \text{Diagram 3} \times \text{bubbles}^{(2)} + \\ &- \text{Diagram 4} \times \text{bubbles}^{(1)} = j(j+1) \text{Diagram 5}, \end{aligned} \quad (4.2.64)$$

where the last diagram denotes just a kinematical integral stripped of the color factor. All in all, the two-loop contributions are

$$\begin{aligned} I_c^{(2)}(\tau_1, \tau_2) = \sum \Gamma_c^{(2)} = j(j+1) & \left(\text{Diagram 6} + \text{Diagram 7} + 2 \text{Diagram 8} + \right. \\ & + 2 \text{Diagram 9} + \text{Diagram 10} + \text{Diagram 11} + \text{Diagram 12} + \\ & + \text{Diagram 13} + \text{Diagram 14} + \text{Diagram 15} + \text{Diagram 16} + \\ & \left. + 2 \text{Diagram 17} \right). \end{aligned} \quad (4.2.65)$$

This sum can be reorganized and further simplified, since an exponentiation of the previous orders occurs. Indeed we have

$$\begin{aligned} I_c^{(2)}(\tau_1, \tau_2) = \frac{j(j+1)}{2} & \left(\text{Diagram 18} + \text{Diagram 19} \right)^2 + j(j+1) \left(\text{Diagram 20} + \right. \\ & + \text{Diagram 21} + \text{Diagram 22} + \text{Diagram 23} + \text{Diagram 24} + \\ & \left. + \text{Diagram 25} + \text{Diagram 26} + \text{Diagram 27} + \text{Diagram 28} \right). \end{aligned} \quad (4.2.66)$$

Furthermore, it's worth noting that specular diagrams contribute equally. Therefore, we are left with evaluating only five diagrams. The integrals are straightforward, and the results are

$$\begin{aligned}
\text{Diagram 1} &= \zeta_0^4 |\tau_1 - \tau_2|^{2\varepsilon} \frac{\delta_{ab}}{3} \cdot \frac{2^{-1-2\varepsilon} \Gamma(\frac{1}{2} - \varepsilon) \Gamma(\varepsilon - 1)}{\sqrt{\pi}(\varepsilon - 1)\varepsilon}, \\
\text{Diagram 2} &= \zeta_0^4 |\tau_1 - \tau_2|^{2\varepsilon} \frac{\delta_{ab}}{3} \cdot \left(\frac{1}{2(\varepsilon - 1)\varepsilon^2(2\varepsilon - 1)} - \frac{\Gamma(\varepsilon - 1)\Gamma(-2\varepsilon)}{\Gamma(2 - \varepsilon)} \right), \\
\text{Diagram 3} &= \zeta_0^4 |\tau_1 - \tau_2|^{2\varepsilon} \frac{\delta_{ab}}{3} \cdot \left(-\frac{1}{2(\varepsilon - 1)^2\varepsilon^2} + \frac{\Gamma(\varepsilon - 1)\Gamma(-2\varepsilon)}{\Gamma(2 - \varepsilon)} \right), \\
\text{Diagram 4} &= \zeta_0^4 |\tau_1 - \tau_2|^{2\varepsilon} \frac{\delta_{ab}}{3} \cdot \left(\frac{-1 + \frac{2^{1-2\varepsilon}\sqrt{\pi}\varepsilon\Gamma(\varepsilon)}{\Gamma(\frac{1}{2} + \varepsilon)}}{2(\varepsilon - 1)^2\varepsilon^2} \right), \\
\text{Diagram 5} &= \zeta_0^4 |\tau_1 - \tau_2|^{2\varepsilon} \frac{\delta_{ab}}{3} \cdot \left(\frac{-\Gamma(1 + \varepsilon)^2 + \Gamma(1 + 2\varepsilon)}{(\varepsilon - 1)^2\varepsilon^2\Gamma(1 + 2\varepsilon)} \right).
\end{aligned} \tag{4.2.67}$$

Substituting these into (4.2.66) gives the two loops contribution to the bare two-point function. Notably, the same diagrams contribute to both the free and interacting bulk cases because, at this order, the only new diagram in the interacting case would be a mass correction to the bulk propagator, which is zero.

Once all diagrams are evaluated, one can introduce the wavefunction renormalization coefficient $Z_{\hat{S}}$ and rewrite the bare coupling constant in terms of the renormalized one, keeping in mind that $Z_{\hat{S}} = Z_{\zeta}^{-1}$. Imposing finiteness of $Z_{\hat{S}}^{-2} \langle \hat{S}_0^a(\tau_1) \hat{S}_0^b(\tau_2) \rangle_{\mathcal{D}_j}$ at this order in the coupling constant yields

$$Z_{\hat{S}} = 1 - \frac{\zeta^2}{\varepsilon} - \frac{\zeta^4}{2\varepsilon^2} + \frac{\zeta^4}{2\varepsilon} + O(\zeta^6). \tag{4.2.68}$$

Putting everything together, the renormalized two-point function evaluated at the free bulk fixed point (4.2.24) is

$$\langle \hat{S}_a(\tau_1) \hat{S}_b(\tau_2) \rangle_{\mathcal{D}_j} = \frac{\mathcal{N}_{\hat{S}}}{|\tau_1 - \tau_2|^{2\hat{\Delta}_{\hat{S}}}} \cdot \frac{\delta_{ab}}{3}, \tag{4.2.69}$$

where $\hat{\Delta}_{\hat{S}} = \varepsilon/2$ and

$$\mathcal{N}_{\hat{S}} = j(j+1) \left(1 - \varepsilon + \varepsilon^2 \frac{12 + \pi^2}{24} \right) + O(\varepsilon^3). \tag{4.2.70}$$

By conformal symmetry and the fact that \hat{S}_a is protected, we already knew that (4.2.69) holds at the non-perturbative level. However, the computation is necessary to determine the constant $\mathcal{N}_{\hat{S}}$.²⁴

²⁴Note that the normalization of \hat{S}_a is already fixed from the bulk through the Ward identity (4.2.49).

We can use this result together with (4.2.50) to compute the bulk-to-defect two-point function between ϕ^a and \hat{S}^b

$$\langle \phi^a(0, x^i) \hat{S}^b(0) \rangle_{\mathcal{D}_j} = \sqrt{\kappa} \zeta \int d\tau \frac{\langle \hat{S}^a(\tau) \hat{S}^b(0) \rangle_{\mathcal{D}_j}}{(\tau^2 + |x^i|^2)^{1-\frac{\varepsilon}{2}}}, \quad (4.2.71)$$

which is exact in the free-bulk theory.²⁵ Using (4.2.69), solving the integral, and evaluating at the fixed point yields

$$\langle \phi^a(0, x^i) \hat{S}^b(0) \rangle_{\mathcal{D}_j} = \frac{\delta^{ab}}{3|x^i|} \cdot \frac{\sqrt{\kappa} \zeta_* \mathcal{N}_{\hat{S}} \sqrt{\pi} \Gamma\left(\frac{1-\varepsilon}{2}\right)}{\Gamma\left(1-\frac{\varepsilon}{2}\right)} \equiv \frac{\delta^{ab}}{3|x^i|} b_{\phi\hat{S}}. \quad (4.2.72)$$

Interestingly, the above correlator contains a factor $\Gamma\left(\frac{1-\varepsilon}{2}\right)$ that diverges in the $\varepsilon \rightarrow 1$ limit. At this stage, it remains unclear whether this divergence could be cured by the ε -dependent term $\zeta_* \mathcal{N}_{\hat{S}}$. Nevertheless, this suggests that the theory might be problematic for $\varepsilon = 1$, i.e. in three dimensions, as we will prove in the bootstrap section.

When the bulk interaction is turned on, using (4.2.36) and (4.2.56), we obtain

$$\mathcal{N}_{\hat{S}} = j(j+1) \left[1 - \varepsilon + \varepsilon^2 \left(\frac{1512 - 55\pi^2}{2904} + \frac{2\pi^2 j(j+1)}{11} \right) \right] + O(\varepsilon^3). \quad (4.2.73)$$

The displacement operator and the defect stress-energy tensor

It is natural to consider the Ward identity arising from the translational invariance of the bulk theory. The defect explicitly breaks this symmetry, leading to a modification in the conservation of the bulk stress-energy tensor by a term localized on the defect [128, 38]

$$\partial_\mu T^{\mu\nu}(0, x^i) = - \left(\delta_i^\nu \hat{D}^i(0) + \partial_\tau x^\nu(0) \partial_\tau \hat{T}_{\mathcal{D}_j}(0) \right) \delta^{d-1}(x^i). \quad (4.2.74)$$

where $x^\nu(\tau)$ is the embedding function that describes the defect and τ is the coordinate that parametrizes the line. The operator \hat{D}^i , known as the *displacement* operator, is a primary operator with protected dimension $\hat{\Delta}_D = 2$. The explicit expression for the bare displacement operator is derived from the variation of the action with respect to $x^i(\tau)$

$$\hat{D}_0^i(x(\tau)) = \frac{1}{|\dot{x}(\tau)|} \frac{\delta S_{\text{defect}}}{\delta x_i(\tau)}. \quad (4.2.75)$$

Computing this functional derivative²⁶ and at the end evaluating it for a straight line with $|\dot{x}(\tau)| = 1$, one finds

$$\hat{D}_0^i(\tau) = \frac{\zeta_0}{\sqrt{\kappa}} \partial^i \phi_a(\tau) \frac{\text{Tr}(\mathcal{D}_j(-\infty, \tau) T_a \mathcal{D}_j(\tau, \infty))}{\text{Tr} \mathcal{D}_j}. \quad (4.2.76)$$

²⁵Since we are interested in the correlator at the fixed point, it suffices to evaluate it with vanishing parallel distance between the operators. The kinematics is already fixed by conformal symmetry.

²⁶Note that one needs to first reintroduce the arc length element $|\dot{x}(\tau)|$ in the integral of the defect action (4.2.44) since a generic variation of the embedding spoils the unit speed parametrization.

For correlators, the bare displacement operator inserted at a point τ on the defect satisfies

$$\langle \mathcal{O}_1(x_1) \dots \hat{D}_0^i(\tau) \dots \mathcal{O}_n(x_n) \rangle_{\mathcal{D}_j} = \frac{\zeta_0}{\sqrt{\kappa}} \langle \mathcal{O}_1(x_1) \dots \partial^i \phi^a(\tau) T_a \dots \mathcal{O}_n(x_n) \rangle_{\mathcal{D}_j}. \quad (4.2.77)$$

This can be rewritten as

$$\hat{D}_i(\tau) \sim \partial_i \phi^a T_a(\tau). \quad (4.2.78)$$

This analysis is valid regardless of whether the bulk is interacting, as the bulk stress-energy tensor is always conserved.

The other operator in (4.2.74) is the *defect stress-energy tensor* $\hat{T}_{\mathcal{D}_j}$. By the Ward identity, it has protected dimension $\hat{\Delta}_{\hat{T}_{\mathcal{D}_j}} = 1$. This operator breaks conformal invariance on the line defect, so it must vanish at the fixed point. In our case, the defect stress-energy tensor is given by ²⁷

$$\hat{T}_{\mathcal{D}_j}(\tau) = \frac{\beta_\zeta}{\sqrt{\kappa}} \hat{\Phi}(\tau), \quad (4.2.79)$$

where we define $\hat{\Phi}(\tau) = \phi_a T^a(\tau)$. Using the definition of conformal dimension $\mu \frac{\partial \hat{\mathcal{O}}}{\partial \mu} = -\hat{\Delta}_{\hat{\mathcal{O}}} \hat{\mathcal{O}}$ and the fact that $\hat{T}_{\mathcal{D}_j}$ is protected, we obtain

$$\hat{\Delta}_{\hat{\Phi}} = 1 + \frac{\partial \beta_\zeta}{\partial \zeta} + \frac{\beta_\lambda}{\beta_\zeta} \frac{\partial \beta_\zeta}{\partial \lambda}. \quad (4.2.80)$$

This formula is exact and holds for both free and interacting bulk theories.

From the last equation and the definition of the anomalous dimension of $\hat{\Phi}$ in terms of the wave function normalization of the operator, we find in free theory

$$Z_{\hat{\Phi}} = -\frac{2\beta_\zeta}{\varepsilon \zeta Z_\zeta}. \quad (4.2.81)$$

Using the expression for the beta function in the case of free bulk theory and the value of ζ at the critical point, the conformal dimension of the defect operator $\hat{\Phi}$ is

$$\hat{\Delta}_{\hat{\Phi}} = 1 + \varepsilon - \frac{\varepsilon^2}{2} + \frac{\varepsilon^3}{2} \left[1 - \pi^2 \left(j(j+1) - \frac{1}{3} \right) \right] + O(\varepsilon^4). \quad (4.2.82)$$

Similarly, in the interacting case

$$\hat{\Delta}_{\hat{\Phi}} = 1 + \varepsilon - \varepsilon^2 \left[\frac{257}{484} - \frac{4\pi^2}{11} \left(j(j+1) - \frac{1}{3} \right) \right] + O(\varepsilon^3). \quad (4.2.83)$$

²⁷For a generic line defect with a Lagrangian of the form $\mathcal{L}_{\text{defect}} = g\hat{\mathcal{O}}$, the defect stress tensor reads $\hat{T} = \beta_g \hat{\mathcal{O}}$. This follows from the more general result $\partial_\nu T_\mu^\nu x^\mu = \beta_i \frac{\partial \mathcal{L}}{\partial g_i}$, which is a consequence of Noether's theorem applied to the renormalized Lagrangian in the case of scale transformations.

Correlators of $\hat{\Phi}$

In this section, we calculate the one-loop two-point function of $\hat{\Phi}$ for both the free and the interacting bulk cases. This computation serves a dual purpose: it validates the arguments presented in the previous section and demonstrates the practical evaluation of correlators involving operators that incorporate both generator insertions and fundamental fields.

At tree level there is only one diagram

$$\begin{array}{c} \text{---} \circ \text{---} \\ \text{---} \circ \text{---} \end{array} = j(j+1) \frac{\kappa}{|\tau_1 - \tau_2|^{2-\varepsilon}}. \quad (4.2.84)$$

At one loop, there are two types of connected diagrams: one where the two operators are connected by a free bulk propagator, and another where they interact with the defect. Importantly, even in the interacting bulk case, no additional diagrams appear at this order, as bulk interactions contribute only at the subsequent order. The first type of diagrams are those where the operators are connected by a free bulk propagator

$$\begin{array}{c} \text{---} \bullet \text{---} \\ \text{---} \circ \text{---} \end{array} \quad \begin{array}{c} \text{---} \circ \text{---} \\ \text{---} \bullet \text{---} \end{array} \quad (4.2.85)$$

the computation of these integrals is analogous to the one for the operators \hat{S}_a , with the only difference that now everything is multiplied by a free propagator. The result is

$$I_1^{(1)}(\tau_1, \tau_2) = -\frac{\zeta_0^2 j(j+1) \Gamma(2 - \frac{\varepsilon}{2})}{\pi^{2-\frac{\varepsilon}{2}} (2-\varepsilon)(1-\varepsilon) \varepsilon |\tau_1 - \tau_2|^{2-2\varepsilon}}. \quad (4.2.86)$$

The remaining diagrams involve interactions between the two operators and the defect. There are twelve such diagrams, which can be categorized into two distinct color structures: eight diagrams are associated with $\text{Tr}(T_a T_a T_b T_b) \sim j^2(j+1)^2$, and the remaining four are associated with $\text{Tr}(T_a T_a T_b T_b) \sim j(j+1)(j^2+j-1)$. When summing all these diagrams, there is a component proportional to $j^2(j+1)^2$, which represents the sum of the ordered integral of two propagators over all possible orders. This results in the expression $\kappa^2 \int d\sigma_1 |\sigma_1 - \tau_1|^{-2+\varepsilon} \int d\sigma_2 |\sigma_2 - \tau_2|^{-2+\varepsilon}$, which vanishes in our regularization scheme. Consequently, we need to evaluate the remaining four diagrams

$$\begin{aligned} \begin{array}{c} \text{---} \circ \text{---} \\ \text{---} \bullet \text{---} \end{array} &= -\frac{\zeta_0^2 j(j+1) \Gamma(2-2\varepsilon) \Gamma(1-\frac{\varepsilon}{2}) \Gamma(\varepsilon)}{4\pi^{2-\frac{\varepsilon}{2}} (1-\varepsilon) \Gamma(2-\varepsilon) |\tau_1 - \tau_2|^{2-2\varepsilon}}, \\ \begin{array}{c} \text{---} \bullet \text{---} \\ \text{---} \circ \text{---} \end{array} &= -\frac{\zeta_0^2 j(j+1) \Gamma(1-\frac{\varepsilon}{2}) (\Gamma(\varepsilon)^2 - \Gamma(2\varepsilon-1))}{8\pi^{2-\frac{\varepsilon}{2}} (1-\varepsilon)^3 \Gamma(-2+2\varepsilon) |\tau_1 - \tau_2|^{2-2\varepsilon}}, \\ \begin{array}{c} \text{---} \bullet \text{---} \\ \text{---} \bullet \text{---} \end{array} &= -\frac{\zeta_0^2 j(j+1) \Gamma(1-\frac{\varepsilon}{2})}{4\pi^{2-\frac{\varepsilon}{2}} (1-\varepsilon)^2 |\tau_1 - \tau_2|^{2-2\varepsilon}}, \\ \begin{array}{c} \text{---} \circ \text{---} \\ \text{---} \circ \text{---} \end{array} &= -\frac{\zeta_0^2 j(j+1) \Gamma(2-2\varepsilon) \Gamma(1-\frac{\varepsilon}{2}) \Gamma(\varepsilon)}{4\pi^{2-\frac{\varepsilon}{2}} (1-\varepsilon) \Gamma(2-\varepsilon) |\tau_1 - \tau_2|^{2-2\varepsilon}}. \end{aligned} \quad (4.2.87)$$

After summing all the contributions and introducing the wavefunction renormalization coefficient $Z_{\hat{\Phi}}$, we impose the condition that $Z_{\hat{\Phi}}^{-2} \langle \hat{\Phi}(\tau_1) \hat{\Phi}(\tau_2) \rangle_{\mathcal{D}_j}$ remains finite at one loop. This leads to the result

$$\begin{aligned} Z_{\hat{\Phi}} &= 1 - \frac{3\zeta^2}{\varepsilon} + O(\zeta^4, \zeta^2\lambda, \lambda^2), \\ \gamma_{\hat{\Phi}}|_{\zeta^*, \lambda^*} &= \beta_{\zeta} \frac{\partial \log Z_{\hat{\Phi}}}{\partial \zeta} \Big|_{\zeta^*, \lambda^*} + O(\varepsilon^2) = \frac{3}{2} \varepsilon + O(\varepsilon^2). \end{aligned} \quad (4.2.88)$$

The renormalized two-point function evaluated at the fixed point is

$$\langle \hat{\Phi}(\tau_1) \hat{\Phi}(\tau_2) \rangle_{\mathcal{D}_j} = \frac{\mathcal{N}_{\hat{\Phi}}}{|\tau_1 - \tau_2|^{\hat{\Delta}_{\hat{\Phi}}}}, \quad (4.2.89)$$

where both in the free bulk and in the interacting bulk case

$$\begin{aligned} \mathcal{N}_{\hat{\Phi}} &= \frac{j(j+1)}{4\pi^2} \left(1 + \varepsilon \left(-2 + \frac{\gamma_E}{2} + \frac{\log \pi}{2} \right) \right) + O(\varepsilon^2), \\ \hat{\Delta}_{\hat{\Phi}} &= 1 + \varepsilon + O(\varepsilon^2). \end{aligned} \quad (4.2.90)$$

General defect operators

The defect spin and displacement operators appeared as defect corrections to Ward identities. It is natural to wonder if there are other defect operators with protected dimensions that can be constructed in a similar way. In particular, in the bulk-free theory, an infinite series of conserved higher spin currents exists, represented schematically as [135, 136]

$$\mathcal{J}_{\mu_1 \dots \mu_{s+1}}^{ab}(x) \sim \sum_{k=0}^s c_{s,k} \partial_{\{\mu_1 \dots \mu_k} \phi^a \partial_{\mu_{k+1} \dots \mu_{s+1}} \phi^b(x), \quad (4.2.91)$$

where the brackets denote traceless symmetrization, and $s \geq 1$ ²⁸. These currents have dimensions $\Delta_{J_{s+1}} = s + 1 - \varepsilon$. From the modified Ward identity

$$\partial^\nu \mathcal{J}_{\nu \mu_1 \dots \mu_s}^{ab}(0, x^i) = \frac{\zeta_0}{\sqrt{\kappa}} \hat{\mathcal{J}}_{\mu_1 \dots \mu_s}^{ab}(0) \delta^{d-1}(x^i), \quad (4.2.92)$$

we identify a tower of defect operators with protected dimensions $\hat{\Delta}_{\hat{\mathcal{J}}_s} = s + 1 \in \mathbb{N}$. In (4.2.92), the operators are defect primaries only when all free spatial indices are orthogonal to the defect, as parallel derivatives produce descendants. Therefore, we focus on $\hat{\mathcal{J}}_{i_1 \dots i_s}^{ab}$, which has orthogonal spin s . For the color indices, it is convenient to use $\mathfrak{so}(3)$

²⁸For $s = 0$, the resulting expression, up to an antisymmetric tensor, gives the Noether current associated with the $SU(2)$ global symmetry $\mathcal{J}_\mu^a \sim \epsilon^{abc} \phi_b \partial_\mu \phi_c$, which remains conserved even in the defect theory.

rather than $\mathfrak{su}(2)$. For even s , the two color indices are in the antisymmetric representation, equivalent to the vector representation $\hat{\mathcal{J}}_{i_1 \dots i_s}^a$. For odd s , the representations can be the traceless symmetric $\hat{\mathcal{J}}_{i_1 \dots i_s}^{\{ab\}}$ and the singlet $\hat{\mathcal{J}}_{i_1 \dots i_s}$. When bulk interactions are introduced, these higher spin currents are weakly broken and their dimensions receive corrections starting at second order in ε .

It is possible to obtain more information on the defect spectrum by examining Ward identities for specific correlators. Following [137], we can consider the bulk-to-defect two-point function of ϕ and $\hat{\phi}$, which by conformal symmetry takes the form

$$\langle \phi_a(0, x^i) \hat{\phi}_b(0) \rangle_{\mathcal{D}_j} = \frac{b_{\phi\hat{\phi}}}{|x^i|^{\Delta_\phi - \hat{\Delta}_\phi} |x^i|^{2\hat{\Delta}_\phi}} \delta_{ab}. \quad (4.2.93)$$

Here $\hat{\phi}$ is the fundamental field evaluated on the defect. Specializing to the free-bulk case and applying the Laplacian \square_x at a point away from the defect x , we find

$$0 = \langle \square \phi_a(0, x) \hat{\phi}_b(0) \rangle_{\mathcal{D}_j} = (\hat{\Delta}_\phi + \Delta_\phi - 1)(\hat{\Delta}_\phi - \Delta_\phi) \frac{b_{\phi\hat{\phi}}}{|x^i|^{\Delta_\phi - \hat{\Delta}_\phi + 2} |x^i|^{2\hat{\Delta}_\phi}} \delta_{ab}, \quad (4.2.94)$$

Given that $\hat{\Delta}_\phi = 1 + O(\varepsilon)$ and $b_{\phi\hat{\phi}} \neq 0$, as one can immediately see from tree-level diagrams, it follows that $\hat{\Delta}_\phi = \Delta_\phi$ non-perturbatively. The same argument applies to transverse spin- s operators $\hat{\mathcal{O}}_{i_1 \dots i_s}^a \sim \partial_{i_1} \dots \partial_{i_s} \hat{\phi}^a$, leading to the exact dimension $\hat{\Delta}_s = \Delta_\phi + s$. These dimensions receive corrections in the interacting bulk case, starting at second order in ε .

In previous sections, we observed that certain defect operators, such as the defect spin and displacement operators, incorporate insertions of a generator T_a , making them matrix-valued. A generic local defect operator is a $(2j+1) \times (2j+1)$ Hermitian matrix, with entries composed of fundamental fields and their derivatives. When the matrix is proportional to the identity, operators like the fundamental fields $\hat{\phi}_a$ can be factored outside the trace of the path-ordering. To construct and identify all possible defect operators, it is helpful to choose a convenient basis for these matrices.

For the simplest case $j = \frac{1}{2}$, corresponding to the fundamental representation of $\mathfrak{su}(2)$, the three generators and the identity span the entire real vector space of 2×2 Hermitian matrices. Thus, a defect operator with an arbitrary Hermitian matrix insertion can be decomposed into operators with insertions linear in the generators T^a . For higher spin $j > \frac{1}{2}$, the space of possible Hermitian matrix insertions has a real dimension of $(2j+1)^2$. This space can be spanned by Hermitian combinations of symmetrized traceless products of the generators $T^{\{a_1 \dots a_k\}}$, with $k = 0, \dots, 2j$. In particular, there are $4j(j+1)$ defect primary operators defined by the basis elements $\hat{S}^{\{a_1 \dots a_k\}}(x) \equiv T^{\{a_1 \dots a_k\}}(x)$ for $k \geq 1$ inserted in the path-ordered exponential, without any fundamental field. These operators are expected to be among the lightest in the theory, since their classical dimension is zero. Additionally, no mixing occurs between

them for representation theory reasons. For operators involving powers of fundamental fields and their derivatives, it is still useful to organize them by their color index structure. However, in general there will be several operators in the same representation and with the same classical dimension, therefore they may mix.

Finally, it is crucial to note that defect descendants are defined by the defect covariant derivative (4.2.52), not the ordinary one. For example, as shown in (4.2.53), the defect operator $\epsilon^{abc}\phi_b T_c(\tau)$ is not a new primary, but a descendant.

Correlators of $\hat{\phi}_a$ and $\hat{\mathcal{O}}_{i_1\dots i_s}^a$

In the free bulk case, there are interesting exact relations between the correlators of defect operators we've discussed. For instance, consider the defect operator $\hat{\phi}_a$, which is just the fundamental field placed on the defect. Using the analogue of (4.2.50) for $\hat{\phi}_a$ (i.e. when $x^i = 0$), we can express its two-point function in terms of the correlator of the defect spin operator

$$\langle \hat{\phi}_a(\tau_1)\hat{\phi}_b(\tau_2)\rangle_{\mathcal{D}_j} = \frac{\kappa j(j+1)\delta_{ab}}{3|\tau_1 - \tau_2|^{2-\varepsilon}} + \kappa \zeta^2 \int d\sigma_1 \int d\sigma_2 \frac{\langle \hat{S}(\sigma_1)\hat{S}(\sigma_2)\rangle_{\mathcal{D}_j}}{(|\tau_1 - \sigma_1||\tau_2 - \sigma_2|)^{2-\varepsilon}}. \quad (4.2.95)$$

This relation holds non-perturbatively. In particular, at the fixed point we obtain

$$\langle \hat{\phi}_a(\tau_1)\hat{\phi}_b(\tau_2)\rangle_{\mathcal{D}_j} = \frac{\delta_{ab}}{3|\tau_1 - \tau_2|^{2-\varepsilon}} \left(\kappa j(j+1) - \frac{\zeta_*^2 \mathcal{N}_{\hat{S}} \Gamma(1-\varepsilon) \Gamma(\frac{\varepsilon-1}{2}) \sin(\frac{\pi\varepsilon}{2})}{2^{2-\varepsilon} \pi^{\frac{3-\varepsilon}{2}}} \right). \quad (4.2.96)$$

This confirms that $\hat{\phi}_a$ has zero anomalous dimension, as we already knew from Ward identities.

Similarly, we can examine the two-point function involving one bulk operator and one defect operator. At the fixed point, we find

$$\langle \phi_a(0, x^i)\hat{\phi}_b(\tau)\rangle_{\mathcal{D}_j} = \frac{\delta_{ab}}{3(|x^i|^2 + \tau^2)^{1-\frac{\varepsilon}{2}}} \left(\kappa j(j+1) - \frac{\zeta_*^2 \mathcal{N}_{\hat{S}} \Gamma(1-\frac{\varepsilon}{2}) \tan(\frac{\pi\varepsilon}{2})}{\pi^{1-\frac{\varepsilon}{2}}(\varepsilon-1)} \right). \quad (4.2.97)$$

Notably, this two-point function depends only on the four-dimensional distance between the bulk and defect fields, because they have the same conformal dimension. This logic also extends to correlators involving $\hat{\mathcal{O}}_{i_1\dots i_s}^a \sim \partial_{i_1}\dots\partial_{i_s}\hat{\phi}^a$, where one needs to compute orthogonal derivatives in (4.2.50) before setting $x^i = 0$.

Finally, a similar approach can be used to compute the two-point function of two bulk fields, as will see in Section 4.2.5.

In the interacting bulk case, corrections to the correlators (4.2.96) and (4.2.97) will appear starting from order ε^2 .

Time reversal symmetry for defect operators

We are now ready to extend the discussion of time reversal symmetry to general defect operators. Their behavior under this symmetry will be a valuable tool for classifying these operators.

Defect operators composed only of fundamental fields and their derivatives, without any additional generator insertions, behave just like bulk operators under time reversal symmetry. However, for defect operators with insertions, we need a more detailed analysis. We can apply the same logic as in Section 4.2.2 to operators with insertions into the defect.

A careful examination shows that under the effect of T_t we have

$$T_t : T^a(\tau) \mapsto -T^a(-\tau) \quad (4.2.98)$$

Since $T_{\mathbb{Z}_2}$ does not act on generators, it follows that T^a is odd under \bar{T}_t . This is evident, for instance, from the Ward identity

$$\square\phi_a(0, x^i) = \frac{\zeta_0}{\sqrt{\kappa}} \hat{S}_a(0) \delta^{d-1}(x^i). \quad (4.2.99)$$

For cases where more than one generator is inserted at the same point (for $j \geq 1$), time reversal not only introduces a factor of (-1) for each generator, but also reverses the order of the insertions. In the matrix basis introduced earlier, the action of time reversal is

$$\bar{T}_t : T_{\{a_1 \dots a_k\}}(\tau) \mapsto (-1)^k T_{\{a_1 \dots a_k\}}(-\tau) \quad (4.2.100)$$

This symmetry imposes useful constraints on correlators. For instance, it can resolve certain degeneracies, since two defect operators with different parities must have a vanishing two-point function at the non-perturbative level. This rule also applies to the two-point function involving a bulk operator and a defect operator, giving useful selection rules for the coefficients in the defect block expansion.

However, this conclusion does not necessarily extend to correlators with more than two defect operators. In one-dimensional defects, the three-point function of three defect operators can be antisymmetric [137]²⁹. For example, one can check that

$$\langle \hat{S}_a(\tau_1) \hat{S}_b(\tau_2) \hat{S}_c(\tau_3) \rangle \propto i\epsilon_{abc}. \quad (4.2.101)$$

Classification of low-lying defect operators

In this section, we conveniently collect all the information about the low-lying spectrum of the defect obtained so far through various methods. Defect operators are classified

²⁹Given any two points on an ordered straight line it is possible to invert their order through a special conformal transformation that preserves the line, but the same cannot be done for three points.

based on their transverse spin s , their $\mathfrak{su}(2)$ representation (characterized by its dimension), their parity under time reversal symmetry \bar{T}_t and their classical scaling dimension. Note that some of these operators only exist for sufficiently high values of j , where j specifies the $\mathfrak{su}(2)$ -representation of the generators T_a in the definition of the defect (4.2.1).

Compiling a complete list of defect operators at twist zero is straightforward.³⁰ For twist-one operators, it is sufficient to construct all possible composite operators using a single fundamental field ϕ_a and an arbitrary number of generators T_a and orthogonal derivatives ∂_i . These must then be decomposed into irreducible representations of $\mathfrak{su}(2)$. Furthermore, since the defect covariant derivative increases the twist by one, all descendants of the twist-zero primaries must be excluded. In principle, this classification can be extended to higher twist operators, which can be constructed using multiple fundamental fields and orthogonal Laplacians \square_\perp . Again, all descendants of lower-twist primaries must be excluded. The number of primary operators grows combinatorially with the defect twist.

In table 4.1, we list all the defect twist-zero and defect twist-one primary operators, along with their quantum numbers and scaling dimensions at the fixed point (both for the free bulk and interacting bulk cases). In Table 4.2, we provide the explicit definition of these operators in perturbation theory.

³⁰Recall that the defect twist $\hat{\tau}$ of a defect operator with dimension $\hat{\Delta}$ and orthogonal spin s is defined as $\hat{\tau} \equiv \hat{\Delta} - s$.

$\hat{\mathcal{O}}$	s	$\dim R_{\text{su}(2)}$	\bar{T}_t	$\hat{\Delta}_{\hat{\mathcal{O}}} _{\lambda=0}$	$\hat{\Delta}_{\hat{\mathcal{O}}} _{\lambda_*}$
\hat{S}^a	0	3	−	$\frac{\varepsilon}{2}$	(4.2.56)
$\hat{S}^{\{a_1 \dots a_k\}}$	0	$2k + 1$	$(-)^k$	$O(\varepsilon)$	$O(\varepsilon)$
$\hat{\phi}^a$	0	3	−	$1 - \frac{\varepsilon}{2}$	$1 - \frac{\varepsilon}{2} + O(\varepsilon^2)$
$\hat{\Phi}$	0	1	+	(4.2.82)	(4.2.83)
\hat{D}_i	1	1	+	2	2
$\hat{\mathcal{J}}_{i_1 \dots i_s}^a$	s	3	+	$s + 1$	$s + 1 + O(\varepsilon^2)$
$\hat{\mathcal{J}}_{i_1 \dots i_s}^{\{ab\}}$	s	5	+	$s + 1$	$s + 1 + O(\varepsilon^2)$
$\hat{\mathcal{J}}_{i_1 \dots i_s}$	s	1	+	$s + 1$	$s + 1 + O(\varepsilon^2)$
$\hat{\mathcal{O}}_{i_1 \dots i_s}^a$	s	3	−	$s + 1 - \frac{\varepsilon}{2}$	$s + 1 - \frac{\varepsilon}{2} + O(\varepsilon^2)$
$\hat{U}_{i_1 \dots i_s}^{\{a_1 \dots a_k\}}$	s	$2k + 1$	$(-)^k$	$s + 1 + O(\varepsilon)$	$s + 1 + O(\varepsilon)$
$\hat{V}_{i_1 \dots i_s}^{\{a_1 \dots a_k\}}$	s	$2k + 1$	$(-)^k$	$s + 1 + O(\varepsilon)$	$s + 1 + O(\varepsilon)$
$\hat{W}_{i_1 \dots i_s}^{\{a_1 \dots a_k\}}$	s	$2k + 1$	$(-)^{k+1}$	$s + 1 + O(\varepsilon)$	$s + 1 + O(\varepsilon)$

Table 4.1: Defect twist-zero and twist-one primary operators with their quantum numbers and scaling dimensions.

Operator	Perturbative definition	Existence
\hat{S}^a	T^a	
$\hat{S}^{\{a_1 \dots a_k\}}$	$T^{\{a_1 \dots T^{a_k}\}}$	$2 \leq k \leq 2j$
$\hat{\phi}^a$	ϕ^a	
$\hat{\Phi}$	$\phi^a T_a$	
\hat{D}_i	$\partial_i \phi^a T_a$	
$\hat{J}_{i_1 \dots i_s}^a$	$\epsilon^{abc} \partial_{i_1} \dots \partial_{i_s} \phi_b T_c$	even s , $s \geq 2$
$\hat{J}_{i_1 \dots i_s}^{\{ab\}}$	$\partial_{i_1} \dots \partial_{i_s} \phi^{\{a T^b\}}$	odd s , $s \geq 1$
$\hat{J}_{i_1 \dots i_s}$	$\partial_{i_1} \dots \partial_{i_s} \phi^a T_a$	odd s , $s \geq 3$
$\hat{O}_{i_1 \dots i_s}^a$	$\partial_{i_1} \dots \partial_{i_s} \phi^a$	$s \geq 1$
$\hat{U}_{i_1 \dots i_s}^{\{a_1 \dots a_k\}}$	$\partial_{i_1} \dots \partial_{i_s} \phi_b T^{\{b T^{a_1} \dots T^{a_k}\}}$	$1 \leq k \leq 2j - 1$, $s \geq 0$
$\hat{V}_{i_1 \dots i_s}^{\{a_1 \dots a_k\}}$	$\partial_{i_1} \dots \partial_{i_s} \phi^{\{a_1 T^{a_2} \dots T^{a_k}\}}$	$3 - \delta_{0,s} \leq k \leq 2j + 1$, $s \geq 0$
$\hat{W}_{i_1 \dots i_s}^{\{a_1 \dots a_k\}}$	$\partial_{i_1} \dots \partial_{i_s} \phi^b \epsilon^{bc} \{a_1 T^c T^{a_2} \dots T^{a_k}\}$	$2 \leq k \leq 2j$, $s \geq 1$

Table 4.2: Schematic perturbative definition of defect twist-zero and twist-one operators.

Note that for some of these operators, the form provided is only schematic. Beyond the tree level, mixing among operators with the same quantum numbers can occur, and orthogonalization with respect to the two-point functions must be performed. For instance, the explicit form of the operator $\hat{U}^a = \phi_b T^{\{b T^a\}}$ is accurate only at tree level. At higher loop orders, this operator must be orthogonalized relative to $\hat{\phi}_a$.

Further results about defect operators will be obtained in the next section through analytic bootstrap techniques.

4.2.4 Analytic bootstrap of the bulk two-point function

In this section, we do a similar bootstrap analysis as in Section 4.1. We use the dispersion relation (3.2.1) to calculate the bulk two-point function

$$\langle \phi_a(x_1) \phi_b(x_2) \rangle_{\mathcal{D}_j} = \frac{\delta_{ab} F_{\phi\phi}(r, w)}{|x_1^i|^{\Delta_\phi} |x_2^i|^{\Delta_\phi}}, \quad (4.2.102)$$

and then we extract the bulk and defect CFT data, similar to what we did in Sections 4.1.4 and 4.1.5. There are small differences compared to the case of the localized magnetic field. First of all, the operators that appear in the defect block expansion

(2.5.15) transform according to the representations of $O(3)$, since the spin impurity does not break the global symmetry. Additionally, the operators that appear in the bulk OPE are all singlets of $O(3)$. For this reason, contrary to Section 4.1, we often omit the representation labels in the CFT data of the operators. In this section, we will consider the two-point function both in the free and interacting (Wilson-Fisher) bulk cases.

The computation at the Wilson-Fisher fixed point is very similar to the one in Section 4.1.3. The reason is straightforward: we compute the discontinuity by expanding the two-point function into bulk blocks and evaluating the discontinuity of each block. As we saw in Section 4.1.3, at first order in perturbation theory the discontinuity of a block is proportional to the anomalous dimension of the corresponding bulk operator, which is independent of the defect. As observed in (4.1.33), in the $O(3)$ model all the operators that appear in the bulk OPE at order ε have vanishing anomalous dimensions, except for the ϕ^2 operator. Therefore also in this case the discontinuity will be given by a single bulk block.

Analytic bootstrap for the free bulk

We begin by examining the spin impurity (4.2.1) in a free bulk theory in $d = 4 - \varepsilon$ dimensions, a case for which we can find certain results exactly in ε .

In this case, the bulk OPE includes only the identity and twist-two operators (4.1.24). As discussed in Section 4.1.3, the discontinuity of twist-two operators is proportional to their anomalous dimension. However, in a free theory, bulk operators do not possess an anomalous dimension, meaning that the discontinuity arises solely from the identity operator. It reads

$$\text{Disc}[F_{\phi\phi}] = \text{Disc} \left[\left(\frac{rw}{(1-rw)(w-r)} \right)^{\Delta_\phi} \right] = 2i \sin(\pi\Delta_\phi) \left(\frac{rw}{(1-rw)(r-w)} \right)^{\Delta_\phi}, \quad (4.2.103)$$

where $\Delta_\phi = 1 - \frac{\varepsilon}{2}$. Notice that this equation holds to all orders in ε . Using the dispersion relation (3.2.1), and adding a potential low-spin ($s \leq s^*$) ambiguity³¹, we obtain

$$F_{\phi\phi}(r, w) = \left(\frac{rw}{(1-rw)(w-r)} \right)^{\Delta_\phi} + \text{low-spin ambiguity}. \quad (4.2.104)$$

To resolve the low-spin ambiguity, we can leverage the results of Section 4.2.3 regarding the operators that may appear in the defect channel. As previously discussed, the equation of motion $\square\phi_a = 0$ constrains the dimensions of the defect operators that couple to it. In particular, following [137], we can infer the existence of two families of

³¹For more details on the low spin ambiguity, see (2.5.25) and the discussion below.

operators from the relation

$$\square \langle \phi_a(x) \hat{\mathcal{O}}_b(\tau) \rangle = 0, \quad (4.2.105)$$

These families include:

- Modes $\hat{\mathcal{O}}_{0,s}^a \sim (\partial_\perp)^s \phi^a$ with $s \geq 0$ and $\hat{\Delta}_{0,s} = \Delta_\phi + s = 1 - \varepsilon/2 + s$.
- An operator \hat{S}^a , with $s = 0$ and $\hat{\Delta} = \varepsilon/2$.³² This is the spin operator discussed in Section 4.2.3, and perturbatively defined by (4.2.47). Due to the inverted Ward identity (4.2.50) and the non-vanishing two-point function of \hat{S}^a , the spin operator has a non-trivial coupling to the bulk fundamental field (4.2.71).

As seen in Section 4.1.2, the defect-channel expansion of the bulk identity (4.2.104) contains the $\hat{\mathcal{O}}_{0,s}^a$ operators, but it does not include any operator with the quantum numbers of \hat{S}^a . Thus, we conclude that the dispersion relation fails to account for the contribution from spin $s = 0$. Consequently, the most general ansatz for the correlator is

$$F_{\phi\phi}(r, w) = \left(\frac{rw}{(1-rw)(w-r)} \right)^{\Delta_\phi} + k_1 \hat{f}_{1-\varepsilon/2,0}(r, w) + k_2 \hat{f}_{\varepsilon/2,0}(r, w), \quad (4.2.106)$$

where the extra terms are the defect blocks associated with the low-spin ambiguities. The coefficients k_1 and k_2 are not arbitrary. They must be chosen to ensure the absence of spurious terms and logarithms that are incompatible with a bulk-channel expansion. To be more explicit, consider changing from radial coordinates (r, w) to lightcone coordinates (z, \bar{z}) , defined in (2.5.9). In this coordinate system, one can see that the expansion of (4.2.106) around $|1-z| \ll |1-\bar{z}| \ll 1$ contains spurious powers $(1-z)^n(1-\bar{z})^{-m}$ for $m \geq 2$, and spurious logarithms $\log(1-\bar{z})$ which are not accompanied by $\log(1-z)$. These terms are incompatible with an expansion in terms of bulk-channel conformal blocks (2.5.18), and therefore we must choose the relative size of k_1 and k_2 to make sure they are absent. After carrying out this procedure, we find that the free correlator is

$$F_{\phi\phi}(r, w) = \left(\frac{rw}{(1-rw)(w-r)} \right)^{\Delta_\phi} + a\lambda_{\phi^2} J_\varepsilon(r), \quad (4.2.107)$$

where we introduced³³

$$J_\varepsilon(r) = \frac{\Gamma\left(\frac{1-\varepsilon}{2}\right)}{\sqrt{\pi}\Gamma\left(\frac{2-\varepsilon}{2}\right)} \hat{f}_{\varepsilon/2,0}(r, w) + \frac{\Gamma\left(\frac{\varepsilon-1}{2}\right)}{\sqrt{\pi}\Gamma\left(\frac{\varepsilon}{2}\right)} \hat{f}_{1-\varepsilon/2,0}(r, w). \quad (4.2.108)$$

This correlation function is exact to all orders in ε , though it depends on one parameter $a\lambda_{\phi^2}$ that cannot be fixed by the bootstrap. Since (4.2.107) is exact in ε , it is possible

³²More generally, we would find spinning operators with $\hat{\Delta} = \varepsilon/2 - s$, but they break unitarity for $s > 0$.

³³Note that this function does not depend on w because it is a sum of two $s = 0$ blocks (2.5.15).

to investigate the properties of the fixed point in three dimensions by simply setting $\varepsilon = 1$. Even though in (4.2.108) there are some divergent factors, one can check that $J_\varepsilon(r)$ is finite in the $\varepsilon \rightarrow 1$ limit. We are left with two possibilities: either $a\lambda_{\phi^2}|_{\varepsilon=1} = 0$, or $a\lambda_{\phi^2}|_{\varepsilon=1} \neq 0$. In the first case, $F_{\phi\phi}$ is just a free correlator. This is sufficient to show that ϕ satisfies the free-field equations of motion, and therefore all its correlators are those of the free theory. Instead, if $a\lambda_{\phi^2}|_{\varepsilon=1}$ is a finite non-zero number, we can try to expand the correlator in the defect channel by taking $r \ll 1$. However, this expansion contains terms with factors of $\log r$ that cannot be reproduced by the defect blocks. Therefore, this correlator does not obey the defect bootstrap equation (2.5.14). Thus, in three dimensions and a free bulk, no non-trivial spin impurity exists.

For $0 < \varepsilon < 1$, instead, the function $J_\varepsilon(r)$ is a truncated solution of crossing ³⁴, meaning that it has sensible bulk and defect expansions on its own, and it involves finitely many transverse spins. From the full two-point function, we can extract the CFT data for $\varepsilon < 1$ in both OPE channels as a function of $a\lambda_{\phi^2}$. Let us start with the defect expansion, which from the discussion above takes the form

$$F_{\phi\phi}(r, w) = b_{0,0}^2 \hat{f}_{1-\varepsilon/2,0}(r, w) + b_{\phi\hat{S}}^2 \hat{f}_{\varepsilon/2,0}(r, w) + \sum_{s=1}^{\infty} b_{0,s}^2 \hat{f}_{\Delta_\phi+s,s}(r, w), \quad (4.2.109)$$

where $b_{0,s}^2 \equiv b_{\phi\hat{\mathcal{O}}_{0,s}}^2$. Comparing the expansion above with (4.2.107) and using the definition of conformal blocks (2.5.15), we obtain

$$b_{0,0}^2 = 1 + \frac{\Gamma(\frac{\varepsilon-1}{2})}{\sqrt{\pi}\Gamma(\frac{\varepsilon}{2})} a\lambda_{\phi^2}, \quad b_{\phi\hat{S}}^2 = \frac{\Gamma(\frac{1-\varepsilon}{2})}{\sqrt{\pi}\Gamma(\frac{2-\varepsilon}{2})} a\lambda_{\phi^2}, \quad b_{0,s}^2 = \frac{2^s (\Delta_\phi)_s}{s!}. \quad (4.2.110)$$

Alternatively, one can extract the last result using the the defect inversion formula (2.5.21) with the discontinuity given in (4.2.103).

Similarly, using the formulas for the bulk blocks (2.5.19), we find the expansion

$$F_{\phi\phi}(r, w) = \left(\frac{rw}{(1-rw)(w-r)} \right)^{\Delta_\phi} + \left(\frac{rw}{(1-rw)(w-r)} \right)^{\Delta_\phi} \sum_{\ell=0}^{\infty} a\lambda_{0,\ell} f_{2\Delta_\phi+\ell,\ell}(r, w). \quad (4.2.111)$$

where, as usual, we define $a\lambda_{\mathcal{O}} \equiv a_{\mathcal{O}}\lambda_{\phi\phi\mathcal{O}}$. The bulk expansion includes only twist-two operators (4.1.24), as expected in the bulk-free theory. The three-point OPE coefficients are known exactly

$$\lambda_{\phi\phi\mathcal{J}_{0,\ell}} = \sqrt{\frac{2}{3}} \frac{2^{\frac{\ell}{2}} (\Delta_\phi)_\ell}{\sqrt{\ell!(2\Delta_\phi + \ell - 1)_\ell}}. \quad (4.2.112)$$

³⁴This is an analog of the solutions of crossing with finite support in spin of [138], which play an important role in the ε -expansion bootstrap for four-point functions [79, 80, 139, 140, 54].

As a result, from the block expansion (4.2.111), we can predict the one-point functions of all twist-two operators

$$a_{\mathcal{J}_{0,0}} \equiv a_{\phi^2} = \sqrt{\frac{3}{2}} a_{\lambda_{\phi^2}}, \quad a_{\mathcal{J}_{0,\ell}} = \frac{(1-\varepsilon)_\ell \left(\frac{\ell-\varepsilon+2}{2}\right)_{\frac{\ell}{2}} \sqrt{\ell!(\ell-\varepsilon+1)_\ell}}{2^{5\ell/2} \left(\frac{\ell}{2}!\right)^2 \left(\frac{\ell-\varepsilon+1}{2}\right)_{\frac{\ell}{2}} \left(1-\frac{\varepsilon}{2}\right)_\ell} a_{\phi^2}. \quad (4.2.113)$$

For the special case of $\ell = 2$, corresponding to the stress tensor, the one-point function is conjectured to be positive [44].³⁵ Therefore, in the bulk-free theory, we should have $a_{\phi^2} > 0$.

Ultimately, the two-point function of ϕ_a and the CFT data are completely determined by the bootstrap analysis, up to an undetermined constant corresponding to the one-point function a_{ϕ^2} . We shall compute this to order $O(\varepsilon^3)$ in equation (4.2.136) below.

Analytic bootstrap for the interacting bulk

Let us now consider the bulk theory to be the $O(3)$ model at the Wilson-Fisher fixed point in $d = 4 - \varepsilon$ dimensions, focusing on the first non-trivial order in the perturbative expansion for small ε .

As we saw in Section 4.1.3, the bulk OPE contains twist-two operators and the identity. In the case of $O(3)$, the dimensions of twist-two operators are³⁶

$$\Delta_{0,\ell} = 2\Delta_\phi + \ell + \varepsilon \frac{5}{11} \delta_{\ell,0} + O(\varepsilon^2), \quad (4.2.114)$$

and their coefficients can be expanded as

$$\lambda_{\phi\phi\mathcal{J}_{0,\ell}} = \lambda_{\phi\phi\mathcal{J}_\ell}^{(0)} + \varepsilon \lambda_{\phi\phi\mathcal{J}_\ell}^{(1)} + \varepsilon^2 \lambda_{\phi\phi\mathcal{J}_\ell}^{(2)} + O(\varepsilon^3), \quad a_{\mathcal{J}_\ell} = a_{\mathcal{J}_\ell}^{(0)} + \varepsilon a_{\mathcal{J}_\ell}^{(1)} + \varepsilon^2 a_{\mathcal{J}_\ell}^{(2)} + O(\varepsilon^3). \quad (4.2.115)$$

For higher-twist operators, we have

$$\Delta_{n,\ell} = 2\Delta_\phi + 2n + \ell + \varepsilon \gamma_{n,\ell}^{(1)} + O(\varepsilon^2), \quad \lambda_{\phi\phi\mathcal{O}_{n,\ell}} = \varepsilon \lambda_{\phi\phi\mathcal{O}_{n,\ell}}^{(1)} + \varepsilon^2 \lambda_{\phi\phi\mathcal{O}_{n,\ell}}^{(2)} + O(\varepsilon^3). \quad (4.2.116)$$

Therefore only the bulk identity and ϕ^2 operators contribute to the discontinuity. All the other operators do not contribute at the order we are working because their anomalous dimension or OPE coefficients are higher order. Ultimately, the discontinuity is given by³⁷

$$\text{Disc} F_\phi(r, w) = 2i \sin(\pi \Delta_\phi) \left(\frac{rw}{(1-rw)(r-w)} \right)^{\Delta_\phi} + \varepsilon^2 \frac{5\pi i}{11} a_{\phi^2}^{(1)} \lambda_{\phi\phi\phi^2}^{(0)} \frac{rw}{(1-rw)(w-r)} f_{2,0}(r, w) + \mathcal{O}(\varepsilon^3), \quad (4.2.117)$$

³⁵In the $\mathcal{N} = 4$ SYM literature, this observable is often referred to as the Bremsstrahlung function.

³⁶This follows from (4.1.33) with $N = 3$.

³⁷The discontinuity is obtained following the exact same steps as for the singlet contribution in Section 4.1.3.

where the first contribution comes from the identity (4.2.103), with Δ_ϕ given in (4.1.20) and expanded up to order ε^2 . It is worth noticing that a_{ϕ^2} , at leading order, matches the tree-level result from free theory [116], and in particular $a_{\phi^2} \sim \varepsilon$. Therefore the first non-trivial correction to the discontinuity arises at order ε^2 . The discontinuity (4.2.117) is similar to the result found in (4.1.43), differing only by a factor that depends on the specific defect through the one-point function coefficient a_{ϕ^2} . The other coefficient $\lambda_{\phi\phi\phi^2}$ does not depend on the defect, just like the anomalous dimensions of bulk operators, and has the value [141, 79, 80]

$$\lambda_{\phi\phi\phi^2} = \sqrt{\frac{2}{3}} \left(1 - \varepsilon \frac{5}{22} \right) + O(\varepsilon^2). \quad (4.2.118)$$

Specifically, at leading order, $\lambda_{\phi\phi\phi^2}^{(0)} = \sqrt{\frac{2}{3}}$. The discontinuity and the dispersion relation result can be evaluated explicitly in terms of special functions, as in (4.1.43). Ultimately, the dispersion relation yields

$$F_{\phi\phi}(r, w) = \left(\frac{rw}{(1-rw)(w-r)} \right)^{\Delta_\phi} + \varepsilon^2 \frac{5a\lambda_{\phi^2}^{(1)}}{11} H(r, w) + \text{low spin} + O(\varepsilon^3), \quad (4.2.119)$$

where $H(r, w)$ is defined in (4.1.47). This function can be represented in a variety of different ways which are better suited for explicit evaluation or the extraction of the CFT data, as we saw in (4.1.44). Like in the free bulk case, the dispersion relation result may miss low spin contributions. In the free theory discussed previously, a truncated solution to crossing, $J_\varepsilon(r)$, had to be added to the correlator. Expanding this function for small ε , we obtain

$$J_\varepsilon(r) = 1 + \frac{\varepsilon}{2} \log \frac{4r}{(1+r)^2} + O(\varepsilon^2). \quad (4.2.120)$$

We anticipate a similar correction in the interacting case. Our goal is to find the most general truncated solution to be added to the final interacting correlator. Following the same reasoning as in the case of the localized magnetic field, we assume that only operators with defect twist equal to one appear in the defect OPE. As explained in Section 4.1.3, this assumptions leads to

$$F_{\text{amb}}(r, w) = q_0 \hat{f}_{0,0}(r, w) + r_0 \left(\partial_{\hat{\Delta}} \hat{f}_{0,0}(r, w) - 2\hat{f}_{1,0}(r, w) \right) = q_0 + r_0 \log \frac{r}{(1+r)^2}, \quad (4.2.121)$$

Both equation (4.2.120) and (4.2.121) suggest the ambiguities of interest are a constant and a logarithm. Ultimately, the ansatz for the correlator is

$$F_{\phi\phi}(r, w) = \left(\frac{rw}{(1-rw)(w-r)} \right)^{\Delta_\phi} + \varepsilon^2 \frac{5a\lambda_{\phi^2}^{(1)}}{11} H(r, w) + q_0 + r_0 \log \frac{r}{(1+r)^2} + O(\varepsilon^3), \quad (4.2.122)$$

The constants $a\lambda_{\phi^2}^{(1)}$, q_0 , r_0 cannot be fixed from the bootstrap alone. However, they are not independent. One can fix r_0 in terms of $a\lambda_{\phi^2}^{(1)}$ exploiting the analysis on the defect spectrum in Section 4.2.3. Indeed, the defect expansion has the same form as in the case of the free bulk

$$F_{\phi\phi}(r, w) = b_{0,0}^2 \hat{f}_{\hat{\Delta}_{0,0},0}(r, w) + b_{\phi\hat{S}}^2 \hat{f}_{\hat{\Delta}_{\hat{S}},0}(r, w) + \sum_{s=1}^{\infty} b_{0,s}^2 \hat{f}_{\Delta_{\phi+s},s}(r, w). \quad (4.2.123)$$

and in particular it contains the spin operator \hat{S}^a . As discussed in Section 4.2.3, while this operator has no longer protected dimension if the bulk is not free, one can see from the Ward identity that the correction to the anomalous dimension starts at order ε^2 . Therefore, the leading dimension must coincide with the one in the free bulk case. This fixes $r_0 = \frac{\varepsilon}{2} a\lambda_{\phi^2}^{(1)}$. Notice that this is different to what happened in the case of the localized magnetic field, where no analogue of \hat{S}^a exists. Finally, one can fix q_0 in terms of $a\lambda_{\phi^2}$ just by expanding the correlator in the bulk channel, namely

$$F(r, w) = \left(\frac{rw}{(1-rw)(w-r)} \right)^{\Delta_{\phi}} + \varepsilon^2 \frac{5a\lambda_{\phi^2}^{(1)}rw}{22(1-rw)} (\tilde{f}_{2,0}(r, w) \log(w-r) + \partial_{\Delta} \tilde{f}_{2,0}(r, w)) + \sum_{\ell>0} a\lambda_{0,\ell} f_{2\Delta_{\phi+\ell},\ell}(r, w) + \mathcal{O}(\varepsilon^3). \quad (4.2.124)$$

By comparing with (4.2.122) we fix $q_0 = a\lambda_{\phi^2} + \varepsilon^2 a\lambda_{\phi^2}^{(1)} \left(\frac{5}{11} + \frac{16}{11} \log 2 \right)$. Thus, the correlator and all CFT data are fixed in terms of a single unknown one-point function coefficient a_{ϕ^2} , giving

$$F(r, w) = \left(\frac{rw}{(1-rw)(w-r)} \right)^{\Delta_{\phi}} + a\lambda_{\phi^2} \left(1 + \frac{\varepsilon}{2} \log \frac{4r}{(1+r)^2} + \varepsilon \frac{5}{11} (1 + \log 2 + H(r, w)) \right) + \mathcal{O}(\varepsilon^3), \quad (4.2.125)$$

where as always $a\lambda_{\phi^2} = \lambda_{\phi\phi\phi^2} a_{\phi^2} = \sqrt{\frac{2}{3}} (1 - \varepsilon \frac{5}{22}) \left(\varepsilon a_{\phi^2}^{(1)} + \varepsilon^2 a_{\phi^2}^{(2)} \right) + \mathcal{O}(\varepsilon^3)$. From the full correlator, we can extract defect and bulk CFT data, either by comparing (4.2.125) with the explicit form of the defect and bulk expansions, (2.5.15) and (2.5.19), or using the Lorentzian inversion formulas, as in Sections 4.1.4 and 4.1.5. The CFT data for the defect spin operator reads

$$\hat{\Delta}_{\hat{S}} = \frac{\varepsilon}{2} + \mathcal{O}(\varepsilon^2), \quad (4.2.126)$$

$$b_{\phi\hat{S}}^2 = a\lambda_{\phi^2} + \varepsilon^2 a\lambda_{\phi^2}^{(1)} \left(\frac{5}{11} + \frac{16}{11} \log 2 \right) + \mathcal{O}(\varepsilon^3). \quad (4.2.127)$$

Notice that from (4.2.125) we can extract the defect spin dimension up to $\mathcal{O}(\varepsilon)$ because $b_{\phi\hat{S}}$ is also $\mathcal{O}(\varepsilon)$. However let us stress that the $\mathcal{O}(\varepsilon^2)$ for $\hat{\Delta}_{\hat{S}}$ is known and we reported it in (4.2.56). Moving on to the other operators in the defect channel, the CFT data

for the operator $\hat{\mathcal{O}}_{0,0}$ is

$$\hat{\Delta}_{0,0} = \Delta_\phi + \varepsilon^2 \frac{10a\lambda_{\phi^2}^{(1)}}{11} + O(\varepsilon^3), \quad (4.2.128)$$

$$b_{0,0}^2 = 1 - \varepsilon^2 a\lambda_{\phi^2}^{(1)} \left(\frac{31}{11} - \frac{20}{11} \log 2 \right) + O(\varepsilon^3). \quad (4.2.129)$$

Finally, we find a single infinite family of defect operators $\hat{\mathcal{O}}_{0,s}$ with

$$\hat{\Delta}_{0,s} = \Delta_\phi + s + \varepsilon^2 \frac{5a\lambda_{\phi^2}^{(1)}}{11} \frac{1}{s+1/2} + O(\varepsilon^3), \quad (4.2.130)$$

$$b_{0,s}^2 = 2^s \left(\frac{(\Delta_\phi)_s}{s!} + \varepsilon^2 \frac{5a\lambda_{\phi^2}^{(1)}}{11} \left(\frac{H_s - H_{s-1/2}}{s+1/2} - \frac{1}{(s+1/2)^2} \right) + O(\varepsilon^3) \right). \quad (4.2.131)$$

In the bulk channel we have the twist-two operators $\mathcal{J}_{0,\ell}$ with

$$a\lambda_{0,\ell} = \frac{\Gamma(\frac{\ell+1}{2}) \Gamma(\ell+1)^2}{8^\ell (\frac{\ell}{2}!)^2 \Gamma(\frac{\ell+2}{2}) \Gamma(\frac{2\ell+1}{2})} \times \quad (4.2.132)$$

$$\times \left[a\lambda_{\phi^2} + \varepsilon^2 a\lambda_{\phi^2}^{(1)} \left(\frac{5}{11} (1 + \log 2) + \frac{1}{2} \left(H_{\frac{\ell}{2}} - H_{\frac{\ell-1}{2}} + H_{\ell-\frac{1}{2}} - 3H_\ell \right) \right) + O(\varepsilon^3) \right].$$

Notice the absence of double-twist operators with twist higher than 2. This is consistent with the fact that [79, 142] $\lambda_{\phi\phi\mathcal{J}_{n,\ell}} \sim \varepsilon$ and $a_{\mathcal{J}_{n,\ell}} \sim \varepsilon^2$. The latter fact follows immediately by considering tree-level Feynman diagrams.

4.2.5 Diagrammatic computation

In this section we will outline the diagrammatic computation for the correlators of bulk fields ϕ_a and ϕ^2 and compare it with the bootstrap results of Section 4.2.4.

Free bulk

We begin by computing the one-point function of ϕ^2 in the free theory³⁸. This calculation has already been performed up to next-to-leading order in [116]. This observable is not accessible by our bootstrap analysis and indeed it is the only information needed to completely fix the two point function of ϕ_a . Given that the bulk is free, we have two approaches for the computation: we can exploit the Ward identity to express the bulk correlator in terms of an integrated defect correlator using (4.2.50), or perform a direct computation of the bulk correlator using Feynman diagrams. In terms of the defect correlator, we have

$$\langle \phi^2(0, x^i) \rangle_{\mathcal{D}_j} = \kappa \zeta^2 \int d\tau \int d\tau' \frac{\langle \hat{S}^a(\tau) \hat{S}^a(\tau') \rangle_{\mathcal{D}_j}}{(\tau^2 + |x^i|^2)^{1-\frac{\varepsilon}{2}} (\tau'^2 + |x^i|^2)^{1-\frac{\varepsilon}{2}}}. \quad (4.2.133)$$

³⁸The one-point function of ϕ^a is zero because of symmetry.

At the fixed point, $\langle \hat{S}^a(\tau) \hat{S}^a(\tau') \rangle_{\mathcal{D}_j}$ is given by (4.2.69). By evaluating the integrals, we find ³⁹

$$\begin{aligned} \langle \phi^2(0, x^i) \rangle_{\mathcal{D}_j} &= \frac{\kappa \zeta_*^2 \mathcal{N}_{\hat{S}} \pi^{3/2} \Gamma\left(\frac{1}{2} - \frac{\varepsilon}{2}\right)}{|x^i|^{2-\varepsilon} \Gamma\left(1 - \frac{\varepsilon}{2}\right)} = \\ &\equiv \frac{\mathcal{N}_{\phi^2} a_{\phi^2}}{|x^i|^{2-\varepsilon}}. \end{aligned} \quad (4.2.134)$$

Here \mathcal{N}_{ϕ^2} is the normalization of the two-point function, which according to our conventions is

$$\langle \phi^2(x) \phi^2(0) \rangle = \frac{\mathcal{N}_{\phi^2}^2}{|x|^{2\Delta_{\phi^2}}}, \quad \mathcal{N}_{\phi^2}^2 = 6\kappa^2. \quad (4.2.135)$$

If we substitute the value of the coupling at the fixed point (4.2.24) and the normalization constant $\mathcal{N}_{\hat{S}}$ (4.2.70), we obtain ⁴⁰

$$a_{\phi^2} = \frac{\pi^2 j(j+1)\varepsilon}{2\sqrt{6}} \left(1 + \varepsilon \frac{\log 4 - 1}{2} + \varepsilon^2 \frac{2\pi^2 j(j+1) + (\log 4 - 2) \log 4}{8} \right) + O(\varepsilon^4). \quad (4.2.136)$$

We checked that this result can be reproduced from Feynman diagrams.

Moving on to the two point function of the order parameter ϕ_a , we can apply the same method as before, and compute it in terms of an integrated defect two-point function. Specifically, using (4.2.50), we find

$$\begin{aligned} \langle \phi_a(0, x_1^i) \phi_b(0, x_2^i) \rangle_{\mathcal{D}_j} &= \kappa \zeta^2 \int d\tau d\tau' \frac{\langle \hat{S}_a(\tau) \hat{S}_b(\tau') \rangle_{\mathcal{D}_j}}{(\tau^2 + |x_1^i|^2)^{1-\frac{\varepsilon}{2}} (\tau'^2 + |x_2^i|^2)^{1-\frac{\varepsilon}{2}}} + \\ &+ \langle \phi_a^{\text{free}}(0, x_1^i) \phi_b^{\text{free}}(0, x_2^i) \rangle_{\mathcal{D}_j}. \end{aligned} \quad (4.2.137)$$

At the fixed point, using (4.2.24) and (4.2.69), we obtain

$$\begin{aligned} \langle \phi_a \phi_b \rangle_{\mathcal{D}_j} &= \frac{\kappa \zeta_*^2 \mathcal{N}_{\hat{S}}}{3} \int d\tau \int d\tau' \frac{\delta_{ab}}{|\tau - \tau'|^{2\Delta_{\hat{S}}} (\tau^2 + r^2)^{1-\frac{\varepsilon}{2}} (\tau'^2 + 1)^{1-\frac{\varepsilon}{2}}} + \frac{\mathcal{N}_{\phi}^2 \delta_{ab} \left(\frac{rw}{(1-rw)(w-r)} \right)^{\Delta_{\phi}}}{|x_1^i|^{\Delta_{\phi}} |x_2^i|^{\Delta_{\phi}}} = \\ &\equiv \frac{\mathcal{N}_{\phi}^2 \delta_{ab} F_{\phi\phi}(r, w)}{|x_1^i|^{\Delta_{\phi}} |x_2^i|^{\Delta_{\phi}}}, \end{aligned} \quad (4.2.138)$$

where $\mathcal{N}_{\phi} = \sqrt{\kappa}$ and we exploited symmetry to set the first operator at $x = (0, z, \bar{z}, 0, \dots)$ and the other one at $(0, 1, 0, \dots)$. We expressed the integral in radial coordinates (2.5.9)

³⁹In the bootstrap computation, the operators are taken to be unit-normalized, as is customary in the CFT literature. However, in the diagrammatic calculation, a different normalization is more convenient, resulting in an additional factor in the one-point function compared to (2.5.6).

⁴⁰Our result for the one-point function at the fixed point differs from equation 2.14 of [116] at order ε^2 . We believe that this discrepancy arises because the authors of [116] used the leading-order critical coupling instead of the next-to-leading order, thereby missing a contribution of order ε^2 in the one-point coefficient.

in order to simplify the computation. The integral can be solved in terms of hypergeometric functions and we obtain

$$\begin{aligned}
F_{\phi\phi}(r, w) &= \text{free} + \frac{\zeta_*^2 \mathcal{N}_{\hat{S}}}{3} \left(\frac{2\pi \tan(\frac{\pi\varepsilon}{2}) r^{1-\frac{\varepsilon}{2}} {}_2F_1(\frac{1}{2}, 1-\frac{\varepsilon}{2}; \frac{3}{2}-\frac{\varepsilon}{2}; r^2)}{\varepsilon-1} + \frac{\pi r^{\frac{\varepsilon}{2}} \Gamma(\frac{1}{2}-\frac{\varepsilon}{2})^2 {}_2F_1(\frac{1}{2}, \frac{\varepsilon}{2}; \frac{\varepsilon+1}{2}; r^2)}{\Gamma(1-\frac{\varepsilon}{2})^2} \right) = \\
&= \left(\frac{rw}{(1-rw)(w-r)} \right)^{\Delta_\phi} + \lambda_{\phi\phi\phi^2} a_{\phi^2} J_\varepsilon(r), \tag{4.2.139}
\end{aligned}$$

where the free part is given by the bulk identity contribution, $\left(\frac{rw}{(1-rw)(w-r)}\right)^{\Delta_\phi}$. The second line was derived using the expression for the one-point function (4.2.134), the three-point function coefficient (4.2.112), and well-known identities for the hypergeometric function. This result is valid for all ε and perfectly matches the bootstrap prediction (4.2.107). Notably, the non-trivial integral corresponds to $J_\varepsilon(r)$, the contribution of spin $s = 0$ defect operators defined in (4.2.120).

We can also compute the two-point function of ϕ^2 , which we did not present in the bootstrap section. Using (4.2.50), we can express it in terms of defect correlators as follows:

$$\begin{aligned}
\langle \phi^2 \phi^2 \rangle_{\mathcal{D}_j} &= \kappa^2 \zeta_*^4 \int d\tau_1 \int d\tau_2 \int d\tau_3 \int d\tau_4 \frac{\langle \hat{S}_a(\tau) \hat{S}^a(\tau_1) \hat{S}_b(\tau_2) \hat{S}^b(\tau_3) \rangle_{\mathcal{D}_j}}{(\tau_1^2+r^2)^{1-\frac{\varepsilon}{2}} (\tau_2^2+r^2)^{1-\frac{\varepsilon}{2}} (\tau_3^2+1)^{1-\frac{\varepsilon}{2}} (\tau_4^2+1)^{1-\frac{\varepsilon}{2}}} + \\
&+ 2\kappa \zeta_*^2 \int d\tau_1 \int d\tau_2 \frac{\langle \hat{S}^a(\tau_1) \hat{S}^b(\tau_2) \rangle_{\mathcal{D}_j} \langle \phi_a^{\text{free}} \phi_b^{\text{free}} \rangle_{\mathcal{D}_j}}{(\tau_1^2+r^2)^{1-\frac{\varepsilon}{2}} (\tau_2^2+1)^{1-\frac{\varepsilon}{2}}} + \langle \phi_{\text{free}}^2 \phi_{\text{free}}^2 \rangle_{\mathcal{D}_j} = \\
&= \kappa^2 \zeta_*^4 \int d^4\tau \frac{\langle \hat{S}_a(\tau_1) \hat{S}^a(\tau_2) \hat{S}_b(\tau_3) \hat{S}^b(\tau_4) \rangle_{\mathcal{D}_j}}{(\tau_1^2+r^2)^{1-\frac{\varepsilon}{2}} (\tau_2^2+r^2)^{1-\frac{\varepsilon}{2}} (\tau_3^2+1)^{1-\frac{\varepsilon}{2}} (\tau_4^2+1)^{1-\frac{\varepsilon}{2}}} + \\
&+ \frac{1}{|x_1^i|^{\Delta_{\phi^2}} |x_2^i|^{\Delta_{\phi^2}}} \left[\left(\frac{rw}{(1-rw)(w-r)} \right)^{\Delta_{\phi^2}} + 2a\lambda_{\phi^2} \left(\frac{rw}{(1-rw)(w-r)} \right)^{\Delta_\phi} J_\varepsilon(r) \right] \tag{4.2.140}
\end{aligned}$$

where we suppressed the explicit dependence on the external coordinates and used the results from the previous computations to simplify the expression. Since we are in free theory, $\Delta_{\phi^2} = 2\Delta_\phi$. Unlike previous cases, we cannot simplify the result further without expanding in ε . This limitation arises because the four-point function of the defect operator is not completely determined by conformal invariance⁴¹ and we cannot perform the first integral without knowing its explicit form. At tree level, the four-point function of \hat{S}^a is simply given by traces of the generators T^a , similar to the two-point function. However, one must be careful regarding the order of the positions where the generators are inserted, which corresponds to different step functions. This is because, as discussed in Section 4.2.3, the defect spin operator must be interpreted as a generator

⁴¹See (2.4.1) for the structure of the four-point function in a one-dimensional CFT.

inserted at a specific position in the path ordering. In summary, we obtain

$$\begin{aligned} \langle \hat{S}_a(\tau_1) \hat{S}^a(\tau_2) \hat{S}_b(\tau_3) \hat{S}^b(\tau_4) \rangle_{\mathcal{D}_j} &= \frac{1}{2j+1} [\text{Tr}(T_a T_a T_b T_b) (\theta_{1>2>3>4} + \text{cyclic perm.}) + \\ &\quad + \text{Tr}(T_a T_b T_a T_b) (\theta_{1>3>2>4} + \theta_{1>4>2>3} + \text{cyclic perm.})] + O(\varepsilon) = \\ &= j^2(j+1)^2 (\theta_{1>2>3>4} + \theta_{1>3>2>4} + \theta_{1>4>2>3} + \text{cyclic perm.}) + \\ &\quad - j(j+1) (\theta_{1>3>2>4} + \theta_{1>4>2>3} + \text{cyclic perm.}) + O(\varepsilon), \end{aligned} \quad (4.2.141)$$

where we indicated the order of the points using theta functions. When we substitute this result into (4.2.140) and use the symmetry of the integrand, the term proportional to $j^2(j+1)^2$ reproduces the square of the one-point function. The other term reduces to

$$- \int_{\tau_1 > \tau_3 > \tau_2 > \tau_4} d\tau^4 (\tau_1^2 + r^2)^{-1} (\tau_2^2 + r^2)^{-1} (\tau_3^2 + 1)^{-1} (\tau_4^2 + 1)^{-1} \equiv \frac{\pi^2}{2r^2} W(r). \quad (4.2.142)$$

where $W(r)$ is

$$W(r) = 2\text{Li}_2\left(\frac{1-r}{2}\right) - \text{Li}_2(1-r) - \text{Li}_2(-r) + \log(r+1) \log\left(\frac{r+1}{4r}\right) + \log^2 2. \quad (4.2.143)$$

Ultimately, the two-point function reads

$$\langle \phi^2(0, x_1^i) \phi^2(0, x_2^i) \rangle_{\mathcal{D}_j} = \frac{\mathcal{N}_{\phi^2}^2 F_{\phi^2 \phi^2}(r, w)}{|x_1^i|^{\Delta_{\phi^2}} |x_2^i|^{\Delta_{\phi^2}}}. \quad (4.2.144)$$

where

$$\begin{aligned} F_{\phi^2 \phi^2}(r, w) &= \left(\frac{rw}{(1-rw)(w-r)} \right)^{\Delta_{\phi^2}} + a_{\phi^2}^2 - \frac{\pi^2 j(j+1)}{6} \varepsilon^2 W(r) + \\ &\quad + 2a\lambda_{\phi^2} \left(\frac{rw}{(1-rw)(w-r)} \right)^{\Delta_{\phi}} \left(1 + \frac{\varepsilon}{2} \log \frac{4r}{(1+r)^2} \right) + O(\varepsilon^3). \end{aligned} \quad (4.2.145)$$

Expanding (4.2.145) in the defect channel (4.1.17) we find two families of operators. The first family has the interpretation $\hat{\mathcal{O}}_{n,s} \sim (\partial_{\perp})^s \square^n \phi^2$, with

$$\hat{\Delta}_{\hat{\mathcal{O}}_{n,s}} = 2\Delta_{\phi} + s + 2n, \quad (4.2.146)$$

$$b_{\phi \hat{\mathcal{O}}_{n,s}}^2 = a\lambda_{\phi^2} \frac{2^s \left(\frac{3}{2}\right)_{n-1} \Gamma\left(\frac{\varepsilon-1}{2}\right) \left(1-\frac{\varepsilon}{2}\right)_n^2 \left(n-\frac{\varepsilon}{2}+1\right)_s \left(n+s-\varepsilon+2\right)_n}{\sqrt{\pi n} \Gamma\left(\frac{\varepsilon}{2}\right) (n+s)! \left(\frac{3}{2}-\frac{\varepsilon}{2}\right)_n \left(n+s-\frac{\varepsilon}{2}+1\right)_n} + \frac{2^s \left(1-\frac{\varepsilon}{2}\right)_n \left(2-\varepsilon\right)_{2n+s}}{n! (n+s)! \left(n+s-\frac{\varepsilon}{2}+1\right)_n}, \quad (4.2.147)$$

whereas the second family is $\hat{\mathcal{J}}_{n,s} \sim (\partial_{\perp})^s \square^n \phi^a T_a$, with $s > 0$ ⁴²

$$\hat{\Delta}_{\hat{\mathcal{J}}_{n,s}} = 1 + s + 2n, \quad (4.2.148)$$

$$b_{\phi \hat{\mathcal{J}}_{n,s}}^2 = a\lambda_{\phi^2} \frac{2^s (-4)^n \left(\frac{3}{2}\right)_{n-1} \Gamma\left(\frac{1-\varepsilon}{2}\right) (2n+s)! \left(\frac{\varepsilon}{2}\right)_n \left(-n-\frac{\varepsilon}{2}+1\right)_{2n+s}}{\sqrt{\pi n} \Gamma\left(1-\frac{\varepsilon}{2}\right) ((n+s)!)^2 (\varepsilon)_{2n} \left(n+s+\frac{\varepsilon}{2}\right)_n}. \quad (4.2.149)$$

⁴²Notice that the operators $\hat{\mathcal{J}}_{n,s}$ have integer scaling dimension. In particular, the operators $\hat{\mathcal{J}}_{0,s}$ are related to the higher spin symmetries in the free bulk theory which are broken by the defect, as we discussed in Section 4.2.3.

For $n, s = 0$, we have the operator $\phi^a T_a \equiv \hat{\Phi}$, with dimension

$$\hat{\Delta}_{\hat{\Phi}} = 1 + \varepsilon + O(\varepsilon^2). \quad (4.2.150)$$

This result matches with the expression computed from the beta function (4.2.82). One can also extract the bulk CFT data from (4.2.145) but the results are not particularly illuminating. Therefore we do not present them here.

Interacting bulk

When interactions are introduced, expressing the bulk correlator in terms of a defect correlator becomes less convenient. This is because the Ward identity (4.2.42) is corrected and the relation between the two correlators is more complicated. Consequently, we will perform the computation using Feynman diagrams. The diagrams contributing to the one-point function $\langle \phi^2 \rangle_{\mathcal{D}_j}$ up to order ε^2 are

$$\langle \phi^2 \rangle_{\mathcal{D}_j} = \text{diagram 1} + \text{diagram 2} + \text{diagram 3} + \text{diagram 4} + \text{diagram 5} + \text{diagram 6}. \quad (4.2.151)$$

In the last equation, it is implied that one should also consider the mirror images of diagrams such as the third and fifth ones. The diagrams without bulk interactions were previously computed in the free bulk case in [116]. However, due to the shift in the critical coupling (4.2.36), the results will be slightly different in the interacting case. The only diagram involving bulk interactions was computed in [112]. For detailed calculations, we refer to these papers. All in all, we find

$$a_{\phi^2} = \frac{\pi^2 j(j+1)\varepsilon}{2\sqrt{6}} \left(1 - \frac{2\pi^2}{11} \left(j(j+1) - \frac{1}{3} \right) \varepsilon - \frac{181\varepsilon}{242} + \frac{6}{11}\varepsilon \log 2 \right) + O(\varepsilon^3). \quad (4.2.152)$$

Moving on to the two-point function of ϕ , we have

$$\langle \phi_a \phi_a \rangle_{\mathcal{D}_j} = \text{diagram 1} + \text{diagram 2} + \text{diagram 3} + \text{diagram 4} + \text{diagram 5}, \quad (4.2.153)$$

where, again, the contribution from the specular version of the third diagram is implied. The first two diagrams represent the free propagator and the square of the one-point function of ϕ^a , which is zero. The only non-trivial diagram is the last one, and it was already computed in Section 4.1.6. All in all, at order ε^2 we obtain

$$F_{\phi\phi}(r, w) = \left(\frac{rw}{(1-rw)(w-r)} \right)^{\Delta_{\phi}} + a\lambda_{\phi^2} \left(1 + \frac{\varepsilon}{2} \log \frac{4r}{(1+r)^2} + \varepsilon \frac{5}{11} (1 + \log 2 + H(r, w)) \right), \quad (4.2.154)$$

where as always $a\lambda_{\phi^2} = \lambda_{\phi\phi\phi^2}a_{\phi^2}$, with $\lambda_{\phi\phi\phi^2}$ given by (4.2.118) and a_{ϕ^2} by (4.2.152). This result perfectly matches the bootstrap prediction (4.2.125).

Finally, for the two-point function of ϕ^2 , the relevant diagrams are

$$\langle \phi^2 \phi^2 \rangle = \begin{array}{c} \text{---} \\ \text{---} \\ \text{---} \end{array} + \begin{array}{c} \square \\ \text{---} \\ \text{---} \end{array} + \begin{array}{c} \square \\ \text{---} \\ \text{---} \\ \text{---} \end{array} + \begin{array}{c} \triangle \\ \text{---} \\ \text{---} \\ \text{---} \end{array} + \begin{array}{c} \triangle \\ \text{---} \\ \text{---} \\ \text{---} \end{array} + \\ + \begin{array}{c} \text{---} \\ \text{---} \\ \text{---} \\ \text{---} \end{array} + \begin{array}{c} \text{---} \\ \text{---} \\ \text{---} \\ \text{---} \end{array}, \quad (4.2.155)$$

As before, we did not write down the contributions from mirror diagrams. The first diagram represents bulk corrections to the propagator up to $\mathcal{O}(\varepsilon^2)$. These contributions have been computed previously in the theory without the defect, and give corrections to the dimension Δ_{ϕ^2} in the bulk identity term $\left(\frac{rw}{(1-rw)(w-r)}\right)^{\Delta_{\phi^2}}$. The only non-trivial diagram is the fifth, which can be computed in terms of $W(r)$ (4.2.142). All the other diagrams were already computed in [127], therefore we only write the final result, namely

$$F_{\phi^2\phi^2}(r, w) = \left(\frac{rw}{(1-rw)(w-r)}\right)^{\Delta_{\phi^2}} + a_{\phi^2}^2 - \frac{\varepsilon^2\pi^2 j(j+1)}{6}W(r) + \quad (4.2.156) \\ + \frac{\pi^2 j(j+1)\varepsilon[(1-rw)(w-r)]^{1-\frac{\varepsilon}{22}}}{3(rw)^{-1+\frac{\varepsilon}{22}}} \left[1 + \varepsilon \log 2 + \right. \\ \left. + \frac{\varepsilon}{11} \left(-\frac{118}{11} + 5H(r, w) - 2\pi^2 \left(j(j+1) - \frac{1}{3} \right) + \frac{1}{2} \log \frac{4r}{(r+1)^2} \right) \right] + \mathcal{O}(\varepsilon^3),$$

where $\Delta_{\phi^2} = 2 - \frac{6}{11}\varepsilon + \frac{415}{2662}\varepsilon^2 + \mathcal{O}(\varepsilon^3)$ [123]. It would be difficult to compute this result using bootstrap methods, since the discontinuity would receive contributions from all the double-twist operators [127].

4.3 The boundary in the $O(N)$ model

In this section, we consider our last example of defect in the $O(N)$ model, namely the boundary at the Wilson-Fisher fixed point. We perform a similar analysis as in Sections 4.1 and 4.2. Specifically, we compute the two-point function

$$\langle \phi_a(x_1)\phi_a(x_2) \rangle = \frac{F(z)}{(4|x_1^i||x_2^i|)^{\Delta_\phi}}, \quad (4.3.1)$$

using the boundary dispersion relation (3.2.37). This correlator was computed up to second order in the ε -expansion in [47], using a different approach.

We begin with the free scalar theory in $d = 4$ in the presence of a boundary. This setup was initially examined using bootstrap techniques in [46] and it was determined that the two solutions to the boundary crossing equation (2.5.36) are

$$F_N^{(0)}(z) = \left(\frac{z}{1-z}\right)^{\Delta_\phi} + z^{\Delta_\phi}, \quad F_D^{(0)}(z) = \left(\frac{z}{1-z}\right)^{\Delta_\phi} - z^{\Delta_\phi}, \quad (4.3.2)$$

with Δ_ϕ given in (4.1.20). These solutions correspond respectively to Neumann and Dirichlet boundary conditions. At this order, the bulk OPE contains a single primary operator ϕ^2 , with OPE coefficient $a_{\phi^2}^{(0)}\lambda_{\phi\phi^2}^{(0)} = \pm 1$ (the upper sign refers to Neumann and the lower one to Dirichlet). Similarly, in the boundary channel expansion, only one defect operator is exchanged. In the case of Neumann boundary conditions, it corresponds to the operator ϕ evaluated at the boundary and has dimension $\hat{\Delta} = \Delta_\phi$, while for Dirichlet it is $\partial_\perp\phi$ with dimension $\hat{\Delta} = \Delta_\phi + 1$. The corresponding squared bulk-to-boundary coefficients are respectively $b_{\phi\phi}^{2(0)} = 2$ or $b_{\phi\phi}^{2(0)} = \frac{d}{2} - 1$.

If we turn on interactions and consider $d = 4 - \varepsilon$ with ε small, the theory can flow to the Wilson-Fisher fixed point. In the bulk channel, we define as before $a\lambda_{\mathcal{O}} \equiv a_{\mathcal{O}}\lambda_{\phi\phi\mathcal{O}}$ and assume the perturbative expansion

$$\begin{aligned}\Delta &= \Delta^{(0)} + \varepsilon\gamma^{(1)} + \varepsilon^2\gamma^{(2)} + \mathcal{O}(\varepsilon^3), \\ a\lambda &= a\lambda^{(0)} + \varepsilon a\lambda^{(1)} + \varepsilon^2 a\lambda^{(2)} + \mathcal{O}(\varepsilon^3).\end{aligned}\tag{4.3.3}$$

An analogous expansion applies in the defect channel as well

$$\begin{aligned}\hat{\Delta} &= \hat{\Delta}^{(0)} + \varepsilon\hat{\gamma}^{(1)} + \varepsilon^2\hat{\gamma}^{(2)} + \mathcal{O}(\varepsilon^3), \\ b_{\phi\hat{\mathcal{O}}}^2 &= b^{2(0)} + \varepsilon b^{2(1)} + \varepsilon^2 b^{2(2)} + \mathcal{O}(\varepsilon^3).\end{aligned}\tag{4.3.4}$$

We want to obtain the discontinuities of the correlators following the same strategy that worked in the case of the localized magnetic field or the spin impurity, namely computing the discontinuity term by term in the OPE expansion. We recall that the advantage of doing this is that, in perturbation theory, very few terms in the OPE expansion are necessary to compute the discontinuity. Examining the boundary OPE expansion (2.5.32), we observe that the discontinuity at $z = 0$ at a given order arises from two sources: logarithms coming from anomalous dimensions of operators that appeared in prior orders and poles coming from the prefactors, which are necessary to suppress the contributions at infinity in the dispersion relation, see (3.2.40). We should always keep in mind that the discontinuity must be interpreted in a distributional sense. Therefore, if the function $F(z)$ has a pole at $z = 0$, its discontinuity will be given by

$$\text{Disc}_{z<0}[z^{-n}] = \frac{2\pi i(-1)^n \partial^{n-1}(\delta(z))}{(n-1)!}.\tag{4.3.5}$$

A similar story holds for the discontinuity at $z = 1$, which is controlled by the bulk channel (2.5.33).

Before presenting the derivation of the two-point function, we point out the relationship between our approach and the work of [47]. In their study, the authors also used discontinuity techniques to bootstrap results similar to those we are investigating here ⁴³. They computed one particular discontinuity of the crossing equation,

⁴³A similar derivation was also independently obtained in [143] by relating the problem to AdS and solving bulk equations of motion

which allowed them to extract the boundary CFT data using only consistency of the crossing equation. In contrast, our method involves using two distinct discontinuities to reconstruct the correlator, which they derived resumming the OPE expansion. In this sense the two approaches are complementary. Additionally, it's important to note that throughout our analysis, we always use the OPE expansions in their regions of convergence, thereby avoiding certain subtleties discussed in [47].

4.3.1 Next-to-leading order correlator

From now on, we will concentrate on the Neumann case, but the computation is almost identical for Dirichlet. In order to control the large z behaviour and avoid ambiguities in the dispersion relation, we define the rescaled correlator ⁴⁴

$$\tilde{F}(z) = \frac{1}{z(1-z)} F(z). \quad (4.3.6)$$

As shown in [46], the only new operator that appears in the OPE at order ε is the bulk operator ϕ^4 , with classical dimension $\Delta_{\phi^4} = 2d - 4$.

The discontinuity of $\tilde{F}(z)$ at $z = 0$ is controlled by the boundary expansion (2.5.32). Since only $\hat{\phi}$ ⁴⁵ is exchanged in the boundary channel, the order ε term for \tilde{F} reads

$$\tilde{F}^{(1)}(z) = \frac{b_{\hat{\phi}\hat{\phi}}^{2(1)} \hat{f}_1(z) + b_{\hat{\phi}\hat{\phi}}^{2(0)} (\hat{\gamma}_{\hat{\phi}}^{(1)} - 1/2) \partial_{\hat{\Delta}} \hat{f}_{\hat{\Delta}}(z)|_{\hat{\Delta}=1}}{z(1-z)}, \quad (4.3.7)$$

where we used

$$\hat{\Delta}_{\hat{\phi}} = \frac{d}{2} - 1 + \varepsilon \gamma_{\hat{\phi}}^{(1)} + O(\varepsilon^2) = 1 + \varepsilon (\hat{\gamma}_{\hat{\phi}}^{(1)} - 1/2) + O(\varepsilon^2), \quad (4.3.8)$$

and expanded the boundary OPE (2.5.32) up to order ε . Given that $\hat{f}_1(z) = z(1 + \frac{1}{1-z})$, the discontinuity is determined only by the derivative $\partial_{\hat{\Delta}} \hat{f}_{\hat{\Delta}}(z)|_{\hat{\Delta}=1}$ and specifically from the logarithm that is generated by the action of the derivative on the term $z^{\hat{\Delta}}$ in (2.5.34). Thus we have

$$\text{Disc}_{z<0}[\tilde{F}^{(1)}(z)] = 2\pi i b_{\hat{\phi}\hat{\phi}}^{2(0)} (\hat{\gamma}_{\hat{\phi}}^{(1)} - 1/2) \left(\frac{1}{1-z} + \frac{1}{(1-z)^2} \right). \quad (4.3.9)$$

A similar argument allows to derive the discontinuity at $z = 1$ using the bulk expansion (2.5.33) with only two exchanged operators [79]

$$\Delta_{\phi^2} = 2 + \varepsilon (\gamma_{\phi^2}^{(1)} - 1) + O(\varepsilon^2) \quad a\lambda_{\phi^2} = 1 + \varepsilon a \lambda_{\phi^2}^{(1)} + O(\varepsilon^2) \quad (4.3.10)$$

$$\Delta_{\phi^4} = 4 + O(\varepsilon) \quad a\lambda_{\phi^4} = \varepsilon a \lambda_{\phi^4}^{(1)} + O(\varepsilon^2), \quad (4.3.11)$$

⁴⁴The large z behaviour of the bulk two-point function is fixed in terms of the external dimension Δ_{ϕ} , see (3.2.39). The choice of the prefactor is arbitrary, as long as it does not introduce new singularities.

⁴⁵In principle, we could ignore the results of [46] and assume that there are infinitely many defect operators at order ε , see for example [53]. However, since these operators would appear in the defect block expansion with their classical dimensions, they would not contribute to the discontinuity at this order. Therefore, one would obtain the same result for the correlator and see that they were not there in the first place.

Note that we can neglect the order ε contribution to Δ_{ϕ^4} , since the OPE coefficient $a\lambda_{\phi^4}$ is already of order ε . For the bulk channel, we also need to take into account the prefactor $\left(\frac{z}{1-z}\right)^{\Delta_\phi}$ in equation (2.5.33) with Δ_ϕ given in (4.1.20). All in all we get

$$\tilde{F}^{(1)} = \frac{a\lambda_{\phi^2}^{(1)}f_2(z) + a\lambda_{\phi^4}^{(1)}f_4(z) + a\lambda_{\phi^2}^{(0)}(\gamma_{\phi^2}^{(1)} - 1)\partial_\Delta f_\Delta(z)|_{\Delta=2} + \log\frac{1-z}{z}(\gamma_\phi^{(1)} - 1/2)f_2(z)}{(1-z)^2}. \quad (4.3.12)$$

Here all terms contribute to the discontinuity: some contribute with a delta-function and some with a logarithm, according to (4.3.5) and (4.1.42). The only contribution requiring special attention is the one involving $\log(1-z)$, in the last term of (4.3.12), which gives rise to $\text{Disc}\left[\frac{\log(1-z)}{1-z}\right]$. It is possible to interpret this discontinuity in terms of a distribution. For a given test function $f(x)$, we have

$$\int_{-\infty}^0 dx f(x) \text{Disc}_{x<0} \left[\frac{\log x}{x} \right] = -2\pi i \int_{-\infty}^0 dx \partial_x f(x) \log(-x). \quad (4.3.13)$$

Using this formula and (4.3.9) in the dispersion relation (3.2.37), we obtain

$$F^{(1)}(z) = z \left(\alpha + \frac{1}{2-2z} \right) \log(1-z) + z(\hat{\gamma}_{\hat{\phi}}^{(1)} + a\lambda_{\phi^2}^{(1)}) + \frac{(2\hat{\gamma}_{\hat{\phi}}^{(1)} - 1)(z-2)z \log(z)}{2(z-1)}, \quad (4.3.14)$$

where we used with the bulk CFT data computed from the theory without defects (4.1.33)

$$\gamma_\phi^{(1)} = 0, \quad \gamma_{\phi^2}^{(1)} = 2\alpha, \quad \alpha \equiv \frac{1}{2} \frac{N+2}{N+8}. \quad (4.3.15)$$

The result seems to depend on unknown bulk and boundary data, however we can fix the undetermined coefficients by comparing our result with the bulk (2.5.33) and boundary (2.5.32) block expansions. We find

$$\hat{\gamma}_{\hat{\phi}}^{(1)} = -\alpha, \quad a\lambda_{\phi^2}^{(1)} = \alpha, \quad (4.3.16)$$

and finally

$$F^{(1)}(z) = z \left(\alpha + \frac{1}{2-2z} \right) \log(1-z) - \frac{(2\alpha+1)(z-2)z \log(z)}{2(z-1)}, \quad (4.3.17)$$

which agrees with the result of [46]. From the correlator, we can deduce the squared bulk-to-defect coupling $b_{\phi\hat{\phi}}^{2(1)}$, which turns out to be zero.

4.3.2 NNLO correlator

At second order one expects, from diagrammatic considerations [47], the appearance of an infinite tower of double-twist operators $\mathcal{J}_{n,0}$ in the bulk channel. The double-twist

operators have spin $\ell = 0$ and appear with their classical dimensions $\Delta = 2\Delta_\phi + 2n$. Similarly, in the defect channel one expects operators $\hat{\mathcal{O}}_n$ with dimensions $\hat{\Delta}_n = n$, with n an odd integer for Neumann boundary conditions⁴⁶. As we saw in previous sections, even when the OPE contains infinite operators, the dispersion relation offers a significant advantage: it requires only a finite subset of these operators to completely reconstruct the correlator.

We can compute the discontinuity at $z = 0$ by looking at the perturbative expansion in the boundary OPE. In this case it reads

$$\begin{aligned} F^{(2)}(z) &= b_{\phi\phi}^{2(2)} \hat{f}_{\hat{\Delta}_\phi^{(0)}}(z) + (b_{\phi\phi}^{2(0)} \gamma_\phi^{(2)} + b_{\phi\phi}^{2(1)} \gamma_\phi^{(1)}) \partial \hat{f}_{\hat{\Delta}_\phi^{(0)}}(z) \\ &+ \frac{1}{2} b_{\phi\phi}^{2(0)} (\gamma_\phi^{(1)})^2 \partial^2 \hat{f}_{\hat{\Delta}_\phi^{(0)}}(z) + \sum_{n=0}^{\infty} b_{\phi\hat{\mathcal{O}}_n}^{2(2)} \hat{f}_{\hat{\Delta}_n}(z), \end{aligned} \quad (4.3.18)$$

where we used the short-hand notation $\partial \hat{f}_{\hat{\Delta}_\phi^{(0)}}(z) \equiv \partial_{\hat{\Delta}} \hat{f}_{\hat{\Delta}}(z)|_{\hat{\Delta}=\hat{\Delta}_\phi^{(0)}}$. The factor $1/z$ in the prefactor (4.3.6) is always canceled by the blocks or their derivatives, so that this discontinuity is given only by the logarithmic terms arising from the derivatives of the block. These terms can be computed from the OPE data at lower order plus the anomalous dimension of $\hat{\phi}$ at order ε^2 . Note that the new operators do not contribute.

When we explicitly evaluate the perturbative expansion (4.3.18) and retain only terms with logarithms, we find

$$\begin{aligned} \tilde{F}^{(2)}(z) &\approx -\frac{(2\alpha+1)^2(z-2)\log^2(z)}{8(z-1)^2} - \frac{\hat{\gamma}_\phi^{(2)}(z-2)\log(z)}{(z-1)^2} \\ &+ \frac{(2\alpha+1)(2\alpha(z-1)-1)\log(1-z)\log(z)}{4(z-1)^2} + \text{regular at } (z=0). \end{aligned} \quad (4.3.19)$$

The discontinuity therefore is

$$\begin{aligned} \text{Disc}_{z<0}[\tilde{F}^{(2)}(z)] &= -\frac{\pi i(2\alpha+1)^2(z-2)\log(-z)}{2(z-1)^2} - \frac{2\pi i\hat{\gamma}_\phi^{(2)}(z-2)}{(z-1)^2} \\ &+ \frac{\pi i(2\alpha+1)(2\alpha(z-1)-1)\log(1-z)}{2(z-1)^2}. \end{aligned} \quad (4.3.20)$$

The discontinuity at $z = 1$ is more complicated, due to the prefactor introducing poles that are proportional to contributions from both the identity and ϕ^2 . Nevertheless, it remains the case that the new operators do not contribute. We can compute this discontinuity using the following finite set of bulk OPE data

$$\begin{aligned} \gamma_\phi^{(2)} &= -\frac{1}{12}\alpha(2\alpha-1), \\ \gamma_{\phi^2}^{(2)} &= -\frac{1}{6}\alpha(2\alpha-1)(20\alpha+3). \end{aligned} \quad (4.3.21)$$

⁴⁶In the case of Dirichlet boundary conditions, n would be even.

The computation is analogous to the previous case and yields the following singular terms at $z = 1$

$$\begin{aligned}
\tilde{F}^{(2)}(z) \approx & \log(1-z) \left[\frac{\alpha(2\alpha-1)(-20\alpha+4(5\alpha-1)z+5)}{12(z-1)^2} + \frac{(2\alpha(z-2)-1)\log(z)}{4(z-1)^2} \right] \\
& + \frac{(1-4\alpha^2(z-1))\log^2(1-z)}{8(z-1)^2} + \frac{\alpha(40\alpha^2-30\alpha+(-40\alpha^2+28\alpha+8)z-7)\log(z)}{12(z-1)^2} \\
& + \frac{(4\alpha-(4\alpha+1)z+2)\log^2(z)}{8(z-1)^2} + \frac{\pi^2\alpha^2-6a\lambda_{\phi^2}^{(2)}-6\alpha^2\text{Li}_2(z)}{6(z-1)} + \text{regular at } (z=1).
\end{aligned} \tag{4.3.22}$$

From this, we can extract the discontinuity at $z = 1$, which will get contributions from the logarithms and the negative powers. By plugging the two discontinuities in the dispersion relation (3.2.37) and using (4.3.13) we can compute the correlator

$$\begin{aligned}
F^{(2)}(z) = & \hat{\gamma}_{\hat{\phi}}^{(2)}z + \frac{1}{12}\alpha(2\alpha-1)z + a\lambda_{\phi^2}^{(2)}z + \frac{1}{8}z \left(4\alpha^2 + \frac{1}{1-z} \right) \log^2(1-z) + \\
& + \frac{(2\alpha+1)^2(z-2)z\log^2(z)}{8(z-1)} - \frac{\alpha(2\alpha-1)z(20\alpha(z-1)-4z+5)\log(1-z)}{12(z-1)} \\
& - \frac{(2\alpha+1)z(2\alpha(z-1)-1)\log(z)\log(1-z)}{4(z-1)} + \frac{\hat{\gamma}_{\hat{\phi}}^{(2)}(z-2)z\log(z)}{z-1}.
\end{aligned} \tag{4.3.23}$$

Once again we can fix the remaining unknowns by demanding consistency with the bulk and boundary OPE expansions. All in all, we obtain

$$\begin{aligned}
\gamma_{\hat{\phi}}^{(2)} &= \frac{5}{12}\alpha(8\alpha^2-6\alpha+1), \\
a\lambda_{\phi^2}^{(2)} &= -\frac{1}{3}\alpha(\alpha(10\alpha-7)+1),
\end{aligned} \tag{4.3.24}$$

and finally

$$\begin{aligned}
F^{(2)}(z) = & \frac{1}{8}z \left(4\alpha^2 + \frac{1}{1-z} \right) \log^2(1-z) + \frac{5\alpha(8\alpha^2-6\alpha+1)(z-2)z\log(z)}{12(z-1)} \\
& + \frac{(2\alpha+1)^2(z-2)z\log^2(z)}{8(z-1)} - \frac{\alpha(2\alpha-1)z(-20\alpha+4(5\alpha-1)z+5)\log(1-z)}{12(z-1)} \\
& - \frac{(2\alpha+1)z(2\alpha(z-1)-1)\log(z)\log(1-z)}{4(z-1)},
\end{aligned} \tag{4.3.25}$$

which corresponds to the result in [47]. One can follow the same procedure for the Dirichlet case and find again perfect agreement with the literature.

Before concluding this section, let us briefly comment on the next orders in the perturbative expansion. If we wanted to compute the correlator at order ε^3 , we would run

into two problems. First, the operators $\mathcal{J}_{n,0}$ and $\hat{\mathcal{O}}_n$ would start contributing with their anomalous dimensions. This means that both discontinuities could receive infinite ⁴⁷ contributions, making the computation harder. In particular, the discontinuity in the boundary channel would depend on infinite unknown dimensions $\hat{\Delta}_n^{(1)}$. The second problem is the mixing between operators, which means that we can only extract the average of the OPE coefficients. If the degeneracy between operators were lifted at this order, we would not be able to use the averaged coefficients from previous orders to compute the discontinuities from the block expansions.

4.4 The supersymmetric Wilson line in $\mathcal{N} = 4$ SYM

In this section, we examine another significant example of a conformal defect that has been extensively studied in the literature: the supersymmetric Wilson line in $\mathcal{N} = 4$ SYM. It is explicitly defined as [121]

$$\mathcal{W} = \frac{1}{N} \text{Tr} \mathcal{P} \exp \left[\int_{\mathcal{C}} d\tau (iA_\mu \dot{x}^\mu + |\dot{x}| \theta_I \phi^I) \right]. \quad (4.4.1)$$

Here, the contour is a straight line parameterized by τ , and θ^I is a constant unit vector in $SO(6)$, chosen such that $\theta^6 = 1$ and $\theta^i = 0$ for $i = 1, \dots, 5$. With this choice of parameters, the Wilson line is 1/2 BPS, meaning that it preserves half of the supercharges of $\mathcal{N} = 4$ SYM. It is holographically dual to a string worldsheet in $AdS_5 \times S^5$, which ends on the specified contour. At large N and strong 't Hooft coupling $\lambda = g_{YM}^2 N$, insertions of the fundamental fields Φ^i on the line correspond to fluctuations of the worldsheet of the dual fundamental string and can be thought of as light fields propagating on an AdS_2 worldsheet [144]. Correlators of defect insertions generate a one-dimensional CFT and have been studied using various techniques, including integrability [145–149], supersymmetric localization [150–152], holography [144, 153–155], and the conformal bootstrap [50, 156, 51, 157, 158, 55, 104]. In particular, the authors of [51] succeeded in bootstrapping the four-point function of the super-displacement multiplet at fourth order in a strong 't Hooft coupling expansion, using an Ansatz involving polylogarithms and rational functions. A key step in their derivation is the resolution of an operator mixing problem. Building on that analysis, in this section we reproduce their result using the dispersion relation (3.1.1), bypassing the need for an Ansatz. Given the complexity of the computation of the four-point function on the Wilson line, we first introduce a simpler toy model of a scalar theory in AdS_2 to clarify the procedure.

Another interesting observable in this setup is the two-point function of single-trace 1/2 BPS bulk operators. In the holographic description, these operators are dual to certain Kaluza-Klein modes arising from the compactification of type IIB string theory

⁴⁷It could also be the case that some anomalous dimensions are suppressed, and only a finite number of operators contribute to the discontinuity as in Sections 4.1 and 4.2.

on S^5 . As pointed out in [104], these modes can be created at the boundary of AdS_5 , propagate through the bulk, and be absorbed by the string worldsheet dual to the Wilson line. This process corresponds to a non-trivial one-point function of a bulk operator in presence of the Wilson line. Higher-point correlators have an analogous interpretation. Perturbative results for the bulk two-point function at strong coupling were derived in [104] using the Lorentzian inversion formula (2.5.21) to extract the defect CFT data and then resumming the block expansion. In this section, we will reproduce these results directly using the defect dispersion relation (3.2.1), thereby skipping the technically challenging intermediate steps.

4.4.1 Toy model: scalar theory in AdS_2

Before we study the theory on the Wilson line, we will present a detailed computation of a four-point function in a simpler scalar theory defined on the boundary of AdS_2 . We consider the theory of a massive scalar in AdS_2 , with the following Lagrangian

$$\mathcal{L} = \frac{1}{2}(\partial\Phi)^2 - \frac{m^2}{2}\Phi^2 - \frac{\lambda}{4!}\Phi^4. \quad (4.4.2)$$

The four-point function of the corresponding boundary field $\hat{\phi}$ with integer⁴⁸ dimension $\hat{\Delta}_{\hat{\phi}}$ is

$$\langle \hat{\phi}(\tau_1)\hat{\phi}(\tau_2)\hat{\phi}(\tau_3)\hat{\phi}(\tau_4) \rangle = \frac{1}{(\tau_{12}\tau_{34})^{2\hat{\Delta}_{\hat{\phi}}}} \mathcal{G}(z). \quad (4.4.3)$$

At $\lambda = 0$, the four-point function corresponds to that of a generalized free field (GFF) theory and can be computed diagrammatically using Wick contractions. The result is given by⁴⁹

$$\mathcal{G}^{(0)}(z) = 1 + z^{2\hat{\Delta}_{\hat{\phi}}} + \frac{z^{2\hat{\Delta}_{\hat{\phi}}}}{(1-z)^{2\hat{\Delta}_{\hat{\phi}}}}. \quad (4.4.4)$$

The only operators that appear in the conformal block expansion (2.4.6) are double-trace operators $\hat{\phi}\partial^{2\Delta_{\phi}+2n}\hat{\phi}$, with OPE data

$$\begin{aligned} \hat{\Delta}^{(0)} &= 2\hat{\Delta}_{\hat{\phi}} + 2n, \\ \hat{a}_n^{(0)} &= \frac{2\Gamma^2(2\hat{\Delta}_{\hat{\phi}} + 2n)\Gamma(4\hat{\Delta}_{\hat{\phi}} + 2n - 1)}{\Gamma^2(2\hat{\Delta}_{\hat{\phi}})\Gamma(4\hat{\Delta}_{\hat{\phi}} + 4n - 1)\Gamma(2n + 1)}. \end{aligned} \quad (4.4.5)$$

We assume the following expansion for the CFT data up to second order (one loop in AdS_2)

$$\begin{aligned} \hat{\Delta} &= 2\hat{\Delta}_{\hat{\phi}} + 2n + \lambda\hat{\gamma}_n^{(1)} + \lambda^2\hat{\gamma}_n^{(2)} + \mathcal{O}(\lambda^3), \\ \hat{a}_{\hat{\Delta}} &= \hat{a}_n^{(0)} + \lambda\hat{a}_n^{(1)} + \lambda^2\hat{a}_n^{(2)} + \mathcal{O}(\lambda^3), \end{aligned} \quad (4.4.6)$$

⁴⁸We assume we can adjust m^2 in such a way that $\hat{\Delta}_{\hat{\phi}}$ is integer, as was done in [98].

⁴⁹In this section we denote with $\mathcal{G}^{(\ell)}(z)$ the ℓ th-order correlator in the perturbative expansion. The zeroth order term should not be confused with $\mathcal{G}^{(0)}(z)$ in (2.4.3).

and expand the four-point function $\mathcal{G}(z)$ around the GFF solution

$$\mathcal{G}(z) = \mathcal{G}^{(0)}(z) + \lambda \mathcal{G}^{(1)}(z) + \lambda^2 \mathcal{G}^{(2)}(z) + \mathcal{O}(\lambda^3). \quad (4.4.7)$$

Inserting the CFT data (4.4.6) in the one-dimensional OPE expansion (2.4.6) we find, in the t-channel,

$$\mathcal{G}^{(0)}(z) = \left(\frac{z}{1-z}\right)^{2\hat{\Delta}_\phi} \sum_n \hat{a}_n^{(0)} G_{2\hat{\Delta}_\phi+2n}(1-z), \quad (4.4.8)$$

$$\mathcal{G}^{(1)}(z) = \left(\frac{z}{1-z}\right)^{2\hat{\Delta}_\phi} \sum_n \left[\hat{a}_n^{(1)} G_{2\hat{\Delta}_\phi+2n}(1-z) + \hat{a}_n^{(0)} \hat{\gamma}_n^{(1)} \partial_n G_{2\hat{\Delta}_\phi+2n}(1-z) \right], \quad (4.4.9)$$

$$\begin{aligned} \mathcal{G}^{(2)}(z) = & \left(\frac{z}{1-z}\right)^{2\hat{\Delta}_\phi} \sum_n \left[\hat{a}_n^{(2)} G_{2\hat{\Delta}_\phi+2n}(1-z) + (\hat{a}_n^{(0)} \hat{\gamma}_n^{(2)} + \hat{a}_n^{(1)} \hat{\gamma}_n^{(1)}) \partial_n G_{2\hat{\Delta}_\phi+2n}(1-z), \right. \\ & \left. + \frac{1}{2} \hat{a}_n^{(0)} (\hat{\gamma}_n^{(1)})^2 \partial_n^2 G_{2\hat{\Delta}_\phi+2n}(1-z) \right]. \end{aligned} \quad (4.4.10)$$

Similar expressions hold in the s-channel. Notice that the derivatives of the conformal blocks⁵⁰ produce logarithmic terms

$$\partial_n G_{2\hat{\Delta}_\phi+2n}(1-z) = \log(1-z) G_{2\hat{\Delta}_\phi+2n}(1-z) + (1-z)^{2\hat{\Delta}_\phi+2n} \partial_n \left[\frac{G_{2\hat{\Delta}_\phi+2n}(1-z)}{(1-z)^{2\hat{\Delta}_\phi+2n}} \right] \quad (4.4.11)$$

We aim to compute the first two orders⁵¹ in the expansion (4.4.7) using the dispersion relation (3.1.1). Since the theory lacks derivative interactions, we anticipate that the bound in the Regge limit (2.4.22) will hold, allowing us to use the dispersion kernel (3.1.23). The double discontinuity of the correlator, using the expansion (4.4.6) in (2.4.14), is then given by

$$\text{dDisc}[\mathcal{G}(z)] = \lambda^2 \pi^2 \sum_n \frac{1}{2} \hat{a}_n^{(0)} (\hat{\gamma}_n^{(1)})^2 \frac{z^{2\hat{\Delta}_\phi}}{(1-z)^{2\hat{\Delta}_\phi}} G_{2\hat{\Delta}_\phi+2n}(1-z) + \mathcal{O}(\lambda^3). \quad (4.4.12)$$

In other words, the double discontinuity up to second order is entirely determined by zeroth- and first-order data, a pattern that persists at higher orders. This crucial fact is the CFT equivalent of the so-called AdS unitarity⁵². By comparing (4.4.12) with (4.4.8) and using (4.4.11), it is evident that the double discontinuity is completely determined by the terms in (4.4.8) which are proportional to $\log^n(1-z)$ with $n > 1$. Therefore, an alternative method of determining the double discontinuity is to compute the terms proportional to $\log^n(1-z)$ from the OPE and replace $\log^n(1-z)$ with its double discontinuity (2.4.12). As seen from (4.4.12), the double discontinuity at first

⁵⁰See (2.3.3) for the explicit expression of the one-dimensional conformal block.

⁵¹This correlator was originally computed up to one-loop in AdS_2 in [98].

⁵²For a comprehensive discussion of the relationship between unitarity cuts in Witten diagrams and the computation of the double discontinuity, see [159].

order (tree-level in AdS) vanishes. This implies that the tree-level correlator results solely from the two infinitesimal contour integrals in (3.1.22).

$$\mathcal{G}^{(1)}(z) = \lim_{\rho \rightarrow 0} \int_{C_\rho^+} \frac{dw}{2w^2} K_{\Delta_\phi}^{\text{bd}}(z, w) \mathcal{G}^{(1)}(w) + \lim_{\rho \rightarrow 0} \int_{C_\rho^-} \frac{dw}{2w^2} K_{\Delta_\phi}^{\text{bd}}(z, w) \mathcal{G}^{(1)}(w), \quad (4.4.13)$$

which can be evaluated by expanding both the kernel (3.1.19) and $\mathcal{G}^{(1)}(w)$ around $w = 1$. In particular, the correlator can be expanded using the t-channel OPE (4.4.9). Setting $\hat{\Delta}_{\hat{\phi}} = 1$ for simplicity, we obtain

$$\begin{aligned} \mathcal{G}^{(1)}(z) &= \lim_{\rho \rightarrow 0} \int_{C_\rho^+} dw I(z, w) + \lim_{\rho \rightarrow 0} \int_{C_\rho^-} dw I(z, w), \quad (4.4.14) \\ I &= \left[\frac{z^2}{\pi^2(1-w)^3} \left(\frac{\log(1-z)}{z} + \frac{\log(z)}{1-z} \right) + \mathcal{O}\left(\frac{1}{(1-w)^2}\right) \right] \sum_n \left[\hat{a}_n^{(1)} G_{2+2n}(1-w) + \hat{a}_n^{(0)} \hat{\gamma}_n^{(1)} \partial_n G_{2+2n}(1-w) \right] \end{aligned}$$

Switching to radial coordinates $1-w \equiv \rho e^{i\theta}$ and using that $G_{2+2n}(1-w) \sim (1-w)^{2+2n}$, the integrals become

$$\begin{aligned} \mathcal{G}^{(1)}(z) &= \lim_{\rho \rightarrow 0} z^2 \left(\frac{\log(1-z)}{z} + \frac{\log(z)}{1-z} \right) \int_0^\pi d\theta \frac{1}{\pi^2 \rho^2} \left[\hat{a}_0^{(1)} G_2(\rho e^{i\theta}) + \hat{a}_0^{(0)} \hat{\gamma}_0^{(1)} \partial_n G_2(\rho e^{i\theta}) + O(\rho^3) \right] \\ &\quad + \lim_{\rho \rightarrow 0} z^2 \left(\frac{\log(1-z)}{z} + \frac{\log(z)}{1-z} \right) \int_{2\pi}^\pi d\theta \frac{1}{\pi^2 \rho^2} \left[\hat{a}_0^{(1)} G_2(\rho e^{i\theta}) + \hat{a}_0^{(0)} \hat{\gamma}_0^{(1)} \partial_n G_2(\rho e^{i\theta}) + O(\rho^3) \right] \\ &= \lim_{\rho \rightarrow 0} \hat{\gamma}_0^{(1)} z^2 \left(\frac{\log(1-z)}{z} + \frac{\log(z)}{1-z} \right) \left(\int_0^\pi d\theta \log(\rho e^{i\theta}) + \int_{2\pi}^\pi d\theta \log(\rho e^{i\theta}) \right) \\ &= 2 \hat{\gamma}_0^{(1)} z^2 \left(\frac{\log(1-z)}{z} + \frac{\log(z)}{1-z} \right). \quad (4.4.15) \end{aligned}$$

In the third line, the logarithm arises from the derivative of the conformal block with respect to the conformal dimension, and we used the value of $\hat{a}_0^{(0)}$ from (4.4.5). All terms with $n > 0$ in the OPE expansion of the correlator are suppressed as $\rho \rightarrow 0$, so the only contributing term is the one proportional to $\hat{\gamma}_{n=0}^{(1)}$. This is a constant that can be absorbed into the renormalization of the coupling at each order in perturbation theory. To align with the results in the bootstrap literature, we follow [98, 102] and define our coupling by setting

$$\hat{\gamma}_0^{(1)} = 1, \quad \hat{\gamma}_0^{(\ell)} = 0 \quad \text{for } \ell > 1. \quad (4.4.16)$$

Using this convention we find

$$\mathcal{G}^{(1)}(z) = 2 z^2 \left[\frac{\log(1-z)}{z} + \frac{\log(z)}{1-z} \right], \quad (4.4.17)$$

from which one extracts the tree-level OPE data

$$\hat{\gamma}_n^{(1)} = \frac{1}{(2n+1)(n+1)}, \quad \hat{a}_n^{(1)} = \frac{1}{2} \partial_n [a_n^{(0)} \hat{\gamma}_n^{(1)}]. \quad (4.4.18)$$

At second order, the double discontinuity (4.4.12) can be computed from the order zero (4.4.5) and order one (4.4.18) data, and reads simply

$$\text{dDisc}[\mathcal{G}^{(2)}(z)] = \frac{\pi^2 z^2}{(1-z)^2} \log^2 z. \quad (4.4.19)$$

To obtain this result, the sum in (4.4.12) was computed using a standard integral representation for the hypergeometric function that defines the conformal block (2.3.3), allowing for the exchange of summation and integration. By inserting (4.4.19) into the dispersion relation (3.1.22), we obtain

$$\begin{aligned} \mathcal{G}^{(2)}(z) &\stackrel{?}{=} \int_0^1 \frac{dw}{w^2} K_{\Delta_\phi=1}^{\text{bd}}(z, w) \frac{\pi^2 w^2}{(1-w)^2} \log^2 w + \\ &+ \lim_{\rho \rightarrow 0} \int_{C_\rho^+} \frac{dw}{2w^2} K_{\Delta_\phi=1}^{\text{bd}}(z, w) \mathcal{G}^{(2)}(w) + \lim_{\rho \rightarrow 0} \int_{C_\rho^-} \frac{dw}{2w^2} K_{\Delta_\phi=1}^{\text{bd}}(z, w) \mathcal{G}^{(2)}(w). \end{aligned} \quad (4.4.20)$$

However, the first integral does not converge due to a pole at $w = 1$. As discussed around (3.1.23) and (2.4.26), we can fix this by defining a regularized correlator with the following subtraction:

$$\mathcal{G}^{\text{reg}}(z) = \mathcal{G}^{(2)}(z) - \frac{1}{2} \left(z^2 \log^2 \left(\frac{z}{1-z} \right) + \log^2(1-z) + \frac{z^2}{(1-z)^2} \log^2(z) \right). \quad (4.4.21)$$

Remember that we are free to subtract any function, provided the resulting regularized correlator remains Regge-bounded and crossing symmetric. With the specific subtraction above, the double discontinuity becomes

$$\text{dDisc}[\mathcal{G}^{\text{reg}}(z)] = \pi^2 \left(\frac{z^2}{(1-z)^2} \log^2 z - \frac{1+z^2}{2} \right), \quad (4.4.22)$$

and the dispersion relation (3.1.22) is now a sum of convergent integrals

$$\begin{aligned} \mathcal{G}^{\text{reg}}(z) &= \int_0^1 \frac{dw}{w^2} K_{\Delta_\phi=1}^{\text{bd}}(z, w) \pi^2 \left(\frac{w^2}{(1-w)^2} \log^2 w - \frac{1+w^2}{2} \right) + \\ &+ \lim_{\rho \rightarrow 0} \int_{C_\rho^+} \frac{dw}{2w^2} K_{\Delta_\phi=1}^{\text{bd}}(z, w) \mathcal{G}^{\text{reg}}(w) + \lim_{\rho \rightarrow 0} \int_{C_\rho^-} \frac{dw}{2w^2} K_{\Delta_\phi=1}^{\text{bd}}(z, w) \mathcal{G}^{\text{reg}}(w). \end{aligned} \quad (4.4.23)$$

For the two semi-circle integrals above, one follows the same strategy as at tree-level, finding

$$\int_{C_+} \frac{dw}{2w^2} K_{\Delta_\phi=1}^{\text{bd}}(z, w) \mathcal{G}^{\text{reg}}(w) + \int_{C_-} \frac{dw}{2w^2} K_{\Delta_\phi=1}^{\text{bd}}(z, w) \mathcal{G}^{\text{reg}}(w) = 2z^2 \left(\frac{\log(1-z)}{z} + \frac{\log(z)}{1-z} \right) \quad (4.4.24)$$

Notice that the result is proportional to the tree-level term (4.4.17). Computing the integrals in (4.4.23) and using (4.4.21), the correlator at second order (one loop in AdS)

finally reads

$$\begin{aligned}
\mathcal{G}^{(2)}(z) = & \frac{1}{(1-z)^2} \left[4(z-2)z^3\text{Li}_4(1-z) + 4(z^2-1)(1-z)^2\text{Li}_4(z) \right. \\
& - 2(1-z)^2\text{Li}_3(1-z) \left((z^2-1)\log(1-z) + (z^2+2)\log(z) \right) \\
& - 2z^2\text{Li}_3(z) \left((z^2-2z+3)\log(1-z) + (z-2)z\log z \right) + 4(2z-1)\text{Li}_4\left(\frac{z}{z-1}\right) \\
& - \frac{1}{90}\pi^4 z^2(z^2-2z-6) + \left(\frac{1}{3}\pi^2(2z-1) - (z-1)^2(z^2+1)\log^2(z)\right)\log^2(1-z) + \\
& + (1-z)^2\left(\frac{1}{3}\pi^2(z^2+2)\log z + z\right)\log(1-z) - (z-1)z^2\log(z) \\
& + \zeta_3(2\log(z) - 2(2z^3-3z^2+4z-1)\log\left(\frac{z}{1-z}\right)) + \frac{1}{6}(2z-1)\log^4(1-z) \\
& \left. - \frac{1}{3}(4z-2)\log(z)\log^3(1-z) \right], \tag{4.4.25}
\end{aligned}$$

reproducing the result in [98]. A comment is in order: as is often the case in perturbation theory, the spectrum of operators exchanged in the OPE of $\hat{\phi} \times \hat{\phi}$ is degenerate. This means there are multiple distinct operators with the same dimension at a given order in perturbation theory. Consequently, all the CFT data should be interpreted as an average over the degenerate operators, as discussed in detail in [51, 157]. At first order, we can only extract $\langle \hat{\gamma}_n^{(1)} \rangle$ instead of $\hat{\gamma}_n^{(1)}$. If the degeneracy were lifted at first order, we would then not be able to compute the double discontinuity

$$\text{dDisc}[\mathcal{G}^{(2)}(z)] = \pi^2 \sum_n \frac{1}{2} \langle \hat{a}_n^{(0)} (\hat{\gamma}_n^{(1)})^2 \rangle \frac{z^{2\hat{\Delta}_\phi}}{(1-z)^{2\hat{\Delta}_\phi}} G_{2\hat{\Delta}_\phi+2n}(1-z), \tag{4.4.26}$$

because

$$\langle \hat{a}_n^{(0)} (\hat{\gamma}_n^{(1)})^2 \rangle \neq \langle \hat{a}_n^{(0)} \rangle \langle \hat{\gamma}_n^{(1)} \rangle^2. \tag{4.4.27}$$

To compute $\langle \hat{a}_n^{(0)} (\hat{\gamma}_n^{(1)})^2 \rangle$ in (4.4.26), we would need to first solve the degeneracy by properly diagonalizing the dilatation operator. This issue is commonly known as operator mixing⁵³. In this section, we have disregarded this subtlety because, in the specific scenario considered here, the degeneracy among operators remains intact and the mixing problem can be safely ignored, at least up to one-loop order [98]. However, for computations involving higher loops, a careful analysis of the operator spectrum would be necessary.

4.4.2 Defect four-point function on the Wilson line in $\mathcal{N} = 4$ SYM

In this section, we now turn our attention to correlators involving fundamental scalars Φ^i , where $i = 1, \dots, 5$, inserted on the supersymmetric Wilson line given by (4.4.1). The corresponding defect operators $\hat{\Phi}^i$ belong to the super-displacement⁵⁴ multiplet [156]

⁵³This issue also affects the computation of the two-point function of bulk operators, as we mentioned in Sections 4.1 and 4.3.

⁵⁴The displacement operator was defined in (4.2.74). We refer to [156] for details on the generalization to superconformal field theory.

and have protected dimension $\hat{\Delta}_{\hat{\Phi}} = 1$. Their four-point function reads

$$\langle \hat{\Phi}^i(\tau_1) \hat{\Phi}^j(\tau_2) \hat{\Phi}^k(\tau_3) \hat{\Phi}^l(\tau_4) \rangle_{\mathcal{W}} = \frac{\langle \Phi^i(\tau_1) \Phi^j(\tau_2) \Phi^k(\tau_3) \Phi^l(\tau_4) \mathcal{W} \rangle}{\langle \mathcal{W} \rangle} = \frac{\mathcal{G}^{ijkl}(z)}{(\tau_{12} \tau_{34})^2}, \quad (4.4.28)$$

We restrict our attention to the case of identical operators, e.g. $i = j = k = l = 1$. Using superconformal Ward identities [156], one obtains for $\mathcal{G}^{1111}(z) \equiv \mathcal{G}(z)$ the structure

$$\mathcal{G}(z) = \mathbb{F}(\lambda) z^2 + (2z^{-1} - 1)f(z) - (z^2 - z + 1) f'(z), \quad (4.4.29)$$

where $\mathbb{F}(\lambda)$ is a constant that depends on the t'Hooft coupling $\lambda = g_{\text{YM}}^2 N$, and $f(z)$ is a crossing-antisymmetric function

$$f(z) = -\frac{z^2}{(1-z)^2} f(1-z) \quad (4.4.30)$$

that can be expanded in superconformal blocks

$$f(z) = F_{\mathcal{I}}(z) + \hat{a}_{\mathcal{B}_2} F_{\mathcal{B}_2}(z) + \sum_{\hat{\Delta}} \hat{a}_{\hat{\Delta}} F_{\hat{\Delta}}(z). \quad (4.4.31)$$

This is an analogue of the conformal block expansion (2.4.6), where the blocks are replaced with superblocks in presence of supersymmetry. Above, $\hat{\Delta}$ are the dimensions of operators belonging to a long ⁵⁵ supermultiplet, $\hat{a}_{\mathcal{B}_2}$ is the squared OPE coefficient of a short operator and the superconformal blocks are

$$\begin{aligned} F_{\mathcal{I}}(z) &= z, \\ F_{\mathcal{B}_2}(z) &= z - z {}_2F_1(1, 2, 4; z), \\ F_{\hat{\Delta}}(z) &= \frac{z^{\hat{\Delta}+1}}{1-\hat{\Delta}} {}_2F_1(\hat{\Delta}+1, \hat{\Delta}+2, 2\hat{\Delta}+4; z). \end{aligned} \quad (4.4.32)$$

The constant $\mathbb{F}(\lambda)$ in (4.4.29) can be computed using supersymmetric localization [150, 156], and at strong coupling reads

$$\mathbb{F}(\lambda) = 1 + \hat{a}_{\mathcal{B}_2} = 3 - \frac{3}{\lambda^{\frac{1}{2}}} + \frac{45}{8\lambda^{\frac{3}{2}}} + \frac{45}{4\lambda^2} + \mathcal{O}\left(\frac{1}{\lambda^{\frac{5}{2}}}\right). \quad (4.4.33)$$

Building on previous work [144, 156], the large λ expansion of the correlator

$$\mathcal{G}(z) = \mathcal{G}^{(0)}(z) + \frac{1}{\lambda^{\frac{1}{2}}} \mathcal{G}^{(1)}(z) + \frac{1}{\lambda} \mathcal{G}^{(2)}(z) + \frac{1}{\lambda^{\frac{3}{2}}} \mathcal{G}^{(3)}(z) + \frac{1}{\lambda^2} \mathcal{G}^{(4)}(z) + \mathcal{O}\left(\frac{1}{\lambda^{\frac{5}{2}}}\right) \quad (4.4.34)$$

has been recently computed [51, 157] up to fourth order (three loops in AdS_2) using analytic bootstrap techniques. This impressive result was obtained using an Ansatz in terms of a linear combination of Harmonic PolyLogarithms (HPL) multiplied by rational functions, and fixing the unknowns using:

⁵⁵Short supermultiplets are annihilated by some of the supercharges of the superconformal algebra, while long multiplets are not subject to any such constraint.

- Bose symmetry of the correlator, and in particular crossing symmetry.
- The terms proportional to $\log^n(1-z)$ (or $\log^n(z)$) with $n > 1$ in the OPE expansion, which are fixed at each order by lower order data, see (B.8). In order to compute them one has to take care of operator mixing, especially beyond one-loop.

- The assumption ⁵⁶

$$\hat{\gamma}_n^{(\ell)} \sim n^{\ell+1}, \quad (4.4.35)$$

on the behaviour of the anomalous dimensions at each perturbative order ℓ . This corresponds to a divergence $\sim t^\ell$ of the correlator in the Regge limit [102], see (2.4.24).

- Compatibility with the OPE (4.4.31), which combined with the localization result (4.4.33) implies

$$f(z) \sim -\frac{\mathbb{F}(\lambda)}{2} z^2 \quad \text{for } z \sim 0, \quad (4.4.36)$$

There is a similar condition at $z = 1$, thanks to crossing. This point is essentially equivalent to giving a definition of the coupling.

The aim of this section is to reproduce this result from first principles using our dispersion relation, rather than an Ansatz. This means that we will not need to input crossing symmetry or Bose symmetry, or assume the type of functions that appear in the correlator. However, we will see that the results obtained from the dispersion relation depend on undetermined constants, just like in section 4.4.1. We will then need some theory-specific assumptions to fix them, such as the behaviour in the Regge limit and the definition of the coupling.

Our strategy will be the following:

- Compute the terms proportional to $\log^n(1-z)$ in the OPE expansion (B.8) with $n > 1$ from lower order data and find $\text{dDisc}[\mathcal{G}(z)]$, just like we did at one-loop in (4.4.12). Regarding the problem of operator mixing, which may prevent us from computing the logarithmic terms from lower order CFT data, we will rely on the analysis of [157].
- At each perturbative order ℓ , assume a Regge-behaviour compatible with $\hat{\gamma}_n^{(\ell)} \sim n^{\ell+1}$ and derive the corresponding unbounded kernel (3.1.25), using the strategy outlined around (2.4.31).
- Solve the integrals in (3.1.22) with the appropriate kernel and regularized correlator. We choose the convenient subtraction

$$\mathcal{G}^{\text{reg}}(w) = \mathcal{G}(w) - \sum_{m,n} S_{m,n} \left(\frac{\log^n(1-z)}{z^m} + \frac{z^2 \log^n(z)}{(1-z)^{m+2}} \right), \quad (4.4.37)$$

⁵⁶For the OPE data of the long operators, we define a perturbative expansion as in (4.4.6).

where the coefficients $S_{m,n}$ are fixed demanding that the integrals (3.1.22) do not have singularities at $w = 1$. The number of such coefficients depends on the specific case. Notice that the double discontinuity of the extra term in $\mathcal{G}^{\text{reg}}(z)$ can be easily computed using the definition (2.4.12), once all the $S_{m,n}$ are fixed. We stress that (4.4.37) is not the only possible subtraction.

- Finally, we fix any undetermined constant using the localization result (4.4.36), or equivalently⁵⁷

$$\int_0^1 dz z^{-2} \mathcal{G}(z) = 0, \quad (4.4.39)$$

and, if needed, the following identities for integrated correlators [148, 160]

$$\begin{aligned} \int_0^1 dz \left[\left(\mathcal{G}(z) - \frac{2(z-1)z+1}{(z-1)^2} \right) \left(\frac{1+\log z}{z^2} \right) \right] &= \frac{3\mathbb{C}(\lambda) - \mathbb{B}(\lambda)}{8\mathbb{B}^2(\lambda)}, \\ \int_0^1 dz \left[\frac{f(z)}{z} - 2 + \frac{1}{z-1} \right] &= \frac{\mathbb{C}(\lambda)}{4\mathbb{B}^2(\lambda)} + \mathbb{F}(\lambda) - 3, \end{aligned} \quad (4.4.40)$$

where $\mathbb{B}(\lambda)$ is the Brehemstraalung function [161, 162] and $\mathbb{C}(\lambda)$ is the curvature function [163]. Their explicit expressions at large N read

$$\begin{aligned} \mathbb{B}(\lambda) &= \frac{\sqrt{\lambda} I_2(\sqrt{\lambda})}{4\pi^2 I_1(\sqrt{\lambda})} \\ \mathbb{C}(\lambda) &= \frac{(2\pi^2 - 3)\sqrt{\lambda}}{24\pi^4} + \frac{-24\zeta_3 + 5 - 4\pi^2}{32\pi^4} + \frac{11 + 2\pi^2}{64\pi^4\sqrt{\lambda}} + \frac{96\zeta_3 + 75 + 8\pi^2}{1024\pi^5\lambda} \\ &\quad + \frac{3(408\zeta_3 - 240\zeta_5 + 213 + 14\pi^2)}{16384\pi^6\lambda^{\frac{3}{2}}} + \frac{3(315\zeta_3 - 240\zeta_5 + 149 + 6\pi^2)}{16384\pi^7\lambda^2} \\ &\quad + O\left(\frac{1}{\lambda^{\frac{5}{2}}}\right) \end{aligned} \quad (4.4.41)$$

In what follows we will sketch the computation up to three loops. Just like in Section 4.4.1, we start by computing the order zero term using Wick contractions [144]

$$\mathcal{G}^{(0)}(z) = \frac{2z^2 - 2z + 1}{(z-1)^2}. \quad (4.4.43)$$

Comparing the above result with (4.4.29) and (4.4.31), one obtains the CFT data for long double-trace operators,

$$\hat{\Delta}^{(0)} = 2 + 2n, \quad \langle \hat{a}_n^{(0)} \rangle = \frac{\Gamma(5 + 2n)\Gamma(3 + 2n)(1 + 2n)}{\Gamma(6 + 4n)}. \quad (4.4.44)$$

⁵⁷This last equality can be proved by noticing that (4.4.29) implies

$$z^{-2} \mathcal{G}(z) = \partial_z \left(\mathbb{F}(\lambda) z - \left(1 - \frac{1}{z} + \frac{1}{z^2} \right) f(z) \right). \quad (4.4.38)$$

Integrating between $z = 0$ and $z = 1$ and using (4.4.36) and its equivalent condition at $z = 1$ one obtains (4.4.39).

Above, we use the average symbol because in this setup operator mixing turns out to be important at higher orders. Moving on to the tree-level result (first order in the expansion (4.4.34)), we see that the assumption $\hat{\gamma}_n^{(1)} \sim n^2$ implies that the correlator will diverge linearly in the Regge limit. This means we need to use the unbounded kernel (3.1.25), which in this case becomes ⁵⁸

$$\begin{aligned}
\bar{K}(z, w) &\equiv K_{\Delta_\phi=1}(z, w) - \sum_{n=0}^2 (A_{0,n} \hat{H}_{0,2}^B(w) + A_{1,n} \hat{H}_{1,2}^B(w)) \mathcal{C}^n \left[\frac{2}{\pi^2} \left(\frac{z^2 \log(z)}{1-z} + z \log(1-z) \right) \right] \\
&- (\tilde{A}_{0,n} \hat{H}_{0,2}^B(w) + \tilde{A}_{1,n} \hat{H}_{1,2}^B(w)) G_{2+2n}(z) \\
&= \frac{-2w^2(2w^4-9w^3+16w^2-14w+7)(z^2-z+1)^2}{7\pi^2(w-1)^3(z-1)^2} - \frac{w(2w^4-5w^3+5w-2)z^2(z^2-z+1)^2 \log(1-w)}{\pi^2(w(z-1)+1)(w-z)(w(z-1)-z)(w+z-1)((w-1)wz^2+z-1)} \\
&+ \left[-\frac{w^2(w^2-w+1)(2w^2-7w+7)z^4}{(w-1)^3} - \frac{w^2(w^2-w+1)(2w^2-7w+7)(z-1)z^3}{(w-1)^3} + \frac{7w^2(2-z)z^2}{(w-z)(w(-z)+w+z)} \right. \\
&+ \frac{w^2(w^2-w+1)(2w^2-7w+7)(z-2)}{(w-1)^3} + \frac{2(w^2-w+1)(2w^4-7w^3+14w-7)z^2}{(w-1)^3} + \frac{7(w-1)z^2}{w(z-1)+1} + \left. \frac{7z^2}{wz-1} \right] \frac{\log(1-z)}{7\pi^2 z} \\
&+ \frac{w^4(w^2-w+1)z^6(2w^4(2z^3-9z^2+14z-7)+w^3(4z^4-40z^3+131z^2-182z+91)) \log(z)}{7\pi^2(w-1)^3(z-1)^3(w(z-1)+1)(w+z-1)((w-1)wz^2+z-1)} \\
&+ \frac{w^4(w^2-w+1)z^6(w^2(-18z^4+131z^3-365z^2+468z-234)+2w(14z^4-91z^3+234z^2-286z+143)) \log(z)}{7\pi^2(w-1)^3(z-1)^3(w(z-1)+1)(w+z-1)((w-1)wz^2+z-1)} \\
&+ \frac{w^4(w^2-w+1)z^6(-14z^4+91z^3-234z^2+286z-143) \log(z)}{7\pi^2(w-1)^3(z-1)^3(w(z-1)+1)(w+z-1)((w-1)wz^2+z-1)}, \tag{4.4.45}
\end{aligned}$$

where the coefficients were fixed demanding that $\bar{K}(z, w) \sim w^3$, see (2.4.24). The discontinuity at this order is zero, just like in the scalar case. However, since $\bar{K}(z, w) \sim (1-w)^{-3}$ and $\mathcal{G}(w) \sim (1-w)^0$ from (4.4.31) and (4.4.29), the two contour integrals in (3.1.22) diverge because of the singularity at $w = 1$. We introduce the regularization (4.4.37) and fix the coefficients by imposing

$$w^{-2} \bar{K}(z, w) \mathcal{G}^{\text{reg}}(w) \sim (1-w)^0 \quad \text{for } w \rightarrow 1. \tag{4.4.46}$$

Since the expansion of $\mathcal{G}(w)$ around $w = 1$ can be read from the t-channel OPE (B.8), the condition above fixes the coefficients of the subtraction (4.4.37) in terms of known and unknown OPE data. In particular, since the block expansion goes schematically like $(1-z)^{2n}$, see (B.8), this means that at tree level with $\bar{K}(z, w) \sim (1-w)^{-3}$ the subtraction will depend on $\langle \hat{a}_0^{(1)} \rangle$, $\langle \hat{a}_0^{(0)} \hat{\gamma}_0^{(1)} \rangle$, $\langle \hat{a}_1^{(1)} \rangle$, $\langle \hat{a}_1^{(0)} \hat{\gamma}_1^{(1)} \rangle$. From (4.4.46), the contour integrals in (3.1.22) vanish

$$\lim_{\rho \rightarrow 0} \int_{C_\rho^+} \frac{dw}{2w^2} \bar{K}(z, w) \mathcal{G}^{\text{reg}}(w) + \lim_{\rho \rightarrow 0} \int_{C_\rho^-} \frac{dw}{2w^2} \bar{K}(z, w) \mathcal{G}^{\text{reg}}(w) = 0. \tag{4.4.47}$$

The only integral we need to compute is the one involving the double discontinuity of the regularized correlator. The latter can be computed from the explicit form of the

⁵⁸We choose to subtract $\hat{H}_{1,2}^B(w)$, but we could have used $\hat{H}_{0,1}^B(w)$ instead. The difference boils down to having a $\frac{\log(1-w)}{1-w}$ singularity at $w = 1$, rather than a second-order pole. We choose the latter for simplicity.

subtraction (4.4.37) and the definition of double discontinuity (2.4.12), and it will depend on the unknown coefficients $\langle \hat{a}_0^{(1)} \rangle$, $\langle \hat{a}_0^{(0)} \hat{\gamma}_0^{(1)} \rangle$, $\langle \hat{a}_1^{(1)} \rangle$, $\langle \hat{a}_1^{(0)} \hat{\gamma}_1^{(1)} \rangle$. Solving the integral of the double discontinuity in (3.1.22) with the kernel $\bar{K}(z, w)$ defined in (4.4.45) and removing the subtraction, we obtain

$$\begin{aligned} \mathcal{G}^{(1)}(z) = & -\frac{(5\langle \hat{\gamma}_1^{(1)} \rangle(z(2z-7)+7)z^4 + 7\langle \hat{\gamma}_0^{(1)} \rangle(z(z(5z(2z-7)+49)-28)+14)z^2) \log(z)}{245(z-1)^3} + \\ & + \frac{2(7\langle \hat{\gamma}_0^{(1)} \rangle + \langle \hat{\gamma}_1^{(1)} \rangle)((z-1)z+1)^2}{49(z-1)^2} + \frac{(5\langle \hat{\gamma}_1^{(1)} \rangle(z(2z+3)+2)(z-1)^2 + 7\langle \hat{\gamma}_0^{(1)} \rangle(z(z(5z(2z-1)+4)-5)+10)) \log(1-z)}{245z} \end{aligned} \quad (4.4.48)$$

Notice that two of the unknown constants (the OPE coefficients) are automatically canceled once we remove the subtraction. Using the theory-dependent constraints (4.4.39) and one of (4.4.40), we fix the remaining constants and find

$$\mathcal{G}^{(1)}(z) = -\frac{2(z^2-z+1)^2}{(z-1)^2} + \frac{(-2z^4+z^3+z-2) \log(1-z)}{z} + \frac{(2z^4-7z^3+9z^2-4z+2)z^2 \log(z)}{(z-1)^3}, \quad (4.4.49)$$

which is precisely the result obtained in [144]. The only non trivial step of the derivation is the computation of the integral in (3.1.22). While expressions like (4.4.45) look complicated, an efficient way to do the integrals is the repeated use of

$$\int_0^1 dw \frac{w^a(1-w)^b}{w-x} = \pi e^{-i\pi a} \left(-x^a \csc(\pi a) (1-x)^b + \frac{\cot(\pi a) + i \Gamma(b+1) {}_2\tilde{F}_1(1, -a-b; 1-a; x)}{\Gamma(a+b+1)} \right), \quad (4.4.50)$$

and its derivatives with respect to parameters a and b , to compute the integrals involving logarithms and rational functions. From (4.4.49), one can solve (4.4.29) for $f(z)$ and then extract the CFT data [156]

$$\langle \hat{\gamma}_n^{(1)} \rangle = \frac{(2+2n)(5+2n)}{2}, \quad \langle \hat{a}_n^{(1)} \rangle = \frac{1}{2} \partial_n \langle \hat{a}_n^{(0)} \hat{\gamma}_n^{(1)} \rangle. \quad (4.4.51)$$

Moving on to one-loop, one should worry about mixing⁵⁹. However, the authors of [51] found that since at first order the anomalous dimension of any operator is proportional to the eigenvalue of the superconformal Casimir⁶⁰ $\tilde{\mathcal{C}}F_{\hat{\Delta}}(z) = \hat{\Delta}(\hat{\Delta}+3)F_{\hat{\Delta}}(z)$, the degeneracy is actually not lifted. Therefore we can compute the higher logarithmic terms and the double discontinuity at one-loop from tree level data, just like we did in (4.4.12). The double discontinuity in this case reads

$$\text{dDisc}[\mathcal{G}^{(2)}(z)] = \frac{\pi^2 (9z^6 - 8z^5 + 4z^4 + 4z^2 - 8z + 9)}{2z^2}. \quad (4.4.52)$$

Assuming $\hat{\gamma}_n^{(2)} \sim n^3$, we see that the correlator diverges as t^2 in the Regge limit. We can still use the same kernel as for the tree level (4.4.45), since it goes like $\mathcal{O}(w^4)$ for small w . We fix the coefficients in the subtraction (4.4.37) by demanding that the integral of the double discontinuity in (3.1.22) converges and that $w^{-2} \bar{K}(z, w) \mathcal{G}^{\text{reg}}(w) \sim$

⁵⁹See the discussion around (4.4.27).

⁶⁰We refer to [51] for the explicit expression of the superconformal Casimir operator.

$(1-w)^0$, killing the contour integrals. Performing the remaining integral and removing the subtraction, we find

$$\begin{aligned}
\mathcal{G}^{(2)}(z) &= \frac{z^2(9z^6-46z^5+99z^4-116z^3+83z^2-30z+10)\log^2(z)}{2(z-1)^4} + \frac{(z((z(9z-8)+4)z^3+4z-8)+9)\log^2(1-z)}{2z^2} \\
&+ \frac{(118z^6+125z^5+4388z^4-10102z^3+4388z^2+125z+118)\log(1-z)}{840(z-1)^2z} + \frac{(-118z^6+833z^5-6783z^4)\log(z)}{840(z-1)^3} \\
&- \frac{(3(z-1)z+1)(6z^6-18z^5+19z^4-8z^3+z-2)\log(z)\log(1-z)}{2(z-1)^3z} + \frac{(11060z^3-3430z^2-2520z+840)\log(z)}{840(z-1)^3} \\
&+ \langle \hat{\gamma}_0^{(2)} \rangle \left[-\frac{(z(z(5z(2z-7)+49)-28)+14)z^2\log(z)}{35(z-1)^3} + \frac{2((z-1)z+1)^2}{7(z-1)^2} + \frac{(z(z(5z(2z-1)+4)-5)+10)\log(1-z)}{35z} \right] \\
&+ \langle \hat{\gamma}_1^{(2)} \rangle \left[-\frac{(z(2z-7)+7)z^4\log(z)}{49(z-1)^3} + \frac{2((z-1)z+1)^2}{49(z-1)^2} + \frac{(z-1)^2(z(2z+3)+2)\log(1-z)}{49z} \right] - \frac{1831((z-1)z+1)^2}{420(z-1)^2}.
\end{aligned} \tag{4.4.53}$$

Using (4.4.39) and one of the integrated correlators in (4.4.40), we obtain [156]

$$\begin{aligned}
\mathcal{G}^{(2)}(z) &= \frac{(9z^6-8z^5+4z^4+4z^2-8z+9)\log^2(1-z)}{2z^2} + \frac{(26z^6-63z^5+66z^4-62z^3+66z^2-63z+26)\log(1-z)}{4(z-1)^2z} \\
&+ \frac{z^2(9z^6-46z^5+99z^4-116z^3+83z^2-30z+10)\log^2(z)}{2(z-1)^4} + \frac{(-26z^6+93z^5-141z^4+92z^3-36z^2-12z+4)\log(z)}{4(z-1)^3} \\
&+ \frac{(-18z^8+72z^7-117z^6+99z^5-43z^4+5z^3+9z^2-7z+2)\log(z)\log(1-z)}{2(z-1)^3z} + \frac{2(z^2-z+1)^2}{(z-1)^2}.
\end{aligned} \tag{4.4.54}$$

From which one can extract the same CFT data that was found in [157]

$$\begin{aligned}
\langle \hat{\gamma}^{(2)} \rangle_n &= \hat{\gamma}_n^{(1)} \frac{1}{2} \partial_n \hat{\gamma}_n^{(1)} + \frac{j_n^2}{8} \left(-11 - \frac{6}{j_n^2+2} + 4H_{3+2n} \right), \\
\langle \hat{a}^{(2)} \rangle_n &= \frac{1}{2} \partial_n \langle \hat{a}^{(0)} \hat{\gamma}^{(2)} + \hat{a}^{(1)} \hat{\gamma}^{(1)} \rangle_n - \frac{1}{4} \partial_n^2 \langle \hat{a}^{(0)} (\hat{\gamma}^{(1)})^2 \rangle_n \\
&+ \langle \hat{a}^{(0)} \rangle_n \left(\frac{j_n^2(j_n^2-2)}{2} (S_{-2}(2+2n) + \frac{1}{2}\zeta(2)) - \frac{1068+5000n+8772n^2+7616n^3+3424n^4+736n^5+64n^6}{4(j_n^2+2)} \right),
\end{aligned} \tag{4.4.55}$$

where $j_n^2 = (2+2n)(5+2n)$ is the Casimir eigenvalue for the long operators and

$$H_n^{(m)} = \sum_{k=1}^n \frac{1}{k^m}, \quad H_n \equiv H_n^{(1)}, \tag{4.4.56}$$

$$S_{-2}(n) = \sum_{k=1}^n \frac{(-1)^k}{k^2} = \frac{(-1)^n}{4} \left(H_{n/2}^{(2)} - H_{(n-1)/2}^{(2)} \right) - \frac{1}{2} \zeta_2. \tag{4.4.57}$$

The procedure can be carried on at the next two orders, we will however skip the details of the computations and highlight the differences with respect to the previous orders. First of all, in order to compute the double discontinuity at three loops one needs $\langle \hat{a}^{(0)} (\hat{\gamma}^{(2)})^2 \rangle_n$.

It turns out that at this order the degeneracy is lifted, therefore

$$\langle \hat{a}^{(0)} (\hat{\gamma}^{(2)})^2 \rangle_n \neq \langle \hat{a}^{(0)} \rangle_n \langle \hat{\gamma}^{(2)} \rangle_n^2, \tag{4.4.58}$$

and one has to solve the operator mixing problem in order to compute the double discontinuity. This was done in [51] and we report their result

$$\frac{\langle \hat{a}^{(0)} (\hat{\gamma}^{(2)})^2 \rangle_n}{\langle \hat{a}^{(0)} \rangle_n} = \langle \hat{\gamma}^{(2)} \rangle_n^2 + \frac{1}{2} j_n^2 (j_n^2 - 2) S_{-2}(3 + 2n) + \frac{1}{8} j_n^2 (3j_n^2 - 4) H_{3+2n}^2 \quad (4.4.59)$$

$$+ \left(-j_n^4 + \frac{3}{4} \left(5 + \frac{2}{j_n^2 + 2} \right) \right) H_{3+2n} + \frac{1}{32} \left(-156 + 50j_n^2 + 29j_n^4 + \frac{24}{j_n^2 + 2} \right).$$

Using this result, together with the other OPE data from previous orders, we can compute all the higher logarithmic terms in the OPE (B.8) up to three loops and the corresponding contributions to the double discontinuity. A second new aspect of the calculation at this order is that, since the behaviour in the Regge limit gets worse, see (4.4.35), one is forced to subtract an extra term from the dispersion kernel

$$\begin{aligned} \bar{K}(z, w) &\equiv K_{\Delta_\phi=1}(z, w) - \sum_{m=0}^3 \sum_n A_{m,n} \hat{H}_{m,2}^B(w) \mathcal{C}^n \left[\frac{2}{\pi^2} \left(\frac{z^2 \log(z)}{1-z} + z \log(1-z) \right) \right] \\ &\quad - \sum_{m=0}^3 \sum_n \tilde{A}_{m,n} \hat{H}_{m,2}^B(w) G_{2+2n}(z), \end{aligned} \quad (4.4.60)$$

where the coefficients are fixed demanding that $\bar{K}(z, w) \sim w^6$ for small w , according to (2.4.24). We do not report here the (huge) explicit expression. Now $\bar{K}(z, w) \sim (1-w)^{-5}$ for $w \sim 1$, and demanding that the integrals in the dispersion relation (3.1.22) converge introduces a dependence on extra OPE data. This means that, to fix the unknown constants, one has to impose an additional constraint, and one can use (4.4.39) and both integrated correlators (4.4.40). For the third and fourth-order four-point function (4.4.28), the results obtained using the dispersion relation (3.1.22) reproduce the ones in [157]. The explicit expressions of the correlators are presented in (B.9) and (B.10).

4.4.3 Bulk correlator in presence of the Wilson line in $\mathcal{N} = 4$ SYM

In this section we are interested in the two-point function of 1/2 BPS bulk operators of protected dimension $\Delta = P$, where P is their R-charge. For the case $P = 2$

$$\mathcal{O}_{20'}^{IJ}(x) = \text{Tr} \left[\Phi^I(x) \Phi^J(x) - \frac{1}{6} \delta^{IJ} \Phi^K(x) \Phi_K(x) \right]. \quad (4.4.61)$$

This operator is the superprimary of the $\mathcal{N} = 4$ stress tensor multiplet and it transforms in the $\mathbf{20}'$ representation of the $SO(6)$ R-symmetry group⁶¹. To manage the dependence on R-symmetry indices, it is often convenient to introduce the complex null vector Y^I , satisfying $Y^I Y_I = 0$, and define

$$\mathcal{O}_2(x, y) \propto \text{Tr} (Y \cdot \Phi(x))^2. \quad (4.4.62)$$

⁶¹The 1/2 BPS operators in $\mathcal{N} = 4$ SYM are commonly identified by the Dynkin labels $[0, P, 0]$, with the operator (4.4.61) corresponding to the $[0, 2, 0]$ case.

By acting with a suitable differential operator it is always possible to transform functions of Y into $SO(6)$ tensor structures. This expression readily generalizes for higher-dimensional BPS operators

$$\mathcal{O}_P(x, y) \propto \text{Tr}(Y \cdot \Phi(x))^P. \quad (4.4.63)$$

We normalize the operators (4.4.63) as

$$\langle \mathcal{O}_P(Y_1, x_1) \mathcal{O}_P(Y_2, x_2) \rangle = \left(\frac{Y_1 \cdot Y_2}{x_{12}^2} \right)^P. \quad (4.4.64)$$

In the presence of the Wilson line these operators have a non-vanishing one-point function, which is fixed by superconformal invariance up to a coefficient a_P

$$\langle \mathcal{O}_P(Y, x) \rangle_{\mathcal{W}} \equiv \frac{\langle \mathcal{O}_P(Y, x) \mathcal{W} \rangle}{\langle \mathcal{W} \rangle} = a_P \left(\frac{Y \cdot \theta}{|x^i|} \right)^P, \quad (4.4.65)$$

where x^i are the coordinates on the plane orthogonal to the defect. We are interested in the two-point function in the presence of the Wilson line

$$\langle \mathcal{O}_P(Y_1, x_1) \mathcal{O}_P(Y_2, x_2) \rangle_{\mathcal{W}} = \frac{\langle \mathcal{O}_P(Y_1, x_1) \mathcal{O}_P(Y_2, x_2) \mathcal{W} \rangle}{\langle \mathcal{W} \rangle}, \quad (4.4.66)$$

which can be written as [164, 55]

$$\langle \mathcal{O}_P(Y_1, x_1) \mathcal{O}_P(Y_2, x_2) \rangle_{\mathcal{W}} = \left(\frac{Y_1 \cdot \theta \ Y_2 \cdot \theta}{|x_{1\perp}| |x_{2\perp}|} \right)^P \mathcal{F}_P(z, \bar{z}, \sigma), \quad (4.4.67)$$

where z and \bar{z} are the same kinematical cross-ratios as in (2.2.9) and σ is the R-symmetry cross-ratio

$$\sigma = \frac{Y_1 \cdot Y_2}{Y_1 \cdot \theta \ Y_2 \cdot \theta}. \quad (4.4.68)$$

The function $\mathcal{F}_P(z, \bar{z}, \sigma)$ is a polynomial in σ of order P , namely

$$\mathcal{F}_P(z, \bar{z}, \sigma) = \sum_{n=0}^P \sigma^{P-n} F_{P,n}(z, \bar{z}). \quad (4.4.69)$$

The dispersion relation (3.2.1) applies individually to the functions $F_{P,n}(z, \bar{z})$, provided we understand their behavior as $w \rightarrow 0$. Before we move to the computation of these functions at strong t'Hooft coupling, we examine their superconformal OPE expansions.

Selection rules and superconformal block expansion

The function $\mathcal{F}_P(z, \bar{z}, \sigma)$ can be expanded in the bulk and in the defect channel. The block expansions discussed in Section 2.5.1 are improved to superblock expansions in the presence of supersymmetry. Here we summarize the results for the selection rules

and the superblocks derived in [164, 55] and we refer the reader to these works for a thorough discussion.

The operators \mathcal{O}_P are superprimaries of the 1/2 BPS multiplet $\mathcal{B}_{[0,P,0]}$ (here we used the notation of [165] for the $\mathcal{N} = 4$ supermultiplets). In the bulk channel, we are interested in taking the fusion $\mathcal{B}_{[0,P,0]} \times \mathcal{B}_{[0,P,0]}$ and select the supermultiplets with a non-vanishing defect one-point function. Combining the results of [166] and [50, 55], we have

$$\mathcal{B}_{[0,P,0]} \otimes \mathcal{B}_{[0,P,0]} \rightarrow \mathbb{1} \oplus \sum_{k=1}^P \mathcal{B}_{[0,2k,0]} \oplus \sum_{k=1}^{P-1} \sum_{\ell} \mathcal{C}_{[0,2k,0],\ell} \oplus \sum_{k=0}^{P-2} \sum_{\Delta,\ell} \mathcal{A}_{[0,2k,0],\ell}^{\Delta}, \quad (4.4.70)$$

where $\mathcal{C}_{[0,2k,0],\ell}$ are semishort multiplets with protected scaling dimension $\Delta = 2 + 2k + \ell$, while $\mathcal{A}_{[0,2k,0],\ell}^{\Delta}$ are long multiplets with arbitrary scaling dimension $\Delta > 2 + 2k + \ell$. Each exchanged supermultiplet corresponds to a superblock $\mathcal{F}_{\Delta,\ell}(z, \bar{z}, \sigma)$, which encodes the contributions of all the superdescendants in the associated supermultiplet and for this reason it can be expressed as a linear combination of ordinary bulk blocks. Then the correlator can be expanded as

$$\mathcal{F}_P(z, \bar{z}, \sigma) = \left(\frac{\sqrt{z\bar{z}} \sigma}{(1-z)(1-\bar{z})} \right)^P \sum_{\mathcal{O}} \lambda_{PP\mathcal{O}} a_{\mathcal{O}} \mathcal{F}_{\Delta,\ell}(z, \bar{z}, \sigma), \quad (4.4.71)$$

where the sum is taken over the superprimary operators \mathcal{O} for each of the supermultiplets that are allowed to appear in the OPE (4.4.70). The coefficients are given by a product of a bulk three-point function $\lambda_{\mathcal{O}}$ and a one-point function $a_{\mathcal{O}}$. For single-trace short exchanged multiplets, the OPE coefficients are known exactly from supersymmetric localization. Their large- N expression reads

$$\begin{aligned} \lambda_{P_1 P_2 P_3} &= \frac{\sqrt{P_1 P_2 P_3}}{N}, \\ a_P &= \frac{\sqrt{\lambda P} I_P(\sqrt{\lambda})}{2^{\frac{P}{2}+1} N I_1(\sqrt{\lambda})}. \end{aligned} \quad (4.4.72)$$

Each superconformal block $\mathcal{F}_{\Delta,\ell}(z, \bar{z}, \sigma)$ can be expressed as a linear combination of ordinary bulk conformal blocks $f_{\Delta,\ell}(z, \bar{z})$ (2.5.18). We refer to Appendix B.3 for the explicit expressions.

In the defect channel, each supermultiplet $\mathcal{B}_{[0,P,0]}$ is expanded in defect superblocks. Here we will not need the details of this expansion, which can be found in [164, 55]. Our next goal is to understand the implications of the dispersion relation (3.2.1) for this setup.

Strong coupling computation

At large N and strong coupling λ , where the supersymmetric Wilson loop is described as the string worldsheet of minimal area ending on the contour of the loop, the correlator

of bulk operators can be computed perturbatively by Witten diagrams with some propagators ending on the worldsheet. The leading contribution to the correlator $\langle \mathcal{O}_P \mathcal{O}_P \rangle_{\mathcal{W}}$ is just (4.4.64), i.e. the two-point function without the defect. At order $1/N^2$ we have many contributions and we focus on the first two: the disconnected one, which is simply given by the product of two one-point functions at leading order, and the leading connected contribution, which is suppressed by $1/\sqrt{\lambda}$. Explicitly

$$\langle \mathcal{O}_P \mathcal{O}_P \rangle_{\mathcal{W}} = \langle \mathcal{O}_P \mathcal{O}_P \rangle + \frac{\lambda}{N^2} \left(\langle \mathcal{O}_P \rangle_{\mathcal{W}}^{(0)} \langle \mathcal{O}_P \rangle_{\mathcal{W}}^{(0)} + \frac{1}{\sqrt{\lambda}} \langle \mathcal{O}_P \mathcal{O}_P \rangle_{\mathcal{W}}^{(1)} + \mathcal{O} \left(\frac{1}{\lambda} \right) \right) + \mathcal{O} \left(\frac{1}{N^4} \right), \quad (4.4.73)$$

Correspondingly, the function $\mathcal{F}_P(z, \bar{z}, \sigma)$ reads

$$\mathcal{F}_P(z, \bar{z}, \sigma) = \left(\frac{\sqrt{z\bar{z}} \sigma}{(1-z)(1-\bar{z})} \right)^P + \frac{\lambda}{N^2} \left(\frac{P}{2^{P+2}} + \frac{1}{\sqrt{\lambda}} \mathcal{F}_P^{(1)}(z, \bar{z}, \sigma) + \mathcal{O} \left(\frac{1}{\lambda} \right) \right) + \mathcal{O} \left(\frac{1}{N^4} \right), \quad (4.4.74)$$

where we used the result for the one-point function (4.4.72). The function $\mathcal{F}_P^{(1)}(z, \bar{z}, \sigma)$ has been computed for $P = 2, 3, 4$ in [55] extracting the defect CFT data using the Lorentzian inversion formula and resumming the defect block expansion. Here, using the dispersion relation (3.2.1) we can skip the intermediate step and recover the result performing a very simple integration. This gives a clear understanding of the reason why the final result for the correlator is particularly simple.

The crucial observation of [55] is that very few operators contribute to the discontinuity at $\bar{z} = 1$. In particular, at large N and large λ , the bulk theory is described by an effective supergravity theory in AdS_5 and the spectrum of light excitations contains only the protected Kaluza-Klein modes in the short $\mathcal{B}_{[0,P,0]}$ multiplets and double trace operators with dimension

$$\Delta = 2P + 2n + \ell + O(N^{-2}). \quad (4.4.75)$$

Notice that the twist of the double trace operators ($\tau = \Delta - \ell = 2P + 2n$) is higher than the lower bound allowed by the selection rules (4.4.70) which would allow for long operators of twist as low as two. As mentioned before, double trace operators will not contribute to the discontinuity. This fact seems to suggest that the full correlator can be computed just from the CFT data of short operators (4.4.72). However, the dispersion relation (3.2.1) is able to reconstruct the full correlator only if the two-point function decays fast enough at infinity, see (2.5.25). Otherwise, it fails to account for the contribution of low-spin defect operators. Alternatively, the correlator can be reconstructed using the improved dispersion relation (3.2.24), though this approach introduces new poles, which contribute to the discontinuity. In [55] it was argued that the behaviour of the functions $F_{P,n}^{(1)}(z, \bar{z})$ in (4.4.69) for $w \rightarrow 0$ ⁶² is $F_{P,n}^{(1)}(r, w) \sim w^{P-n-1}$

⁶²The behaviour of $F_{P,n}^{(1)}(r, w)$ at $w \rightarrow 0$ is related to the one at infinity by the symmetry $F_{P,n}^{(1)}(r, w) = F_{P,n}^{(1)}(r, \frac{1}{w})$.

so that the improvement is needed only for $F_{P,P-1}^{(1)}$ and $F_{P,P}^{(1)}$. For all the cases when the improvement is not needed, only short operators contribute to the discontinuity.

For $P = 2$, no improvement is needed to compute $F_{2,0}^{(1)}(z, \bar{z})$. In this case, the discontinuity arises solely from the negative powers in the superblock expansion, originating from the contributions of short operators. As recalled in (4.3.5), these contributions correspond to δ -function terms in the discontinuity. In this case we find

$$\text{Disc}(F_{2,0}^{(1)}(r, w)) = -2\pi i \lambda_{222}^{(1)} \delta(r-w) \frac{(r^2 w (r^4 - 2r^2 \log(r^2) - 1))}{(r^2 - 1)^3 (rw - 1)}, \quad (4.4.76)$$

where $\lambda_{222}^{(1)}$ is the strong coupling expansion of (4.4.72). More generally, in this section we define

$$\lambda_{PP\mathcal{O}a\mathcal{O}} = \frac{\sqrt{\lambda}}{N^2} \lambda_{PP\mathcal{O}}^{(1)} + O(\lambda). \quad (4.4.77)$$

Equation (4.4.76) can be immediately integrated in (3.2.1) obtaining with no effort the final result of [55]

$$F_{2,0}^{(1)}(r, w) = -\lambda_{222}^{(1)} \frac{r^2 w (r^4 - 2r^2 \log(r^2) - 1)}{(r^2 - 1)^3 (r-w)(rw - 1)}. \quad (4.4.78)$$

In principle, we could follow a similar procedure for the other R-symmetry components, but in that case we would need to take care of the low-spin ambiguities. In [55], it was argued that these ambiguities can be fixed using superconformal Ward identities.

In general, we can carry out this same procedure for all $\langle \mathcal{O}_P \mathcal{O}_P \rangle$, confirming and extending the results of [55]. Indeed, in this holographic setup only short operators contribute to the discontinuity in all the cases where we do not have low-spin ambiguities. Specifically, only the multiplets $\mathcal{B}_{[0,2k,0]}$ in (4.4.70) need to be considered for the discontinuity. Furthermore the multiplet $\mathcal{B}_{[0,2P,0]}$ is too high in dimension to generate a negative power in the OPE expansion and therefore it does not contribute to the discontinuity. For generic P , we can compute the discontinuity at the order we are interested in as

$$\text{Disc}(\mathcal{F}_P^{(1)}(z, \bar{z}, \sigma)) = \text{Disc} \left[\left(\frac{\sqrt{z\bar{z}\sigma}}{(1-z)(1-\bar{z})} \right)^{P-1} \sum_{k=1}^{P-1} \lambda_{PP2k} a_{2k} \mathcal{G}_{[0,2k,0]}(z, \bar{z}, \sigma) \right], \quad (4.4.79)$$

and use the dispersion formula to find the $F_{P,p}^{(1)}$ up to $p = P - 2$. Notice that, as for the case $P = 2$, all the contributions are distributions, specifically δ -functions or derivatives thereof. For example for $P = 3$

$$\begin{aligned} \text{Disc}(F_{3,0}^{(1)}(r, w)) &= \lambda_{334}^{(1)} \delta(w-r) \frac{(r^3 w (r^6 + 9r^4 - 9r^2 - 6(r^4 + r^2) \log(r^2) - 1))}{4(r^2 - 1)^5 (rw - 1)} \\ &- \frac{\lambda_{332}^{(1)} \delta'(w-r) r^3 w}{4(r^2 - 1)^5 (rw - 1)^2} \left(2r^2 (-5r^4 w + 3r^3 (w^2 + 1) - 2r^2 w + 3r (w^2 + 1) - 5w) \log(r^2) \right. \\ &\left. + (r^2 - 1) (3r^6 w - r^5 (w^2 + 1) + 9r^4 w - 10r^3 (w^2 + 1) + 9r^2 w - r (w^2 + 1) + 3w) \right), \end{aligned} \quad (4.4.80)$$

which gives the expected result [55]

$$F_{3,0}^{(1)}(r, w) = -\frac{3}{4} \frac{r^3 w^2 (r^4 - 4r^2 \log(r) - 1)}{(r^2 - 1)^3 (r - w)^2 (rw - 1)^2}. \quad (4.4.81)$$

Computing at higher P does not involve any conceptual obstacle and it is only an algorithmic procedure. We checked the conjecture of [55] for the function $F_{P,0}^{(1)}$

$$F_{P,0}^{(1)}(z, \bar{z}) = -\frac{P}{4} \frac{(z\bar{z})^{\frac{P}{2}}}{[(1-z)(1-\bar{z})]^{P-1}} \left[\frac{1+z\bar{z}}{(1-z\bar{z})^2} + \frac{2z\bar{z} \log(z\bar{z})}{(1-z\bar{z})^3} \right] \quad (4.4.82)$$

up to very high values of P and we always found perfect agreement. We also derived the functions $F_{P,p}^{(1)}(z, \bar{z})$ with $p \leq P-2$ for several values of P . As an example, in Appendix B.4 we spell out the results for $F_{5,p}^{(1)}$, which is the first case that did not appear in [55].

Chapter 5

Conclusions

This thesis focused on developing new tools for the analytic bootstrap of defect conformal field theories and applying these techniques to defects of interest in condensed matter physics and holography.

The first objective was accomplished in Chapter 3, where we introduced new dispersion relations to compute defect and bulk correlators from their singularities. In particular, we derived a dispersion relation for the four-point function of defect operators in one-dimensional CFTs from the corresponding Lorentzian inversion formula. The formula expresses the correlator as an integral over its double discontinuity. Specifically, we presented the integration kernel for the case of identical bosonic (fermionic) operators with integer (half-integer) dimensions. We saw that the dispersion relation may receive extra contributions depending on the behaviour of the correlator at infinity. These contributions depend on the CFT data of low-dimensional operators. Moreover, we formulated two different dispersion relations for the two-point functions of bulk operators in presence of a defect. The first relation represents the correlator as an integral over a single discontinuity, which is influenced by the OPE data of the bulk channel expansion. The second relation reconstructs the correlator using a double discontinuity governed by the defect channel OPE. Additionally, we derived a separate dispersion relation for codimension-one defects. In this case, the dispersion relation involves both defect and bulk discontinuities. Since all these dispersion relations are derived using a contour deformation argument in the complex plane, which necessitates that the correlator decays sufficiently fast at infinity, they inherently involve some ambiguities. These ambiguities correspond to the exchange of low transverse spin operators in the defect channel OPE. We addressed this issue either by subtracting these low-spin contributions or by introducing an appropriate prefactor to improve the asymptotic behavior of the correlator.

The second objective of this thesis – bootstrapping defects of interest in condensed matter physics and holography – was achieved in Chapter 4. There, we explored line defects in the $O(N)$ model, employing both the analytic bootstrap and conventional

methods. By applying analytic bootstrap and diagrammatic techniques, we computed the two-point function of the fundamental field at the first non-trivial order in the ε -expansion, extracting a wealth of new defect CFT data. We performed this analysis for both a localized magnetic field and a spin impurity. In both scenarios, we found that the discontinuity of the correlator is determined by a single bulk conformal block and is proportional to the anomalous dimension of the corresponding operator. This allowed us to reconstruct the correlator, up to low-spin ambiguities, using only this single piece of known bulk data. We then resolved the ambiguities with the aid of diagrammatic input. For the spin impurity, we analyzed both the free and the interacting bulk cases, thoroughly examining the RG flow on the defect by computing the beta function up to third loop and investigating the defect spectrum. Combining bootstrap and diagrammatic methods, we determined that the spin impurity in the free bulk case flows to a trivial defect CFT. We concluded our exploration of defects in the $O(N)$ model by reproducing known results for the bulk two-point function in the presence of a boundary, at second order in the ε -expansion. In the final section of the thesis, we turned our attention to holographic correlators in presence of the supersymmetric Wilson line in $\mathcal{N} = 4$ Super Yang-Mills theory. Exploiting the analytic bootstrap techniques developed in the previous sections, we successfully reproduced the four-point function of fundamental fields inserted on the line, achieving results up to the fourth order in the large 't Hooft coupling expansion. This correlator was previously obtained using an Ansatz involving polylogarithms and rational functions, and our derivation validates this approach a posteriori. We also streamlined the derivation of existing results for the two-point function of half-BPS single-trace bulk operators.

This thesis demonstrated that the analytic bootstrap is a powerful method for studying conformal defects that admit a small parameter expansion. A natural extension of this work is to perform a similar analysis for other defects. For example, one could study line defects in the Gross-Neveu-Yukawa and cubic models [167–169]. The former are relevant for modeling impurities in graphene undergoing a second-order phase transition, while the latter provide a more accurate description of defects in real-world magnets, which are often not isotropic (i.e. they do not preserve the full $O(3)$ symmetry group but only a discrete subgroup). Another fascinating research direction is the analytic bootstrap of defect CFTs that admit a large N limit [112, 170–172]. The expansion in inverse powers of N is relevant both in holography, where $1/N$ is proportional to the dual string coupling, and in condensed matter physics. In the latter case, it is a powerful alternative to the ε -expansion to study strongly coupled defect CFTs in three dimensions. Moreover, one could analyze higher-dimensional defects in the $O(N)$ model [173–176], as well as superconformal defects with holographic descriptions [117, 177–179]. The latter are interesting because they highlight the interplay between the analytic bootstrap and various other techniques such as integrability, su-

persymmetric localization, and holography. A more ambitious goal is to apply the analytic techniques used in this thesis beyond perturbation theory. In absence of defects, the numerical bootstrap can be used to extract non-perturbative CFT data from the crossing equation for the four-point function. This approach can be extended to the case of defect four-point functions [39, 42]. However, due to the lack of positivity in the bulk channel, the numerical bootstrap cannot be used for extracting the CFT data from bulk two-point functions in the presence of a defect. A possible strategy to overcome this limitation is to combine non-perturbative bulk data from the defect-free numerical bootstrap with the defect Lorentzian inversion formula and dispersion relation, as it has been done in CFTs without defects [33, 180–182]. Another interesting extension of the ideas explored in this thesis is to consider correlators involving multiple defects. For example, one can study the correlator of two parallel line defects or of two lines forming a cusp. From these two-point functions, one can extract interesting observables such as the (generalized) Casimir energy [183]. In this setup, one would like to obtain an analogue of the crossing equation by expanding each defect in terms of local operators [184, 185] and comparing this expansion with the one obtained from the fusion of two defects [186–188]. At the present time, it is not known if this "fusion OPE" can be turned into a convergent block expansion. Finally, it is important to address certain technical issues in the derivation of the dispersion relations. First of all, it would be useful to derive a non-perturbative bound on the growth of the bulk two-point function at $|w| \rightarrow \infty$ for a generic defect, in order to control the low-spin ambiguities. In the case of a CFT without defects, the positivity of the OPE expansion can be used to prove the existence of a bound. For defect CFTs, positivity is absent in one of the OPE channels, therefore an alternative strategy is required. In the context of the one-dimensional dispersion relation, it would be interesting to find a general form of the dispersion kernel, valid for any value of the dimension of the external operators and for non-identical operators. In order to do this, we would first need to generalize the Lorentzian inversion formula introduced in [85]. Additionally, we would like to further investigate the connection between the dispersion relation and other analytic bootstrap tools, such as Mellin amplitudes [68, 189] and analytic functionals [66, 96–98]. In higher dimensions, it is possible to show that these approaches imply completely equivalent sum rules [67]. However, each formalism highlights different features of the correlators. For example, Mellin amplitudes have a simpler analytic structure compared to their counterparts in position space [190]. Moreover, they can be related to flat-space scattering amplitudes [69]. It would be interesting to explore this connection for certain one-dimensional CFTs defined at the boundary of AdS_2 , looking for evidence of integrability such as S-matrix factorization.

Appendices

A Polyakov blocks from the dispersion relation

The dispersion relation (3.1.22) can be used to compute the 1d Polyakov blocks. The Polyakov blocks [21, 70] are crossing symmetric¹ and Regge-bounded functions that satisfy [97, 98, 85]

$$\mathcal{G}(z) = \sum_{\Delta} a_{\Delta} \mathcal{P}_{\Delta}^{\Delta_{\phi}}(z). \quad (\text{A.1})$$

Roughly speaking, they are a crossing symmetric version of the conformal blocks. Since the four-point function $\mathcal{G}(z)$ can be also expanded in conformal blocks $G_{\Delta}(z)$ with the same coefficients (2.4.6), the above equation implies

$$\sum_{\Delta} a_{\Delta} G_{\Delta}(z) = \sum_{\Delta} a_{\Delta} \mathcal{P}_{\Delta}^{\Delta_{\phi}}(z). \quad (\text{A.2})$$

Building on the original study of [21, 70] in higher-dimensions, equation (A.2) can be turned into a powerful set of constraints on the OPE data [102]. See also [99–101, 52] for more recent applications.

As mentioned in Section 2.4, the Polyakov block can be expressed as the crossing-symmetric combination of exchange diagrams in AdS_2 in the s -, t - and u -channel, Regge-improved – in the bosonic case – via the subtraction of the scalar contact diagram of the ϕ^4 interaction in AdS_2 [85]. Alternative representations of the Polyakov blocks exist, such as in terms of linear combinations of conformal blocks and their derivatives [85]. Using their representation in terms of master functionals [96], they have been computed in the flat space limit – the limit of both Δ and Δ_{ϕ} large² – in [191], where their sum lead to a dispersion relation for the related analytic S-matrix. For specific choices of integer exchanged dimensions Δ (and $\Delta_{\phi} = 1$) they were computed in [192] at tree level, using their explicit definition as sum of exchanged Witten diagrams in AdS_2 .

The dispersion relation (3.1.1) (for the fermionic case) or (3.1.22) (for the bosonic case) can be used to obtain an integral representation of the Polyakov block, as noticed

¹The fact that Polyakov blocks are crossing symmetric implies that their functional form depends on the external dimension Δ_{ϕ} .

²In this limit [191], the ratio Δ/Δ_{ϕ} is fixed and strictly different from two.

in [96]. Indeed, from (A.2) and the fact that the double discontinuity (2.4.12) commutes with the t-channel OPE, in the bosonic case one has

$$\text{dDisc}[\mathcal{P}_{\Delta}^{\Delta_{\phi}}(z)] = 2 \sin^2 \frac{\pi}{2} (\Delta - 2\Delta_{\phi}) \frac{z^{2\Delta_{\phi}}}{(1-z)^{2\Delta_{\phi}}} G_{\Delta}(1-z), \quad (\text{A.3})$$

whereas in the fermionic one one obtains

$$\text{dDisc}[\mathcal{P}_{\Delta}^{\Delta_{\phi}}(z)] = 2 \cos^2 \frac{\pi}{2} (\Delta - 2\Delta_{\phi}) \frac{z^{2\Delta_{\phi}}}{(1-z)^{2\Delta_{\phi}}} G_{\Delta}(1-z). \quad (\text{A.4})$$

Therefore, in the bosonic case and for $\Delta > 2\Delta_{\phi}$, the Polyakov block can be computed as

$$\mathcal{P}_{\Delta}^{\Delta_{\phi}}(z) = 2 \sin^2 \left(\frac{\pi}{2} (\Delta - 2\Delta_{\phi}) \right) \int_0^1 dw w^{-2} K_{\Delta_{\phi}}^{\text{bd}}(z, w) \frac{w^{2\Delta_{\phi}}}{(1-w)^{2\Delta_{\phi}}} (1-w)^{\Delta} {}_2F_1(\Delta, \Delta, 2\Delta, 1-w), \quad (\text{A.5})$$

with $K_{\Delta_{\phi}}^{\text{bd}}(z, w)$ defined in (3.1.23). Notice that the condition $\Delta > 2\Delta_{\phi}$ is necessary to have a convergent integral ³. In the fermionic case instead, one has

$$\mathcal{P}_{\Delta}^{\Delta_{\phi}}(z) = 2 \cos^2 \left(\frac{\pi}{2} (\Delta - 2\Delta_{\phi}) \right) \int_0^1 dw w^{-2} K_{\Delta_{\phi}}(z, w) \frac{w^{2\Delta_{\phi}}}{(1-w)^{2\Delta_{\phi}}} (1-w)^{\Delta} {}_2F_1(\Delta, \Delta, 2\Delta, 1-w), \quad (\text{A.6})$$

with $K_{\Delta_{\phi}}(z, w)$ defined in (3.1.19). If Δ is integer, the above integrals can be computed in closed form, for any fixed Δ_{ϕ} , and reduce to a combination of polylogarithms and rational functions. This is consistent with the Ansatz discussed in [102] and with the Witten diagrams computation of [192]. For generic Δ the integrals can be expressed in terms of infinite series. For example, for $\Delta_{\phi} = 1$ and $\Delta = 3$ we find

$$\begin{aligned} \mathcal{P}_{\Delta=3}^{\Delta_{\phi}=1}(z) = & -\frac{60z^2(6z^2-6z+1)\text{Li}_2(1-z)\log(1-z)}{\pi^2} - \frac{60\text{Li}_2(z)\left((z^2-6z+6)(z-1)^4\log(1-z)\right)}{\pi^2(z-1)^4z^2} + \\ & -\frac{60\text{Li}_2(z)\left((z-2)z\left(6(z^2-z+1)^2(2z^3-z^2-2z+1)+(6z^4-18z^3+25z^2-14z+7)z^4\log(z)\right)\right)}{\pi^2(z-1)^4z^2} + \\ & +\frac{60(6z^6-6z^5+z^4-3z^2+18z-18)\text{Li}_3(1-z)}{\pi^2z^2} + \frac{60z^2(6z^6-30z^5+61z^4-64z^3+33z^2-22z-2)\text{Li}_3(z)}{\pi^2(z-1)^4} + \\ & -\frac{120z^2(6z^2-6z+1)\text{Li}_3\left(\frac{z}{z-1}\right)}{\pi^2} + \frac{20z^2(6(z-1)z+1)\log^3(1-z)}{\pi^2} - \frac{60\left(z(6z^5-6z^4+z^3+z-6)+6\right)\log^2(1-z)\log(z)}{\pi^2z^2} \\ & +\frac{5(306z^6-471z^5+(279-62\pi^2)z^4-153z^3+219z^2-144z+36)\log(z)}{\pi^2(z-1)^4} + \frac{60(-192z^3+183z^2-90z+18)\zeta_3}{\pi^2(z-1)^4z^2} + \\ & -\frac{180((z-1)z+1)^2(2z^4-5z^3+5z-2)\log(z)\log(1-z)}{\pi^2(z-1)^4z} + \frac{\log(1-z)(-1710z^7+3075z^6+5(56\pi^2-498)z^5+5(306+4\pi^2)z^4)}{\pi^2(z-1)^4z} \\ & +\frac{\log(1-z)(-10(249+7\pi^2)z^3+5(615+4\pi^2)z^2-1710z+360)}{\pi^2(z-1)^4z} + \frac{20z^5(36z^2+\pi^2(z(6(z-5)z+61)-62))\tanh^{-1}(1-2z)}{\pi^2(z-1)^4} + \\ & +\frac{30\left(\left((z-3)z+3\right)(2z^4-z^3+2z-7)+\frac{3(z-1)((z-1)z+1)^2}{\pi^2}+\frac{6}{z}\right)}{(z-1)^3} + \frac{60(12z^{10}-60z^9+122z^8-128z^7+78z^6-38z^5+113z^4)\zeta_3}{\pi^2(z-1)^4z^2} \end{aligned} \quad (\text{A.7})$$

³This condition has also the effect of killing the extra contour integrals in the bosonic dispersion relation (3.1.22), something in fact necessary as they are defined in terms of the full, unknown, Polyakov block.

For generic Δ and $\Delta_\phi = 1$ one has instead

$$\begin{aligned}
\mathcal{P}_\Delta^{\Delta_\phi=1}(z) = & \sin^2\left(\frac{\pi\Delta}{2}\right) \left\{ 2 \csc^2(\pi\Delta) z^\Delta {}_2F_1(\Delta, \Delta; 2\Delta; z) \right. \\
& + \frac{2(-2\Delta z((1-z)\log(1-z)+z\log(z))+\Delta(z-1)\log(z)+z-1)}{\pi^2\Delta^2(z-1)} {}_3F_2(\Delta, \Delta, \Delta; 2\Delta, \Delta+1; 1) + \\
& - \frac{4^\Delta \Gamma(\Delta+\frac{1}{2})}{\pi^{5/2}(\Delta-2)(\Delta-1)(z-1)^2 \Gamma(\Delta+2)} \left(2(2-3(\Delta-1)\Delta)z \tanh^{-1}(1-2z) + \right. \\
& + ((\Delta-1)\Delta + ((\Delta-1)\Delta-1)z^4 - 3(\Delta-1)\Delta z^3 + 2(\Delta-1)\Delta z^2 - 1) \log(1-z) + \\
& + 2z^3 \log((1-z)z) + (-2(\Delta-1)\Delta - 3z^2 + 2) \log(z) \left. \right) + \\
& - \frac{2\partial_a {}_3F_2(\Delta, \Delta, \Delta; 2\Delta, \Delta+1+a; 1)}{\pi^2\Delta} + \frac{2\partial_a {}_3F_2(\Delta, \Delta, \Delta+a; 2\Delta, \Delta+1; 1)}{\pi^2\Delta} + \\
& + \sum_{n=0}^{\infty} \left[\frac{2z^n}{\pi^2} \left(\frac{z^2 {}_4F_3(\Delta, \Delta, \Delta, n+\Delta, n+\Delta; 2\Delta, n+\Delta+1, n+\Delta+1; 1)}{(\Delta+n)^2} - \frac{\log(z) {}_3F_2(\Delta, \Delta, n+\Delta-2; 2\Delta, n+\Delta-1; 1)}{\Delta+n-2} \right) + \right. \\
& + \frac{2z^n}{\pi^2(n-\Delta)^2} \left(((n-\Delta)\log(z) - 1) {}_3F_2(\Delta, \Delta, \Delta-n; 2\Delta, -n+\Delta+1; 1) + \right. \\
& - (n-\Delta)(\partial_a {}_3F_2(\Delta, \Delta, \Delta-n; 2\Delta, \Delta-n+1+a; 1) + \\
& + \partial_a {}_3F_2(\Delta, \Delta, \Delta-n+a; 2\Delta, \Delta-n+1; 1)) \left. \right) + \\
& - \frac{2z}{\pi^2} \Gamma(2\Delta)(1-z)^{n-2} \Gamma(n+1) \left(z^2 \Gamma(\Delta-2) \log\left(\frac{1-z}{z}\right) {}_3\tilde{F}_2(\Delta-2, \Delta, \Delta; 2\Delta, n+\Delta-1; 1) \right. \\
& + (z-1)^2 \Gamma(\Delta) (\psi^{(0)}(\Delta) {}_3\tilde{F}_2(\Delta, \Delta, \Delta; 2\Delta, n+\Delta+1; 1) + \\
& + \partial_a {}_3\tilde{F}_2(\Delta, \Delta, \Delta; 2\Delta, \Delta+n+1+a; 1) + \partial_a {}_3F_2(\Delta, \Delta, \Delta+a; 2\Delta, \Delta+n+1; 1)) \left. \right) \left. \right\} \\
& + \frac{z^2}{(1-z)^2} (z \rightarrow 1-z). \tag{A.8}
\end{aligned}$$

where $({}_3\tilde{F}_2) {}_3F_2$ are (regularized) generalized hypergeometric functions and ∂_a indicates the derivative with respect to a evaluated at $a = 0$. The structure of Polyakov blocks is quite similar in the fermionic case. For example, for $\Delta_\phi = 1/2$ and $\Delta = 1$ the Polyakov blocks reads

$$\begin{aligned}
\mathcal{P}_{\Delta=1}^{\Delta_\phi=1/2}(z) = & - \frac{(6z^2-6)\log^2(1-z)\log(z)}{3\pi^2(z-1)} - \frac{(-6(z-2)z\text{Li}_2(z) - \pi^2 z^2)\log(z)}{3\pi^2(z-1)} + \\
& - \frac{(6(z^2-1)\text{Li}_2(z) - 2\pi^2 z^2 + 2\pi^2 z)\log(1-z)}{3\pi^2(z-1)} - \frac{18(z^2-1)\text{Li}_3(1-z) + (18z^2-36z)\text{Li}_3(z) + 18\zeta_3}{3\pi^2(z-1)} \tag{A.9}
\end{aligned}$$

B Details on the supersymmetric Wilson line in $\mathcal{N} = 4$ SYM

B.1 Superconformal block expansion for the defect four-point function

We consider the four-point function defined in (4.4.28),

$$\langle \hat{\Phi}^1(\tau_1) \hat{\Phi}^1(\tau_2) \hat{\Phi}^1(\tau_3) \hat{\Phi}^1(\tau_4) \rangle = \frac{\mathcal{G}(z)}{(\tau_{12} \tau_{34})^2}, \tag{B.1}$$

with

$$\mathcal{G}(z) = \mathbb{F}(\lambda) z^2 + (2z^{-1} - 1)f(z) - (z^2 - z + 1) f'(z), \quad (\text{B.2})$$

where $\mathbb{F}(\lambda)$ is given in (4.4.33) and $f(z)$ is an arbitrary crossing-antisymmetric function. As explained in Section 4.4.2, the function $f(z)$ be expanded in superconformal blocks

$$f(z) = F_{\mathcal{I}}(z) + \hat{a}_{\mathcal{B}_2} F_{\mathcal{B}_2}(z) + \sum_{\hat{\Delta}} \hat{a}_{\hat{\Delta}} F_{\hat{\Delta}}(z), \quad (\text{B.3})$$

where $\hat{\Delta}$ are the dimensions of unprotected long operators and

$$\hat{a}_{\mathcal{B}_2} = 2 - \frac{3}{\lambda^{1/2}} + \frac{45}{8\lambda^{3/2}} + \frac{45}{4\lambda^2} + \mathcal{O}\left(\frac{1}{\lambda^{5/2}}\right). \quad (\text{B.4})$$

The explicit form of the superconformal blocks is

$$\begin{aligned} F_{\mathcal{I}}(z) &= z, \\ F_{\mathcal{B}_2}(z) &= z - z {}_2F_1(1, 2, 4; z), \\ F_{\hat{\Delta}}(z) &= \frac{z^{\hat{\Delta}+1}}{1 - \hat{\Delta}} {}_2F_1(\hat{\Delta} + 1, \hat{\Delta} + 2, 2\hat{\Delta} + 4; z). \end{aligned} \quad (\text{B.5})$$

We assume the following perturbative expansion

$$\begin{aligned} \hat{\Delta} &= 2 + 2n + \frac{1}{\lambda^{1/2}} \hat{\gamma}_n^{(1)} + \frac{1}{\lambda} \hat{\gamma}_n^{(2)} + \frac{1}{\lambda^{3/2}} \hat{\gamma}_n^{(3)} + \frac{1}{\lambda^2} \hat{\gamma}_n^{(4)} + \mathcal{O}\left(\frac{1}{\lambda^{5/2}}\right), \\ \hat{a}_{\hat{\Delta}} &= \hat{a}_n^{(0)} + \frac{1}{\lambda^{1/2}} \hat{a}_n^{(1)} + \frac{1}{\lambda} \hat{a}_n^{(2)} + \frac{1}{\lambda^{3/2}} \hat{a}_n^{(3)} + \frac{1}{\lambda^2} \hat{a}_n^{(4)} + \mathcal{O}(\lambda^3) + \mathcal{O}\left(\frac{1}{\lambda^{5/2}}\right), \\ f(z) &= f^{(0)}(z) + \frac{1}{\lambda^{1/2}} f^{(1)}(z) + \frac{1}{\lambda} f^{(2)}(z) + \frac{1}{\lambda^{3/2}} f^{(3)}(z) + \frac{1}{\lambda^2} f^{(4)}(z) + \mathcal{O}\left(\frac{1}{\lambda^{5/2}}\right). \end{aligned} \quad (\text{B.6})$$

If we introduce the notation

$$F_{\hat{\Delta}}^{(\ell)}(z) = z^{\hat{\Delta}} (\partial_{\hat{\Delta}})^{\ell} z^{-\hat{\Delta}} F_{\hat{\Delta}}(z), \quad (\text{B.7})$$

where $F_{\hat{\Delta}}(z)$ are conformal blocks for long operators (B.5), then the s-channel OPE expansion of $f(z)$ reads [51]

$$\begin{aligned} f^{(0)}(z) &= F_{\mathcal{I}}(z) + \hat{a}_{\mathcal{B}_2}^{(0)} F_{\mathcal{B}_2}(z) + \sum_n \hat{a}_n^{(0)} F_{2+2n}(z), \\ f^{(1)}(z) &= \sum_n \left[\hat{a}_n^{(0)} \hat{\gamma}_n^{(1)} F_n(z) \right] \log(z) + \hat{a}_{\mathcal{B}_2}^{(1)} F_{\mathcal{B}_2}(z) + \sum_n \left[\hat{a}_n^{(1)} F_{2+2n}(z) + \hat{a}_n^{(0)} \hat{\gamma}_n^{(1)} F_{2+2n}^{(1)}(z) \right], \end{aligned} \quad (\text{B.8})$$

$$\begin{aligned}
f^{(2)}(z) &= \sum_n \left[\frac{1}{2} \hat{a}_n^{(0)} (\hat{\gamma}_n^{(1)})^2 F_{2+2n}(z) \right] \log^2(z) + \hat{a}_{\mathcal{B}_2}^{(2)} F_{\mathcal{B}_2}(z) \\
&+ \sum_n \left[(\hat{a}_n^{(0)} \hat{\gamma}_n^{(2)} + a_n^{(1)} \hat{\gamma}_n^{(1)}) F_{2+2n}(z) + \hat{a}_n^{(0)} (\hat{\gamma}_n^{(1)})^2 F_{2+2n}^{(1)}(z) \right] \log(z) \\
&+ \sum_n \left[a_n^{(2)} F_{2+2n}(z) + (\hat{a}_n^{(0)} \hat{\gamma}_n^{(2)} + a_n^{(1)} \hat{\gamma}_n^{(1)}) F_{2+2n}^{(1)}(z) + \frac{1}{2} \hat{a}_n^{(0)} (\hat{\gamma}_n^{(1)})^2 F_{2+2n}^{(2)}(z) \right], \\
f^{(3)}(z) &= \sum_n \left[\frac{1}{6} \hat{a}_n^{(0)} (\hat{\gamma}_n^{(1)})^3 F_{2+2n}(z) \right] \log^3(z) \\
&+ \sum_n \left[\left(\hat{a}_n^{(0)} \hat{\gamma}_n^{(1)} \hat{\gamma}_n^{(2)} + \frac{1}{2} a_n^{(1)} (\hat{\gamma}_n^{(1)})^2 \right) F_{2+2n}(z) + \frac{1}{2} \hat{a}_n^{(0)} (\hat{\gamma}_n^{(1)})^3 F_{2+2n}^{(1)}(z) \right] \log^2(z) \\
&+ \sum_n \left[(\hat{a}_n^{(0)} \hat{\gamma}_n^{(3)} + a_n^{(1)} \hat{\gamma}_n^{(2)} + a_n^{(2)} \hat{\gamma}_n^{(1)}) F_{2+2n}(z) + \left(2 \hat{a}_n^{(0)} \hat{\gamma}_n^{(1)} \hat{\gamma}_n^{(2)} + a_n^{(1)} (\hat{\gamma}_n^{(1)})^2 \right) F_{2+2n}^{(1)}(z) \right. \\
&+ \left. \frac{1}{2} \hat{a}_n^{(0)} (\hat{\gamma}_n^{(1)})^3 F_{2+2n}^{(2)}(z) \right] \log(z) + \hat{a}_{\mathcal{B}_2}^{(3)} F_{\mathcal{B}_2}(z) \\
&+ \sum_n \left[a_n^{(3)} F_{2+2n}(z) + (\hat{a}_n^{(0)} \hat{\gamma}_n^{(3)} + a_n^{(1)} \hat{\gamma}_n^{(2)} + a_n^{(2)} \hat{\gamma}_n^{(1)}) F_{2+2n}^{(1)}(z) \right. \\
&+ \left. \left(\hat{a}_n^{(0)} \hat{\gamma}_n^{(1)} \hat{\gamma}_n^{(2)} + \frac{1}{2} a_n^{(1)} (\hat{\gamma}_n^{(1)})^2 \right) F_{2+2n}^{(2)}(z) + \frac{1}{6} \hat{a}_n^{(0)} (\hat{\gamma}_n^{(1)})^3 F_{2+2n}^{(3)}(z) \right], \\
f^{(4)}(z) &= \sum_n \left[\frac{1}{24} \hat{a}_n^{(0)} (\hat{\gamma}_n^{(1)})^4 F_{2+2n}(z) \right] \log^4(z) \\
&+ \sum_n \left[\left(\frac{1}{2} \hat{a}_n^{(0)} (\hat{\gamma}_n^{(1)})^2 \hat{\gamma}_n^{(2)} + \frac{1}{6} a_n^{(1)} (\hat{\gamma}_n^{(1)})^3 \right) F_{2+2n}(z) + \frac{1}{6} \hat{a}_n^{(0)} (\hat{\gamma}_n^{(1)})^4 F_{2+2n}^{(1)}(z) \right] \log^3(z) \\
&+ \sum_n \left[\left(\hat{a}_n^{(0)} \hat{\gamma}_n^{(1)} \hat{\gamma}_n^{(3)} + \frac{1}{2} \hat{a}_n^{(0)} (\hat{\gamma}_n^{(2)})^2 + a_n^{(1)} \hat{\gamma}_n^{(1)} \hat{\gamma}_n^{(2)} + \frac{1}{2} a_n^{(2)} (\hat{\gamma}_n^{(1)})^2 \right) F_{2+2n}(z) \right. \\
&+ \left. \left(\frac{1}{2} a_n^{(1)} (\hat{\gamma}_n^{(1)})^3 + \frac{3}{2} \hat{a}_n^{(0)} (\hat{\gamma}_n^{(1)})^2 \hat{\gamma}_n^{(2)} \right) F_{2+2n}^{(1)}(z) + \frac{1}{4} \hat{a}_n^{(0)} (\hat{\gamma}_n^{(1)})^4 F_{2+2n}^{(2)}(z) \right] \log^2(z) \\
&+ \sum_n \left[(\hat{a}_n^{(0)} \hat{\gamma}_n^{(4)} + a_n^{(1)} \hat{\gamma}_n^{(3)} + a_n^{(2)} \hat{\gamma}_n^{(2)} + a_n^{(3)} \hat{\gamma}_n^{(1)}) F_{2+2n}(z) \right. \\
&+ \left. \left(\hat{a}_n^{(0)} (\hat{\gamma}_n^{(2)})^2 + 2 \hat{a}_n^{(0)} \hat{\gamma}_n^{(1)} \hat{\gamma}_n^{(3)} + 2 a_n^{(1)} \hat{\gamma}_n^{(1)} \hat{\gamma}_n^{(2)} + (a_n^{(2)} (\hat{\gamma}_n^{(1)})^2 \right) F_{2+2n}^{(1)}(z) \right. \\
&+ \left. \left(\frac{3}{2} \hat{a}_n^{(0)} (\hat{\gamma}_n^{(1)})^2 \hat{\gamma}_n^{(2)} + \frac{1}{2} a_n^{(1)} (\hat{\gamma}_n^{(1)})^3 \right) F_{2+2n}^{(2)}(z) + \frac{1}{24} \hat{a}_n^{(0)} (\hat{\gamma}_n^{(1)})^4 F_{2+2n}^{(3)}(z) \right] \log(z) \\
&+ \hat{a}_{\mathcal{B}_2}^{(4)} F_{\mathcal{B}_2}(z) + \sum_n \left[a_n^{(4)} F_{2+2n}(z) + (\hat{a}_n^{(0)} \hat{\gamma}_n^{(4)} + a_n^{(1)} \hat{\gamma}_n^{(3)} + a_n^{(2)} \hat{\gamma}_n^{(2)} + a_n^{(3)} \hat{\gamma}_n^{(1)}) F_{2+2n}^{(1)}(z) \right. \\
&+ \left. \left(\frac{1}{2} \hat{a}_n^{(0)} (\hat{\gamma}_n^{(1)})^2 \hat{\gamma}_n^{(2)} + \frac{1}{6} a_n^{(1)} (\hat{\gamma}_n^{(1)})^3 \right) F_{2+2n}^{(3)}(z) + \frac{1}{24} \hat{a}_n^{(0)} (\hat{\gamma}_n^{(1)})^4 F_{2+2n}^{(4)}(z) \right].
\end{aligned}$$

We can obtain the t-channel expansion by sending $z \rightarrow 1-z$ and multiplying by $-\frac{z^2}{(1-z)^2}$. Using (B.2), we can obtain an analogous expansion for $\mathcal{G}(z)$.

B.2 Defect correlators at two and three loop

In this section we present the explicit form of the third and fourth order correlators, which were obtained following the procedure outlined in Section 4.4.2. The third order (two loops) four-point function reads

$$\begin{aligned}
\mathcal{G}^{(3)}(z) = & -\frac{z^2(111z^6-560z^5+1215z^4-1480z^3+1165z^2-510z+170)\log^2(z)}{4(z-1)^4} \\
& + \frac{(55z^6-191z^5+312z^4-245z^3+130z^2-9z+3)\log(z)}{4(z-1)^3} + \frac{36z^8\zeta_3-176z^7\zeta_3+15z^6(24\zeta_3+1)-20z^5(20\zeta_3+3)}{8(z-1)^4} \\
& + \frac{40z^4(7\zeta_3+3)-6z^3(16\zeta_3+25)+8z^2(4\zeta_3+15)-60z+15}{8(z-1)^4} \\
& + \frac{z^2(72z^8-477z^7+1391z^6-2345z^5+2515z^4-1751z^3+817z^2-200z+50)\log^3(z)}{6(z-1)^5} \\
& + \left[\frac{-55z^6+139z^5-182z^4+193z^3-182z^2+139z-55}{4(z-1)^2z} - \frac{z^2(72z^7-396z^6+940z^5-1260z^4+1040z^3-536z^2+156z-25)\log^2(z)}{2(z-1)^4} \right. \\
& \left. + \frac{(222z^8-888z^7+1497z^6-1383z^5+707z^4-145z^3-45z^2+35z-10)\log(z)}{4(z-1)^3z} \right] \log(1-z) \\
& + \left[\frac{-111z^9+442z^8-741z^7+684z^6-441z^5+439z^4-684z^3+746z^2-449z+114}{4(z-1)^3z^2} \right. \\
& \left. + \frac{(144z^{10}-639z^9+1197z^8-1233z^7+747z^6-247z^5+17z^4+45z^3-55z^2+35z-9)\log(z)}{4(z-1)^3z^2} \right] \log^2(1-z) \\
& + \frac{(-144z^{11}+639z^{10}-1197z^9+1233z^8-747z^7+281z^6-247z^5+657z^4-1123z^3+1127z^2-621z+144)\log^3(1-z)}{12(z-1)^3z^3} \\
& + \frac{(3z^8-10z^7+15z^6-15z^5+13z^4-15z^3+15z^2-10z+3)\text{Li}_2\left(\frac{z}{z-1}\right)}{2(z-1)^3z^2} \\
& + \frac{(-2z^9+9z^8-16z^7+14z^6-36z^5+76z^4-116z^3+99z^2-46z+9)\text{Li}_3(z)}{2(z-1)^4z^2} \\
& - \frac{(9z^9-35z^8+55z^7-45z^6+17z^5+17z^4-45z^3+55z^2-35z+9)\text{Li}_3\left(\frac{z}{z-1}\right)}{2(z-1)^3z^2} \\
& + \frac{\text{Li}_2(z)(3z^9-13z^8+25z^7-30z^6+28z^5-28z^4+30z^3-25z^2+13z-3)}{2(z-1)^4z^2} \\
& + \frac{\text{Li}_2(z)\log(1-z)(9z^{10}-44z^9+90z^8-100z^7+62z^6-62z^4+100z^3-90z^2+44z-9)}{2(z-1)^4z^2} \\
& + \frac{z\log(z)\text{Li}_2(z)(-9z^9+46z^8-99z^7+116z^6-76z^5+36z^4-14z^3+16z^2-9z+2)}{2(z-1)^4z^2}. \tag{B.9}
\end{aligned}$$

The fourth order (three-loops) correlator is

$$\begin{aligned}
\mathcal{G}^{(4)}(z) = & -\frac{3(46z^8-175z^7+287z^6-271z^5+254z^4-271z^3+287z^2-175z+46)\text{Li}_2(z)}{16(z-1)^3z^2} \\
& - \frac{3(96z^{11}-423z^{10}+785z^9-799z^8+477z^7-137z^6-137z^5+477z^4-799z^3+785z^2-423z+96)\text{Li}_2(z)\log^2(1-z)}{8(z-1)^3z^3} \\
& + \frac{3(264z^{11}-1572z^{10}+4097z^9-6169z^8+5713z^7-3107z^6+190z^5+1460z^4-1466z^3+796z^2-236z+30)\text{Li}_2(z)\log(z)}{16(z-1)^5z^2} \\
& - \frac{3(96z^{11}-633z^{10}+1835z^9-3071z^8+3265z^7-2292z^6+980z^5-262z^4-30z^3+25z^2-11z+2)\text{Li}_2(z)\log^2(z)}{8(z-1)^5z} \\
& + \log(1-z) \left[-\frac{3\text{Li}_2(z)(264z^{10}-1086z^9+1893z^8-1797z^7+740z^6+456z^5-1293z^4+1255z^3-580z^2+30z+48)}{16(z-1)^3z^3} \right]
\end{aligned}$$

$$\begin{aligned}
& \left[\frac{3(1-z)(96z^{11}-528z^{10}+1252z^9-1674z^8+1376z^7-700z^6+228z^5-86z^4+100z^3-90z^2+44z-9)\text{Li}_2(z)\log(z)}{4(z-1)^5z^2} \right. \\
& - \frac{3(z^2-z+1)(46z^8-175z^7+241z^6-142z^5+142z^4-241z^3+175z^2-46z)\text{Li}_2\left(\frac{z}{z-1}\right)}{16(z-1)^4z^3} \\
& - \frac{3(z^2-z+1)(24z^9-93z^8+136z^7-90z^6+26z^5-26z^4+90z^3-136z^2+93z-24)\text{Li}_2\left(\frac{z}{z-1}\right)\log(1-z)}{8(z-1)^4z^3} \\
& + \frac{3(z^2-z+1)(24z^8-108z^7+188z^6-156z^5+58z^4+32z^3-66z^2+52z-15)\text{Li}_2\left(\frac{z}{z-1}\right)\log(z)}{8(z-1)^4z^2} \\
& - \frac{3(72z^{11}-396z^{10}+900z^9-1080z^8+94z^7+1939z^6-4005z^5+4625z^4-3193z^3+1260z^2-216z)\text{Li}_3(z)}{16(z-1)^5z^3} \\
& - \frac{3(27z^{12}-163z^{11}+424z^{10}-620z^9+570z^8-226z^7-388z^6+1320z^5-2240z^4+2368z^3-1564z^2+588z-96)\text{Li}_3(z)\log(1-z)}{8(z-1)^5z^3} \\
& + \frac{3(27z^{11}-161z^{10}+413z^9-595z^8+540z^7-488z^6+592z^5-972z^4+1025z^3-703z^2+271z-45)\text{Li}_3(z)\log(z)}{8(z-1)^5z^2} \\
& + \frac{(648z^{11}-3348z^{10}+7419z^9-9156z^8+6099z^7-6099z^5+9156z^4-7419z^3+3348z^2-648z)\text{Li}_3\left(\frac{z}{z-1}\right)}{16(z-1)^4z^3} + \\
& - \frac{3(96z^{12}-519z^{11}+1208z^{10}-1584z^9+1276z^8-614z^7+614z^5-1276z^4+1584z^3-1208z^2+519z-96)\text{Li}_3\left(\frac{z}{z-1}\right)\log(1-z)}{8(z-1)^4z^3} \\
& - \frac{3(96z^{11}-564z^{10}+1432z^9-2052z^8+1808z^7-1024z^6+444z^5-410z^4+532z^3-468z^2+224z-45)\text{Li}_3\left(\frac{z}{z-1}\right)\log(z)}{8(z-1)^4z^2} \\
& - \frac{(1800z^{13}-9144z^{12}+20115z^{11}-25093z^{10}+19259z^9-9009z^8+2403z^7-1581z^6)\log^4(1-z)}{48(z-1)^3z^4} \\
& - \frac{(6147z^5-14465z^4+20383z^3-17577z^2+8568z-1800)\log^4(1-z)}{48(z-1)^3z^4} \\
& + \frac{(1728z^8-8446z^7+17973z^6-21752z^5+17642z^4-8178z^3+2824z^2-84z+21)\log^2(z)}{16(z-1)^4} \\
& + \frac{(-3024z^{10}+19629z^9-56379z^8+94369z^7-101549z^6+71379z^5-34041z^4+8808z^3-2232z^2+20z-4)\log^3(z)}{24(z-1)^5} \\
& + \frac{z^2(900z^{10}-7272z^9+26487z^8-57436z^7+82346z^6-81720z^5+56934z^4-26952z^3+8613z^2-1250z+250)\log^4(z)}{24(z-1)^6} \\
& + \log^3(1-z) \left[\frac{12096z^{11}-55620z^{10}+110010z^9-122387z^8+82023z^7-35200z^6}{96(z-1)^3z^3} \right. \\
& - \frac{31084z^5-71961z^4+112931z^3-105816z^2+55566z-12528}{96(z-1)^3z^3} \\
& + \frac{(-7200z^{12}+42912z^{11}-112473z^{10}+170512z^9-164340z^8+102980z^7)\log(z)}{48(z-1)^4z^2} \\
& \left. + \frac{(-40586z^6+9300z^5-1996z^4+1800z^3-1620z^2+792z-162)\log(z)}{48(z-1)^4z^2} \right] \\
& \log^2(1-z) \left[\frac{3456z^9-14350z^8+25751z^7-26307z^6}{32(z-1)^3z^2} \right. \\
& + \frac{19443z^5-19392z^4+26259z^3-26087z^2+14737z-3594}{32(z-1)^3z^2} \\
& + \frac{(-12096z^{11}+66492z^{10}-159516z^9+219295z^8-188716z^7+102443z^6)\log(z)}{32(z-1)^4z^2} \\
& + \frac{(-32956z^5+6317z^4-2608z^3+2251z^2-1050z+198)\log(z)}{32(z-1)^4z^2} + \frac{(3600z^{12}-21312z^{11}+55404z^{10}-83184z^9)\log^2(z)}{16(z-1)^4z^2} \\
& \left. + \frac{(79272z^8-49008z^7+18976z^6-4116z^5+602z^4-332z^3+288z^2-136z+27)\log^2(z)}{16(z-1)^4z^2} \right]
\end{aligned}$$

$$\begin{aligned}
& + \frac{-648z^8\zeta_3 + 3348z^7\zeta_3 + z^6(26 - 7451\zeta_3) + 4z^5(2321\zeta_3 - 26) + z^4(208 - 7369\zeta_3) + z^3(3362\zeta_3 - 260)}{16(z-1)^4} \\
& + \frac{z^2(208 - 1270\zeta_3) + 8z(16\zeta_3 - 13) - 32\zeta_3 + 26}{16(z-1)^4} \\
& + \frac{(2304z^{10}\zeta_3 - 15840z^9\zeta_3 + 152z^8(316\zeta_3 - 7) + z^7(5583 - 84320\zeta_3) + z^6(94240\zeta_3 - 14343)) \log(z)}{64(z-1)^5} \\
& + \frac{(z^5(22559 - 68768\zeta_3) + z^4(33376\zeta_3 - 23629) + z^3(17036 - 8960\zeta_3) + z^2(2240\zeta_3 - 8294) + 2690z - 538) \log(z)}{64(z-1)^5} \\
& + \log(1 - z) \left[\frac{(-3456z^8 + 13824z^7 - 23847z^6 + 23157z^5 - 13699z^4 + 4931z^3 - 2289z^2 + 1379z - 388) \log(z)}{16(z-1)^3 z} \right. \\
& + \frac{-2304z^{10}\zeta_3 + 12456z^9\zeta_3 - 56z^8(520\zeta_3 - 19) + z^7(38592\zeta_3 - 5057) - 8z^6(3956\zeta_3 - 1497) + z^5(16752\zeta_3 - 18877)}{64(z-1)^4 z} \\
& + \frac{z^4(21788 - 5088\zeta_3) + z^3(2016\zeta_3 - 18877) - 8z^2(128\zeta_3 - 1497) + z(576\zeta_3 - 5057) - 128\zeta_3 + 1064}{64(z-1)^4 z} \\
& + \frac{(6048z^{10} - 33030z^9 + 78696z^8 - 107437z^7 + 91780z^6 - 49499z^5 + 15706z^4 - 2762z^3 + 532z^2 - 274z + 60) \log^2(z)}{16(z-1)^4 z} \\
& + \frac{(-1800z^{12} + 12528z^{11} - 38799z^{10} + 70469z^9 - 83015z^8 + 65845z^7) \log^3(z)}{12(z-1)^5 z} \\
& \left. + \frac{(-34966z^6 + 11946z^5 - 2256z^4 + 280z^3 - 25z^2 + 11z - 2) \log^3(z)}{12(z-1)^5 z} \right]. \tag{B.10}
\end{aligned}$$

B.3 Superconformal block expansion for the bulk two-point function

In this section we present the expression of the superconformal blocks that were found in [50] and that we used in Section 4.4.3. We follow the conventions of [55]. After defining the R-symmetry block

$$h_k = \sigma^{-\frac{k}{2}} {}_2F_1 \left(-\frac{k}{2}, -\frac{k}{2}; -k - 1; \frac{\sigma}{2} \right), \tag{B.11}$$

then the superconformal blocks are expressed as a combination of ordinary bulk blocks $f_{\Delta,\ell}(z, \bar{z})$ (2.5.18) as

$$\begin{aligned}
\mathcal{G}_{\mathcal{B}_{[0,P,0]}} &= h_P f_{P,0}(z, \bar{z}) + \frac{(P+2)^2 P}{128(P+1)^2(P+3)} h_{P-2} f_{P+2,2}(z, \bar{z}) \\
&+ \frac{(P-2)(P+2)P^2}{16384(P-1)^2(P+1)(P+3)} h_{P-4} f_{P+4,0}(z, \bar{z}), \\
\mathcal{G}_{\mathcal{C}_{[0,2,0],\ell}} &= h_2 f_{\ell+4,\ell} + b_1 h_0 f_{\ell+6,\ell-2} + (b_{21} h_4 + b_{22} h_2 + b_{23} h_0) f_{\ell+6,\ell+2} + (b_{31} h_2 + b_{32} h_0) f_{\ell+8,\ell} \\
&+ b_4 h_2 f_{\ell+8,\ell+4} + b_5 h_0 f_{\ell+10,\ell+2}, \\
\mathcal{G}_{\mathcal{A}_{[0,0,0],\ell}} &= h_0 f_{\Delta,\ell} + (h_2 \eta_{11} + h_0 \eta_{12}) f_{\Delta+2,\ell-2} + (h_2 \eta_{21} + h_0 \eta_{22}) f_{\Delta+2,\ell+2} + \eta_3 h_0 f_{\Delta+4,\ell-4} \\
&+ (h_4 \eta_{41} + h_2 \eta_{42} + h_0 \eta_{43}) f_{\Delta+4,\ell} + \eta_5 h_0 f_{\Delta+4,\ell+4} + (h_2 \eta_{61} + h_0 \eta_{62}) f_{\Delta+6,\ell-2} \\
&+ (h_2 \eta_{71} + h_0 \eta_{72}) f_{\Delta+6,\ell+2} + \eta_8 h_0 f_{\Delta+8,\ell}. \tag{B.12}
\end{aligned}$$

The explicit form of the coefficients b_{ij} and η_{ij} is not particularly illuminating, and can be found in the ancillary file of [164].

B.4 Bulk correlators for $P = 5$

In this section we present the results for the components $F_{5,p}^{(1)}$, defined in (4.4.67) and (4.4.69), with $p < P - 1$,

$$\begin{aligned}
F_{5,0}^{(1)} &= -\frac{5}{4} \left[\frac{r^5(r^2+1)w^4}{(r^2-1)^2(r-w)^4(rw-1)^4} - \frac{2r^7w^4 \log(r^2)}{(r^2-1)^3(r-w)^4(rw-1)^4} \right], \\
F_{5,1}^{(1)} &= \frac{5}{4} \left[\frac{(r^4-38r^2+1)r^5w^3}{(r^2-1)^4(r-w)^3(rw-1)^3} \right. \\
&\quad \left. + \frac{r^6w^3(r^6(w^2+1)+5r^5w-10r^4(w^2+1)+26r^3w-10r^2(w^2+1)+5rw+w^2+1) \log(r^2)}{(r^2-1)^5(r-w)^4(rw-1)^4} \right], \\
F_{5,2}^{(1)} &= \frac{5}{4} \left[-\frac{3r^6w^2(8r^6(w^2+1)+43r^5w-83r^4(w^2+1)+214r^3w-83r^2(w^2+1)+43rw+8w^2+8)}{(r^2-1)^6(r-w)^3(rw-1)^3} \right. \\
&\quad + \frac{3r^5w^2(r(r^9w+7r^8(w^2+1)+15r^7w-46r^6(w^2+1)+284r^5w)+w) \log(r^2)}{2(r^2-1)^7(r-w)^3(rw-1)^3} \\
&\quad \left. + \frac{3r^5w^2(r(-222r^4(w^2+1)+284r^3w-46r^2(w^2+1)+15rw+7w^2+7)+w) \log(r^2)}{2(r^2-1)^7(r-w)^3(rw-1)^3} \right], \\
F_{5,3}^{(1)} &= \frac{5}{4} \left[\frac{5r^5w(r(3r^{11}w+15r^{10}(w^2+1)+20r^9w-35r^8(w^2+1)+833r^7w-960r^6(w^2+1))+3w) \log(r^2)}{2(r^2-1)^9(r-w)^2(rw-1)^2} \right. \\
&\quad + \frac{5r^5w(r(+2208r^5w-960r^4(w^2+1)+833r^3w-35r^2(w^2+1)+20rw+15(w^2+1))+3w) \log(r^2)}{2(r^2-1)^9(r-w)^2(rw-1)^2} \\
&\quad - \frac{5r^5w(r(9r^9w+72r^8(w^2+1)+188r^7w-503r^6(w^2+1)+2743r^5w-2078r^4(w^2+1)+2743r^3w)+9w)}{3(r^2-1)^8(r-w)^2(rw-1)^2} \\
&\quad \left. - \frac{5r^5w(r(-503r^2(w^2+1)+188rw+72(w^2+1))+9w)}{3(r^2-1)^8(r-w)^2(rw-1)^2} \right].
\end{aligned} \tag{B.13}$$

They were derived following the approach outlined in Section 4.4.3.

Bibliography

- [1] T. Andrews, “*Bakerian Lecture: On the Continuity of the Gaseous and Liquid States of Matter.*”, Proceedings of the Royal Society of London 18, 42 (1869), <http://www.jstor.org/stable/112707>.
- [2] M. Smoluchowski, “*Molekular-kinetische Theorie der Opaleszenz von Gasen im kritischen Zustande, sowie einiger verwandter Erscheinungen*”, *Annalen der Physik* 330, 205 (1908).
- [3] A. M. Polyakov, “*Conformal symmetry of critical fluctuations*”, JETP Lett. 12, 381 (1970).
- [4] Y. Nakayama, “*Scale invariance vs conformal invariance*”, *Phys. Rept.* 569, 1 (2015), [arxiv:1302.0884](https://arxiv.org/abs/1302.0884).
- [5] L. Onsager, “*Crystal Statistics. I. A Two-Dimensional Model with an Order-Disorder Transition*”, *Phys. Rev.* 65, 117 (1944), <https://link.aps.org/doi/10.1103/PhysRev.65.117>.
- [6] L. D. Landau, “*On the theory of phase transitions*”, *Zh. Eksp. Teor. Fiz.* 7, 19 (1937).
- [7] L. P. Kadanoff, “*Critical behaviour. Universality and scaling*”.
- [8] D. J. Gross and F. Wilczek, “*Ultraviolet Behavior of Nonabelian Gauge Theories*”, *Phys. Rev. Lett.* 30, 1343 (1973).
- [9] L. P. Kadanoff, “*Scaling laws for Ising models near $T(c)$* ”, *Physics Physique Fizika* 2, 263 (1966).
- [10] K. G. Wilson and J. Kogut, “*The renormalization group and the ϵ -expansion*”, *Physics Reports* 12, 75 (1974), <https://www.sciencedirect.com/science/article/pii/0370157374900234>.
- [11] K. G. Wilson, “*The renormalization group and critical phenomena*”, *Rev. Mod. Phys.* 55, 583 (1983), <https://link.aps.org/doi/10.1103/RevModPhys.55.583>.
- [12] J. M. Maldacena, “*The large N limit of superconformal field theories and supergravity*”, *Adv. Theor. Math. Phys.* 2, 231 (1998), [hep-th/9711200](https://arxiv.org/abs/hep-th/9711200).
- [13] E. Witten, “*Anti-de Sitter space and holography*”, *Adv. Theor. Math. Phys.* 2, 253 (1998), [hep-th/9802150](https://arxiv.org/abs/hep-th/9802150).

- [14] S. S. Gubser, I. R. Klebanov and A. M. Polyakov, “*Gauge theory correlators from non-critical string theory*”, *Phys. Lett. B* **428**, 105 (1998), [hep-th/9802109](#).
- [15] K. G. Wilson and M. E. Fisher, “*Critical exponents in 3.99 dimensions*”, *Phys. Rev. Lett.* **28**, 240 (1972).
- [16] J. C. Le Guillou and J. Zinn-Justin, “*Critical Exponents from Field Theory*”, *Phys. Rev. B* **21**, 3976 (1980).
- [17] R. Guida and J. Zinn-Justin, “*Critical exponents of the N vector model*”, *J. Phys. A* **31**, 8103 (1998), [cond-mat/9803240](#).
- [18] M. Moshe and J. Zinn-Justin, “*Quantum field theory in the large N limit: A Review*”, *Phys. Rept.* **385**, 69 (2003), [hep-th/0306133](#).
- [19] M. Campostrini, M. Hasenbusch, A. Pelissetto, P. Rossi and E. Vicari, “*Critical exponents and equation of state of the three-dimensional Heisenberg universality class*”, *Phys. Rev. B* **65**, 144520 (2002), [cond-mat/0110336](#).
- [20] S. Ferrara, A. F. Grillo and R. Gatto, “*Tensor representations of conformal algebra and conformally covariant operator product expansion*”, *Annals Phys.* **76**, 161 (1973).
- [21] A. M. Polyakov, “*Nonhamiltonian approach to conformal quantum field theory*”, *Zh. Eksp. Teor. Fiz.* **66**, 23 (1974).
- [22] A. A. Belavin, A. M. Polyakov and A. B. Zamolodchikov, “*Infinite Conformal Symmetry in Two-Dimensional Quantum Field Theory*”, *Nucl. Phys. B* **241**, 333 (1984).
- [23] R. Rattazzi, V. S. Rychkov, E. Tonni and A. Vichi, “*Bounding scalar operator dimensions in 4D CFT*”, *JHEP* **0812**, 031 (2008), [arxiv:0807.0004](#).
- [24] K. G. Wilson, “*Non-Lagrangian Models of Current Algebra*”, *Phys. Rev.* **179**, 1499 (1969), <https://link.aps.org/doi/10.1103/PhysRev.179.1499>.
- [25] D. Poland, S. Rychkov and A. Vichi, “*The Conformal Bootstrap: Theory, Numerical Techniques, and Applications*”, *Rev. Mod. Phys.* **91**, 015002 (2019), [arxiv:1805.04405](#).
- [26] S. Rychkov and N. Su, “*New Developments in the Numerical Conformal Bootstrap*”, [arxiv:2311.15844](#).
- [27] S. El-Showk, M. F. Paulos, D. Poland, S. Rychkov, D. Simmons-Duffin and A. Vichi, “*Solving the 3D Ising Model with the Conformal Bootstrap*”, *Phys. Rev. D* **86**, 025022 (2012), [arxiv:1203.6064](#).
- [28] S. El-Showk, M. F. Paulos, D. Poland, S. Rychkov, D. Simmons-Duffin and A. Vichi, “*Solving the 3d Ising Model with the Conformal Bootstrap II. c -Minimization and Precise Critical Exponents*”, *J. Stat. Phys.* **157**, 869 (2014), [arxiv:1403.4545](#).
- [29] F. Kos, D. Poland, D. Simmons-Duffin and A. Vichi, “*Precision Islands in the Ising and $O(N)$ Models*”, *JHEP* **1608**, 036 (2016), [arxiv:1603.04436](#).

- [30] L. F. Alday, “*Large Spin Perturbation Theory for Conformal Field Theories*”, *Phys. Rev. Lett.* **119**, 111601 (2017), [arxiv:1611.01500](#).
- [31] S. Caron-Huot, “*Analyticity in Spin in Conformal Theories*”, *JHEP* **1709**, 078 (2017), [arxiv:1703.00278](#).
- [32] Z. Komargodski and A. Zhiboedov, “*Convexity and Liberation at Large Spin*”, *JHEP* **1311**, 140 (2013), [arxiv:1212.4103](#).
- [33] D. Simmons-Duffin, “*The Lightcone Bootstrap and the Spectrum of the 3d Ising CFT*”, *JHEP* **1703**, 086 (2017), [arxiv:1612.08471](#).
- [34] K. G. Wilson, “*Confinement of Quarks*”, *Phys. Rev. D* **10**, 2445 (1974).
- [35] G. 't Hooft, “*On the Phase Transition Towards Permanent Quark Confinement*”, *Nucl. Phys. B* **138**, 1 (1978).
- [36] I. Affleck, “*Conformal field theory approach to the Kondo effect*”, *Acta Phys. Polon. B* **26**, 1869 (1995), [cond-mat/9512099](#).
- [37] C.-M. Chang, Y.-H. Lin, S.-H. Shao, Y. Wang and X. Yin, “*Topological Defect Lines and Renormalization Group Flows in Two Dimensions*”, *JHEP* **1901**, 026 (2019), [arxiv:1802.04445](#).
- [38] M. Billo, V. Goncalves, E. Lauria and M. Meineri, “*Defects in conformal field theory*”, *JHEP* **1604**, 091 (2016), [arxiv:1601.02883](#).
- [39] D. Gaiotto, D. Mazac and M. F. Paulos, “*Bootstrapping the 3d Ising twist defect*”, *JHEP* **1403**, 100 (2014), [arxiv:1310.5078](#).
- [40] A. Gimenez-Grau and P. Liendo, “*Bootstrapping line defects in $\mathcal{N} = 2$ theories*”, *JHEP* **2003**, 121 (2020), [arxiv:1907.04345](#).
- [41] J. Padayasi, A. Krishnan, M. A. Metlitski, I. A. Gruzberg and M. Meineri, “*The extraordinary boundary transition in the 3d $O(N)$ model via conformal bootstrap*”, *SciPost Phys.* **12**, 190 (2022), [arxiv:2111.03071](#).
- [42] A. Gimenez-Grau, E. Lauria, P. Liendo and P. van Vliet, “*Bootstrapping line defects with $O(2)$ global symmetry*”, *JHEP* **2211**, 018 (2022), [arxiv:2208.11715](#).
- [43] C. Behan, L. Di Pietro, E. Lauria and B. C. Van Rees, “*Bootstrapping boundary-localized interactions*”, *JHEP* **2012**, 182 (2020), [arxiv:2009.03336](#).
- [44] M. Lemos, P. Liendo, M. Meineri and S. Sarkar, “*Universality at large transverse spin in defect CFT*”, *JHEP* **1809**, 091 (2018), [arxiv:1712.08185](#).
- [45] P. Liendo, Y. Linke and V. Schomerus, “*A Lorentzian inversion formula for defect CFT*”, *JHEP* **2008**, 163 (2020), [arxiv:1903.05222](#).
- [46] P. Liendo, L. Rastelli and B. C. van Rees, “*The Bootstrap Program for Boundary CFT_d*”, *JHEP* **1307**, 113 (2013), [arxiv:1210.4258](#).
- [47] A. Bissi, T. Hansen and A. Söderberg, “*Analytic Bootstrap for Boundary CFT*”, *JHEP* **1901**, 010 (2019), [arxiv:1808.08155](#).

- [48] D. Mazáč, L. Rastelli and X. Zhou, “An analytic approach to $BCFT_d$ ”, *JHEP* 1912, 004 (2019), [arxiv:1812.09314](#).
- [49] A. Kaviraj and M. F. Paulos, “The Functional Bootstrap for Boundary CFT”, *JHEP* 2004, 135 (2020), [arxiv:1812.04034](#).
- [50] P. Liendo and C. Meneghelli, “Bootstrap equations for $\mathcal{N} = 4$ SYM with defects”, *JHEP* 1701, 122 (2017), [arxiv:1608.05126](#).
- [51] P. Ferrero and C. Meneghelli, “Bootstrapping the half-BPS line defect CFT in $N=4$ supersymmetric Yang-Mills theory at strong coupling”, *Phys. Rev. D* 104, L081703 (2021), [arxiv:2103.10440](#).
- [52] P. Dey and K. Ghosh, “Bootstrapping conformal defect operators on a line”, [arxiv:2404.06576](#).
- [53] A. Gimenez-Grau, P. Liendo and P. van Vliet, “Superconformal boundaries in $4 - \epsilon$ dimensions”, *JHEP* 2104, 167 (2021), [arxiv:2012.00018](#).
- [54] A. Gimenez-Grau and P. Liendo, “Bootstrapping monodromy defects in the Wess-Zumino model”, *JHEP* 2205, 185 (2022), [arxiv:2108.05107](#).
- [55] J. Barrat, A. Gimenez-Grau and P. Liendo, “Bootstrapping holographic defect correlators in $\mathcal{N} = 4$ super Yang-Mills”, *JHEP* 2204, 093 (2022), [arxiv:2108.13432](#).
- [56] L. Bianchi and D. Bonomi, “Conformal dispersion relations for defects and boundaries”, *SciPost Phys.* 15, 055 (2023), [arxiv:2205.09775](#).
- [57] D. Bonomi and V. Forini, “Dispersion relation from Lorentzian inversion in 1d CFT”, [arxiv:2406.10220](#).
- [58] L. Bianchi, D. Bonomi and E. de Sabbata, “Analytic bootstrap for the localized magnetic field”, *JHEP* 2304, 069 (2023), [arxiv:2212.02524](#).
- [59] L. Bianchi, D. Bonomi, E. de Sabbata and A. Gimenez-Grau, “Analytic bootstrap for magnetic impurities”, *JHEP* 2405, 080 (2024), [arxiv:2312.05221](#).
- [60] S. Rychkov, “EPFL Lectures on Conformal Field Theory in $D \geq 3$ Dimensions”.
- [61] D. Simmons-Duffin, “The Conformal Bootstrap”, [arxiv:1602.07982](#), in: “Theoretical Advanced Study Institute in Elementary Particle Physics: New Frontiers in Fields and Strings”, 1–74p.
- [62] A. Bissi, A. Sinha and X. Zhou, “Selected topics in analytic conformal bootstrap: A guided journey”, *Phys. Rept.* 991, 1 (2022), [arxiv:2202.08475](#).
- [63] H. Osborn, “Lectures on conformal field theories in more than two dimensions”, <https://www.damtp.cam.ac.uk/user/ho/CFTNotes.pdf>, (2019).
- [64] D. Pappadopulo, S. Rychkov, J. Espin and R. Rattazzi, “OPE Convergence in Conformal Field Theory”, *Phys. Rev. D* 86, 105043 (2012), [arxiv:1208.6449](#).
- [65] V. S. Rychkov and A. Vichi, “Universal Constraints on Conformal Operator Dimensions”, *Phys. Rev. D* 80, 045006 (2009), [arxiv:0905.2211](#).

- [66] D. Mazac, “*Analytic bounds and emergence of AdS₂ physics from the conformal bootstrap*”, *JHEP* 1704, 146 (2017), [arxiv:1611.10060](#).
- [67] S. Caron-Huot, D. Mazac, L. Rastelli and D. Simmons-Duffin, “*Dispersive CFT Sum Rules*”, *JHEP* 2105, 243 (2021), [arxiv:2008.04931](#).
- [68] G. Mack, “*D-independent representation of Conformal Field Theories in D dimensions via transformation to auxiliary Dual Resonance Models. Scalar amplitudes*”, [arxiv:0907.2407](#).
- [69] J. Penedones, “*Writing CFT correlation functions as AdS scattering amplitudes*”, *JHEP* 1103, 025 (2011), [arxiv:1011.1485](#).
- [70] R. Gopakumar, A. Kaviraj, K. Sen and A. Sinha, “*Conformal Bootstrap in Mellin Space*”, *Phys. Rev. Lett.* 118, 081601 (2017), [arxiv:1609.00572](#).
- [71] J. Penedones, J. A. Silva and A. Zhiboedov, “*Nonperturbative Mellin Amplitudes: Existence, Properties, Applications*”, *JHEP* 2008, 031 (2020), [arxiv:1912.11100](#).
- [72] F. Dolan and H. Osborn, “*Conformal four point functions and the operator product expansion*”, *Nucl. Phys. B* 599, 459 (2001), [hep-th/0011040](#).
- [73] F. A. Dolan and H. Osborn, “*Conformal partial waves and the operator product expansion*”, *Nucl. Phys. B* 678, 491 (2004), [hep-th/0309180](#).
- [74] F. A. Dolan and H. Osborn, “*Conformal Partial Waves: Further Mathematical Results*”, [arxiv:1108.6194](#).
- [75] V. K. Dobrev, G. Mack, V. B. Petkova, S. G. Petrova and I. T. Todorov, “*Harmonic Analysis on the n-Dimensional Lorentz Group and Its Application to Conformal Quantum Field Theory*”.
- [76] M. S. Costa, V. Goncalves and J. Penedones, “*Conformal Regge theory*”, *JHEP* 1212, 091 (2012), [arxiv:1209.4355](#).
- [77] L. F. Alday and S. Caron-Huot, “*Gravitational S-matrix from CFT dispersion relations*”, *JHEP* 1812, 017 (2018), [arxiv:1711.02031](#).
- [78] L. F. Alday, A. Bissi and E. Perlmutter, “*Genus-One String Amplitudes from Conformal Field Theory*”, *JHEP* 1906, 010 (2019), [arxiv:1809.10670](#).
- [79] L. F. Alday, J. Henriksson and M. van Loon, “*Taming the ϵ -expansion with large spin perturbation theory*”, *JHEP* 1807, 131 (2018), [arxiv:1712.02314](#).
- [80] J. Henriksson and M. Van Loon, “*Critical O(N) model to order ϵ^4 from analytic bootstrap*”, *J. Phys. A* 52, 025401 (2019), [arxiv:1801.03512](#).
- [81] A. Fitzpatrick, J. Kaplan, D. Poland and D. Simmons-Duffin, “*The Analytic Bootstrap and AdS Superhorizon Locality*”, *JHEP* 1312, 004 (2013), [arxiv:1212.3616](#).
- [82] A. Kaviraj, K. Sen and A. Sinha, “*Analytic bootstrap at large spin*”, *JHEP* 1511, 083 (2015), [arxiv:1502.01437](#).

- [83] A. Kaviraj, K. Sen and A. Sinha, “*Universal anomalous dimensions at large spin and large twist*”, [JHEP 1507, 026 \(2015\)](#), [arxiv:1504.00772](#).
- [84] D. Simmons-Duffin, D. Stanford and E. Witten, “*A spacetime derivation of the Lorentzian OPE inversion formula*”, [JHEP 1807, 085 \(2018\)](#), [arxiv:1711.03816](#).
- [85] D. Mazáč, “*A Crossing-Symmetric OPE Inversion Formula*”, [JHEP 1906, 082 \(2019\)](#), [arxiv:1812.02254](#).
- [86] Harish-Chandra, “*Plancherel formula for the 2×2 real unimodular group*”, [Proceedings of the National Academy of Sciences of the United States of America 38 \(4\), 337–342 \(1952\)](#).
- [87] J. Maldacena, S. H. Shenker and D. Stanford, “*A bound on chaos*”, [JHEP 1608, 106 \(2016\)](#), [arxiv:1503.01409](#).
- [88] M. Isachenkov, P. Liendo, Y. Linke and V. Schomerus, “*Calogero-Sutherland Approach to Defect Blocks*”, [JHEP 1810, 204 \(2018\)](#), [arxiv:1806.09703](#).
- [89] D. M. McAvity and H. Osborn, “*Conformal field theories near a boundary in general dimensions*”, [Nucl. Phys. B 455, 522 \(1995\)](#), [cond-mat/9505127](#).
- [90] R. de L. Kronig, “*On the Theory of Dispersion of X-Rays*”, [J. Opt. Soc. Am. 12, 547 \(1926\)](#), <https://opg.optica.org/abstract.cfm?URI=josa-12-6-547>.
- [91] K. H. A., “*La diffusion de la lumiere par les atomes*”, [Atti Cong. Intern. Fisica \(Transactions of Volta Centenary Congress\) Como 2, 545 \(1927\)](#), <https://cir.nii.ac.jp/crid/1571135649980336384>.
- [92] R. J. Eden, P. V. Landshoff, D. I. Olive and J. C. Polkinghorne, “*The analytic S-matrix*”, Cambridge Univ. Press (1966), Cambridge.
- [93] Z. Bern, L. J. Dixon, D. C. Dunbar and D. A. Kosower, “*One loop n point gauge theory amplitudes, unitarity and collinear limits*”, [Nucl. Phys. B 425, 217 \(1994\)](#), [hep-ph/9403226](#).
- [94] R. Britto, F. Cachazo and B. Feng, “*Generalized unitarity and one-loop amplitudes in $N=4$ super-Yang-Mills*”, [Nucl. Phys. B 725, 275 \(2005\)](#), [hep-th/0412103](#).
- [95] D. Carmi and S. Caron-Huot, “*A Conformal Dispersion Relation: Correlations from Absorption*”, [JHEP 2009, 009 \(2020\)](#), [arxiv:1910.12123](#).
- [96] M. F. Paulos, “*Dispersion relations and exact bounds on CFT correlators*”, [JHEP 2108, 166 \(2021\)](#), [arxiv:2012.10454](#).
- [97] D. Mazac and M. F. Paulos, “*The analytic functional bootstrap. Part I: 1D CFTs and 2D S-matrices*”, [JHEP 1902, 162 \(2019\)](#), [arxiv:1803.10233](#).
- [98] D. Mazac and M. F. Paulos, “*The analytic functional bootstrap. Part II. Natural bases for the crossing equation*”, [JHEP 1902, 163 \(2019\)](#), [arxiv:1811.10646](#).
- [99] K. Ghosh, A. Kaviraj and M. F. Paulos, “*Charging up the functional bootstrap*”, [JHEP 2110, 116 \(2021\)](#), [arxiv:2107.00041](#).

- [100] A. Kaviraj, “*Crossing antisymmetric Polyakov blocks + dispersion relation*”, *JHEP* **2201**, 005 (2022), [arxiv:2109.02658](https://arxiv.org/abs/2109.02658).
- [101] K. Ghosh, A. Kaviraj and M. F. Paulos, “*Polyakov blocks for the 1D conformal field theory mixed-correlator bootstrap*”, *Phys. Rev. D* **109**, L061703 (2024), [arxiv:2307.01257](https://arxiv.org/abs/2307.01257).
- [102] P. Ferrero, K. Ghosh, A. Sinha and A. Zahed, “*Crossing symmetry, transcendentality and the Regge behaviour of 1d CFTs*”, *JHEP* **2007**, 170 (2020), [arxiv:1911.12388](https://arxiv.org/abs/1911.12388).
- [103] A. Bissi, P. Dey and T. Hansen, “*Dispersion Relation for CFT Four-Point Functions*”, *JHEP* **2004**, 092 (2020), [arxiv:1910.04661](https://arxiv.org/abs/1910.04661).
- [104] J. Barrat, A. Gimenez-Grau and P. Liendo, “*A dispersion relation for defect CFT*”, *JHEP* **2302**, 255 (2023), [arxiv:2205.09765](https://arxiv.org/abs/2205.09765).
- [105] A. Allais, “*Magnetic defect line in a critical Ising bath*”, <https://arxiv.org/abs/1412.3449>.
- [106] F. P. Toldin, F. F. Assaad and S. Wessel, “*Critical behavior in the presence of an order-parameter pinning field*”, *Physical Review B* **95**, (2017).
- [107] S. Ebadi et al., “*Quantum phases of matter on a 256-atom programmable quantum simulator*”, *Nature* **595**, 227 (2021), [arxiv:2012.12281](https://arxiv.org/abs/2012.12281).
- [108] B. M. Law, “*Wetting, adsorption and surface critical phenomena*”, *Progress in Surface Science* **66**, 159 (2001).
- [109] M. Fisher and P. de Gennes, “*Phenomenes aux parois dans un melange binaire critique*”, *World Scientific Simple Views on Condensed Matter*, 237–241 (2003).
- [110] A. Hanke, “*Critical Adsorption on Defects in Ising Magnets and Binary Alloys*”, *Phys. Rev. Lett.* **84**, 2180 (2000), <https://link.aps.org/doi/10.1103/PhysRevLett.84.2180>.
- [111] A. Allais and S. Sachdev, “*Spectral function of a localized fermion coupled to the Wilson-Fisher conformal field theory*”, *Phys. Rev. B* **90**, 035131 (2014), [arxiv:1406.3022](https://arxiv.org/abs/1406.3022).
- [112] G. Cuomo, Z. Komargodski and M. Mezei, “*Localized magnetic field in the $O(N)$ model*”, *JHEP* **2202**, 134 (2022), [arxiv:2112.10634](https://arxiv.org/abs/2112.10634).
- [113] M. Vojta, C. Buragohain and S. Sachdev, “*Quantum impurity dynamics in two-dimensional antiferromagnets and superconductors*”, *Physical Review B* **61**, 15152 (2000).
- [114] S. Sachdev, C. Buragohain and M. Vojta, “*Quantum Impurity in a Nearly Critical Two-Dimensional Antiferromagnet*”, *Science* **286**, 2479 (1999), Publisher: American Association for the Advancement of Science, <https://www.science.org/doi/10.1126/science.286.5449.2479>.

- [115] S. Liu, H. Shapourian, A. Vishwanath and M. A. Metlitski, “*Magnetic impurities at quantum critical points: Large N expansion and connections to symmetry protected topological states*”, *Physical Review B* 104, (2021).
- [116] G. Cuomo, Z. Komargodski, M. Mezei and A. Raviv-Moshe, “*Spin impurities, Wilson lines and semiclassics*”, *JHEP* 2206, 112 (2022), [arxiv:2202.00040](#).
- [117] M. Beccaria, S. Giombi and A. A. Tseytlin, “*Wilson loop in general representation and RG flow in 1D defect QFT*”, *J. Phys. A* 55, 255401 (2022), [arxiv:2202.00028](#).
- [118] A. Zaffaroni, “*Introduction to the AdS-CFT correspondence*”, *Class. Quant. Grav.* 17, 3571 (2000).
- [119] V. E. Hubeny, “*The AdS/CFT Correspondence*”, *Class. Quant. Grav.* 32, 124010 (2015), [arxiv:1501.00007](#).
- [120] M. Ammon and J. Erdmenger, “*Gauge/Gravity Duality: Foundations and Applications*”, Cambridge University Press (2015).
- [121] J. M. Maldacena, “*Wilson loops in large N field theories*”, *Phys.Rev.Lett.* 80, 4859 (1998), [hep-th/9803002](#).
- [122] A. Kapustin, “*Wilson-’t Hooft operators in four-dimensional gauge theories and S-duality*”, *Phys. Rev. D* 74, 025005 (2006), [hep-th/0501015](#).
- [123] J. Henriksson, “*The critical $O(N)$ CFT: Methods and conformal data*”, *Phys. Rept.* 1002, 1 (2023), [arxiv:2201.09520](#).
- [124] T. Huber and D. Maitre, “*HypExp: A Mathematica package for expanding hypergeometric functions around integer-valued parameters*”, *Comput. Phys. Commun.* 175, 122 (2006), [hep-ph/0507094](#).
- [125] T. Huber and D. Maitre, “*HypExp 2, Expanding Hypergeometric Functions about Half-Integer Parameters*”, *Comput. Phys. Commun.* 178, 755 (2008), [arxiv:0708.2443](#).
- [126] H. M. Srivastava and M. C. Daoust, “*A Note on the Convergence of KAMPÉ DE FÉRIET’s Double Hypergeometric Series*”, *Mathematische Nachrichten* 53, 151 (1972).
- [127] A. Gimenez-Grau, “*Probing magnetic line defects with two-point functions*”, [arxiv:2212.02520](#).
- [128] G. Cuomo, Z. Komargodski and A. Raviv-Moshe, “*Renormalization Group Flows on Line Defects*”, *Phys. Rev. Lett.* 128, 021603 (2022), [arxiv:2108.01117](#).
- [129] N. Drukker and D. J. Gross, “*An Exact prediction of $N=4$ SUSYM theory for string theory*”, *J. Math. Phys.* 42, 2896 (2001), [hep-th/0010274](#).
- [130] V. S. Dotsenko and S. N. Vergeles, “*Renormalizability of Phase Factors in the Nonabelian Gauge Theory*”, *Nucl. Phys. B* 169, 527 (1980).
- [131] M. Beccaria, S. Giombi and A. A. Tseytlin, “*Higher order RG flow on the Wilson line in $\mathcal{N} = 4$ SYM*”, *JHEP* 2201, 056 (2022), [arxiv:2110.04212](#).

- [132] A. M. Sengupta, “*Spin in a fluctuating field: The Bose(+Fermi) Kondo models*”, *Phys. Rev. B* **61**, 4041 (2000), <https://link.aps.org/doi/10.1103/PhysRevB.61.4041>.
- [133] S. Sachdev, “*Static hole in a critical antiferromagnet: Field theoretic renormalization group*”, *Physica C* **357**, 78 (2001), [cond-mat/0011233](https://doi.org/10.1016/S0921-4534(01)00123-3).
- [134] M. Billò, M. Caselle, D. Gaiotto, F. Gliozzi, M. Meineri and R. Pellegrini, “*Line defects in the 3d Ising model*”, *JHEP* **1307**, 055 (2013), [arxiv:1304.4110](https://arxiv.org/abs/1304.4110).
- [135] A. V. Belitsky, J. Henn, C. Jarczak, D. Mueller and E. Sokatchev, “*Anomalous dimensions of leading twist conformal operators*”, *Phys. Rev. D* **77**, 045029 (2008), [arxiv:0707.2936](https://arxiv.org/abs/0707.2936).
- [136] S. Giombi and V. Kirilin, “*Anomalous dimensions in CFT with weakly broken higher spin symmetry*”, *JHEP* **1611**, 068 (2016), [arxiv:1601.01310](https://arxiv.org/abs/1601.01310).
- [137] E. Lauria, P. Liendo, B. C. Van Rees and X. Zhao, “*Line and surface defects for the free scalar field*”, *JHEP* **2101**, 060 (2021), [arxiv:2005.02413](https://arxiv.org/abs/2005.02413).
- [138] L. F. Alday, “*Solving CFTs with Weakly Broken Higher Spin Symmetry*”, *JHEP* **1710**, 161 (2017), [arxiv:1612.00696](https://arxiv.org/abs/1612.00696).
- [139] J. Henriksson, S. R. Kousvos and A. Stergiou, “*Analytic and Numerical Bootstrap of CFTs with $O(m) \times O(n)$ Global Symmetry in 3D*”, *SciPost Phys.* **9**, 035 (2020), [arxiv:2004.14388](https://arxiv.org/abs/2004.14388).
- [140] J. Henriksson and A. Stergiou, “*Perturbative and Nonperturbative Studies of CFTs with MN Global Symmetry*”, *SciPost Phys.* **11**, 015 (2021), [arxiv:2101.08788](https://arxiv.org/abs/2101.08788).
- [141] P. Dey, A. Kaviraj and A. Sinha, “*Mellin space bootstrap for global symmetry*”, *JHEP* **1707**, 019 (2017), [arxiv:1612.05032](https://arxiv.org/abs/1612.05032).
- [142] S. Kehrein, F. Wegner and Y. Pismak, “*Conformal symmetry and the spectrum of anomalous dimensions in the N vector model in four epsilon dimensions*”, *Nucl. Phys. B* **402**, 669 (1993).
- [143] S. Giombi and H. Khanchandani, “*CFT in AdS and boundary RG flows*”, *JHEP* **2011**, 118 (2020), [arxiv:2007.04955](https://arxiv.org/abs/2007.04955).
- [144] S. Giombi, R. Roiban and A. A. Tseytlin, “*Half-BPS Wilson loop and AdS₂/CFT₁*”, *Nucl. Phys. B* **922**, 499 (2017), [arxiv:1706.00756](https://arxiv.org/abs/1706.00756).
- [145] N. Kiryu and S. Komatsu, “*Correlation Functions on the Half-BPS Wilson Loop: Perturbation and Hexagonalization*”, *JHEP* **1902**, 090 (2019), [arxiv:1812.04593](https://arxiv.org/abs/1812.04593).
- [146] D. Grabner, N. Gromov and J. Julius, “*Excited States of One-Dimensional Defect CFTs from the Quantum Spectral Curve*”, *JHEP* **2007**, 042 (2020), [arxiv:2001.11039](https://arxiv.org/abs/2001.11039).
- [147] A. Cavaglià, N. Gromov, J. Julius and M. Preti, “*Integrability and conformal bootstrap: One dimensional defect conformal field theory*”, *Phys. Rev. D* **105**, L021902 (2022), [arxiv:2107.08510](https://arxiv.org/abs/2107.08510).

- [148] A. Cavaglià, N. Gromov, J. Julius and M. Preti, “*Bootstrability in defect CFT: integrated correlators and sharper bounds*”, [JHEP 2205, 164 \(2022\)](#), [arxiv:2203.09556](#).
- [149] A. Cavaglià, N. Gromov and M. Preti, “*Computing Four-Point Functions with Integrability, Bootstrap and Parity Symmetry*”, [arxiv:2312.11604](#).
- [150] S. Giombi and S. Komatsu, “*Exact Correlators on the Wilson Loop in $\mathcal{N} = 4$ SYM: Localization, Defect CFT, and Integrability*”, [JHEP 1805, 109 \(2018\)](#), [arxiv:1802.05201](#), [Erratum: [JHEP 11, 123 \(2018\)](#)].
- [151] S. Giombi and S. Komatsu, “*More Exact Results in the Wilson Loop Defect CFT: Bulk-Defect OPE, Nonplanar Corrections and Quantum Spectral Curve*”, [J. Phys. A 52, 125401 \(2019\)](#), [arxiv:1811.02369](#).
- [152] S. Giombi, J. Jiang and S. Komatsu, “*Giant Wilson loops and $AdS_2/dCFT_1$* ”, [JHEP 2011, 064 \(2020\)](#), [arxiv:2005.08890](#).
- [153] N. Drukker and B. Fiol, “*All-genus calculation of Wilson loops using D-branes*”, [JHEP 0502, 010 \(2005\)](#), [hep-th/0501109](#).
- [154] J. Gomis and F. Passerini, “*Holographic Wilson Loops*”, [JHEP 0608, 074 \(2006\)](#), [hep-th/0604007](#).
- [155] J. Gomis and F. Passerini, “*Wilson Loops as D3-Branes*”, [JHEP 0701, 097 \(2007\)](#), [hep-th/0612022](#).
- [156] P. Liendo, C. Meneghelli and V. Mitev, “*Bootstrapping the half-BPS line defect*”, [JHEP 1810, 077 \(2018\)](#), [arxiv:1806.01862](#).
- [157] P. Ferrero and C. Meneghelli, “*Unmixing the Wilson line defect CFT. Part II. Analytic bootstrap*”, [JHEP 2406, 010 \(2024\)](#), [arxiv:2312.12551](#).
- [158] P. Ferrero and C. Meneghelli, “*Unmixing the Wilson line defect CFT. Part I. Spectrum and kinematics*”, [JHEP 2405, 090 \(2024\)](#), [arxiv:2312.12550](#).
- [159] D. Meltzer, E. Perlmutter and A. Sivaramakrishnan, “*Unitarity Methods in AdS/CFT* ”, [JHEP 2003, 061 \(2020\)](#), [arxiv:1912.09521](#).
- [160] N. Drukker, Z. Kong and G. Sakkas, “*Broken Global Symmetries and Defect Conformal Manifolds*”, [Phys. Rev. Lett. 129, 201603 \(2022\)](#), [arxiv:2203.17157](#).
- [161] D. Correa, J. Henn, J. Maldacena and A. Sever, “*An exact formula for the radiation of a moving quark in $N=4$ super Yang Mills*”, [JHEP 1206, 048 \(2012\)](#), [arxiv:1202.4455](#).
- [162] B. Fiol, B. Garolera and A. Lewkowycz, “*Exact results for static and radiative fields of a quark in $N=4$ super Yang-Mills*”, [JHEP 1205, 093 \(2012\)](#), [arxiv:1202.5292](#).
- [163] N. Gromov and F. Levkovich-Maslyuk, “*Quantum Spectral Curve for a cusped Wilson line in $\mathcal{N} = 4$ SYM*”, [JHEP 1604, 134 \(2016\)](#), [arxiv:1510.02098](#).
- [164] J. Barrat, P. Liendo and J. Plefka, “*Two-point correlator of chiral primary operators with a Wilson line defect in $\mathcal{N} = 4$ SYM*”, [JHEP 2105, 195 \(2021\)](#), [arxiv:2011.04678](#).

- [165] F. A. Dolan and H. Osborn, “On short and semi-short representations for four-dimensional superconformal symmetry”, *Annals Phys.* **307**, 41 (2003), [hep-th/0209056](#).
- [166] B. Eden and E. Sokatchev, “On the OPE of 1/2 BPS short operators in $N=4$ SCFT(4)”, *Nucl. Phys. B* **618**, 259 (2001), [hep-th/0106249](#).
- [167] J. Barrat, P. Liendo and P. van Vliet, “Line defect correlators in fermionic CFTs”, [arxiv:2304.13588](#).
- [168] W. H. Pannell and A. Stergiou, “Line defect RG flows in the ε expansion”, *JHEP* **2306**, 186 (2023), [arxiv:2302.14069](#).
- [169] D. Rodriguez-Gomez, “A scaling limit for line and surface defects”, *JHEP* **2206**, 071 (2022), [arxiv:2202.03471](#).
- [170] J. Erdmenger, C. Hoyos, A. O’Bannon and J. Wu, “A Holographic Model of the Kondo Effect”, *JHEP* **1312**, 086 (2013), [arxiv:1310.3271](#).
- [171] J. Erdmenger, C. Hoyos, A. O’Bannon, I. Papadimitriou, J. Probst and J. M. S. Wu, “Two-point Functions in a Holographic Kondo Model”, *JHEP* **1703**, 039 (2017), [arxiv:1612.02005](#).
- [172] S. Giombi and A. A. Tseytlin, “Wilson Loops at Large N and the Quantum $M2$ -Brane”, *Phys. Rev. Lett.* **130**, 201601 (2023), [arxiv:2303.15207](#).
- [173] S. Giombi and B. Liu, “Notes on a surface defect in the $O(N)$ model”, *JHEP* **2312**, 004 (2023), [arxiv:2305.11402](#).
- [174] A. Raviv-Moshe and S. Zhong, “Phases of surface defects in Scalar Field Theories”, *JHEP* **2308**, 143 (2023), [arxiv:2305.11370](#).
- [175] F. P. Toldin and M. A. Metlitski, “Boundary Criticality of the 3D $O(N)$ Model: From Normal to Extraordinary”, *Phys. Rev. Lett.* **128**, 215701 (2022), [arxiv:2111.03613](#).
- [176] T. Nishioka, Y. Okuyama and S. Shimamori, “Comments on epsilon expansion of the $O(N)$ model with boundary”, *JHEP* **2303**, 051 (2023), [arxiv:2212.04078](#).
- [177] L. Bianchi, G. Bliard, V. Forini, L. Griguolo and D. Seminara, “Analytic bootstrap and Witten diagrams for the ABJM Wilson line as defect CFT₁”, *JHEP* **2008**, 143 (2020), [arxiv:2004.07849](#).
- [178] J. Baerman, A. Chalabi and C. Kristjansen, “Superconformal two-point functions of the Nahm pole defect in $N=4$ super-Yang-Mills theory”, *Phys. Lett. B* **853**, 138642 (2024), [arxiv:2401.13749](#).
- [179] S. Giombi, R. Ricci and D. Trancanelli, “Operator product expansion of higher rank Wilson loops from D -branes and matrix models”, *JHEP* **0610**, 045 (2006), [hep-th/0608077](#).
- [180] J. Liu, D. Meltzer, D. Poland and D. Simmons-Duffin, “The Lorentzian inversion formula and the spectrum of the 3d $O(2)$ CFT”, *JHEP* **2009**, 115 (2020), [arxiv:2007.07914](#), [Erratum: *JHEP* **01**, 206 (2021)].

- [181] S. Caron-Huot, Y. Gobeil and Z. Zahraee, “*The leading trajectory in the 2+1D Ising CFT*”, *JHEP* **2302**, 190 (2023), [arxiv:2007.11647](#).
- [182] A. Atanasov, A. Hillman, D. Poland, J. Rong and N. Su, “*Precision bootstrap for the $\mathcal{N} = 1$ super-Ising model*”, *JHEP* **2208**, 136 (2022), [arxiv:2201.02206](#).
- [183] O. Diatlyk, H. Khanchandani, F. K. Popov and Y. Wang, “*Defect Fusion and Casimir Energy in Higher Dimensions*”, [arxiv:2404.05815](#).
- [184] A. Gadde, “*Conformal constraints on defects*”, *JHEP* **2001**, 038 (2020), [arxiv:1602.06354](#).
- [185] N. Kobayashi and T. Nishioka, “*Spinning conformal defects*”, *JHEP* **1809**, 134 (2018), [arxiv:1805.05967](#).
- [186] A. Söderberg, “*Fusion of conformal defects in four dimensions*”, *JHEP* **2104**, 087 (2021), [arxiv:2102.00718](#).
- [187] P. Kravchuk, A. Radcliffe and R. Sinha, “*Effective theory for fusion of conformal defects*”, [arxiv:2406.04561](#).
- [188] G. Cuomo, Y.-C. He and Z. Komargodski, “*Impurities with a cusp: general theory and 3d Ising*”, [arxiv:2406.10186](#).
- [189] L. Bianchi, G. Bliard, V. Forini and G. Peveri, “*Mellin amplitudes for 1d CFT*”, *JHEP* **2110**, 095 (2021), [arxiv:2106.00689](#).
- [190] L. Rastelli and X. Zhou, “*Mellin amplitudes for $AdS_5 \times S^5$* ”, *Phys. Rev. Lett.* **118**, 091602 (2017), [arxiv:1608.06624](#).
- [191] L. Córdova, Y. He and M. F. Paulos, “*From conformal correlators to analytic S-matrices: CFT_1/QFT_2* ”, *JHEP* **2208**, 186 (2022), [arxiv:2203.10840](#).
- [192] G. Bliard, “*Notes on n-point Witten diagrams in AdS_2* ”, *J. Phys. A* **55**, 325401 (2022), [arxiv:2204.01659](#).